Department of **MEDICINE, HEMATOLOGY**

CANCER RESEARCH CENTER-IBMCC (USAL-CSIC)

VNiVERSiDAD D SALAMANCA

CAMPUS DE EXCELENCIA INTERNACIONAL

Doctoral Dissertation

Therapy-induced changes in the gene expression profile of patients with hematological diseases

With the approval of Salamanca University, Department of Medicine, this thesis will be defended on 2th September 2019

Supervisors:

Prof. Dr. Jesús María Hernández Rivas

Dra. M del Rocío Benito Sánchez

Dra. Ana E. Rodríguez Vicente

Jesús María Hernández Sánchez, Salamanca, 2019

D. **Jesús María Hernández Rivas**, Doctor en Medicina, Catedrático del Departamento de Medicina de la Universidad de Salamanca, Médico Adjunto del Servicio de Hematología del Hospital Clínico Universitario de Salamanca e Investigador del Centro de Investigación del Cáncer de Salamanca,

D.ª **María del Rocío Benito Sánchez**, Doctora en Ciencias Biológicas e Investigadora del Centro de Investigación del Cáncer de Salamanca,

D.ª **Ana Eugenia Rodríguez Vicente**, Doctora por la universidad de Salamanca e Investigadora del Centro de Investigación del Cáncer de Salamanca,

CERTIFICAN

Que D. **Jesús María Hernández Sánchez** graduado en Farmacia por la Universidad de Salamanca, ha realizado bajo nuestra dirección el trabajo de Tesis Doctoral titulado "**Therapy-induced changes in the gene expression profile of patients with hematological diseases**", y que éste reúne, a nuestro juicio, las condiciones de originalidad y calidad científica requeridas para su presentación y defensa ante el tribunal correspondiente para optar al grado de Doctor, con mención "Doctor International", por la Universidad de Salamanca.

Y para que así conste a los efectos oportunos, firmamos el presente certificado en Salamanca, a 2 de Julio de 2019.

Fdo:

Prof. Dr. Jesús M. Hernández Rivas

HERNANDEZ RIVAS JESUS MARIA - 06541691P

Firmado digitalmente por HERNANDEZ RIVAS JESUS MARIA - 06541691P
Nombre de reconocimiento (DN): c=ES, serialNumber=IDCES-06541691P, givenName=JESUS MARIA, sn=HERNANDEZ RIVAS, cn=HERNANDEZ RIVAS JESUS MARIA - 06541691P
Fecha: 2019.07.09 12:53:29 +02'00'

Dra. M. del Rocío Benito Sánchez

BENITO SANCHEZ MARIA DEL ROCIO - 07875452E

Firmado digitalmente por BENITO SANCHEZ MARIA DEL ROCIO - 07875452E
Nombre de reconocimiento (DN): c=ES, serialNumber=IDCES-07875452E, givenName=MARIA DEL ROCIO, sn=BENITO SANCHEZ, cn=BENITO SANCHEZ MARIA DEL ROCIO - 07875452E
Fecha: 2019.07.09 12:54:05 +02'00'

Dra. Ana Eugenia Rodríguez Vicente

RODRIGUEZ VICENTE ANA EUGENIA - 70982673G

Firmado digitalmente por RODRIGUEZ VICENTE ANA EUGENIA - 70982673G
Nombre de reconocimiento (DN): c=ES, serialNumber=IDCES-70982673G, givenName=ANA EUGENIA, sn=RODRIGUEZ VICENTE, cn=RODRIGUEZ VICENTE ANA EUGENIA - 70982673G
Fecha: 2019.07.09 11:42:45 +01'00'

This thesis was performed being Jesús María Hernández Sánchez partially supported by "Beca de investigación de la fundación española de hematología y hemoterapia"

Acknowledgments:

- PI17/01741: Caracterización de los SMD de bajo riesgo sin sideroblastos en anillo: de las CPH a las vesículas extracelulares circulantes. 2018-2021
- GRS 1873/A/18: Ultrasecuenciación del ARN (RNA-seq) en pacientes con trombocitopenia inmune tratados con eltrombopag. Búsqueda de biomarcadores de respuesta y de nuevos mecanismos de acción de eltrombopag. 2018-2019
- GRS 1349/A/16: Impacto clínico y pronóstico de la presencia de mutaciones somáticas en pacientes con SMD de bajo riesgo sin sideroblastos en anillo. 2016-2017
- Celgene Corporation, Spain. Determinación de la alteración 5q- en pacientes diagnosticados de SMD. 2013
- Novartis Farmacéutica, Spain: Estudio observacional y prospectivo sobre la influencia del tratamiento inhibidor selectivo de JAK 1/2 en el perfil de expresión génica de pacientes con mielofibrosis. 2015
- Roche IVS: IRON-III (Interlaboratory robustness of Next generation Sequencing). 2014-2015

Scientific contribution during the thesis performed by **Jesús María Hernández Sánchez**:

Published papers

[1] M. Hernández-Sánchez, A.E. Rodríguez-Vicente, I. González-Gascón y Marín, M. Quijada-Álamo**, J.M. Hernández-Sánchez**, M. Martín-Izquierdo, J.Á. Hernández-Rivas, R. Benito, J.M. Hernández-Rivas, DNA damage response-related alterations define the genetic background of patients with chronic lymphocytic leukemia and chromosomal gains, Experimental Hematology. 72 (2019) 9–13. doi:10.1016/j.exphem.2019.02.003.

[2] J.M. Bastida, O. López-Godino, A. Vicente-Sánchez, S. Bonanad-Boix, B. Xicoy-Cirici**, J.M. Hernández-Sánchez**, E. Such, J. Cervera, J.C. Caballero-Berrocal, F. López-Cadenas, M. Arnao-Herráiz, I. Rodríguez, I. Llopis-Calatayud, M.J. Jiménez, M.C. del Cañizo-Roldán, M. Díez-Campelo, Hidden myelodysplastic syndrome (MDS): A prospective study to confirm or exclude MDS in patients with anemia of uncertain etiology, International Journal of Laboratory Hematology. 41 (2019) 109–117. doi:10.1111/ijlh.12933.

[3] J.M. Bastida, R. Benito, M.L. Lozano, A. Marín-Quilez, K. Janusz, M. Martín-Izquierdo, **J. Hernández-Sánchez**, V. Palma-Barqueros, J.M. Hernández-Rivas, J. Rivera, J.R. González-Porras, Molecular Diagnosis of Inherited Coagulation and Bleeding Disorders, Semin Thromb Hemost. (2019) s-0039-1687889. doi:10.1055/s-0039-1687889.

[4] I. García-Tuñón, V. Alonso-Pérez, E. Vuelta, S. Pérez- Ramos, M. Herrero, L. Méndez**, J.M. Hernández-Sánchez**, M. Martín-Izquierdo, R. Saldaña, J. Sevilla, F. Sánchez- Guijo, J.M. Hernández-Rivas, M. Sánchez-Martín, Splice donor site sgRNAs enhance CRISPR/Cas9-mediated knockout efficiency, PLoS ONE. 14 (2019) e0216674. doi:10.1371/journal.pone.0216674.

[5] J.M. Bastida, M.L. Lozano, R. Benito, K. Janusz, V. Palma-Barqueros, M. Del Rey, **J.M. Hernández-Sánchez**, S. Riesco, N. Bermejo, H. González-García, A. Rodriguez-Alén, C. Aguilar, T. Sevivas, M.F. López-Fernández, A.E. Marneth, B.A. van der Reijden, N.V. Morgan, S.P. Watson, V. Vicente, J.M. Hernández-Rivas, J. Rivera, J.R. González-Porras, Introducing high-throughput sequencing into mainstream genetic diagnosis practice in inherited platelet disorders, Haematologica. 103 (2018) 148–162. doi:10.3324/haematol.2017.171132.

[6] J. Sanchez-Garcia, J. Falantes, A. Medina Perez, F. Hernandez-Mohedo, L. Hermosin, A. Torres-Sabariego, A. Bailen, **J.M. Hernandez-Sanchez**, M. Solé Rodriguez, F.J. Casaño, C. Calderon, M. Labrador, M. Vahí, J. Serrano, E. Lumbreras, J.M. Hernández-Rivas, On behalf

of Grupo Andaluz SMD, Prospective randomized trial of 5 days azacitidine versus supportive care in patients with lower-risk myelodysplastic syndromes without 5q deletion and transfusion-dependent anemia, Leukemia & Lymphoma. 59 (2018) 1095–1104. doi:10.1080/10428194.2017.1366998.

[7] J.M. Bastida, R. Benito, K. Janusz, M. Díez-Campelo, **J.M. Hernández-Sánchez**, S. Marcellini, M. Girós, J. Rivera, M.L. Lozano, A. Hortal, J.M. Hernández-Rivas, J.R. González-Porras, Two novel variants of the *ABCG5* gene cause xanthelasmas and macrothrombocytopenia: a brief review of hematologic abnormalities of sitosterolemia, Journal of Thrombosis and Haemostasis. 15 (2017) 1859–1866. doi:10.1111/jth.13777.

[8] M. Forero-Castro, C. Robledo, R. Benito, I. Bodega-Mayor, I. Rapado, M. Hernández-Sánchez, M. Abáigar, **J. Maria Hernández-Sánchez**, M. Quijada-Álamo, J. María Sánchez-Pina, M. Sala-Valdés, F. Araujo-Silva, A. Kohlmann, J. Luis Fuster, M. Arefi, N. de las Heras, S. Riesco, J.N. Rodríguez, L. Hermosín, J. Ribera, M. Camos Guijosa, M. Ramírez, C.D. de Heredia Rubio, E. Barragán, J. Martínez, J.M. Ribera, E. Fernández-Ruiz, J.-M. Hernández-Rivas, Mutations in TP53 and JAK2 are independent prognostic biomarkers in B-cell precursor acute lymphoblastic leukaemia, British Journal of Cancer. 117 (2017) 256–265. doi:10.1038/bjc.2017.152.

[9] M. Quijada-Álamo, M. Hernández-Sánchez, C. Robledo, **J.-M. Hernández-Sánchez**, R. Benito, A. Montaño, A.E. Rodríguez-Vicente, D. Quwaider, A.-Á. Martín, M. García-Álvarez, M.J. Vidal-Manceñido, G. Ferrer-Garrido, M.-P. Delgado-Beltrán, J. Galende, J.-N. Rodríguez, G. Martín-Núñez, J.-M. Alonso, A. García de Coca, J.A. Queizán, M. Sierra, C. Aguilar, A. Kohlmann, J.-Á. Hernández, M. González, J.-M. Hernández-Rivas, Next-generation sequencing and FISH studies reveal the appearance of gene mutations and chromosomal abnormalities in hematopoietic progenitors in chronic lymphocytic leukemia, Journal of Hematology & Oncology. 10 (2017) 83. doi:10.1186/s13045-017-0450-y.

[10] A.M. Dubuc, M.S. Davids, M. Pulluqi, O. Pulluqi, K. Hoang, **J.M. Hernandez-Sánchez**, C. Schlich, J.M. Hernández-Rivas, J.R. Brown, P. Dal Cin, FISHing in the dark: How the combination of FISH and conventional karyotyping improves the diagnostic yield in CpG-stimulated chronic lymphocytic leukemia: Combined FISH and Karyotyping Improves Diagnostic Yield in CLL, American Journal of Hematology. 91 (2016) 978–983. doi:10.1002/ajh.24452.

[11] A.E. Rodríguez-Vicente, E. Lumbreras, **J.M. Hernández**, M. Martín, A. Calles, C.L. Otín, S.M. Algarra, D. Páez, M. Taron, Pharmacogenetics and pharmacogenomics as tools in cancer therapy, Drug Metabolism and Personalized Therapy. 31 (2016). doi:10.1515/dmpt-2015-0042.

[12] M. Forero-Castro, C. Robledo, E. Lumbreras, R. Benito, **J.M. Hernández-Sánchez**, M. Hernández-Sánchez, J.L. García, L.A. Corchete-Sánchez, M. Tormo, P. Barba, J. Menárguez, J. Ribera, C. Grande, L. Escoda, C. Olivier, E. Carrillo, A. García de Coca, J.-M. Ribera, J.M. Hernández-Rivas, The presence of genomic imbalances is associated with poor outcome in patients with burkitt lymphoma treated with dose-intensive chemotherapy including rituximab, British Journal of Haematology. 172 (2016) 428–438. doi:10.1111/bjh.13849.

[13] M.A. Dasi, R. Gonzalez-Conejero, S. Izquierdo, J. Padilla, J.L. Garcia, N. Garcia-Barberá, B. Argilés, M.E. de la Morena-Barrio**, J.M. Hernández-Sánchez**, J.M. Hernández-Rivas, V. Vicente, J. Corral, Uniparental disomy causes deficiencies of vitamin K-dependent proteins, Journal of Thrombosis and Haemostasis. 14 (2016) 2410–2418. doi:10.1111/jth.13517.

[14] J.C. Caballero Berrocal, Mercedes Sánchez Barba, **Jesús M. Hernández Sánchez**, Monica del Rey, Kamila Janusz, C. Chillón, Esperanza Such, Guillermo F Sanz, Ana María Hurtado López, C. Calderón Cabrera, David Valcarcel, Eva Lumbreras, Cristina Robledo, María Abáigar, F. López Cadenas, M. Cabrero, A. Redondo-Guijo, J.M. Hernández Rivas, Maria-Consuelo del Cañizo, M. Díez Campelo, Chronic Graft Versus Host Disease could ameliorate the impact of adverse somatic mutations in patients with Myelodysplastic Syndromes and Hematopoietic Stem Cell Transplantation. **Annals of Hematology, 2019 (in press)**

[15] Laura Palomo, Mariam Ibáñez, María Abáigar, Iria Vázquez, Sara Álvarez, Marta Cabezón, Bárbara Tazón-Vega, Inmaculada Rapado, Francisco Fuster-Tormo, José Cervera, Rocío Benito, María José Larrayoz, Juan Cruz Cigudosa, Lurdes Zamora, David Valcárcel, María Teresa Cedena, Pamela Acha**, Jesús María Hernández-Sánchez**, Marta Fernández-Mercado, Guillermo Sanz, Jesús María Hernández-Rivas, María José Calasanz,Francesc Solé, Esperanza Such. On behalf of the Spanish Group of MDS (GESMD). Spanish Guidelines for the use of targeted deep sequencing in myelodysplastic syndromes and chronic myelomonocytic leukaemia. **British Journal of Haematology, 2019 (in press)**

Submitted papers

130876-JCI-RG-1: Defining the biologic impact and therapeutic vulnerabilities of del(11q) in CLL through CRISPR/Cas9-edited models. **The EMBO Journal**

HAEMATOL/2019/228940: Chronic lymphocytic leukemia patients with IGH translocations are characterized by a distinct genetic landscape with prognostic implications. **American Journal of Hematology**

HAEMATOL/2019/226258: The Combination of WGS and RNA-Seq is Superior to Conventional Diagnostic Tests in Multiple Myeloma: Ready for Prime Time? **The Journal of Molecular Diagnostic**

HAEMATOL/2019/223487 Distinct mutational pattern of Myelodysplastic syndromes with and without 5q- treated with lenalidomide. **Haematologica**

Table of Contents

General Introduction

Precision medicine

It is widely recognized that a revolution is taking place in healthcare. The historical approach of classifying diseases within categories and following empirical treat-and-observe therapeutic strategies is being replaced by a targeted way of medical practice, which aims to characterize and treat illnesses on the basis of progressively greater understanding of their underlying molecular pathology. This is known as 'personalized' or 'precision' medicine (PM) [1]. This model moves away from a "one size fit all" approach, and attempt to divide patients with the same disease into groups with specific conditions [2]. PM tailored treatments target on the baseline characteristics of each patient, analyzing genetic, phenotype, biomarkers and also psychosocial aspects [3]. There is an increasing acknowledgment by clinicians, health care and patients, that reflects the importance of this field in the last years [4]. PM is expected to deliver numerous benefits to patients, by significantly improving the state of health, and thus of the population. PM allows healthcare to be finely tuned to each individual. Properly implemented, it has the potential to shift the focus of the health system from the treatment of illness to the protection of health[5].

PM is based on a better scientific understanding of the components of health and disease; thus is enabled by recent advances in genomics, data analysis and availability, and artificial intelligence. The development of novel, powerful, high-throughput technologies has enabled better insight into the genomic, epigenomic, transcriptomic and proteomic landscape of many diseases, resulting in the application of personalized medicine approaches in their treatment [4,6].

There are several technologies that may be chosen for each patient and clinical situation. The most commonly used are: allele-specific PCR, next generation sequencing (whole and exome genome), flow cytometry, genotyping and imaging. Most of them need a powerful informatics support and the new machine learning approaches combined with the artificial intelligence are moving fast to change the health systems. The new era of targeted therapy will require novel strategies for the better understanding of the mechanism of action, enabling to anticipate the adverse effect and losses in response [7]. The discovery that genomic alterations may be related with drug response, which is the subject of study of pharmacogenetics, have enhanced the implementation of PM (Figure 1).

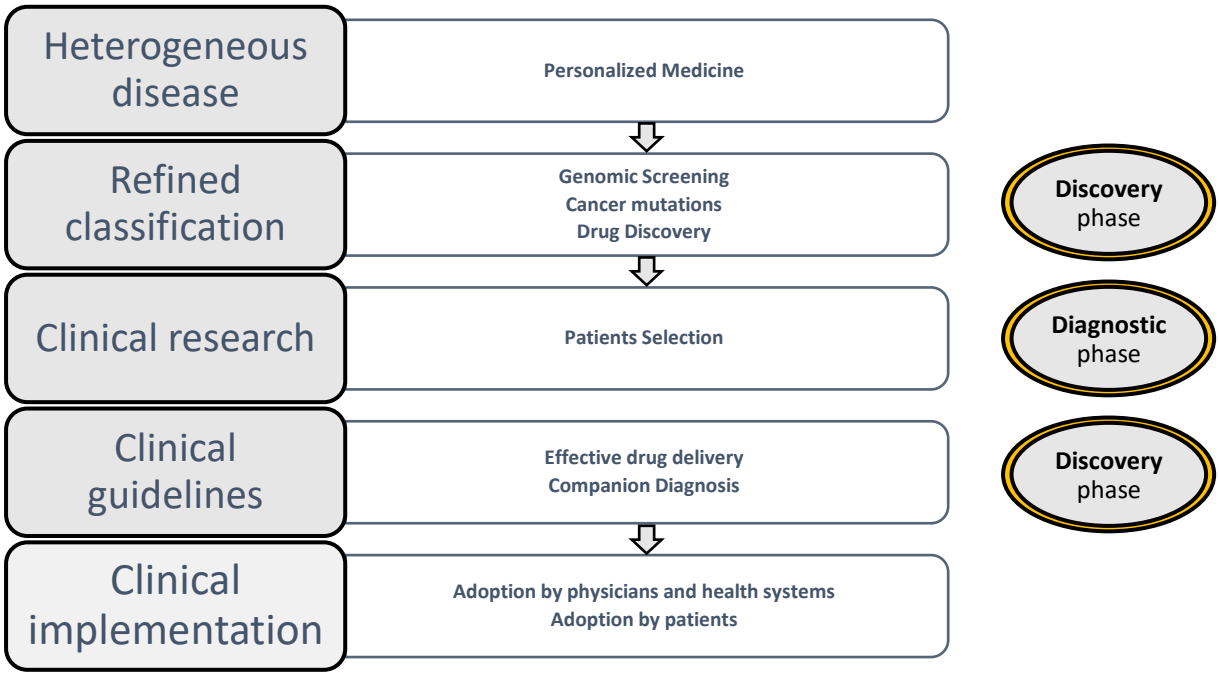

Figure 1. Implementation of personalize medicine. This is a multilayer process involving experts in the field. 1st step requires the analysis of a large number of samples to be analyzed, 2nd the discovering of recurrent genomic alterations in tumor cells, and development of targeted therapy by small molecule inhibitors. 3rd selection of patients carrying this mutation. 4th biomarkers to predict response to therapy, also analyzing side effects. 5th implementation in clinical practice.

Pharmacogenomics

Pharmacogenomics (PKG) is the use of "omic" information to individualize drug selection and use, to minimize adverse reactions and maximize the efficacy [8]. This relative new field has rapidly evolved in the last years, driven by the evidences that genetics may influence drug response. Pharmacogenomics combine the study of drugs (pharmacology) and the study of genes and their functions (genomics). Genomics opens up the shift toward personalized precision treatment, allowing us to examine the underlying causes of disease, rather than just identifying and managing patients once disease has taken hold [9]. The used of gene cloning, DNA genotyping and, in the last ten years, the quick implementation of next generation sequencing (NGS) has increased the knowledge in this field [10–12].

Clinical observations reported that, frequently, drugs with the same indication and administration schedule did not work in the same way. The variation ranges from serious (potentially life threating) to inadequate therapeutic effect, being most of the times difficult to predict who will benefit, who will not response or who will undergo adverse side effect. The results from the Human Genome Project have been a keystone for a better understanding of how differences in genes could affect response to drugs [13,14].

The utility of PKG has been validate in many conditions, for example, PKG may also contribute to test medication adherence [15], one of the biggest problems in chronic diseases. Moreover, PKG can play an important role in identifying responders and non-responders to medications, avoiding adverse events, and optimizing drug dose [16] . There is consensus regarding that PKG and some testing are nowadays essential and could help in the clinical routine. Some examples of the utility of genetic polymorphism are the

warfarin sensitivity (related to the presence of variations in *CYP2C9* or *VKORC1* genes) [17], clopidogrel resistance (in relation to the presence of genetic variations in *CYP2C19* gene) [18] or side-effects related to 6-Mercaptopurine (related to the genetic variants on *TPMT* gene [19]).

The increasing information generated by the clinical laboratories who get massive data has contributed to incorporate this information into electronic health records. This electronic information might be useful with the integration of many patients. This information recently gains the attention of Big Data platforms which aim to merge clinical information with molecular genetic background with the goal of empower the knowledge between clinical information and molecular genetics. Success depends on accessing high-quality genetic and molecular data from large, well-annotated patient cohorts that couple biological samples to comprehensive clinical data, which in conjunction can lead to effective therapies [20,21,22].

However, pharmacogenetics has not reached all potentialities and the use is still quite limited in the clinical setting. Nevertheless, the new target therapies and the use of NGS technologies are enabling the use of pharmacogenetics in more clinical trials. Research and innovation in PM are extensive and expanding as measured by the number of scientific publications biomarker discovery and targeted therapies. However, despite the steady increase in the number of clinically useful molecular diagnostic and targeted therapies, the healthcare system is slow to integrate PM into clinical practice [23].

In recent years, “Cancer Precision Medicine” (CPM) has arisen for the management of cancer patients. CPM system include: cancer screening, monitoring relapse or progression, selection of effective therapies and, at present, personalize

immunotherapy [24]. The results obtained by the use of tyrosine-kinase inhibitors in chronic myeloid leukemia, with overall survival rates over 85% of treated patients, open new avenues for the use of target therapies in other hematological malignancies and solid tumors [25,26]. Breast cancer was one of the first solid tumor to gain advanced based on gene expression or mutations profile, predicting individual response [27]. In accordance, the last years a vast array of new drugs demonstrated their clinical efficacy in terms of survival or in the treatment of secondary effects in breast cancer and other solid tumors as well as hematological malignancies.

Unfortunately, there is no target therapies approved for MDS patients yet. Patients with myelodysplastic syndromes (MDS) are treated with 5-Azacytidine (AZA) or deferasirox [28,29]. Other new drugs are also used in the treatment of benign hematological diseases, such as immune thrombocytopenia (ITP), in which the use of thrombopoietin stimulating agents, as eltrombopag or romiplostim, improved the prognosis of these patients [30,31]. The wide clinical use of these drugs increased in the last years. However, some of the mechanisms of action remains unclear.

Immune thrombocytopenia

Immune thrombocytopenia (ITP) is an infrequent autoimmune disease that leads to a decrease in circulating platelet number due to an abnormal T cell response. This disorder is due to an elevated rate destruction in the spleen and the disability of megakaryocytes (MK) to restore the platelets counts. IPT is characterize by abnormal platelet counts, $<100x10^9/L$ [32]. The low platelet number is the main reason of the clinical manifestations: petechiae, purpura and bleeding episodes. The incidence in adults is 3.3/100,000/year, although, due to the multimodal distribution, can also show up in children and elderly patients [33].

Corticosteroids is the first line management of ITP [33]. Prednisone remains the election drug in most of the patients, scheduled daily 1mg/kg for 2-4 weeks [34]. Nevertheless, new evidences from clinical trials comparing dexamethasone at high doses *versus* prednisone demonstrated that dexamethasone accomplish faster platelet responses, lower hemorrhagic complications and less adverse events [35,36]. When hemorrhage is life-threating intravenous immunoglobulins are required [37].

Classically, splenectomy was the second choice for ITP patients who did not achieve response with corticosteroids. However, splenectomy choice has sifted with the development of thrombopoietin (TPO) agonists. TPO receptor (TPO-R) also known as c-mpl is a growth factor receptor located in the megakaryocytes surface. TPO binds c-mpl being the primer regulator of megakaryopoiesis There are two TPO-R agonists approved for clinical use: romiplostim [38] and eltrombopag [39].

The mechanism behind IPT are characterized by increased platelet destruction and/or reduced platelet production [40]. The first mechanism is related to the innate and adaptive immune system which decreased in regulatory T and B cells [41] involving interleukin-2 (IL-2), interferon-gamma (IFN-γ), IL-17 cytokines, IL-10, transforming growth factor-β1 (TGF-β), IL-4, and IL-35 [42]. It is known that splenic T follicular helper cells induces the differentiation and proliferation of autoreactive B-cells [43]. The B-cells produce mainly the immunoglobulin G isotype (IgG) which is reactive against glycoprotein (GP) receptors: GPIIb/IIIa, GPIb/IX, GPV, GPIa/IIa or GPIV, which are mainly platelet receptors [44]. This reaction induces platelet destruction, although the disease course is not the same in all the patients, depending on the specific autoantibodies and the glycoproteins targeted by the B-cells. Besides the platelet destruction, there is also a loss in bone marrow megakaryocyte proliferation/differentiation. MK are not able to produce platelets normally, boosting thrombocytopenia [43]

Eltrombopag a synthetic, non-peptide TPO mimetics, interacts with the transmembrane and juxtamembrane domains of the TPO-R [45]. For this reason, eltrombopag does not compete with TPO. This interaction activates *JAK2* pathway which directly phosphorylates *STAT*, stimulating megakaryopoiesis. Importantly, eltrombopag does not cause platelet activation or aggregation. Some studies have suggested that eltrombopag may stimulate hematopoietic stem cells, improving hematopoiesis in aplastic anemia and MDS patients [46]. *In vivo* studies are only suitable in chimpanzee and humans because eltrombopag only bind TPO-R in these two species. Moreover, *in vivo* sequential studies are lacking, and potentially they can define which are the potential pathways involved in patients treated with eltrombopag

Myelodysplastic syndromes

Myelodysplastic syndromes (MDS) are a heterogeneous group of hematopoietic disease, that arise in hematopoietic stem cell (HSC) with an increased risk of progression to acute myeloid leukemia (AML) [47]. MDS are characterized by clonal and ineffective hematopoiesis, resulting in a bone marrow (BM) failure with various degrees of peripheral blood (PB) cytopenias, BM hypercellularity, and morphological dysplasia in one or more myeloid lineages (erythroid, granulocytic and megakaryocytic) [48].

MDS present a highly variable clinical course, ranging from indolent conditions with a near normal life expectancy over many years, to an aggressive disease with a rapid progression to acute myeloid leukemia (AML). These diseases are frequent in the elderly, with a median age of 65–70 years at diagnosis, and with <10% of the patients younger than 50 years. The annual incidence of MDS is about 4 cases/100,000 inhabitants/year [49]. However, the incidence rises to 30 per 100,000 per year for people over 70 years of age. MDS more frequently affect males, except for the 5q- syndrome, which is more prevalent in woman [50].

Several risk factors have been implicated in the development of MDS: age, male gender, previous use of radiotherapy or chemotherapy, immunosuppressive agents, viral infections, exposure to ionizing radiation or to benzene, smoking tobacco, excess alcohol intake, and other environmental or occupational exposures [51]. In fact, the incidence of secondary MDS has increased in recent years, maybe in relation to the use of chemotherapy and radiotherapy in cancer[52].

The diagnosis of MDS is based on the presence of cytopenias in a routine analysis of the PB. In general, MDS patients usually show anemia (hemoglobin levels <10 g/dL), and/or thrombocytopenia (platelet count $<50x10^9$/L) and/or neutropenia (neutrophil count $<1.5x10^9$/L). In addition, the diagnosis is confirmed by the morphological examination of the PB smear and BM aspirate. Dysplasia is considered when at least 10% of the cells, of at least one myeloid BM lineage, shows unequivocal morphological changes. The proportion of blasts in the BM must also be assessed to provide a correct classification [53]. Although, BM biopsy is not required, it is important for identifying fibrotic or hypocellular MDS [54].

A careful study must be performed to exclude patients with cytopenia but no dysplasia, which could have similar characteristics to those of MDS. The diagnosis of MDS should be considered in any patient with unexplained cytopenias(s) [55,56]. The implementation of High-Throughput Sequencing (HTS) in clinical routine has allowed the characterization of new entities which share similarities like, idiopathic cytopenia of undetermined significance (ICUS), clonal cytopenia of undetermined significance (CCUS), clonal hematopoiesis of undetermined potential (CHIP) and idiopathic dysplasia of undetermined significance (Table 1).

Table 1: Differential diagnosis of idiopathic cytopenias and MDS (Adapted from Montalban-Bravo et al) [56]

Features	CHIP	IDUS	ICUS	CCUS	MDS
Cytopenias	No	No	Yes	Yes	Yes
Dysplasia	No	Yes < 10% bone marrow cellularity	No MDS diagnosis. Absent of dysplasia or minimal	No MDS diagnosis. Absent of dysplasia or minimal	Yes (>10% of elements per lineage in at least 1 lineage)
Somatic mutations	Yes. Usually in *DNMT3A*, *TET2*, *ASXL1*, *SRSF2* or *TP53* (VAF >2%)	Can be associated with CH	No clonality	• Up to 36% overall with similar mutation VAF compared to MDS • 17% of ICUS without dysplasia • 45% of ICUS with some dysplasia	Up to 85% of patients
Risk of progression	Very low	Unknown	Up to 10% at 5 years	Up to 80% at 5 years	-

CHIP: Clonal hematopoiesis of indeterminate potential. IDUS: Idiopathic dysplasia of undetermined significance. ICUS: Idiopathic cytopenia of undetermined significance. CCUS: Clonal cytopenia of undetermined significance. MDS: Myelodysplastic syndromes.

MDS classification

In 2016 the World Health Organization (WHO) revised its version of 2008 for the myeloid neoplasm classification. Since 2008, there have been many new discoveries of unique biomarkers associated with myeloid neoplasm and acute leukemia [48]. These new advances came from the hand of the implementation of gene expression analysis and next generation sequencing [57]. Thus, in this new version *SF3B1* mutation was include for the diagnosis of MDS with ring sideroblasts. However, other mutations commonly mutated in MDS patients as *TET2*, *SRSF2*, *ASXL1*, *TP53*, *DNMT3A*, *RUNX1*, *U2AF1* or *EZH2* were not included, although this revision highlight the important of *TP53* [48]. Otherwise, some of the patients show myeloproliferative features such as monocytosis in chronic myelomonocytic leukemia or bone marrow fibrosis with an over-representation of mutations in *JAK2*, *SRSF2*, *SETBP1*, *CSF3R* and *BCOR*. Although they are not included as criteria in the WHO 2016 (Table 2) for myeloid classification, evidences suggest the utility of include gene information in future classifications [58].

Table 2. **WHO 2016 criteria for classifying MDS patients**. (Adapted from Arber et al [48]).

Name	Dysplastic lineages	Cytopenias*	Ring sideroblasts as % of marrow erythroid elements	BM and PB blasts	Cytogenetics by conventional karyotype analysis
MDS with single lineage dysplasia (MDS-SLD)	1	1 or 2	<15%/<5%†	BM <5%, PB <1%, no Auer rods	Any, unless fulfills all criteria for MDS with isolated del(5q)
MDS with multilineage dysplasia (MDS-MLD)	2 or 3	1-3	<15%/<5%†	BM <5%, PB <1%, no Auer rods	Any, unless fulfills all criteria for MDS with isolated del(5q)
MDS with ring sideroblasts (MDS-RS)					
MDS-RS with single lineage dysplasia (MDS-RS-SLD)	1	1 or 2	≥15%/≥5%†	BM <5%, PB <1%, no Auer rods	Any, unless fulfills all criteria for MDS with isolated del(5q)
MDS-RS with multilineage dysplasia (MDS-RS-MLD)	2 or 3	1-3	≥15%/≥5%†	BM <5%, PB <1%, no Auer rods	Any, unless fulfills all criteria for MDS with isolated del(5q)
MDS with isolated del(5q)	1-3	1-2	None or any	BM <5%, PB <1%, no Auer rods	del(5q) alone or with 1 additional abnormality except −7 or del(7q)
MDS with excess blasts (MDS-EB)					
MDS-EB-1	0-3	1-3	None or any	BM 5%-9% or PB 2%-4%, no Auer rods	Any
MDS-EB-2	0-3	1-3	None or any	BM 10%-19% or PB 5%-19% or Auer rods	Any
MDS, unclassifiable (MDS-U)					
with 1% blood blasts	1-3	1-3	None or any	BM <5%, PB = 1%,‡ no Auer rods	Any
with single lineage dysplasia and pancytopenia	1	3	None or any	BM <5%, PB <1%, no Auer rods	Any
based on defining cytogenetic abnormality	0	1-3	<15%§	BM <5%, PB <1%, no Auer rods	MDS-defining abnormality
Refractory cytopenia of childhood	1-3	1-3	None	BM <5%, PB <2%	Any

* Cytopenias defined as: hemoglobin, <10 g/dL; platelet count, <100 × 10^9/L; and absolute neutrophil count, <1.8 × 10^9/L. Rarely, MDS may present with mild anemia or thrombocytopenia above these levels. PB monocytes must be <1 × 10^9/L

† If SF3B1 mutation is present.

‡ One percent PB blasts must be recorded on at least 2 separate occasions.

§ Cases with ≥15% ring sideroblasts by definition have significant erythroid dysplasia and are classified as MDS-RS-SLD.

Revised International Prognostic Scoring System (IPSS-R) for MDS Risk

MDS are heterogeneous diseases with large differences regarding survival. Therefore, a scoring system is needed to assess a better prognosis of MDS. The first IPSS was published in 1997 [59]. This was updated in 2012 by the International Working Group for Prognosis in MDS, and called IPSS-R [60]. The prognosis of MDS patients is accurately estimated by the prognostic scoring indexes: IPSS-R and WPSS [61]. The main difference between the IPSS-R and the WHO classification-based prognostic scoring system (WPSS), is the ability of WPSS to predict leukemia progression[62]. IPSS-R prognostic scoring system, classifies MDS patients based on the proportion of blasts in the BM, cytogenetic abnormalities, and the degree of peripheral cytopenias, each considered individually (hemoglobin, platelet and neutrophil levels). These five prognostic variables are shown in Table 3**.**

The five parameters incorporated in the IPSS-R have its own score, and the calculation of the final score assigns the patients in 5 risk groups. Online calculators' tools to facilitate this process are available at https://www.mds-foundation.org/ipss-r-calculator/. The risk groups, from 1 to 5, are significantly different in Overall Survival (OS) and risk of progression to AML. The two lowest and the two highest risk groups are often called "low risk MDS" and "high risk MDS" respectively. The intermediate group, that represents nearly 20% of the MDS patients, is heterogeneous with indolent patients similar to lower risk MDS and other patients with aggressive disease. The IPSS-R recognizes the role of age, performance status, serum ferritin, and lactate dehydrogenase (LDH) levels for overall survival, but not for AML transformation [60].

One of the most important limitations of the IPSS-R is the lack of genetic information. For this reason, it is accepted that IPSS-R can be supplemented by genetic testing where *TP53, NRAS, EZH2* and *ASXL1* mutations are associated with poor outcomes, while *SF3B1* mutation is associated with favorable outcome. Moreover, the IPSS-R has been validated only in the *de novo* disease at diagnosis time and although in the first study therapy related MDS (t-MDS) were excluded from the IPSS-R, a subsequent study showed the prognostic value in these patients [63].

Table 3. Revised International Prognostic Scoring System (IPSS-R). (Adapted from Greenberg et al. [60]).

Cytogenetic risk groups						
	Very good	**Good**	**Intermediate**	**Poor**		**Very poor**
Cytogenetic abnormalities	-Y, del(11q)	Normal, del(5q), del(12p), del(20q), double including del(5q)	del(7q), +8, +19, i(17q), any other single or double independent clones	-7, inv(3)/t(3q)/del(3q), double including -7/del(7q), Complex: 3 abnormalities		Complex: >3 abnormalities
Score Values						
	0	**0.5**	**1**	**1.5**	**2**	**4**
Cytogenetics	Very Good	-	Good	-	Intermediate	Very Poor
BM Blast %	<=2	-	>2-<5%	-	5-10%	-
Hemoglobin	=>10	-	8-<10	<8	-	-
Platelets	=>100	50-<100	<50	-	-	-
ANC	=>0.8	<0.8	-	-	-	-
Category Clinical Outcomes						
	Very Low	**Low**	**Intermediate**	**High**		**Very High**
Patients (%)	19%	38%	20%	13%		10%
Survival*	8.8	5.3	3.0	1.6		0.8
AML/25%**	Not Reached	10.8	3.2	1.4		0.7
Categories/Scores						
	Very Low	**Low**	**Intermediate**	**High**		**Very High**
RISK SCORE	<=1.5	>1.5 - 3	>3 - 4.5	>4.5 - 6		>6

*Medians, years. **Median time to 25% AML evolution

MDS treatment

Allogeneic progenitor stem cell transplantation (SCT) is the only curative therapy for MDS; however, in the majority of the patients is not applicable mainly because of the age. Some drugs have approved by the Food and Drug Administration (FDA) and EMA for MDS patients, such as lenalidomide, an immunomodulatory therapy, and two hypomethylating agents (HMA), 5-Azacytidine (AZA) and decitabine (https://www.centerwatch.com/drug-information/fda-approved-drugs/therapeutic-area/6/hematology). However more than 12 years have passed without any new drug for MDS patients [64]. Furthermore, there is a wide use of erythropoiesis stimulating agents (ESA), such as epoetin and darbepoetin. Since the most frequent symptoms of MDS patients are related to the anemia, blood cell transfusions are largely used in these patients. The use of this therapy is associated with iron overload and the subsequent organ damage due the iron accumulation. For these reason in the last years oral iron-chelators as deferasirox has been extended [65].

High risk MDS and demethylating agents

High-risk MDS patients who are not eligible for SCT, are mainly treated with intensive chemotherapy of demethylating agents, such as 5-Azacitidine (AZA) and decitabine (5-aza-2'-deoxycytidine) (DAC) that can modify the clinical course of these patients. Both hypomethylating agents (HMA), are structurally similar nucleoside analogs (Figure 2) AZA and DAC are converted into their monophosphates, diphosphates and triphosphates [66]. DAC triphosphate is a deoxyribonucleotide that is incorporate only to

DNA. By contrast, AZA triphosphate is mainly incorporate into RNA, although a small part (10-20%) is converted to DAC.

	Azacytidine	Decitabine
Chemical structure	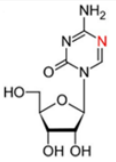	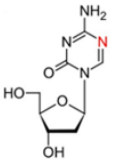
Mechanism of action	Inhibition of DNA methyltransferase	Inhibition of DNA methyltransferase
Administration route	Subcutaneous injection	Intravenous infusion
Cell-cycle specificity	S-phase	S-phase
DNA/RNA	35:65	DNA
Main toxicities	Erythema, Myelosuppression, gastrointestinal toxicities	Myelosuppression, gastrointestinal toxicities
Population	Intermediate/high-risk MDS	Intermediate/high-risk MDS

Figure 2. Comparison between hypomethylating agents, 5-Azacytidine and decitabine. MDS myelodysplastic syndromes.

The main mechanism of action of HMA, is restoring the hypermethylated CpG island, however, the effect on cellular pathways or functions remains unclear. The covalent addition of a methyl group occurs mainly in cytosine within CpG dinucleotide. DNA Methyltransferase 1 (*DNMT1*) gene encodes an enzyme that transfer methyl groups to cytosine nucleotides. This gene is part of the DNA methyltransferase family, being the major protein responsible for maintaining methylation patterns in cancer oncogenesis [67]. Silencing of tumor suppressor genes is one of the studied changes in DNA methylation. These tumor suppressor genes are usually hypermethylated CpG island in the promoter region [68]. Initially, HMA were used at high-dose to achieve chemotherapy effect, however, this therapy can cause also *DNMT1* inactivation at low dose [69].

Decitabine was approved in United States after the results of two randomize clinical trials comparing to best supportive care (D-0007 and EORTC-06011). Although there was not a clear benefit in survival, it was associated with 9% of complete response and 17%

of overall response. In Europe, the randomize study in high MDS treated with decitabine did not achieved the main objective, survival, maybe because the dose and schedule used was not the appropriated.

The effectiveness of 5-Azacytidine in higher-risk MDS was analyzed in two randomize multicenter studies in Europe: CALGB 9221 and AZA-001. In the first trial, MDS patients with a median age of 68 years, showed that AZA had a 60% of response compared to the 5% responses in the best supportive care (BSC) arm ($p < 0.0001$). Furthermore, time to leukemic transformation or death was also longer in AZA arm (21 months vs 12 months, $p = 0.007$) [29]. The AZA-001 trial, with a similar median age, showed that the treatment with AZA was associated with a significantly better mean survival and longer time to AML progression. This trial highlights the improvement regarding red blood cell transfusion requirements and rate of infections in AZA arm [70]. However, the results from these two clinical trials could not be corroborated in real daily life by the cooperative Spanish group of MDS. The study showed, in intermediate-2 and high risk MDS, a lack of improvement in survival over the years [71].

AZA has also been studied in lower-risk MDS lacking del(5q): Patients treated with AZA achieved erythroid response after 9 cycles compare with BSC. ($p < 0.01$) [72]. Analyzing longer AZA treatment, transfusion independence was achieved in all AZA responders with a median duration of 50 weeks (range: 17–231). Furthermore, AZA induced changes in the variant allele burden in some genes such as *RET*, *SF3B1* and *ASXL1*. The study suggests that low risk-MDS patients, lacking del(5q) and resistant to ESAs, may achieve transfusion independence after treatment with AZA[72].

Therefore AZA is widely used in daily treatment for MDS patients. However, there is a need for the identification of predicting factors of response and survival, to select patients that are more likely to be responders.

Low-risk MDS and Iron overload

Low-risk MDS, which covers very low and low IPSS-R risk group, includes asymptomatic patients with slight cytopenias at diagnosis. These patients are usually treated with supportive therapy, because there is not available treatments that had shown any benefit preventing clonal evolution or death [73]. Low-risk MDS are associated with longer survival and RBC transfusion [74]. There are different supportive treatment approaches, and the choice is mainly made by levels of serum erythropoietin or the diagnosis of 5q- syndrome (defined by the isolated deletion of the long arm in chromosome 5) [73]. Patients with low levels of serum erythropoietin, < 100 U/L, have more than 70% chances to response to Erythropoiesis Stimulating Agents (ESAs), while patients with >500 U/L have a response rate <10% [75,76]. Moreover, patients with 5q-syndrome are usually treated with lenalidomide when they are transfusion dependent, reaching a high transfusion independency (65-70%) and 30-40% of cytogenetic responses [77,78].

Beyond these two treatments, red blood transfusion is the only therapeutic option for anemic patients, who usually becoming transfusion dependent. The transfusion and the ineffective erythropoiesis triggers in dysregulation of iron metabolism and finally leads to iron overload (IO). Studies have correlated the IO with a decrease in overall survival in MDS patients [79]. In addition, retrospective studies suggest that MDS with IO have poor

outcomes after SCT [80,81]. All these data support the key role of the iron overload in the management of MDS patients.

Iron is narrowly regulated under normal homeostasis and it is implicated in many process: hemoglobin, myoglobin transport, storage of oxygen and many biochemical reactions [82]. In addition, there is no physiological mechanism of iron excretion and it becomes toxic at excess levels. Transferrin is the protein which binds the iron, as all the biochemical process can be saturated when reached 80% of its capacity [83]. Once transferrin is saturated, non-transferrin-bound iron (NTBI) is generated, being the labile plasma iron (LPI) the most toxic component of NTBI, because is activating redox reactions [84].

Dietary iron is mainly storage in red blood cells (RBCs) and serum ferritin (SF), 60% and 25% respectively, moreover a lesser extent is storage in heme enzymes and non-heme enzymes [85]. Hepatic iron concentration (HIC) correlated with magnitude of total body iron load, and it can predict the threshold for fatal complications. Several iron chelation therapies (ICT) are available: deferasirox, deferoxamine and deferiprone [86]. ICT have shown a clinical benefit in low-risk MDS [87]. Deferoxamine was the standard over the past four decades, however the intravenous administration every 8-12h usually ends in patient's non-compliance. On the other side, deferiprone can cause agranulocytosis. For these reasons deferasirox is considered first-line treatment in MDS [88]. Deferasirox, orally administered, was licensed in 2005 by the FDA, and nowadays is widely used in low and high risk MDS with iron overload. The effect on iron-chelation by deferasirox has been largely demonstrated at clinical level. In addition, in a comparative studied with deferiprone, deferasirox showed a better reduction in serum ferritin [89]. All ICT may

contribute to normalize hepcidin levels, a key protein in iron homeostasis [90]. Deferasirox has also showed an influence in self-renewal and differentiation of hematopoietic stem cell, thus these effects might be the reason for the hematopoiesis improvement observed in MDS patients [91]. However, biological basis of ICT effects on the erythropoiesis and other cellular pathways that can contribute to improve hematopoiesis has not been extensively explored so far.

Next Generation Sequencing (NGS)

Until recently, Sanger sequencing of candidate genes has been the method for mutational molecular diagnosis. However, this technique is time consuming and has a 15-20% detection limit. NGS has revolutionized genetic diagnosis, because allows simultaneous and rapid investigation from whole genome/exome to multiple genes at DNA level with an affordable cost [92,93]. Several NGS large-scale projects all over the world are trying to elucidate its clinical implementation to empower precision medicine [4,94]. Detection of somatic mutations in cancer can be used for diagnosis, prognosis and/or selection and monitoring therapy [95]. For these reasons many clinical laboratories have exchange the detection to one or few numbers of genes, to custom panels that allows the interrogation of dozens to hundreds of genes deeply and simultaneously. Its implementation in research and clinical practice has improved the genetic characterization of hematological and disease [96–100]. The current standard is to validate NGS variations with Sanger sequencing, which has been reported unnecessary after the high validation rate 99.965% of concordance found in some studies [101].

Moreover, in the last years, transcriptomic techniques have changed, moving from microarrays, mainly on Affymetrix platforms, to RNA sequencing (RNAseq). RNA, unlike to DNA, is a dynamic biomolecule involved in many biological processes [102]. Gene expression analysis have evolved from one single gene tests by quantitative reverse transcriptome (qRT-PCR) [103] to multiple genes studies based in hybridization methods using arrayed probes on solid surfaces [104]. Microarray technology coined the terminology “gene expression profiles” (GEP), as the cellular expression patterns indicative of diseases or therapy response. MammaPrint, for example, is a clinical

microarray test that measures simultaneously 70 genes in breast cancer tumors to assessed the risk of recurrence [105]. Actually, many trials in breast cancer tailored the patients according to the GEP. Other clinical platforms are available using qRT-PCR multi-gene profiles, OncoTypeDX [106] and Prolaris [107], for breast and prostate cancer, respectively.

Microarray-based methodologies were an important improvement in the massive genetic studies. However, these approaches have limitations such as variations in sample preparation (collection and extraction) between different laboratories and noise ratios that can affect the limit of detection, especially in low expressed transcripts. Although NGS and microarrays are similar in terms of protein coding genes, RNAseq has a greater dynamic range for quantifying transcription expression [108], providing unprecedented flexibility, accuracy and sensitivity to measure gene expression of low and highly expressed transcripts [102]. High-throughput RNA sequencing has become popular in the last years because enables rapid profiling and deep investigation of the whole transcriptome. Unlike arrays, RNAseq allows not only the quantification of the coding protein genes, but also allow the detection of fusion genes, splicing events , single nucleotide variants (SNV), small insertions and deletions (indels), new transcripts [108] or rare transcripts with oncogenic implications [109,110]. RNAseq is an open methodology because, in contrast to arrays, it does not require species specific probes. There are four main RNAseq procedures: i. custom RNA panel, able to study genes or pathways of interest; ii. mRNA, useful for the sequencing of coding protein genes (it is needed to select these genes by the catching the poly-A tail); iii. total RNAseq technique enable not only coding genes but also quantification of long non-coding and intergenic RNA

(lncRNA/lincRNA), which are transcripts with more than 200 nucleotides (nt) that are not translate into proteins, and non-coding RNA (ncRNA); iv. miRNAseq, which allow the sequencing of microRNAs.

Both microRNAs and circulating RNAs has been widely study as potential biomarkers. However, its implementation is dealing with some unresolved questions, isolation method, quantification, quality control to validate platform accuracy and sample preparation [102].

Many efforts have been done in last years in the bioinformatics area. However, there is still a need of stablish benchmark standards to confirm assay reproducibility and optimization to implement RNAseq in clinical daily routine. The implementation RNAseq, allow the detection of hundreds to thousands expressed transcripts. All these vast amount of data, as well as fusions genes, transcript isoforms and allele-specific expression allow the identification of gene signatures always based in correct, affordable and validated bioinformatics pipelines [102].

Furthermore, the recent development of droplet digital PCR (ddPCR), may help the validation of RNA and DNA sequencing results. This technique divides individual target molecules within oil droplets. ddPCR provides an absolute quantification, that enable with unprecedented precision and sensitivity the detection of rare sequences [111].

In the last years the advances in Genetics, Informatics, Imaging and Biology have provided new tools for the better management of the human disease. The combination of these methodologies has been the basis of the Precision Medicine. However, the

application of these techniques to the better ascertainment and knowledge of the diseases and to the study of the drug effects *in vivo* are still lacking. These studies, analyzing the induced changes by treatments in hematological patients are needed for the better understanding of the mechanism of action and the human response to the drugs. The changes in biological pathways usually have been related with clinical features: hematological response, reduction of blast count or failure/relapse to the treatment. However, few sequential studies have been performed in order to evaluate how the drugs could modify the gene expression in the patient cells. This work is devoting to elucidate which are the pathways involved in these changes.

Hypothesis

Personalized medicine has been boosted by the implementation of high-throughput techniques, such as next generation sequencing (NGS) and droplet digital PCR (ddPCR), both at DNA and RNA level. These techniques are able to detect molecular genetic alterations present at very low levels, with high confidence, thus improving the periodical follow-up of genetic alterations. Gene expression has been at the forefront of advance in personalized medicine, notably in the field of cancer. Changes in the gene expression profile (GEP), have been analyzed by means of microarrays and, more recently, by RNAseq, which has not only validated previous arrays results, but also has empowered the ability to detect low expressed genes, usually key transcription factors and splicing changes. The ability of RNAseq to detect variants also enables the evaluation of allele-specific expression. Furthermore, targeted therapies have increased the need of accurate molecular diagnosis and tracking patients during the treatment. Therefore, it would be desirable to implement all these *omic* techniques into the clinical routine, in order to efficiently combine the genetic information with clinical data, morphology and classical cytogenetics. It is mandatory to unravel the biological mechanisms behind the administration of drugs for the better understanding of the process induced in each patient.

Immune thrombocytopenia is a rare autoimmune disease that causes a decrease in platelet count. The development of new TPO agonists, which stimulate megakaryopoiesis, is widely used. Some studies showed how the drug can also stimulate hematopoietic stem cell, suggesting a positive side effect of the therapy.

Myelodysplastic Syndromes (MDS) are a heterogeneous group of diseases displaying a range of morphological and cytogenetic abnormalities and characterized by a wide array

of genetic alterations. Nowadays, it is accepted that MDS are the consequence of the accumulation of cooperating mutations that could arise from asymptomatic clonal hematopoiesis to symptomatic MDS and, in some patients, end in acute myeloid leukemia. These mutations occur in more than 50 genes related to DNA methylation, histone modifications, RNA splicing, cohesin complex, transcription factors and signal transduction proteins. RNA splicing and DNA methylation mutations are considered the founders events. Moreover, most of the MDS (~90%) have mutations, thus these patients are usually candidate for high-throughput deep sequencing. The most recurrent mutated genes found in MDS are: *SF3B1*, *TET2*, *SRSF2*, *ASXL1*, *DNMT3A*, *U2AF1*, *TP53* and *EZH2*. However, few studies regarding the transcriptome of MDS patients and the relationship with the therapy have been carried out.

In the last years new therapies have improved the clinical outcome of the hematological diseases. Primary IPT treatment is corticosteroids (prednisone), however some patients did not response being the second line treatment, eltrombopag or romiplostim, TPO agonist. Supportive care of MDS patients is based on red blood cell transfusions, being the management of iron overload an essential part of the treatment. Thus, iron chelators are widely used in low-risk MDS patients in the clinical routine. On the other hand, demethylating agents are the standard care for high-risk MDS patients. However, other unexpected clinical effects, such as erythropoiesis improvement in patients treated with deferasirox or the presence of immune abnormalities in patients treated with 5-Azacytidine have not been fully elucidated. One of the reasons could be the lack of transcriptomic studies in patients treated with these drugs. The best way to assess these changes is to perform sequential studies in patients, and to apply, in selected

cases, the *omic* techniques in purified cells. These analyses can contribute to decipher the biological pathways affected by the therapy. This could be of great interest in MDS patients, due to their heterogeneity and the lack of targeted therapies. Nevertheless, *omic* studies are not currently performed in patients treated with new drugs. Consequently, no information coming from the application of these full-scale methodologies is available.

Therefore, I hypothesize that the combination of different transcriptomic high-throughput molecular techniques such as microarrays and RNA-seq, will help us to identify those genes and molecular pathways, as well as to better understand the mechanisms, modified by the therapy, which can be related with the clinical features, the hematological response, the reduction of blast count or the failure/relapse to the treatment. However, although response analysis is important to get insight of the biological process, it is also necessary to compare the induced changes with healthy controls, to understand how the changes can reestablish some pathways to "normality" and also which remains unmodified and could be potentially targeted by other therapies. It is known that transcriptome shift throughout life, being one of the main challenges selecting healthy controls for MDS studies. The MDS patients are usually elderly and, in consonance, the healthy controls have to be aged matched.

Of note, in-depth transcriptomic analysis can also identify biological pathways affected by the treatment and associated with off-target effects, whether adverse but as well therapeutic, which are usually difficult to be detected *in vitro* or in animal models. This is especially challenging in the case of MDS, due to the lack of mouse models. These unknown therapeutic effects might be useful for patients suffering from different

diseases. Moreover, there is a need to gain insight in getting clonal response to therapy, not only to asses mutations that can correlate with response, but also, by analyzing mutational dynamics to identify which variants are more sensitive or which mutations can arise during the treatment. Thus, these new insights may end in new clinical trials.

Aims

General aim:

To analyze, *in vivo,* the pharmacogenomic profile of three commonly used treatments for hematological disorders (eltrombopag, deferasirox and 5-Azacytidine) and to assess the changes in the gene expression profile induced by the therapy in paired samples (before and during the treatment) of treated patients, correlating these changes with the clinical features observed in order to gain insights into the mechanism of action of the drugs. We will analyze the 5-Azacytidine effect in intermediate/high risk MDS, the effect of deferasirox for the iron chelation in low-risk MDS patients as well as eltrombopag, used for the treatment of patients with immune thrombocytopenia

Specific aims:

1. To identify the global transcriptome variations induced by eltrombopag treatment in patients with immune thrombocytopenia and to explore the pathways differentially deregulated depending on the response/failure to the therapy.

2. To analyze, in low-risk MDS patients, the switch induced by deferasirox in the gene and miRNA expression profiles.

3. To assess the changes in the gene expression profile of CD34+ cells from high-risk MDS/AML bone marrow samples before and during 5-Azacytidine treatment.

4. To evaluate the gene expression profile shift in relation to the clinical outcome (hematological and blast response), using baseline profiles and changes in the gene expression.

5. To characterize the mutational profile in high-risk MDS patients treated with 5-Azacytidine by Next-Generation Sequencing (NGS), in the CD34+ and CD34- fractions, in order to assess the variations due to the therapy.

Results

***Chapter 1**: Transcriptomic analysis of patients with immune thrombocytopenia treated with eltrombopag*

Authors

Jesús María Hernández-Sánchez[1,2], José María Bastida[1,2], Diego Alonso-López[3], Rocío Benito[1,2], José Ramón González-Porras[1,2], Javier de las Rivas[3], Jesús María Hernández Rivas[1,2,*], Ana Eugenia Rodríguez-Vicente[1,2,*]

[1] *Department of Hematology, Hospital Universitario Salamanca, Salamanca, Spain.*

[2] *IBSAL, IBMCC-Cancer Research Center, University of Salamanca, Salamanca, Spain.*

[3] *Bioinformatics Unit, Cancer Research Center (CSIC-USAL), Salamanca, Spain*

** Shared authorship*

Correspondence

Ana E Rodríguez Vicente

IBMCC, CIC Universidad de Salamanca-CSIC, Hospital Universitario de Salamanca

Campus Miguel de Unamuno

37007 Salamanca

Spain

e-mail: anaerv@hotmail.com

Running title

Gene expression profile changes in ITP patients treated with eltrombopag

Scientific category: Original Article

Text word count (without references): ~3800
Abstract word count: 236
Figures: 2
Tables: 4
Reference count: 61

Abstract

In the last years, the use of thrombopoietin receptor agonists (TPO-RA), eltrombopag and romiplostim, has improved the management of immune thrombocytopenia (ITP). Moreover, eltrombopag is also active in patients with aplastic anemia and myelodysplastic syndrome. However, their mechanisms of action and signaling pathways still remain controversial. In order to gain insight into the mechanisms underlying eltrombopag therapy, a gene expression profile (GEP) analysis in patients treated with this drug was carried out. Fourteen patients with chronic ITP were studied by means of microarrays before and during eltrombopag treatment. Median age was 78 years (range, 35-87 years); median baseline platelet count was $14x10^9$/L (range, 2-68 $x10^9$/L). Ten patients responded to the therapy, two cases relapsed after an initial response and the remaining two were refractory to the therapy. Eltrombopag induced relevant changes in the hematopoiesis, platelet activation and degranulation, as well as in megakaryocyte differentiation, with overexpression of some transcription factors and the genes *PPBP*, *ITGB3*, *ITGA2B*, *F13A1, F13A1*, *MYL9* and *ITGA2B*. In addition, *GP1BA, PF4,*

ITGA2B, MYL9, HIST1H4H and *HIST1H2BH*, genes regulated by *RUNX1* were also significantly enriched after eltrombopag therapy. Furthermore, in non-responder patients an overexpression of Bcl-X gene and genes involved in erythropoiesis, such as *SLC4A1* and *SLC25A39,* was also observed. To conclude, overexpression in genes involved in megakaryopoiesis, platelet adhesion, degranulation and aggregation was observed in patients treated with eltrombopag. Moreover, an important role regarding heme metabolism was also present in non-responder patients.

Introduction

Primary immune thrombocytopenia (ITP) is an autoimmune disorder, which brings about to isolated thrombocytopenia in the absence of underlying causes.[1] Pathogenic mechanisms are mainly characterized by both increased platelet destruction and/or reduced platelet production.[2] The first mechanism is related to the innate and adaptive immune system which decreased in regulatory T and B cells [3] involving interleukin-2 (IL-2), interferon-gamma (IFN-γ), IL-17 cytokines, IL-10, transforming growth factor-β1 (TGF-β), IL-4, and IL-35.[4] The immune suppression with corticosteroids (CC), immunoglobulins (IVIG) and Rituximab are often used to treat ITP.[5]. In the last 10 years the extended use of thrombopoietin receptor agonists (TPO-RA) has improved the prognosis of patients with ITP.[6] TPO activates Jak2 pathway, which directly phosphorylates STAT family members through transcriptional elements within genes, including Bcl-XL.[7] TPO plasma levels in ITP can be either normal or low, thus these considerations have led to the use of TPO receptor agonists (TPO-RAs) in the treatment of this disease.[8,9] The mechanism of action of TPO-RAs (eltrombopag and romiplostim) still remains controversial being the direct stimulation of BM MKs precursors and possibly the MKs themselves.[10] Eltrombopag, is an oral non-peptide TPO mimetic that binds to the TPO-R near its membrane insertion site, away from the active site, while romiplostim is thought to bind directly to the TPO binding site on TPO-R.[10,11] The interaction of eltrombopag with the TPO receptor, initiate the JAK/STAT signaling pathway which induce the proliferation and differentiation of the MKs and giving rise to an increase in platelet production.[12] However, other signaling pathways might be influenced. Thus the presence of adverse events such as an increased risk of thrombosis

[13] and the responses in aplastic anemia and myelodysplastic syndromes has been described in eltrombopag treatment.[10,14,15] In addition, eltrombopag induces the proliferation of immature MKs rather than platelet production, due to the unbalanced activation of AKT and ERK1/2 signaling molecules.[16,17] Finally, GPVI expression in platelets was upregulated in MKs after TPO stimulation, due to the promoter of GPVI is modulated by a transcription factor, FLI1, which interacts with Sp-1 and GATA-1 to enhance the transcription of GPVI leading to reduce bleeding symptoms.[18]

The application of system-wide "omics" technologies could provide new insights into the knowledge of pathogenic mechanisms of ITP and gene expression profiling (GEP) can provide useful information. Genome-wide gene expression analysis in adult and pediatric ITP patients have revealed gene signatures of differentially expressed genes, as well as altered gene-expression networks in ITP.[19–27] Noticeably, there are several studies reporting a signature expression of miRNAs in ITP patients and indicating the pathogenic role of miRNAs in developing ITP. However, little is known about the gene expression changes induced by the use of eltrombopag in ITP patients.

In this work, we aimed to analyze the gene expression changes in paired samples from ITP patients before and during the treatment with eltrombopag, in order to gain insight into the molecular mechanism of this therapy.

Patients and methods

Patients

Fourteen patients diagnosed as chronic ITP and treated with eltrombopag, were included in the study. Clinical characteristics, laboratory findings and treatment

response were evaluated the day before starting the treatment, as well as at least fourteen days after starting therapy (Tables 1 & 2). Bleeding was evaluated by ITP-BAT score.[28] Venous blood was drawn from each patient collecting whole blood sample in commercial tubes (7.5% K3 EDTA tubes for blood cells count and nucleic acid extraction).

Complete response (CR) was defined as a platelet count of ≥100 x 10^9/L. Response (R) was defined as a platelet count of **≥**30 x 10^9/L and at least two-fold increase in the baseline count. No response (NR) was defined as a platelet count of **<**30 x 10^9/L or less than twofold increase the baseline count.[29] The definition of response required concurrent resolution of bleeding symptoms and the absence of any rescue intervention during the preceding 8 weeks. Treatment failure was defined as a platelet count of **≤**20 x 10^9/L for 4 consecutive weeks at the highest recommended dose of eltrombopag, a major bleeding event, or the need to change therapy (including splenectomy and rescue treatment). The need to increase the dose of a concomitant treatment to eltrombopag at higher levels of the baseline dose was considered as a rescue treatment.

The procedures followed were in accordance with the Helsinki Declaration of 1975, as revised in 2008, with the study receiving official institutional approval (Hospital Universitario, Salamanca, Spain), and samples were obtained after subjects provided informed consent.

Table 1. **Main clinical and biological characteristics of ITP patients included in the study**

Characteristics	Median (range)
Age (years)	77.5 (35-87)
Sex (n, %): Male / Female:	8 (57.1%) / 6 (42.9%)
Treatments before eltrombopag: 1 or ≥2	5 (35.7%) / 9 (64.3%)
Blood cells count basal:	
Platelets (x 10^9/L)	14.45 (1.9-73.8)
White blood cells (x 10^9/L)	6.85 (2.2-19.3)
Hemoglobin (g/dL)	13.85 (8.7-16.2)
Blood cells count at day 14:	
Platelets (x 10^9/L)	119.5 (4.7-230)
White blood cells (x 10^9/L)	7.58 (1.9-14.4)
Hemoglobin (g/dL)	12,85 (8.6-16.3)
Blood cells count at day 28:	
Platelets (x 10^9/L)	132 (1.9-73.8)
White blood cells (x 10^9/L)	9.1 (2.7-14.1)
Hemoglobin (g/dL)	13.35 (81-15.4)
Treatment response (n, %): Complete / Failure	12 (85.7%) / 2 (14.3%)
Day of response (n, %): +14 / +28	10 (71.4%) / 4 (28.6%)
Blood cells count at day RNA analysis:	
Platelets (x 10^9/L)	154.5 (9.6-562)
White blood cells (x 10^9/L)	7.6 (2.7-10.6)
Hemoglobin (g/dL)	13.75 (8.1-16.5)

All blood samples were collected before treatment and after eltrombopag in the days 14^{th} and 28^{th}

Table 2. Detailed clinical characteristics of the ITP patients included in the study.

ID	Age (years)	Sex	Nº previous treatments	Last treatment before eltrombopag	ITP-BAT	Platelets pre (x 10^9/L)	Platelets at day 14 (x 10^9/L)	Platelets at day 28 (x 10^9/L)	Response at day 28	Concomitant treatment
1	76	Male	4	Rituximab	4	5.4	4,7	28	No R	IVIG
2	40	Male	2	IVIG	2	2	230	562	CR	No
3	81	Male	4	CC	0	11	201	6	Relapse	No
4	70	Female	3	Romiplostim	0	68	169	121	CR	No
5	80	Male	1	CC	0	13	47	255	CR	No
6	77	Female	1	CC	0	56	153	3	Relapse	No
7	35	Female	3	CC	0	35	75,9	65	R	No
8	87	Male	2	IVIG	0	27	28	11	No R	CC
9	53	Male	2	Splenectomy	1	14	213	145	CR	No
10	87	Female	1	CC	0	14	104	105	CR	No
11	80	Female	3	CC	0	12	135	131	CR	No
12	78	Male	2	IVIG	0	3	15	442	CR	No
13	68	Male	1	IVIG	0	29	20	133	CR	No
14	79	Female	1	CC	0	23	225	203	CR	No

M: male; F: female; P: platelet count (x10^9/L); IVIG: Intravenous immunoglobulin, CC: corticosteroids, CR Complete Response, No R: no response.

Study design: PBMCs isolation, RNA extraction and gene expression analysis

Peripheral blood mononuclear cells (PBMCs) were isolated from whole blood using Ficoll-Hypaque Plus gradient, snap-frozen and stored at -80ºC. Total RNA was extracted by QIAgen (Qiagen, Valencia, CA, USA), following the manufacturer's recommendations. RNA integrity was assessed on an Agilent 2100 Bioanalyzer (Agilent technologies, Santa Clara, CA, USA) employing the RNA 6000 Nano Assay kit. All RNA samples had an A260/A280 ratio ~1.8 and RNA integrity number (RIN) ≥8.0.

Genome-wide expression analysis of the paired samples (before and during the treatment) was performed using GeneChip Human Gene 2.0 ST Array (Affymetrix, Inc., Santa Clara, CA, USA) following the manufacturer's protocols for the GeneChip platform by Affymetrix. Briefly, cDNA was regenerated through a random-primed reverse transcription (RT) using a dNTP mix containing dUTP. After cDNA was hybridized to the arrays at 60 rpm for 18h at 45°C, the chips were processed in a Genechip Fluidics Station 450 (Affymetrix). Microarray images were collected by Affymetrix GeneChip 3000 scanner, and data were extracted using Affymetrix GCOS Software.

Microarray data analysis

Briefly, the robust microarray analysis (RMA) algorithm was used for background correction, intra- and inter-microarray normalization, and expression signal calculation.[30–32] Once the absolute expression signal for each gene (i.e., the signal value for each probe set) was calculated in each microarray, a method called significance

analysis of microarray (SAM) was applied to calculate significant differential expression and find the gene probe sets that characterized the treated samples.[33] The method uses permutations to provide robust statistical inference of the most significant genes and provides P values adjusted to multiple testing using false discovery rate (FDR).[34]

Filtering, inter-quartile range (IQR)

Filtering was applied to remove genes with consistently low intensity values or low variance across the samples. This technique was especially useful in the case of genome-wide arrays as often a minor of all genes are expressed at all in the peripheral blood mononuclear cells. Inter-quartile range provides a measure of the spread of the middle 50% of the intensity scores for each gene. The IQR was defined as the 75th percentile - the 25th percentile. The advantage of using the IQR was that it is easy to compute and extreme scores in the distribution have less impact, but its strength is also a weakness in that it suffers as a measure of variability because it discards too much data. Gene selection by IQR seems to lead to a higher concentration of differentially expressed genes, whereas for the intensity-based criterion, the effect was less pronounced.[35]

Functional analysis and gene annotation

The functional assignment of the genes was carried out by the Database for Annotation, Visualization and Integrated Discovery (DAVID) [36] and the GeneCodis software [37] which identifies concurrent annotations in GO and KEGG, and thereby constructs several groups of genes of functional significance. Gene set enrichment analysis (GSEA) (http://software.broadinstitute.org/gsea/index.jsp) to evaluate

whether the set of genes were significant between the groups was also carried out. Normalized enrichment score (NES), and false discovery rate (FDR) were used for the statistical significances between the groups in the genes set and defined molecular signatures (MSigDB).[38,39]

The most significant biological mechanisms, pathways and functional categories in the data sets of genes selected by statistical analysis were identified through the use of Reactome.[40]

Results and Discussion

Clinical characteristics of ITP patients treated with eltrombopag

The main clinical and biological characteristics of patients included in the study are summarized in Tables 1 and 2**.** The median age at eltrombopag initiation was 77.5 years [range, 35-87 years]; eight patients were male (57.1%). Nine patients (64.3%) were treated at least with 2 previous lines of therapy before using eltrombopag, based mainly on corticosteroids (CC) and/or immunoglobulins (IVIG). Only three patients were previously splenectomized. Median platelet counts pre-treatment, at day 14 and at day 28 were: 14.4 x 10^9/L [1.9-73.8 x 10^9/L], 119.5 x 10^9/L [4.7-230 x 10^9/L], and 132 x 10^9/L [3-559 x 10^9/L], respectively. A detailed description of patients is provided in Table 2. All but three patients had no bleeding symptoms before and during eltrombopag treatment. Regarding the response, all but two patients (02 and 09) achieved CR, mainly established with 50 mg doses at day 14 (n=9; 75%). while other 3 cases achieved CR at day 28 with 75 mg (25%). Two patients (04 and 07) had eltrombopag treatment failure because they needed concomitant treatment (CC or IVIG) to improve platelet counts.

Thus, four patients were considered as non-responders (treatment failure or relapsed patients).

Gene expression shift induced by eltrombopag

The gene expression profile (GEP) analysis showed 101 genes overexpressed after eltrombopag treatment (supplementary Table 1). The top 10 differentially expressed genes (DEG) are shown in Table 3. Nine out of ten were related with hematopoiesis: several are involved in megakaryocyte differentiation (*PPBP, ITGB3, TUBB1, TREML1, MYL9, ITGA2B, F13A1*), while *CXCR2P1* is an immune checkpoint gene [41] and *MMD* is related to monocyte to macrophage differentiation.[42].

Table 3. Most differentially expressed genes sorted by gene expression values before and during eltrombopag treatment. PPBP, ITGB3, ITGA2B, F13A1 and F13A1 are related with platelet activation (signaling and aggregation) and platelet degranulation respectively, while MYL9 and ITGA2B are involved to megakaryocyte differentiation through RUNX1.

Gene	Official Full Name	Description
PPBP	Pro-Platelet Basic Protein	The protein encoded by this gene is a platelet-derived growth factor that belongs to the CXC chemokine family.
ITGB3	Integrin Subunit Beta 3	Megakaryocyte and platelet marker
TUBB1	Tubulin, Beta 1	Expressed in platelets and megakaryocytes and may be involved in proplatelet production and platelet release.
TREML1	Triggering Receptor Expressed on Myeloid Cells Like 1	Involved in platelet aggregation, inflammation, and cellular activation
MYL9	Myosin Light Chain 9	Proplatelet and platelet release
ITGA2B	Integrin Subunit Alpha 2b	Megakaryocyte and platelet marker
F13A1	Coagulation Factor XIII A Chain	Coagulation factor XIII is the last zymogen to become activated in the blood coagulation cascade
PGRMC1	Progesterone Receptor Membrane Component 1	Heme chaperone or sensor.
CXCR2P1	C-X-C Motif Chemokine Receptor 2 Pseudogene 1	Pseudogene
MMD	Monocyte To Macrophage Differentiation Associated	Expressed by in vitro differentiated macrophages but not freshly isolated monocytes

To gain insight into the biological mechanisms deregulated by eltrombopag, a Gene Ontology (GO) and a GSEA analysis on the paired analysis were carried out (Figure 1). Interestingly, a high enrichment score in megakaryocyte/platelet processes was shown (supplementary Table 2). The regulation of megakaryocyte differentiation process had an enrichment of 17.8-fold (p-value 0.016), while platelet function, involving aggregation, degranulation and activation had a 21.5, 18.5 and 14.8 enrichment fold respectively. Moreover, the regulation of cell differentiation was also enriched due to the treatment (enrichment fold =2.55, p-value = 0.035). Reactome enrichment analysis (data not shown) also highlighted that the most deregulated pathways were platelet activation, signaling and aggregation, being involved key genes: *MPL*, *GP1BA*, *ITGA2B/CD41*, *C6orf25*, *PROS1*, *SERPINE1*, *MMRN1*, *ABCC4*, *SELP*, *ITGB3/CD61*, *TGFB2*, *CLEC1B*, *PF4*, *PPBP*, *F13A1*, *EGF*, *VWF*, *GP9*, *SPARC*, *GP6*, *GNG11* and *CLU* (FDR = 4.41E-13). It is well known that eltrombopag treatment boosts platelet production by megakaryocytes stimulation, instead of reducing immune mediated platelet destruction, in contrast with previous treatments.[43]

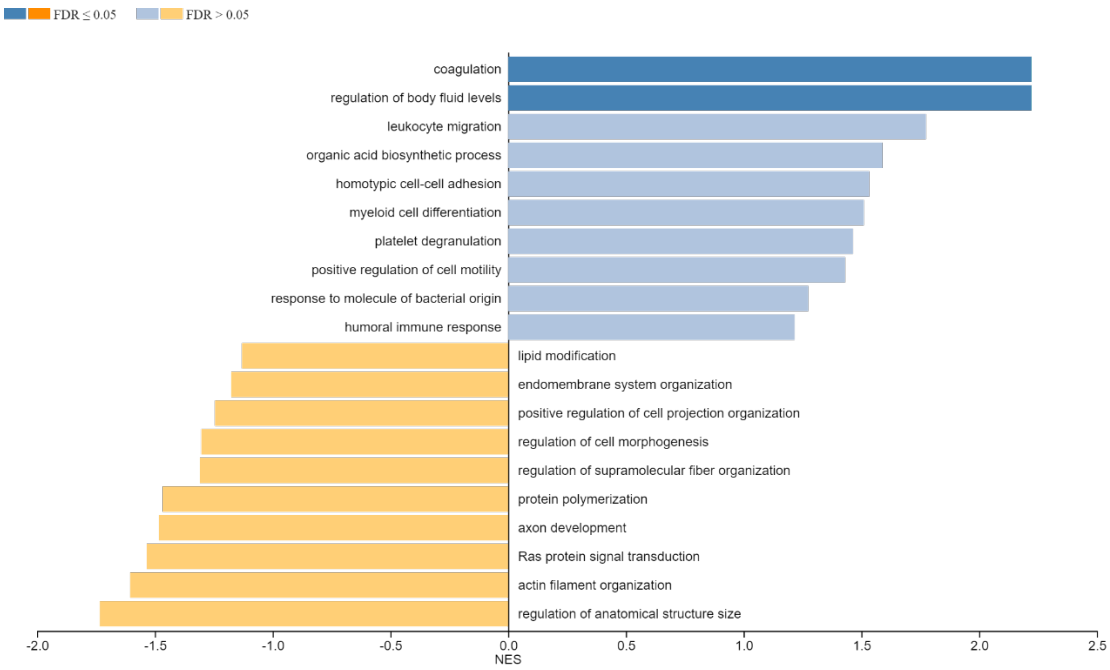

Figure 1. Gene Ontology enrichment analysis based on non-redundant biological process (minimum number of IDs in the category 5 and significant number of ID in the category top 10). Biological process enriched from the differentially expressed genes in the paired comparison in immune thrombocytopenia patients before and during eltrombopag treatment. In blue, biological process upregulated by eltrombopag treatment. Coagulation was the most significant process influenced by the treatment (FDR <0.05). No significant leukocyte migration and myeloid cell differentiation showed high normalize enrichment score (NES). In yellow, downregulated biological process induced by eltrombopag.

In the megakaryopoiesis process, the megakaryocyte-erythroid progenitor (MEP) is able to differentiate into megakaryocytes and erythrocytes [44]. This process is highly regulated by multiple transcription factors such as *GATA1* (and its cofactor *FOG1*), *FLI1* and *RUNX1* [45]. The first two genes induce the expression of *MPL* and *GP6* along megakaryopoiesis, were found overexpressed in our study after eltrombopag treatment. Furthermore, *GP1BA, PF4, ITGA2B, MYL9, HIST1H4H* and *HIST1H2BH*, genes regulated by *RUNX1* were also significantly enriched by the treatment (FDR = 3.85E-9) Thus, these findings point that the platelet increment could be due to a crucial change in megakaryopoiesis-related genes.

Identification of differentially expressed genes and enriched pathways in responder patients

Interestingly, GSEA analysis showed that the top 5 hallmark gene sets (Normalize Enrichment Score, NES) correlating with eltrombopag treatment in responder patients were TNFα signaling via Nf kB (NES = 2.66), interferon gamma response (IFN-γ) (NES = 2.35), coagulation (NES = 2.33), apoptosis (NES = 2.23) and IL2-STAT5 signaling (NES = 2.21), all gene sets showing a FDR q-value < 0.00001 (Table 4). Of note, TNFα and IFN-γ are deregulated in aplastic anemia and its regulation by eltrombopag have been proposed as one of the mechanism to improve hematopoiesis, standing out the upregulation genes such as *KLF4*, *HES1, EGR1* among others.[46], which also play an important role in hematopoiesis. Moreover, *IFN-γ, IFN-α* and *IL2-STAT5*, are involved in the innate and adaptive immune response, which is altered in ITP patients and could be inducing a reduction in platelet counts.[47].

Table 4. Gene sets enriched in responder patients.

GS follow link to MSigDB	SIZE	ES	NES	NOM p-val	FDR q-val	FWER p-val	RANK AT MAX	LEADING EDGE
TNFA SIGNALING VIA NFKB	198	0.64	2.66	<0.001	<0.001	<0.001	2608	tags=47%, list=12%, signal=53%
INTERFERON GAMMA RESPONSE	195	0.57	2.35	<0.001	<0.001	<0.001	4030	tags=48%, list=19%, signal=58%
COAGULATION	132	0.59	2.33	<0.001	<0.001	<0.001	2549	tags=30%, list=12%, signal=33%
APOPTOSIS	159	0.56	2.23	<0.001	<0.001	<0.001	3840	tags=44%, list=18%, signal=53%
IL2 STAT5 SIGNALING	194	0.54	2.21	<0.001	<0.001	<0.001	2873	tags=38%, list=13%, signal=43%
UV RESPONSE DN	140	0.55	2.16	<0.001	<0.001	<0.001	2086	tags=26%, list=10%, signal=29%
ALLOGRAFT REJECTION	190	0.53	2.14	<0.001	<0.001	<0.001	3523	tags=41%, list=16%, signal=49%
EPITHELIAL MESENCHYMAL TRANSITION	198	0.52	2.14	<0.001	<0.001	<0.001	1633	tags=22%, list=8%, signal=23%
INTERFERON ALPHA RESPONSE	96	0.54	2.03	<0.001	<0.001	<0.001	4707	tags=49%, list=22%, signal=62%
COMPLEMENT	194	0.48	2.00	<0.001	<0.001	0.001	2553	tags=28%, list=12%, signal=31%
INFLAMMATORY RESPONSE	199	0.48	1.98	<0.001	<0.001	0.002	2567	tags=33%, list=12%, signal=37%
IL6 JAK STAT3 SIGNALING	83	0.51	1.87	<0.001	<0.001	0.004	2553	tags=31%, list=12%, signal=35%
KRAS SIGNALING UP	193	0.45	1.86	<0.001	0.001	0.005	2542	tags=26%, list=12%, signal=29%
APICAL JUNCTION	194	0.45	1.84	<0.001	0.001	0.009	2858	tags=24%, list=13%, signal=27%
P53 PATHWAY	193	0.44	1.81	<0.001	0.001	0.011	3049	tags=26%, list=14%, signal=30%
HYPOXIA	197	0.42	1.76	<0.001	0.002	0.020	4181	tags=35%, list=19%, signal=42%

ITP patients who did not respond to eltrombopag are characterized by a specific genetic signature

In our study, 4 out of 14 patients (IDs: 02, 04, 07 and 09) did not show a platelet increase at day 28 (Table 2). To find which pathway could be deregulated in these patients, their gene expression profile was explored.

First, we compared responders *vs.* non-responders (10 and 4 patients respectively) before the treatment, hoping to find a genetic signature that could allow us to identify patients who may not benefit from eltrombopag. However, we failed to demonstrate any significantly deregulated gene in this analysis, suggesting other genetic biomarkers of treatment failure.

In a second step, a comparison between samples during eltrombopag administration (responders *vs.* non-responders) was carried out. Twenty-one genes were significantly overexpressed in non-responder patients (supplementary Table 3). Interestingly all these 21 differentially expressed genes were either involved in erythropoiesis or *GATA-1* target genes (*ALAS2*, *SLC4A1*, *HBD*, *GYPA*, *EPB42*, *BCL2L1*, *IFIT1B*, *AHSP*, *SELENBP1*, *SLC14A1*, *FECH*, *TRIM58*, *DCAF12*, *FAM46C*, *SLC25A39*, *MARCH8*, *BPGM*, *TMOD1*, *PLEK2*, *NPRL3* and *CA1*).

BCL2L1 gene, also named *Bcl-X*, belongs to the BCL2 family, which can act as an anti or pro apoptotic regulator. B*cl-X* plays an important role in mega and erythropoiesis. Its expression prevents ineffective erythropoiesis controlling apoptosis in late-stage, and is strongly expressed during late differentiation of erythroblast, reaching the maximum transcript level at hemoglobin synthesis. A previous study has showed that conditional *Bcl-X* knock-out mice develop severe anemia.[48] However, its expression is absent during

late megakaryopoiesis [49], because *Bcl-X* expression inhibits proplatelet formation. Moreover, chromatin immunoprecipitation assays have demonstrated that *GATA-1* binds *Bcl-X* promoter [50] and the transcript levels of *GATA-1* correlated with *Bcl-X*, inducing its expression. We hypothesize that the regulation between *GATA-1* and *Bcl-X* is altered in non-responder patients, since an increment in the hemoglobin levels but not in platelet counts was observed (Figure 2).

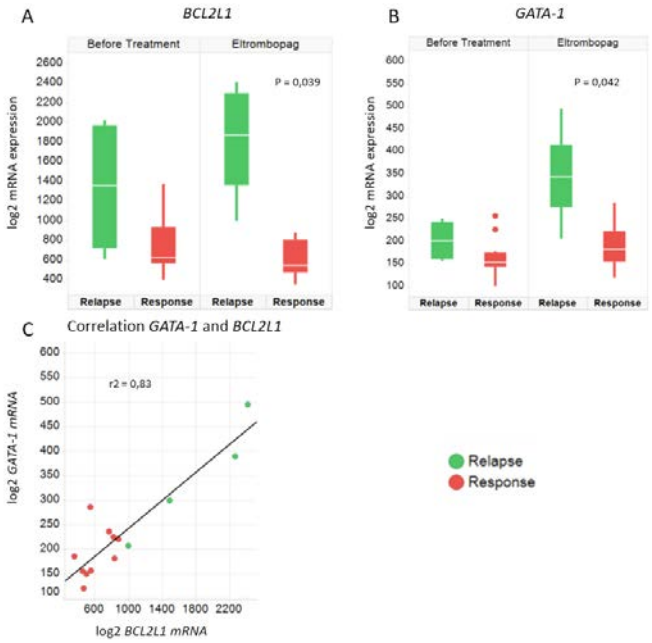

Figure 2. Expression levels of *GATA-1* and *BCL2L1* before and after eltrombopag treatment in ITP patients. A. *Before eltrombopag treatment, BCL2L1* did not show any statistically significant difference between relapse patients and responders. On the other hand, after treatment *BCL2L1 was overexpressed in* relapsed ITP patients compared to responders (P = 0.039). B. *GATA-1* showed the same pattern as *BCL2L1* (P = 0.042). The thick line inside the box plot indicates the median expression levels and the box shows the 25th and 75th percentiles, while the whiskers show the maximum and minimum values. Outliers (extreme values falling out of the main distribution) are represented by circles. Statistical significance was determined using the Bayesian Linear Model (P<0.05). Values are shown on a logarithmic scale. C. A high positive correlation (r^2 = 0.83) between *GATA-1* and *BCL2L1 expression levels was found.* Interestingly this correlation was stronger in relapse ITP patients (r^2 = 0.92).

Furthermore, a deregulation in some genes involved in erythropoiesis, such as *ALAS2*, *HBD*, *EPB42*, *BCL2L1*, *SELENBP1*, *SLC14A1*, *FECH*, *TRIM58*, *FAM46C*, *MARCH8*, *BPGM*, *TMOD1*, and *CA1,* has been recently described after the therapy with recombinant human erythropoietin[51]*. SLC4A1* encodes an anion exchanger family

member expressed in the erythrocyte plasma membrane and strongly induced during erythroid maturation, being reported that chromatin around the promoter and 3´ end of *SLC4A1* is only available during erythroid differentiation.[52] *SLC25A39*, a member of the *SLC25* transporter or mitochondrial carrier family of proteins, is required for normal heme biosynthesis and may play a role in iron homeostasis.[53] These results are in line with the GEP obtained in our study, suggesting that in non-responder patients the erythropoiesis could be highly up-regulated. Moreover, our results indicate that several genes involved in the heme pathway were activated (ES = 0.79, NES = 3.56 and FDR q-value < 0.0001) in non-responder patients (supplementary Figure 1).

In addition, the present study spotlights *GATA1* and *KLF1* (also known as Erythroid-Specific Transcription Factor) as genes altered by eltrombopag therapy. *KLF1* has been described as a critical gene working as a transcription factor to open the chromatin and facilitate the recruitment of *GATA1* .[54]. Moreover, TNFα signaling via NFKβ (ES = -0.57, NES = -2.61 and FDR q-value < 0.0001), inflammatory response (ES = -0.43, NES = -1.96 and FDR q-value < 0.0001) and IL6-JAK-STAT3 signaling (ES = -0.44, NES = -1.72 and FDR q-value =0.006) were enriched in responder patients, suggesting the importance of these pathways in the restoration of normal megakaryopoiesis in ITP patients.

Finally, our analysis also showed enrichment in the metabolism and reactive oxygen species (ROS) gene set (ES = 0.51, NES = 1.84 and FDR q-value = 0.003), supplementary Figure 1. Interestingly, Kao *et al*. demonstrated that eltrombopag not only targets the thrombopoietin receptor, but also works as iron chelator[55], and through this intracellular iron chelating action eltrombopag could stimulate multilineage hematopoiesis.[56] According to our data, when eltrombopag does not work, the lack of

quelation would lead to iron overload, and consequently the high levels of intracellular iron would lead to an increase of oxidative stress.[57,58] In addition, increased reactive oxygen species (ROS) may result in accumulation of DNA damage and unscheduled activation of senescence mechanisms in the stem cell compartment, and it is becoming increasingly clear that deregulated accumulation of ROS in hematopoietic stem cells leads to abnormal hematopoiesis.[59–61] Thus, the tight regulation of oxidative stress in hematopoietic stem cells is essential for the control of homeostasis in hematopoietic tissues, and is achieved in patients responding to eltrombopag.

In summary, our results showed an overexpression in genes involved in megakaryopoiesis, platelet adhesion, degranulation and aggregation in patients treated with eltrombopag. Moreover, an important role regarding heme metabolism and oxidative stress is suggested, although this finding should be confirmed in a larger cohort of patients. These results open new avenues in the knowledge of eltrombopag mechanism of action and should be confirmed in larger series of patients

Acknowledgments

This work was partially supported by grants from the Spanish Fondo de Investigaciones Sanitarias PI17/01966 Instituto de Salud Carlos III (ISCIII), European Regional Development Fund (ERDF) “Una manera de hacer Europa”, “Proyectos de Investigación del SACYL” GRS1873/A18 and IBY17/00006.

JMHS and AERV are supported by a research grant by FEHH (“Fundación Española de Hematología y Hemoterapia”).

We thank Sara González, Irene Rodríguez, Teresa Prieto, Mª Ángeles Ramos, Mª Almudena Martín, Ana Díaz, Ana Simón, María del Pozo, Isabel M Isidro, Vanesa Gutiérrez, Sandra Pujante, Sandra Santos and Cristina Miguel from the Cancer Research Center of Salamanca, Spain, for their technical support.

Authorship Contributions

JMHS and JMBB designed the experiment, interpreted the results and wrote the manuscript; DAL performed bioinformatic analysis; RB contributed to the interpretation of the results; JRGP and JMHR performed patient selection, contributed to the interpretation of the results and provided clinical data; AERV contributed to the interpretation of the results and wrote the manuscript. All authors revised the manuscript.

Conflict-of-interest disclosure

The authors declare no competing financial interests.

References

1. Cines, D. B., Bussel, J. B., Liebman, H. A. & Luning Prak, E. T. The ITP syndrome: pathogenic and clinical diversity. *Blood* **113**, 6511–6521 (2009).
2. Toltl, L. J. & Arnold, D. M. Pathophysiology and management of chronic immune thrombocytopenia: focusing on what matters: Annotation. *British Journal of Haematology* **152**, 52–60 (2011).
3. Ogawara, H. *et al.* High Th1/Th2 ratio in patients with chronic idiopathic thrombocytopenic purpura. *Eur. J. Haematol.* **71**, 283–288 (2003).
4. Schifferli, A. & Kühne, T. Thrombopoietin receptor agonists: a new immune modulatory strategy in immune thrombocytopenia? *Seminars in Hematology* **53**, S31–S34 (2016).
5. Provan, D. & Newland, A. C. Current Management of Primary Immune Thrombocytopenia. *Adv Ther* **32**, 875–887 (2015).
6. Ghanima, W., Cooper, N., Rodeghiero, F., Godeau, B. & Bussel, J. B. Thrombopoietin receptor agonists: Ten Years Later. *Haematologica* haematol.2018.212845 (2019). doi:10.3324/haematol.2018.212845
7. de Groot, R. P., Raaijmakers, J. A. M., Lammers, J.-W. J. & Koenderman, L. STAT5-Dependent CyclinD1 and Bcl-xL Expression in Bcr-Abl-Transformed Cells. *Molecular Cell Biology Research Communications* **3**, 299–305 (2000).
8. González-Porras, J. R. *et al.* Use of eltrombopag after romiplostim in primary immune thrombocytopenia. *British Journal of Haematology* **169**, 111–116 (2015).
9. Stasi, R., Evangelista, M. L. & Amadori, S. Novel thrombopoietic agents: a review of their use in idiopathic thrombocytopenic purpura. *Drugs* **68**, 901–912 (2008).
10. Gonzalez-Porras, J. R. & Bastida, J. M. Eltrombopag in immune thrombocytopenia: efficacy review and update on drug safety. *Therapeutic Advances in Drug Safety* **9**, 263–285 (2018).

11. Basciano, P. A. & Bussel, J. B. Thrombopoietin-receptor agonists: *Current Opinion in Hematology* **19**, 392–398 (2012).
12. Jenkins, J. M. *et al.* Phase 1 clinical study of eltrombopag, an oral, nonpeptide thrombopoietin receptor agonist. *Blood* **109**, 4739–4741 (2007).
13. Nguyen, T.-T. L., Palmaro, A., Montastruc, F., Lapeyre-Mestre, M. & Moulis, G. Signal for Thrombosis with Eltrombopag and Romiplostim: A Disproportionality Analysis of Spontaneous Reports Within VigiBase®. *Drug Safety* **38**, 1179–1186 (2015).
14. Gill, H., Leung, G. M. K., Lopes, D. & Kwong, Y.-L. The thrombopoietin mimetics eltrombopag and romiplostim in the treatment of refractory aplastic anaemia. *British Journal of Haematology* **176**, 991–994 (2017).
15. Platzbecker, U. *et al.* Safety and tolerability of eltrombopag versus placebo for treatment of thrombocytopenia in patients with advanced myelodysplastic syndromes or acute myeloid leukaemia: a multicentre, randomised, placebo-controlled, double-blind, phase 1/2 trial. *The Lancet Haematology* **2**, e417–e426 (2015).
16. Di Buduo, C. A. *et al.* Revealing eltrombopags promotion of human megakaryopoiesis through AKT/ERK-dependent pathway activation. *Haematologica* **101**, 1479–1488 (2016).
17. Mitchell, W. B. *et al.* Effect of thrombopoietin receptor agonists on the apoptotic profile of platelets in patients with chronic immune thrombocytopenia: Effect of Eltrombopag on Platelet Apoptosis. *American Journal of Hematology* **89**, E228–E234 (2014).
18. Chiou, T.-J. *et al.* Eltrombopag enhances platelet adhesion by upregulating the expression of glycoprotein VI in patients with chronic immune thrombocytopenic purpura. *Translational Research* **166**, 750-761.e4 (2015).
19. Bal, G. *et al.* Identification of novel biomarkers in chronic immune thrombocytopenia (ITP) by microarray-based serum protein profiling. *British Journal of Haematology* **172**, 602–615 (2016).

20. Bay, A. *et al.* Plasma microRNA profiling of pediatric patients with immune thrombocytopenic purpura: *Blood Coagulation & Fibrinolysis* **25**, 379–383 (2014).
21. Deng, G. *et al.* MicroRNA profiling of platelets from immune thrombocytopenia and target gene prediction. *Molecular Medicine Reports* **16**, 2835–2843 (2017).
22. Jernas, M. *et al.* Differences in gene expression and cytokine levels between newly diagnosed and chronic pediatric ITP. *Blood* **122**, 1789–1792 (2013).
23. Sehgal, K. *et al.* Plasmacytoid Dendritic Cells, Interferon Signaling, and FcγR Contribute to Pathogenesis and Therapeutic Response in Childhood Immune Thrombocytopenia. *Science Translational Medicine* **5**, 193ra89-193ra89 (2013).
24. Sood, R., Wong, W., Gotlib, J., Jeng, M. & Zehnder, J. L. Gene expression and pathway analysis of immune thrombocytopenic purpura. *Br. J. Haematol.* **140**, 99–103 (2008).
25. Sood, R., Wong, W., Jeng, M. & Zehnder, J. L. Gene expression profile of idiopathic thrombocytopenic purpura (ITP). *Pediatr Blood Cancer* **47**, 675–677 (2006).
26. Ye, Q., Jiang, H., Liao, X., Chen, K. & Li, S. Identification and Validation of Gene Expression Pattern and Signature in Patients with Immune Thrombocytopenia. *SLAS DISCOVERY: Advancing Life Sciences R&D* **22**, 187–195 (2017).
27. Zhao, H. *et al.* Reduced *MIR130A* is involved in primary immune thrombocytopenia via targeting *TGFB1* and *IL18*. *British Journal of Haematology* **166**, 767–773 (2014).
28. Rodeghiero, F. *et al.* Standardization of bleeding assessment in immune thrombocytopenia: report from the International Working Group. *Blood* **121**, 2596–2606 (2013).
29. Rodeghiero, F. *et al.* Standardization of terminology, definitions and outcome criteria in immune thrombocytopenic purpura of adults and children: report from an international working group. *Blood* **113**, 2386–2393 (2009).

30. Bolstad, B. M., Irizarry, R. A., Astrand, M. & Speed, T. P. A comparison of normalization methods for high density oligonucleotide array data based on variance and bias. *Bioinformatics* **19**, 185–193 (2003).

31. Irizarry, R. A. *et al.* Summaries of Affymetrix GeneChip probe level data. *Nucleic Acids Res.* **31**, e15 (2003).

32. Irizarry, R. A. *et al.* Exploration, normalization, and summaries of high density oligonucleotide array probe level data. *Biostatistics* **4**, 249–264 (2003).

33. Tusher, V. G., Tibshirani, R. & Chu, G. Significance analysis of microarrays applied to the ionizing radiation response. *Proc. Natl. Acad. Sci. U.S.A.* **98**, 5116–5121 (2001).

34. Benjamini, Y. & Hochberg, Y. Controlling the False Discovery Rate: A Practical and Powerful Approach to Multiple Testing. *Journal of the Royal Statistical Society: Series B (Methodological)* **57**, 289–300 (1995).

35. *Bioinformatics and Computational Biology Solutions Using R and Bioconductor*. (Springer New York, 2005). doi:10.1007/0-387-29362-0

36. Huang, D. W., Sherman, B. T. & Lempicki, R. A. Systematic and integrative analysis of large gene lists using DAVID bioinformatics resources. *Nature Protocols* **4**, 44–57 (2009).

37. Carmona-Saez, P., Chagoyen, M., Tirado, F., Carazo, J. M. & Pascual-Montano, A. GENECODIS: a web-based tool for finding significant concurrent annotations in gene lists. *Genome Biol.* **8**, R3 (2007).

38. Liberzon, A. *et al.* The Molecular Signatures Database Hallmark Gene Set Collection. *Cell Systems* **1**, 417–425 (2015).

39. Subramanian, A. *et al.* Gene set enrichment analysis: A knowledge-based approach for interpreting genome-wide expression profiles. *Proceedings of the National Academy of Sciences* **102**, 15545–15550 (2005).

40. Fabregat, A. *et al.* The Reactome Pathway Knowledgebase. *Nucleic Acids Res.* **46**, D649–D655 (2018).

41. Choy, C. T., Wong, C. H. & Chan, S. L. Embedding of Genes Using Cancer Gene Expression Data: Biological Relevance and Potential Application on Biomarker Discovery. *Front. Genet.* **9**, 682 (2019).

42. Liu, Q. *et al.* Monocyte to macrophage differentiation-associated (MMD) positively regulates ERK and Akt activation and TNF-α and NO production in macrophages. *Mol Biol Rep* **39**, 5643–5650 (2012).

43. Raslova, H., Vainchenker, W. & Plo, I. Eltrombopag, a potent stimulator of megakaryopoiesis. *Haematologica* **101**, 1443–1445 (2016).

44. Xavier-Ferrucio, J. & Krause, D. S. Concise Review: Bipotent Megakaryocytic-Erythroid Progenitors: Concepts and Controversies: MEP: Concepts and Controversies. *Stem Cells* **36**, 1138–1145 (2018).

45. Guo, T. *et al.* Megakaryopoiesis and platelet production: insight into hematopoietic stem cell proliferation and differentiation. *Stem Cell Investig* **2**, 3 (2015).

46. Scheinberg, P. Activity of eltrombopag in severe aplastic anemia. *Blood Adv* **2**, 3054–3062 (2018).

47. Lazarus, A. H., Semple, J. W. & Cines, D. B. Innate and Adaptive Immunity in Immune Thrombocytopenia. *Seminars in Hematology* **50**, S68–S70 (2013).

48. Rhodes, M. M. Bcl-xL prevents apoptosis of late-stage erythroblasts but does not mediate the antiapoptotic effect of erythropoietin. *Blood* **106**, 1857–1863 (2005).

49. Kaluzhny, Y. *et al.* BclxL overexpression in megakaryocytes leads to impaired platelet fragmentation. *Blood* **100**, 1670–1678 (2002).

50. Kuo, Y.-Y. & Chang, Z.-F. GATA-1 and Gfi-1B interplay to regulate Bcl-xL transcription. *Mol. Cell. Biol.* **27**, 4261–4272 (2007).

51. Durussel, J. *et al.* Blood transcriptional signature of recombinant human erythropoietin administration and implications for antidoping strategies. *Physiological Genomics* **48**, 202–209 (2016).

52. NIH Intramural Sequencing Center *et al.* Establishment of regulatory elements during erythro-megakaryopoiesis identifies hematopoietic lineage-commitment points. *Epigenetics & Chromatin* **11**, 22 (2018).
53. Nilsson, R. *et al.* Discovery of Genes Essential for Heme Biosynthesis through Large-Scale Gene Expression Analysis. *Cell Metabolism* **10**, 119–130 (2009).
54. Kevin R. Gillinder *et al.* KLF1 Acts As a Pioneer Transcription Factor to Open Chromatin and Facilitate Recruitment of GATA1. *Blood* **132**, 501 (2018).
55. Kao, Y.-R. *et al.* Thrombopoietin receptor–independent stimulation of hematopoietic stem cells by eltrombopag. *Sci. Transl. Med.* **10**, eaas9563 (2018).
56. Vlachodimitropoulou, E. *et al.* Eltrombopag: a powerful chelator of cellular or extracellular iron(III) alone or combined with a second chelator. *Blood* **130**, 1923–1933 (2017).
57. Dixon, S. J. & Stockwell, B. R. The role of iron and reactive oxygen species in cell death. *Nature Chemical Biology* **10**, 9–17 (2014).
58. Murillo-Ortiz, B. *et al.* Impact of Oxidative Stress in Premature Aging and Iron Overload in Hemodialysis Patients. *Oxidative Medicine and Cellular Longevity* **2016**, 1–8 (2016).
59. Miyamoto, K. *et al.* Foxo3a Is Essential for Maintenance of the Hematopoietic Stem Cell Pool. *Cell Stem Cell* **1**, 101–112 (2007).
60. Tothova, Z. *et al.* FoxOs Are Critical Mediators of Hematopoietic Stem Cell Resistance to Physiologic Oxidative Stress. *Cell* **128**, 325–339 (2007).
61. Yalcin, S. *et al.* Foxo3 Is Essential for the Regulation of Ataxia Telangiectasia Mutated and Oxidative Stress-mediated Homeostasis of Hematopoietic Stem Cells. *Journal of Biological Chemistry* **283**, 25692–25705 (2008).

Chapter 2: *Genome-wide transcriptomics leads to the identification of deregulated genes after deferasirox therapy in low-risk MDS patients*

Jesús María Hernández Sánchez[1], Eva Lumbreras[1], María Díez-Campelo[2], María Abáigar[1,] Mónica del Rey[1], Ana África Martín[2], Raquel de Paz[3], Sonia Erkiaga[4], Beatriz Arrizabalaga[3], Jesús María Hernández-Rivas[1,2*] Ana Eugenia Rodríguez Vicente[1*]

Affiliations

1 IBSAL. IBMCC. CIC Universidad de Salamanca-CSIC, Spain

2 Servicio de Hematología. Hospital Universitario. Salamanca, Spain

3 Servicio de Hematología. Hospital Universitario La Paz. Madrid, Spain.

4 Servicio de Hematología. Hospital Universitario de Cruces. Barakaldo, Vizcaya, Spain

* Shared authorship

Correspondence

Ana E Rodríguez Vicente

IBMCC, CIC Universidad de Salamanca-CSIC, Hospital Universitario de Salamanca

Campus Miguel de Unamuno

37007 Salamanca

Spain

Running title

Gene expression profile changes induced by deferasirox in MDS patients

Scientific category: Original Article

Text word count (without references): 3150

Abstract word count: 237

Figures: 3

Tables: 3

Reference count: 30

Abstract

The iron chelator deferasirox is widely used in patients with iron overload. Patients with low-grade myelodysplastic syndromes (MDS) get transfusion dependency and need to be treated with deferasirox to avoid iron overload. Moreover, in some patients an increase in both erythroid and platelets have been observed after deferasirox therapy. However, the mechanisms involved in these clinical findings are poorly understood. The aim of this work was to analyze, in patients treated with deferasirox, the changes in the gene expression profile after receiving the treatment. A total of fifteen patients with the diagnosis of low-grade MDS were studied. Microarrays were carried out in RNA from peripheral blood before and after 14 weeks of deferasirox therapy. Changes in 1,457 genes and 54 miRNAs were observed: deferasirox induced the downregulation of genes related to the Nf kB pathway leading of an overall inactivation of this pathway. In addition, the iron chelator also downregulated gamma interferon. Altogether these changes could be related to the improvement of erythroid response observed in these patients after therapy. Moreover, the inhibition of NFE2L2/ NRF2, which was predicted

in silico, could be playing a critical role in the reduction of reactive oxygen species (ROS). Of note, miR-125b, overexpressed after deferasirox treatment, could be involved in the reduced inflammation and increased hematopoiesis observed in the patients after treatment. In summary this study shows, for the first time, the mechanisms that could be governing deferasirox impact *in vivo*.

Introduction

Myelodysplastic syndromes (MDS) are a heterogeneous group of clonal stem cell disorders, usually characterized by the presence of anemia. Red blood cell transfusion is the only therapeutic option for most patients, who usually develop transfusion dependence, which can be correlated with poorer outcomes partially caused by transfusional iron overload. The magnitude of total body iron load correlated with hepatic iron concentration (HIC)[1]. Thresholds of HIC predict the development of potentially fatal complications[2]: HIC exceeding 15 mg iron/gram liver, dry weight, and sustained elevations of serum ferritin (SF) over 2500 µg/L, increase the risk of premature death. Deferoxamine has been the standard drug for iron chelation therapy over the past four decades. However, the major disadvantage is the patient's lack of adherence, because it needs an 8- to 12-hr parenteral administration since it has a short half-life and a very poor oral bioavailability[1–4]. Therefore, in the 1980s, the parenteral requirement for deferoxamine stimulated studies of orally active chelators. Deferasirox was licensed as first line therapy by the FDA in 2005, following randomized trials comparing this drug, and demonstrating its non-inferiority, to deferoxamine[5]. The safety profile is acceptable, the drug is well tolerated and effective even in long term follow up[6]. Deferasirox is widely used in low-risk MDS[1] and also in high-risk MDS[7].

Changes in the gene expression profile (GEP) of MDS have been described[8], being different between low risk and high risk MDS patient groups. Thus, patients with refractory anemia with ring sideroblasts (RARS) showed an overexpression of mitochondrial and iron homeostasis genes[9]. Moreover, iron overload could selectively affect peripheral T lymphocytes and induce an impaired cellular immunity by increasing

ROS level[10]. The application of system-wide "omics" technologies could provide new insights into the knowledge of pathogenic mechanisms involved after deferasirox therapy. In fact, several in vitro studies analyzed the effects of deferasirox in the blood cells, identifying pathways or cellular mechanisms such as Nf kB[11], MTOR[12] or ROS[10] as the most frequently involved during this treatment. However, only few *in vivo* studies have been performed to assess the main cellular mechanisms affected by deferasirox therapy in MDS patients[1].

In this work, we aimed to perform an *in vivo* pharmacogenomic analysis in patients diagnosed as low-risk MDS treated with deferasirox, in order to identify the changes in the GEP induced by the treatment in these patients.

Patients and methods

Patients

Fifteen patients diagnosed as low-risk MDS and treated with deferasirox were included in the study. All patients have the diagnosis of low-risk MDS according to WHO 2008 classification[13]. Blood samples were analyzed before deferasirox and 14 weeks after treatment (range 6-40 weeks). All patients received the treatment without additional drugs during the study. The median age was 77 years (range 62-90 years), and 36% patients were male. This study was performed in accordance with the Declaration of Helsinki guidelines, and approved by the Local Ethical Committees "Comité Ético de Investigación Clínica, Hospital Universitario de Salamanca". All patients provided written informed consent.

Methods

PBMCs and RNA isolation

Peripheral blood mononuclear cells (PBMCs) were isolated from whole peripheral blood using Ficoll gradient, snap-frozen and stored at -80ºC. Total RNA was extracted by QIAgen (Qiagen, Valencia, CA, USA), following the manufacturer's recommendations. RNA integrity was assessed on an Agilent 2100 Bioanalyzer (Agilent technologies, Santa Clara, CA, USA) employing a RNA 6000 Nano Assay kit. All RNA samples had an A260/A280 ratio ~1.8 and RNA integrity number (RIN) ≥8.0.

Gene expression profiling

Genome-wide expression analysis of the paired samples (before and after the treatment) was performed using Human Transcriptome Array 2.0 ST (Affymetrix, Inc., Santa Clara, CA, USA) following the manufacturer's protocols for the GeneChip platform by Affymetrix. Briefly, cDNA was regenerated through a random-primed reverse transcription (RT) using a dNTP mix containing dUTP. After cDNA was hybridized to the arrays at 60 rpm for 18h at 45°C, the chips were processed in a Genechip Fluidics Station 450 (Affymetrix). Microarray images were collected by Affymetrix GeneChip 3 000 scanner, and data were extracted using Affymetrix GCOS Software.

Bioinformatic analysis: normalization, signal calculation and significant differential expression

The Robust Microarray Analysis (RMA) algorithm was used for background correction, intra- and inter-microarray normalization, and expression signal calculation[14]. The absolute expression signal for each gene was calculated for each microarray. Differential gene expression before and after treatment were obtained using the MultiExperiment Viewer 4 (MeV4, TM4 software suite), using the Student's paired t-test for matched samples to analyze the statistical significance. $P<0.05$ was considered statistically significant.

Functional analysis and gene annotation

The functional assignment of the genes included in the expression signature of MDS patients was carried out by the Database for Annotation, Visualization and Integrated Discovery (DAVID)[15,16] and the GeneCodis application[17] which identifies concurrent annotations in GO and KEGG, and thereby constructs several groups of genes of functional significance. The most significant biological mechanisms, pathways and functional categories in the data sets of genes selected by statistical analysis were identified through the use of Ingenuity Pathways Analysis (Ingenuity Systems Inc., Redwood City, CA, USA).

Upstream regulator analysis

The goal of this analysis is to identify the cascade of upstream transcriptional regulators that can explain the observed gene expression changes in a dataset. This analysis is based on prior knowledge of expected effects between transcriptional regulators and their target genes stored in the Ingenuity® Knowledge Base. The analysis examines how many known targets of each transcription regulator are present in the analyzed dataset, and also compares their direction of change to what is expected from the literature in order to predict likely relevant transcriptional regulators. If the observed direction of change is mostly consistent with a particular activation state of the transcriptional regulator ("activated" or "inhibited"), then a prediction is made about that activation state.

Integrative analysis of miRNA and gene expression profile.

MiRNAs with significantly different expression ($P<0.05$) before and after treatment were further analyzed to identify the networks and pathway targets. For this purpose, IPA's microRNA Target Filter, which enables prioritization of experimentally validated and predicted mRNAtargets from TargetScan Knowledge Base was used. This tool identified the putative targets for the input miRNAs and then developed the networks among the targets and identified the known and most relevant biological functions, pathways and annotations in this enriched set of target genes. By applying the expression pairing tool, the analysis was focused on targets exhibiting altered expression in our analysis, finding miRNAs and their target genes with opposite or same expression.

Droplet digital PCR

First-stranded cDNA was synthesized from 500 ng total RNA using SuperScript III First-Strand Synthesis SuperMix assay (Invitrogen) according to manufacturer's instruction. Transcript expression for selected genes were quantified in MDS patients before and after treatment using QX200 ddPCR (Bio-Rad, Hercules, CA, USA). Primers are listed in supplementary Table 1. ddPCR mix were prepared containing 10 µL of 2X QX200 ddPCR EvaGreen Supermix (Bio-Rad, cat. no. 1864034), 8 µL of nuclease-free water, 1 µL of primers 20x and 1 µL of diluted cDNA. A 20µL aliquot was taken from each of the assembled ddPCR mixtures and pipetted into each sample well of an eight-channel disposable droplet generator cartridge (Bio-Rad, Hercules, CA, USA). A 70µL volume of Droplet Generation Oil for EvaGreen (Bio-Rad) was then loaded into each of the eight oil wells. The cartridge was placed into the QX200 droplet generator (Bio-Rad) where a vacuum was applied to the outlet wells to simultaneously partition each 20µL sample into nanoliter sized droplets. After∼1.5 min, the cartridge was removed from the generator, and the droplets that had collected in each of the independent outlet wells were transferred with a multichannel pipet to a 96-well polypropylene plate (Eppendorf, Hamburg, Germany). The plate was heat-sealed with foil using a PX1 PCR Plate Sealer (Bio-Rad) and placed in a conventional thermal cycler (C1000 Touch, Bio-Rad), where an endpoint PCR run was performed with the following program: an activation period (95 °C for 10 minutes), followed by 40 cycles of a two-step thermal profile comprising of a denaturation step (95 °C for 30 seconds), and a combined annealing-extension step (60 °C for 1 minute). A final signal stabilization step was also included (90 °C for 10 minutes) and then cooling to 4 °C. After PCR, the 96-well plate was loaded into the

QX200 Droplet Reader (Bio-Rad), and the appropriate assay information was entered into the analysis software package provided (Quanta-Soft, Bio-Rad). Droplets were automatically aspirated from each well and streamed single-file past a two-color fluorescence detector and finally to waste. The quality of all droplets was analyzed and rare outliers (e.g., doublets, triplets) were gated based on detector peak width. Analysis of the ddPCR data was performed with QuantaSoft analysis software (Bio-Rad) that accompanied the QX200 Droplet Reader. Expression levels of the selected genes before and after treatment were analyzed using the Mann-Whitney U test with a two tailed value of P=0.05 for statistical significance. All tests were performed using SPSS v19.0.

Results and Discussion

GEP was carried out in paired samples before deferasirox and during the treatment. The analysis revealed changes in 1,457 genes (709 overexpressed after the therapy), and 54 miRNAs (thirty-three of them, overexpressed) (supplementary Table 2 and 3). Table 1 shows the top-ten deregulated genes after deferasirox therapy. Of note, several genes from the Nuclear factor-κappa B, Nf kB pathway (NFBIA), and immune system (*IFNG*, *CX3CR1*) as well as miRNAs (miR-2682, miR-147b) were deregulated. Moreover, the functional analysis of the most relevant pathways affected showed an overall downregulation of Nf kB pathway, as well as NO & ROS and hypoxia-related genes (Table 2).

Table 1. Top-ten deregulated genes after deferasirox therapy in low-risk MDS patients

Overexpressed		
Gene ID	**Gene Title**	**Diff exp**
CX3CR1	chemokine (C-X3-C motif) receptor 1	0.5001405
SRRM5	serine/arginine repetitive matrix 5	0.4905514
miR-2682	MicroRNA 2682	0.4834731
OR10J3	olfactory receptor, family 10, subfamily J, member 3	0.432497
OR52B6	Olfactory Receptor Family 52 Subfamily B Member 6	0.4171242
HCG24	HLA Complex Group 24	0.3994102
OR1F2P	olfactory receptor, family 1, subfamily F, member 2, pseudogene	0.3919816
RNU6-64P	RNA, U6 Small Nuclear 64, Pseudogene	0.380795
KPRP	Keratinocyte Proline Rich Protein	0.3738589
OR3A1	Olfactory Receptor Family 3 Subfamily A Member 1	0.3568774
Underexpressed		
Gene ID	**Gene Title**	**Diff exp**
miR-147b	MicroRNA 147b	-1.0768079
DDIT3	DNA Damage Inducible Transcript 3	-1.0100787
IFNG	Interferon Gamma	-0.991313
CD69	CD69 Molecule	-0.967943
CCL3L3	C-C Motif Chemokine Ligand 3 Like 3	-0.8482828
NFKBIA	NFKB Inhibitor Alpha	-0.809967
IL1B	Interleukin 1 Beta	-0.788842
GPR183	G Protein-Coupled Receptor 183	-0.78225
MAPK6	Mitogen-Activated Protein Kinase 6	-0.7801395
HIF1A	Hypoxia Inducible Factor 1 Subunit Alpha	-0.7389716

Diff exp: differential gene expression before and after treatment. The positive sign means overexpressed after treatment and the negative sign, underexpressed.

Table 2. Most relevant altered pathways after deferasirox treatment in low-risk MDS patients

Pathway	P-value	Z-score
NF-κB	0.02	-1.5
NO & ROS	0.01	-1.4
RIG1-like	0.00004	-1.9
NRF2	0.03	-2.6
Hypoxia	0.0003	NC
iNOS	0.03	-2.4
Interferon	0.01	-2.2

Deferasirox treatment downregulated NF kB pathway in low-risk MDS patients

Deferasirox therapy induced an overall downregulation in several genes involved in Nf kB pathway (Table 2). These results now detected in patients confirmed previous *in vitro* observations, in which deferasirox was associated to repression of Nf kB activity in samples showing high basal activity as well as in cell lines, whereas no similar behavior was observed with other iron chelators. This observation has been linked to the hemoglobin improvement showed in some patients treated with this iron chelator[18–20]. Moreover, our results pointed out the genes which could be involved in this downregulation, such as *BCL10*, *IL1B*, *NFKBIA*, *RIPK1*, *RELA*, *BID*, *BIRC2*, and *TANK* (Table 3). The interactions among these genes leading to an overall downregulation of the whole Nf kB pathway is showed in Figure 1. Expression changes in *BIRC2*, *TRAF6*, *BID*, *RELA*, *REL*, *TANK* and *NFKBIA* were validated by ddPCR (supplementary Figure 1).

The overall downregulation of the Nf kB pathway could be related to a decrease in levels of pro inflammatory cytokines and also could be promoting an increased apoptosis in the cells. Altogether, these changes could be related to a decrease in the transfusion

dependency of these patients, as previously reported[1,11,21]

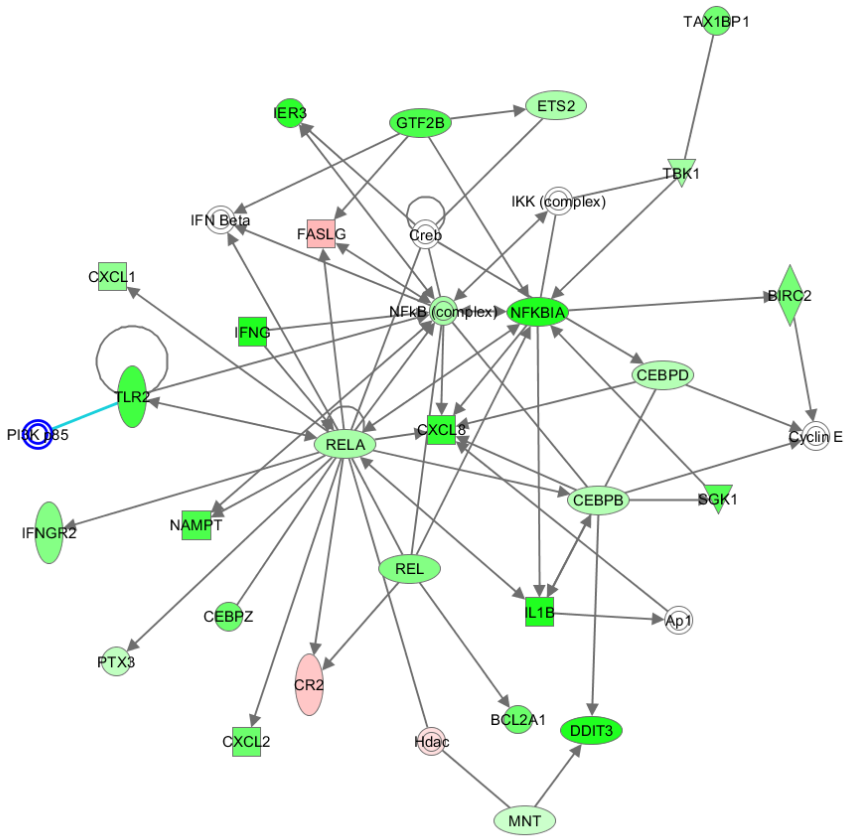

Figure 1. Network analysis of differentially expressed genes (DEG) from the Nf kB pathway in low-risk MDS patients treated with deferasirox (Green color refers to underexpression, while red color indicates overexpression)

Table 3. **Most relevant deregulated genes from the Nf kB pathway in low-risk MDS patients treated with deferasirox**. Ratio = 17/169, Z-score = -1.5, p value = 0.042

Gene	Gene Title	Expression	Diff exp
AZI2	5-Azacytidine Induced 2	DOWN	**-0.219**
BCL10	BCL10 Immune Signaling Adaptor		**-0.341**
EIF2AK2	Eukaryotic Translation Initiation Factor 2 Alpha Kinase 2		**-0.508**
IL1B	Interleukin 1 Beta		**-0.789**
KRAS	KRAS Proto-Oncogene, GTPase		**-0.200**
NFKBIA	NFKB Inhibitor Alpha		**-0.810**
RELA	RELA Proto-Oncogene, NF-KB Subunit		**-0.304**
RIPK1	Receptor Interacting Serine/Threonine Kinase 1		**-0.141**
TANK	TRAF Family Member Associated NFKB Activator		**-0.437**
TLR2	Toll Like Receptor 2		**-0.664**
TRAF3	TNF Receptor Associated Factor 3		**-0.215**
TRAF6	TNF Receptor Associated Factor 6		**-0.200**
PDGFRB	Platelet Derived Growth Factor Receptor Beta	UP	**0.130**
TK1	Thymidine Kinase 1		**0.059**
TNFSF11	TNF Superfamily Member 11		**0.094**

Deferasirox treatment deregulated genes related to reactive oxygen species (ROS) in low-risk MDS patients

In silico upstream regulator analysis predicted the involvement of the transcriptional regulator nuclear factor erythroid 2 (*NFE2L2/NRF2*) as inhibited, pointing it as the responsible for the deregulation of a great number of genes after deferasirox treatment. *NFE2L2/NRF2* is a master gene which controls the response to the oxidative stress induced by the reactive oxygen species (ROS) and regulates over 200 genes (Figure 2). ROS are a group of highly reactive chemicals containing oxygen produced either exogenously or endogenously. They are related to a wide variety of human disorders,

such as chronic inflammation, age-related diseases, and cancers[10,22]. Interestingly, in MDS patients the iron overload is related to an increase of the cytoplasmic ROS. By contrast, the decreased ROS activity observed after deferasirox treatment could be related to the Nf kB activation[22] and linked to the abnormalities in T cell lymphocytes[10]. Our study confirmed that these previous results, mainly based in *in vitro* models, are also observed in patients during deferasirox therapy.

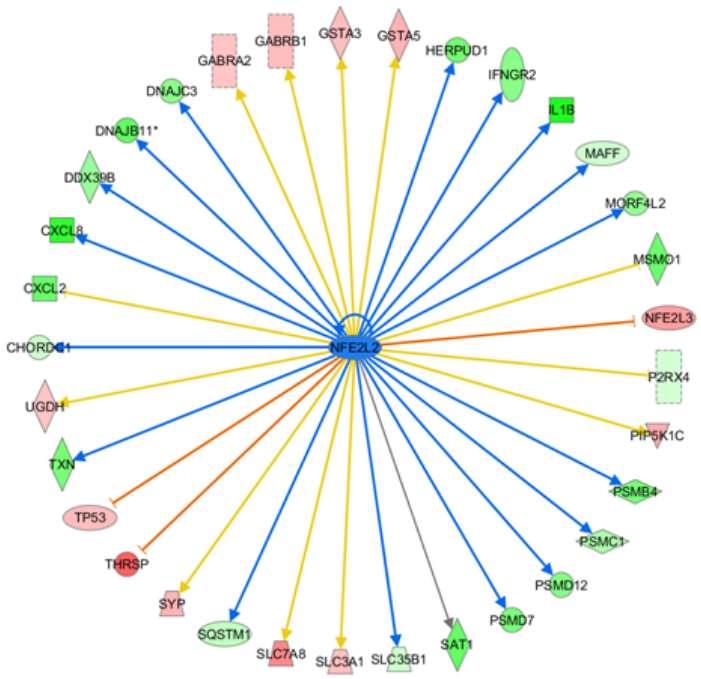

Figure 2. *In silico* upstream regulator analysis predicts the inhibition of nuclear factor erythroid 2 in low-risk MDS patients treated with deferasirox. Most of the genes involved in reactive oxygen species (ROS) were downregulated after the therapy

Erythropoiesis improvement after deferasirox therapy in low-risk MDS patients could be related to the overexpression of GFI1 and the downregulation in the interferon pathway.

The present study showed an activation of the gene Growth Factor Independent 1 Transcriptional Repressor (*GFI1*), a transcription factor which plays a critical role in the hematopoiesis, activating both erythroid and megakaryocyte lineages[23]. Of note, several studies have reported an improvement of hemoglobin and platelet levels in MDS patients treated with deferasirox[18–20,24,25].

Moreover, the GEP of patients after deferasirox therapy showed a marked downregulation of gamma interferon, as well as other cytokines such as *TRAF6*, *IL8*, *ILB* and *IL1RAP.* The role of *IL-1* and gamma interferon as inhibitors of erythropoiesis has been already reported[26]. Thus, our results showing the downregulation of the expression of these genes could be related to an erythropoiesis activation. Taking together, several mechanisms reported in this study, including activation of *GFI1* or repression of gamma interferon, could lead to an erythropoiesis stimulation, thus providing the biological basis for the clinical results observed in MDS patients treated with this iron chelator.

miRNA Deregulation in MDS patients treated with deferasirox

The analysis of miRNA expression revealed that fifty-four miRNAs were deregulated in MDS patients after the treatment: hsa-miR-2682 was the most highly upregulated miRNA (Diff exp = 0.48), while hsa-miR-147b was the most significantly downregulated (Diff exp = -1.08) (supplementary Table 3). Functional analysis of the deregulated miRNAs after treatment (Figure 3) revealed that the most strongly affected cell function by these miRNAs was gene expression, with a total of 7 miRNAs involved (mir-146, mir-

515, mir-665, mir-548, mir-30, mir-154, mir-130). Inflammation (inflammatory disease and inflammatory response), cancer, hematological-related functions (hematological disease and hematological system development and function) and Hematopoiesis were other important functions affected by these miRNAs.

The influence of these deregulated miRNAs on deferasirox treated MDS patients was assessed. Specifically, we investigated whether observed changes in miRNAs were correlated with changes in the expression of genes. Therefore, the post-transcriptional regulatory network of miRNA and genes in MDS patients treated with deferasirox was carried out by analyzing the miRNA-mRNA relationships. Indeed, because miRNAs tend to downregulate the target genes, we focused our study on the subset of 8 miRNAs selected for analysis in IPA and the genes experimentally observed or predicted with high confidence to be regulated by them and characterized by expression profiles stringly anticorrelated. MiR-125b, overexpressed after deferasirox treatment, was negatively correlated with the expression of 20% expected target genes (data not shown) demonstrating the relationship between miRNA and gene deregulation. Interestingly, the expression of miR-125b is modulated by NF-kB signaling. MiR-125b targets the 3'UTR region of TNF-alpha gene to negatively regulate the inflammatory response[27]. By contrast, another study has reported that miR-125b can promote macrophage mediated inflammation and enhance antitumor activities by targeting Interferon regulatory factor 4 (IRF4)[28] These data suggest that miRNAs could play different roles in diverse biological contexts. Of note, a recent study[29] has shown that miR-146b, also overexpressed after deferasirox therapy (supplementary Table 3), can

regulate inflammatory responses by targeting mRNAs encoding TRAF6, a gene downregulated in our work (Table 3, supplementary Table 2).

Moreover, miR125 has recently emerged as a key regulator of hematopoietic stem cells (HSCs)[30], although there are contradictory findings regarding the lineage that is expanded because of the overexpression of miR-125b, lymphoid[31] or myeloid[30]. However, the contribution of miR-125 family members in blood cell production is well recognized[30], as miR-125 has been identified in a subset of miRNAs enriched in HSCs, providing evidence that these miRNAs function to properly manage hematopoietic output.

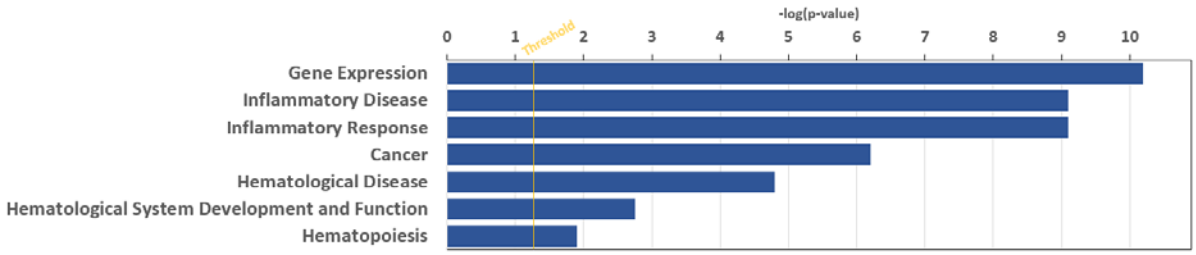

Figure 3. **Most significant cellular functions affected by the deregulation of miRNAs in MDS patients treated with deferasirox**. A functional enrichement analysis was performed in the dataset of 54 deregulated miRNAs. Category names are presented on the vertical axis. Of note, gene expression signaling and inflammatory signaling were among the most significant cellular functions affected. The significance of the association between the dataset and the canonical pathway was measured by the P-value determining the probability of the association between the genes in the dataset and the canonical pathway, calculated by Fisher's exact test. The horizontal axis on the top indicates the −log (P value), the higher value indicates the higher significance.

In summary, in low-risk MDS patients, the treatment with deferasirox induced strong changes both in gene and miRNA expression of the patients. These changes mainly involved the downregulation of Nf kB pathway and ROS-related genes, namely *NRF2*. These changes could be related to the reduced inflammation and oxidative stress observed after deferasirox treatment. In addition, *GFI1* overexpression and the downregulation of gamma interferon could be related to the increase in hemoglobin

and platelets levels observed after deferasirox therapy. Besides, miRNAs may play an important role in the hematopoiesis, controlling diverse biological process.

Acknowledgments

This work was partially supported by grants from the Spanish Fondo de Investigaciones Sanitarias PI15/01471, PI17/01741, PI18/01500, Instituto de Salud Carlos III (ISCIII), European Regional Development Fund (ERDF) “Una manera de hacer Europa”, “Consejería de Educación, Junta de Castilla y León” (SA271P18), “Proyectos de Investigación del SACYL”, Spain: GRS 1847/A/18, GRS 1653/A17, GRS 1850/A/18, Fundación Memoria Don Samuel Solórzano Barruso”, by grants (RD12/0036/0069) from Red Temática de Investigación Cooperativa en Cáncer (RTICC) and Centro de Investigación Biomédica en Red de Cáncer (CIBERONC CB16/12/00233). JM Hernández Sánchez and AE Rodríguez Vicente are supported by a research grant by FEHH (“Fundación Española de Hematología y Hemoterapia”).

We are grateful to I. Rodríguez, S. González, T.Prieto, M. Á. Ramos, A. Martín, A. Díaz, A.Simón, M.del Pozo, V. Gutiérrez and S.Pujante, Sandra Santos and Cristina Miguel from Cancer research Center of Salamanca, Salamanca, for their technical assistance.

Authorship Contributions

JMHS designed the experiment, interpreted the results and performed bioinformatic analysis; EL, MA and MDR contributed to the interpretation of the results; MDC, JGR, SG, AM, RP, SET, BA and JMHR performed patient selection and provided clinical data; JMHR and AERV contributed to the interpretation of the results and wrote the manuscript. All authors revised the manuscript.

Conflict-of-interest disclosure

The authors declare no competing financial interests.

References

1. Gattermann, N. Iron overload in myelodysplastic syndromes (MDS). *International Journal of Hematology* **107**, 55–63 (2018).
2. Cario, H. *et al.* Recent Developments in Iron Chelation Therapy. *Klinische Pädiatrie* **219**, 158–165 (2007).
3. Kushner, J. P., Porter, J. P. & Olivieri, N. F. Secondary iron overload. *Hematology. American Society of Hematology. Education Program* 47–61 (2001).
4. Olivieri, N. F. & Brittenham, G. M. Iron-chelating therapy and the treatment of thalassemia. *Blood* **89**, 739–61 (1997).
5. Olivieri, N. F., Sabouhanian, A. & Gallie, B. L. Single-center retrospective study of the effectiveness and toxicity of the oral iron chelating drugs deferiprone and deferasirox. *PLOS ONE* **14**, e0211942 (2019).
6. Piciocchi, A. *et al.* Update of the GIMEMA MDS0306 study: Deferasirox for lower risk transfusion-dependent patients with myelodysplastic syndromes. *European Journal of Haematology* **102**, 442–443 (2019).
7. Musto, P. *et al.* Iron-chelating therapy with deferasirox in transfusion-dependent, higher risk myelodysplastic syndromes: a retrospective, multicentre study. *British Journal of Haematology* **177**, 741–750 (2017).
8. Mills, K. I. *et al.* Microarray-based classifiers and prognosis models identify subgroups with distinct clinical outcomes and high risk of AML transformation of myelodysplastic syndrome. *Blood* **114**, 1063–1072 (2009).
9. del Rey, M. *et al.* Genome-wide profiling of methylation identifies novel targets with aberrant hypermethylation and reduced expression in low-risk myelodysplastic syndromes. *Leukemia* **27**, 610–618 (2013).

10. Chen, J. *et al.* Reactive oxygen species mediated T lymphocyte abnormalities in an iron-overloaded mouse model and iron-overloaded patients with myelodysplastic syndromes. *Annals of Hematology* **96**, 1085–1095 (2017).
11. Messa, E. *et al.* Deferasirox is a powerful NF- B inhibitor in myelodysplastic cells and in leukemia cell lines acting independently from cell iron deprivation by chelation and reactive oxygen species scavenging. *Haematologica* **95**, 1308–1316 (2010).
12. Ohyashiki, J. H. *et al.* The oral iron chelator deferasirox represses signaling through the mTOR in myeloid leukemia cells by enhancing expression of REDD1. *Cancer Science* **100**, 970–977 (2009).
13. Vardiman, J. W. *et al.* The 2008 revision of the World Health Organization (WHO) classification of myeloid neoplasms and acute leukemia: rationale and important changes. *Blood* **114**, 937–951 (2009).
14. Bolstad, B. M., Irizarry, R. A., Astrand, M. & Speed, T. P. A comparison of normalization methods for high density oligonucleotide array data based on variance and bias. *Bioinformatics* **19**, 185–193 (2003).
15. Huang, D. W., Sherman, B. T. & Lempicki, R. A. Systematic and integrative analysis of large gene lists using DAVID bioinformatics resources. *Nature protocols* **4**, 44–57 (2009).
16. Huang, D. W., Sherman, B. T. & Lempicki, R. A. Bioinformatics enrichment tools: paths toward the comprehensive functional analysis of large gene lists. *Nucleic Acids Research* **37**, 1–13 (2009).
17. Carmona-Saez, P., Chagoyen, M., Tirado, F., Carazo, J. M. & Pascual-Montano, A. GENECODIS: a web-based tool for finding significant concurrent annotations in gene lists. *Genome biology* **8**, R3 (2007).
18. List, A. F. *et al.* Deferasirox Reduces Serum Ferritin and Labile Plasma Iron in RBC Transfusion–Dependent Patients With Myelodysplastic Syndrome. *Journal of Clinical Oncology* **30**, 2134–2139 (2012).

19. Gattermann, N. *et al.* Hematologic responses to deferasirox therapy in transfusion-dependent patients with myelodysplastic syndromes. *Haematologica* **97**, 1364–1371 (2012).
20. Angelucci, E. *et al.* Deferasirox for transfusion-dependent patients with myelodysplastic syndromes: safety, efficacy, and beyond (GIMEMA MDS0306 Trial). *European Journal of Haematology* **92**, 527–536 (2014).
21. Lyle, L. & Hirose, A. Iron Overload in Myelodysplastic Syndromes: Pathophysiology, Consequences, Diagnosis, and Treatment. *Journal of the advanced practitioner in oncology* **9**, 392–405
22. Meunier, M. *et al.* Reactive oxygen species levels control NF-κB activation by low dose deferasirox in erythroid progenitors of low risk myelodysplastic syndromes. *Oncotarget* **8**, (2017).
23. Anguita, E., Candel, F. J., Chaparro, A. & Roldán-Etcheverry, J. J. Transcription Factor GFI1B in Health and Disease. *Frontiers in Oncology* **7**, (2017).
24. Nolte, F. *et al.* Results from a 1-year, open-label, single arm, multi-center trial evaluating the efficacy and safety of oral Deferasirox in patients diagnosed with low and int-1 risk myelodysplastic syndrome (MDS) and transfusion-dependent iron overload. *Ann Hematol* **92**, 191–198 (2013).
25. Molteni, A. *et al.* Hematological improvement during iron-chelation therapy in myelodysplastic syndromes: The experience of the “Rete Ematologica Lombarda”. *Leukemia Research* **37**, 1233–1240 (2013).
26. Morales-Mantilla, D. E. & King, K. Y. The Role of Interferon-Gamma in Hematopoietic Stem Cell Development, Homeostasis, and Disease. *Current Stem Cell Reports* **4**, 264–271 (2018).

27. Tili, E. *et al.* Modulation of miR-155 and miR-125b Levels following Lipopolysaccharide/TNF-α Stimulation and Their Possible Roles in Regulating the Response to Endotoxin Shock. *The Journal of Immunology* **179**, 5082–5089 (2007).
28. Chaudhuri, A. A. *et al.* MicroRNA-125b Potentiates Macrophage Activation. *The Journal of Immunology* **187**, 5062–5068 (2011).
29. Park, H., Huang, X., Lu, C., Cairo, M. S. & Zhou, X. MicroRNA-146a and MicroRNA-146b Regulate Human Dendritic Cell Apoptosis and Cytokine Production by Targeting TRAF6 and IRAK1 Proteins. *Journal of Biological Chemistry* **290**, 2831–2841 (2015).
30. O'Connell, R. M. *et al.* MicroRNAs enriched in hematopoietic stem cells differentially regulate long-term hematopoietic output. *Proceedings of the National Academy of Sciences* **107**, 14235–14240 (2010).
31. Ooi, A. G. L. *et al.* MicroRNA-125b expands hematopoietic stem cells and enriches for the lymphoid-balanced and lymphoid-biased subsets. *Proceedings of the National Academy of Sciences* **107**, 21505–21510 (2010).

Chapter 3: *Sequential Mutational and Gene Expression Profile shows marked changes in CD34 positive cells from MDS patients during 5-Azacytidine treatment*

Authors:

Jesús María Hernández-Sánchez[1,2], Mónica del Rey[2], Rocío Benito[2], Sohini Chakraborty[3], Ana Eugenia Rodríguez-Vicente[2], Teresa González[1,2], Félix Cadenas[1], María Díez-Campelo[1], Christopher Park[3], Jesús María Hernández-Rivas[1,2,4]

Affiliations:

1. Servicio de Hematología. Hospital Universitario. Salamanca, Spain

2 IBSAL. IBMCC. CIC, Universidad de Salamanca-CSIC, Spain.

3. Department of Pathology, School of Medicine, New York University, NY, USA

4. Department of Medicine, Universidad de Salamanca

Correspondence

Jesús M Hernández Rivas

Dept. Medicine, University of Salamanca

Campus Miguel de Unamuno

37007 Salamanca, Spain

Running title

DNA-seq and RNA-seq in CD34 cells in patients treated with 5-Azacytidine

Scientific category: Original Article

Text word count (without references): ~3800

Abstract word count: 297

Figures: 4

Tables: 3

Reference count: 32

Abstract

The use of hypomethylating agents (5-Azacytidine and decitabine) has changed the course of MDS patients, showing an increased survival in higher risk MDS. The emergence of Next Generation Sequencing (NGS) technologies, has increased the sensitivity and specificity of mutational and the gene expression profile (GEP) analysis. However, few studies have explored the changes induced by the therapy with 5-Azacytidine (AZA) in the GEP landscape in patients. In order to identify the biological mechanisms of action of 5-Azacytidine (AZA) a sequential study in patients before and during the treatment was carried out in CD34+ isolated cells from patients suffering high-risk myeloid malignancies. To further validate the biological changes induced by AZA the gene expression profiles were compared to a subset of aged matched healthy control samples. Mutation analysis profiles did not show significant variants between CD34+ population and the bone marrow mononuclear cells, showing also a high correlation variant allele frequency (VAF). Three patients showed a decrease in the mutations of the hematopoietic clone, interestingly all the patients showed mutations in *TP53*. Finally, we identified mutations in *KRAS* and *NRAS* that arose during the treatment in two patients; both mutations have been related with higher risk of transformation. Differentially expressed genes (DEG) foreground the downregulation of rRNA process, translation and metabolism of RNA (FDR <0.0001, NES = 5.3 and ES = 0.67). Moreover, AZA also induced upregulation of immune system pathways, involved in innate and adaptative response. The therapy promotes the expression of hematopoietic cell lineage markers while downregulation of leukemogenesis genes as *HOXA6* and *HOXA9*. Finally, all pathways but translation were restored by AZA when compared with healthy control samples. These results defined potential genes targeted

by AZA, such as *TP53*, and showed an activation of the immune system and a downregulation of the protein synthesis after AZA therapy.

Introduction

Myelodysplastic syndromes (MDS) are a group of heterogeneous clonal hematopoietic stem cell disorders associated with a myeloid differentiation blockade leading to bone marrow (BM) accumulation of myeloid progenitor cells and peripheral blood (PB) cytopenias [1,2]. Cytopenias might affect one or more hematological lineages (erythrocytes, platelets, granulocytes and/or monocytes). Approximately 30% of MDS progress to an acute myeloid leukemia (AML) [3]. Although MDS arise in hematopoietic stem cell, genetic data indicate that they are heterogeneous at genetic level and with respect to therapeutic responses [4–6]. Hypomethylating therapies are among the few therapies available for patients who are not candidate to allogenic stem cell transplantation. 5-Azacytidine (AZA) and decitabine are considered the standard treatment for higher risk MDS (HR-MDS), chronic myelomonocytic leukemia (CMML) and acute myeloid leukemia (AML) with myelodysplastic features [7,8].

AZA is an azanucleoside, analog of cytidine, with antineoplastic effects. Low doses inhibit the DNA methyl-transferase, resulting in DNA hypomethylation finally driving to cytotoxicity in abnormal BM cells. At high dose, azacytidine leads to cell death due to the incorporation into DNA and RNA. This drug was approved in 2004 [9], through two randomize clinical trials (AZA-001 and CALGB 9221) accomplished in HR-MDS patients. AZA-001 showed a survival improved when compare *versus* standard care irrespective of age, karyotype or percentage of BM blast [10]. The time to AML progression and red blood cells transfusion were also significantly improved in AZA arm. Furthermore, in CALGB 9221 study, AZA also exhibit an improvement to leukemic transformation or death, although no differences in survival were observed [11]. However, these findings

could not be confirmed by the Spanish Group of Myelodysplastic Syndromes in unselected high-risk patients [12].

Other studies have shown hematological improvements induced by AZA and some patients also achieved complete response, extending overall survival. However, this effect is only observed in 30-40% of the treated patients [13]. For this reason, there is a need to gain insights to assess the AZA mechanism of action and the identification of predicting factors that may help to select patients who will benefit of the treatment.

Next generation sequencing (NGS) has been widely used in the last years. The analysis of DNA mutations and the use RNA-seq to identify changes in the gene expression profile (GEP) is providing new insights about the characterization of cancer. RNA-seq provides an in-depth view of the transcriptome, detecting low expressed transcripts and splicing changes. Therefore, evolution of NGS technologies facilitates the use of RNA-seq as a methodology to increase the knowledge of the pathways involved in human diseases.

In this study, the changes in CD34+ cells induced by AZA in both DNA and RNA were analyzed in patients with MDS and AML. We studied paired samples, before and during the treatment with this hypomethylating agent. Some changes in the mutational profile as well as a high number of genes deregulated after AZA therapy, mainly involving immune response and translation and metabolism of RNA were observed. These results showed that AZA therapy influences not only the methylation pattern of CD34+ cells but also induces a high deregulation of other pathways involved in myeloid diseases.

Material and methods

Patients and control samples

BM samples from 14 patients with MDS (n= 11) and AML (n = 3) were collected before and during the treatment with 5-Azacytidine. Patient's median age was 70 years (range: 49-85 years). Patients were diagnosed following the WHO 2016 criteria. Baseline patient's characteristics are shown in Table 1.

Table 1. **Main clinical and biological characteristics of MDS/AML patients included in the study**

Characteristics	Median (range)
Age (years)	70 (49-85)
Sex (n, %): Male / Female:	6 (42.9%) / 8 (57.1%)
Blood cells count basal:	
Platelets (x 10^3/mm^3)	138.6 (9-470)
White blood cells (x 10^3/mm^3)	5.8 (1.2-36.6)
Hemoglobin (g/dL)	10.2 (7.2-14.9)
ANC (10^9/L)	5.8(1.2-36.6)
Bone Marrow blast (%)	13 (0.5-70)
IPSS-R Category:	
High / Intermediate	9 / 2
Diagnosis (n, %)	
MDS-EB-1	4, 28.6%
MDS-EB-2	5, 35.7%
MDS-MLD	2, 14.3%
AML-MDS	3, 21.4%
Type of Response (n, %)	
Blast / Hematological	5 (35%) / 8 (57%)

AZA was administrated at 75 mg/m^2 per day for seven days every month. The median number of cycles was 8 per patient (range 4–13). Hematological evaluation to AZA response was performed according to the International Working Group (IWG) criteria for MDS and AML. Patients were considered responders if they achieved complete remission (CR), partial remission (PR), marrow CR (mCR), or hematological improvement

(HI). Moreover, they were considered non-responders whether they exhibited stable disease (SD) or disease progression (PD). Complete clinical data is shown in Supplementary Table 1.

Furthermore, BM specimens from 6 healthy controls were obtained at the Department of Orthopedics of the Hospital Universitario of Salamanca (Spain). Controls were aged matched, 74 years old (range: 67-83 years), compared with the fourteen patients.

The procedures followed were in accordance with the Helsinki Declaration of 1975, as revised in 2008, with the study receiving official institutional approval (Hospital Universitario, Salamanca, Spain), and samples were obtained after subjects provided informed consent.

Thirty-four CD34+ samples were included in the study: Twenty-eight samples corresponding to 14 patients were collected from BM as serial samples (before and during AZA treatment) while the remaining six were form aged matched healthy controls. Blast cell response was achieved in 5/14 patients (35%), while any type of hematological response was achieved in 8/14 patients (57%) (Table 1). No significant differences in response regarding MDS subtype or AML were observed. Most of the patients were classify as high risk by the IPSS-R (9/11), two patients started the treatment as acute myeloid leukemia with myelodysplasia-related changes and one had missing values to calculate the IPSS-R score (Table 1).

Study design: cell separation, nucleic acid and Next Generation sequencing

Cell separation

Mononuclear cells were isolated from BM samples using Ficoll-Paque Plus (GE Healthcare, Massachusetts, US) density gradient. CD34+ cells were isolated by autoMACs Pro Separator (Miltenyi Biotec GmbH, Bergisch Gladbach, Germany) using immunomagnetic separation following manufacturer´s instructions.

Nucleic acids extraction

CD34+ samples and its negative fraction, were snap-frozen and stored at -80ºC. Total DNA and RNA were extracted by QIAgen (Qiagen, Valencia, CA, USA), following the manufacturer's recommendations. RNA integrity was assessed on an Agilent 2100 Bioanalyzer (Agilent technologies, Santa Clara, CA, USA) employing the RNA 6000 Nano Assay kit. All RNA samples had an RNA integrity number (RIN) ≥8.0. DNA and RNA quantity were assessed by qubit 2.0 (ThermoFisher scientific, Massachusetts, U.S.) using double strand kit or RNA kit (high/broad sensitivity).

Next Generation Sequencing

DNA-seq

Custom HTS panel was made using Design Studio (Illumina, California, U.S.) with 3,259 probes targeting 1,740 regions including exons, splicing regions (10nt aside exons) and 3/5 untranslated region (UTR) for 117 genes associated with myeloid neoplasms, the final design covered ~500kb (Supplementary table 2). Libraries were made following nextera rapid capture custom enrichment protocol (Illumina) recommendations. MiSeq or NextSeq platform were used with a read length of 2 × 150 nucleotides.

Raw data quality control was performed with FastQc (v0.11.8) and picard tools (v2.2.4) to collect sequencing metrics. Demultiplexed files (fastq) were aligned to the reference genome (hg19/GRCh37), read duplicates were marked with samtools (v1.3.1) and post-alignment was performed with GATK (v3.5). Coverage for each region was assessed using bedtools (v.2.26.0). Finally, somatic variant calling, and annotation were done with VarScan (v2.4) and ANNOVAR (v.2017Jul16), respectively. Regarding annotation, dbSNP, COSMIC, ClinVar, 1000genomes, ExAC, and *in silico* predictors of functional effects, such as mutationAssessor, SIFT or Polyphen2 (among other databases) were employed.

RNAseq

RNA-seq was performed in paired samples (before and during azacytidine treatment) from 14 patients and 6 control samples by using SMART-Seq v4 Ultra Low Input RNA kit (Clonthech, California, U.S.). In all samples, RNA from CD34+ cells was analyzed following manufacturer's recommendations for the protocol "*Illumina library preparation using Covaris shearing*". Libraries were sequenced in the HiSeq400 platform (Illumina) according to manufacturer´s description with a read length of 2 × 150 nucleotides.

Briefly, *bcl* files were demultiplexing on BaseSpace (Illumina Cloud based resource) to generate *fastq* files. Raw data quality control was performed with fastQc (v0.11.8), globin contamination was assessed with HTSeq Count, FastQ screen evaluated ribosomal RNA contamination and other external possible resources of contamination (Mus musculus, Drosophila melanogaster, Caenorhabditis elegans and mycoplasma). STAR (v020201) was used for the alignment (hg19 reference genome) and FeatureCounts (v1.4.6) to generate the read count matrix. Finally, DESeq2 was used for differentially gene expression analysis. Of noted, DESeq2 model internally corrects for

library size therefore normalizes the values and enables paired comparisons. Principal component analysis (PCA) and heatmaps were performed in R.

Pathways analysis

Gene set enrichment analysis (GSEA) to evaluate whether a set of genes was significantly enriched between the different comparisons was used. The most significant biological mechanisms, pathways and functional categories in the data sets of genes selected by statistical analysis were identified through Reactome. Finally, WEB-based Gene SeT AnaLysis Toolkit (WebGestalt) was performed to get new biological insights.

Results and Discussion

AZA induces changes in the mutational profile

Samples from twelve patients, in which CD34+ DNA was available before and during AZA treatment, were sequenced. Mutations in eleven out of the twelve patients (91.6%) were observed. A total of 48 mutations, and a median of four mutations [0-9], per patient was observed. The most frequently mutated genes were: *TP53*, *DNMT3A* and *BCOR*, mutated in 4 patients (36.3%) while *SRSF2*, *NRAS* and *TET2* were mutated in 3 patients (27.2%). A detailed description of all the mutational is provided in Supplementary table 3. These results are in accordance with other large series of MDS [4–6]. In terms of nucleotide substitution, the proportion of transitions and transversions was 56.6% and 43.4% respectively. Predominance of transition was in concordance with previously data in MDS [14]. Interestingly, AZA showed a higher reduction of transition mutations, 32.6%, whereas only 9.1% of transversion mutations were modified by the treatment. Moreover, C->T change modified its allele burden in 43.4%. Of note, the mutational analysis in the hematopoietic stem cells before and during the treatment revealed how AZA does not induce the same effects in all the patients. Figure 1, shows the mutational profile of the patients and the changes induced by the therapy.

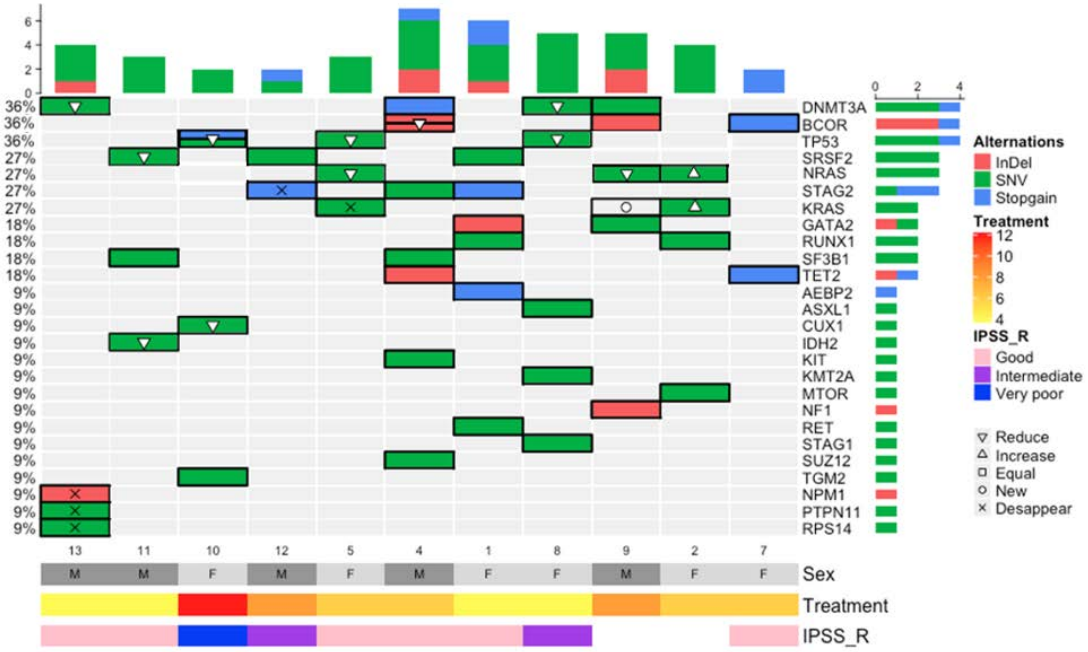

Figure 1. Dynamics of mutations in patients with myeloid malignancies treated with 5-Azacytidine (AZA). Y axis indicates the percentage of each gene mutated in the study. Most of the patients retained the mutations after AZA, while a decrease was shown in *DNMT3A*, *TP53*, *BCOR*, *NRAS*, *CUX1* and *IDH1* gene mutation burden. Only a new mutation, on *KRAS*, was observed during AZA therapy.

In fact, patient 2 which had 2 clonal population carrying mutations in *MTOR* and *RUNX1*, and *KRAS*, *NRAS*, respectively, showed how the clone harboring *KRAS* and *NRAS* increased the burden allele with AZA (1.8 to 7.1, 1.2 to 15.2). Interestingly, this patient had a reduction in blast count, although neither hematological nor clinical response was achieved. In contrast, patient 5 had 3 mutations in *TP53*, *NRAS* and *KRAS*. All the mutations decreased (81.2 to 15.8 and 28 to 6.6, respectively) and *KRAS* mutation disappeared (detection limit 1%) after AZA therapy. In this patient, the mutational profile correlated with complete response observed. Moreover, patient 8 also decreased the variant allele frequency (VAF) in *TP53* and *DNMT3A* (87.48 to 3.9 and 41.7 to 10 respectively) while others mutation remained unchanged (*ASXL1*, *KMT2A* and *STAG1*). This patient had a reduction in blast count and showed a clinical response, however did not achieved hematological response. Regarding patient 9, an additional mutation in *KRAS* was acquired while the *NRAS* burden decreased during the treatment;

this patient remains stable, maybe because the low allele burden. Finally, patient 10 decreased in the entire mutations burden, being the most important *TP53* and *CUX1*. However, he had a complex karyotype and a quick progression. Finally, patients 12 and 13 showed mutations before the treatment (*STAG2; PTPN11*, *RPS14* and *NPM1*, respectively) that were removed after AZA. However, mutation in *SRSF2* (patient 12) was not affected by AZA and mutation in *DNMT3A* (patient 13) although decreased the allele burden (43.1 to 9) did not disappeared completely (Figure 1). This data revealed the heterogeneous mutational dynamics to AZA in high-risk MDS. Some reports showed how patients that achieved complete response to AZA also had a marked reduction of VAF [15]. However there is not an agreement on which mutations can be targeted by hypomethylating agents [16]. For this reason, we suggest to monitor mutation status through AZA treatment, to assess the genetic response to the therapy.

In summary, 5-Azacytidine treatment reduced the mutational allele burden in 7 patients (63%) while in 17 out of the 48 mutations this therapy decreased the VAF (35%). However only six mutations were removed during the therapy (35%). In contrast, 3 mutations (two *KRAS* and one *NRAS*) increased during AZA therapy. Remarkably all the patients harboring mutations in *TP53* reduced the mutational allele burden. These results are in accordance with previously studies that suggest that although *TP53* is associated with shorter overall survival, patients harboring mutations in this gene can be treated with AZA to gain benefit in overall survival [15], therefore the effect of mutations in *TP53* could be controlled by the treatment.

Finally, we sequenced 9 samples where CD34+ and the bone marrow mononuclear cells (BMMNCs) were available. We used the negative fraction to analyze whether hematopoietic stem cells could have the same mutation profile and allelic burden. We wondered if the mutation profile in both cell types change in the same way or whether AZA could target BMMNCs preferentially. Figure 2, shows a strong correlation (r = 0.73) in both cell types, in both situations, before and during AZA treatment. This data suggests that the mutation profile and the allele burden in BMMCs give similar information as the hematopoietic stem cells, making unnecessary the CD34+ isolation for detection or tracking mutations. Previous studies have shown different mutations pattern among common myeloid progenitor (CMP), granulocyte-macrophage progenitor (GMP) and megakaryocyte-erythroid progenitor (MEP) [14,17,18]; however isolation of these progenitor is laborious and not feasible for clinical routine.

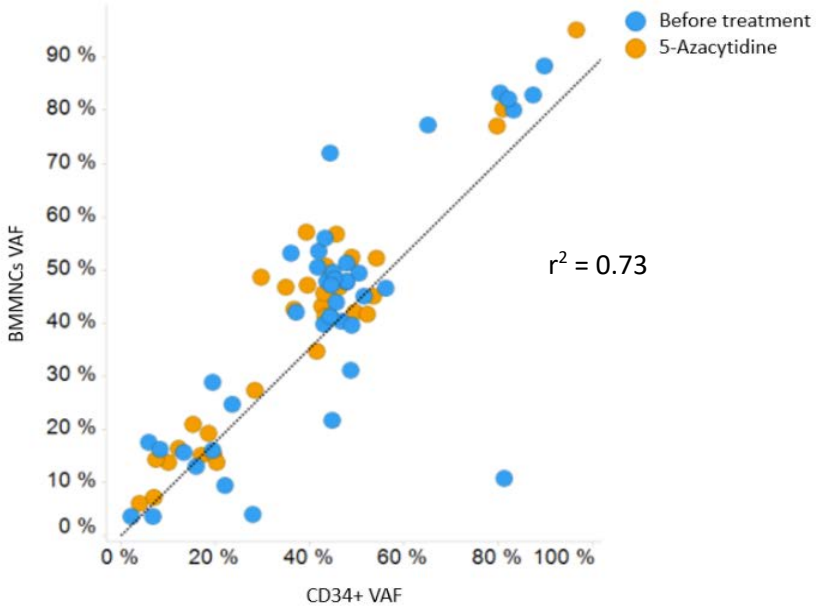

Figure 2. **Correlation of variant allele frequency (VAF) showed in hematopoietic stem cell (CD34+) and bone marrow mononuclear cells (BMMNCs)**. The mutations were present in both cell types with a high correlation before and during the treatment, $r^2 = 0.73$.

Taking all these data together, we can suggest that NGS is an optimal technology to track the mutational status in patients treated with AZA. The mutational status correlates with clinical phenotype and the early detection of mutational changes could help to know the response to the therapy.

5-Azacytidine induces changes in the gene expression profile in MDS/AML patients

The gene expression profile showed a total of 792 differentially expressed genes (536 upregulated and 256 downregulated) after AZA therapy (Supplementary Table 4). Figure 3 shows the top 50 most differentially expressed genes in the analysis (qval <0.01).

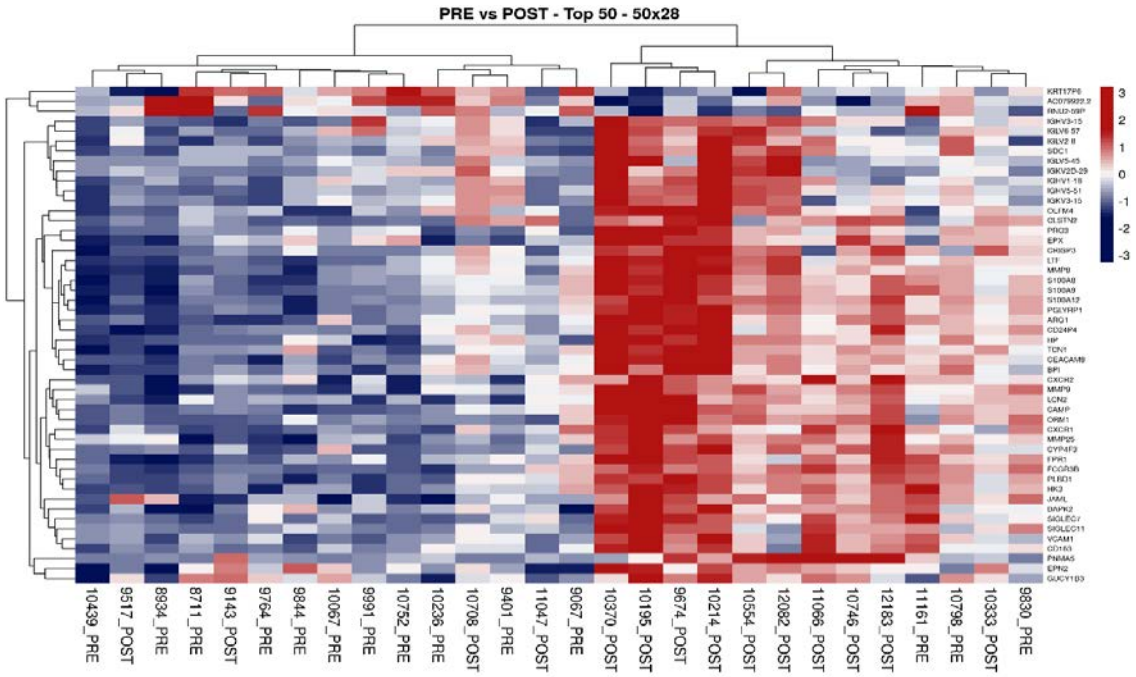

Figure 3. **Heatmap of the top 50 deregulated genes after AZA therapy (qval<0.01)**. Red color means overexpression while blue color means underexpression of the genes.

In addition, the heatmap shows how the treatment induced changes in the gene expression profile (GEP) in most of the patients. Reactome enrichment analysis exhibit the most deregulated pathways groups induced by the treatment were immune system, metabolism of RNA and metabolism of proteins (Figure 4). AZA induced deep changes

in classical antibody-mediated complement activation pathway. Thus sixty-six immunoglobulin (IG) genes were overexpressed after AZA treatment (Supplementary Table 3). Most of them were IG heavy chain genes (40%), and also kappa and lambda related genes were upregulated after AZA therapy (FC = -1.94 [-1.4 to -2.7]. Light chain genes represent 60% of the upregulated IG genes (21 kappa and 19 lambda related genes) while 26 were IG heavy chain genes (40%) (Supplementary Table 3).

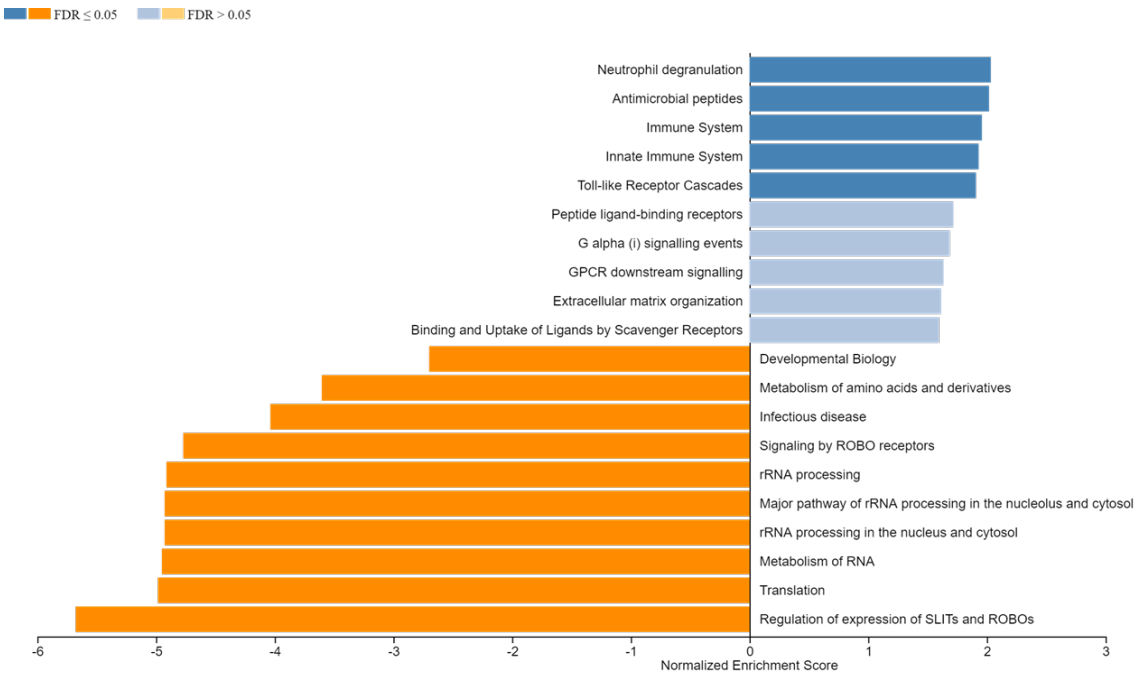

Figure 4. **Reactome enrichment analysis of patients with myeloid malignancies treated with AZA**. AZA induced significant downregulation of RNA, mRNA, ncRNA and translation, while this therapy significantly increased the immune function and granulocyte activation

Figure 4 shows GSEA analysis. The biological enrichment process exhibits also the upregulation of leukocyte migration and granulocyte activation (FDR: 0.034; 0.028 and a NES: -2.01; -1.96, respectively), highlighting *CXCR1*, *S100A12*, *MMP9*, *S100A8*, *CXCR2* genes as the most up/down regulated after AZA. In addition, GSEA enrichment analysis pathway KEGG, showed an important downregulation of ribosomal genes (FDR < 0.0001, ES = 0.778 and NES = 4.55). It is widely known that azacytidine reduces protein synthesis,

one of the reason is because it has a ratio of incorporation into nucleic of 65:35, RNA:DNA [19] ; In contrast decitabine is mainly incorporate in DNA [20]. Few data regarding the down regulation of ribosomal proteins after AZA have been described. However, an upregulation of protein synthesis machinery in Lin-/CD34+/CD38-/CD123+ when compared to Lin-/CD34+/CD38-/CD123- cells has been described [18]. Protein synthesis is highly regulated in hematopoietic stem cell [21] and the up regulation of ribosome genes, have been correlated with malignancy due to the fundamental change in the physiology. Interestingly cytidine deaminase (CDA) that degrades azacytidine was upregulated during the treatment (qval = 0.003) as previously described [22]. Moreover, genes related to mRNA binding were also downregulated by the treatment (*RBFOX3*, *PTBP2*, *SHMT1*, *XPO5*, *RPS3*, *G3BP1*, *RPL7*, *PABPC3*, *PABPC1*, *RPL13A* and *IREB2*).

Finally, three key genes were downregulated in treated samples: *MDM4*, *HOXA6* and *HOXA9*. *MDM4* has similarities with *MDM2* and both inhibit *TP53*, however through different mechanism. *MDM4* binds and inhibits the activity of p53 transactivation domain [23], while *MDM2* degrades the protein. In addition, *MDM4* can also bind *MDM2*, and its overexpression has been seen in many cancers [24]. Disruption of *p53* pathway is one of the first tumorogenic processes, being the overexpression of its major negative regulators (MDM2 and MDM4) also drivers for tumor development [25]. In this study AZA induced a downregulation on *HOXA9* and *HOXA6* gens. Both genes belong to the homeobox gene family. The expression of both genes has been extensively related with hematopoietic stem cell. The overexpression of *HOXA9* and *HOXA6* has been related with leukemogenesis and poor prognosis in AML patients [26].

Of note, several genes involved in the hematopoietic cell lineages were upregulated after AZA administration (P= 0.0097) (Table 2). These data suggest how the treatment could induce hematopoiesis differentiation although these changes are not enough to restore the cytopenias observed in patients treated with AZA [10].

Table 2. Most recurrent overexpressed hematopoietic-related genes after 5-Azacytidine therapy

Hematopoietic cell lineages	**Up regulated genes**
Lymphocyte T	*CD3*, *CD4*, *CD7* and *CD38*
Lymphocyte B	*CD38* and *CD35*
Neutrophils	*CD125* and *CD121*
Megakaryocyte	*CD9*, *CD14*, *CD41* and *CD61*

5-Azacytidine re-establishes the gene expression profile

In the next step of the study, we aimed to analyze the changes in the GEP of patients with myeloid malignancies induced by azacytidine. For this purpose, a gene expression profile comparison between samples before treatment and control samples was carried out. These analyses will foster the understanding of the changes induced by azacytidine by the comparison with age matched healthy control.

MDS/AML pre-treatment samples exhibit a strong up-regulation of ribosomal protein when compared with healthy controls (FDR <0.00001, ES = 0.63 and NES =2.63) (Supplementary Figure 1). Overexpression of ribosomal complex has been related to MDS pathogenesis and also with AML transformation [18,27–29]. Interestingly, none of the overexpressed ribosomal genes in pre-treated samples, were differentially expressed in the comparison between treated samples and healthy controls. This result confirms *in vivo*, one the mechanisms related to the AZA observed i*n vitro* studies. Gagnon-Kugler

et al showed how CpG methylation positively influences into rRNA synthesis and thus the hypomethylation induced by AZA decrease its expression [30]. However, our results show, for the first time *in vivo*, how this reduction in restoring the ribosomal expression genes to a normal status is carried out by AZA in MDS/AML patients.

Previous studies from our group (unpublished data) showed different patterns for MDS to AML progression. Genes with progressively increasing expression levels in low-risk MDS through high-risk MDS patients, getting the maximum in AML samples were: *RPL22*, *RPS5*, *RPL12*, *RPL13*, *RPL3*, *RPS6*, *CCNG1*, *CCNB1IP1*, *HSP90AB1*, *TFPI*, *TOMM20*, *SNHG8*, *TSC22D1* and *UFM1* (Supplementary Table 5). Also, the genes that were significantly up-regulated in AML patients when compared to MDS (either low-risk and high-risk MDS) and non-leukemic controls were *HOXA7*, *HOXA9* and *TWISTNB*. All these genes were overexpressed when compared pre-treatment samples *versus* controls, however there were not significant different when compared with azacytidine treated samples. All these results suggest how the hypomethylating therapy may restore the gene expression profile for a certain period of time, and also reduce the risk of transformation, with the downregulation of *HOXA7, HOXA9, TWISTNB* and other genes related to time-dependent AML time evolution (*RPS19*, *RPS20*, *RPL23*, *RPL6*, *RPL5* and *BMI1*) [31].

Finally, translation was the only pathway that was not affected by azacytidine (Supplementary Figure 2). Translation was upregulated over control samples in MDS/AML patients, disregarding if they were treated with azacytidine. This pathway can be an evasion mechanism for clonal hematopoietic stem cell, to avoid 5-Azacytidine action (Table 3).

Table 3. Main downregulated genes related to mitochondrial and transcription after 5-Azacytidine therapy

Gene Symbol	Score	Gene Name
MRPL50	10.177	mitochondrial ribosomal protein L50
MRPL15	0.9894	mitochondrial ribosomal protein L15
PPA1	0.9606	pyrophosphatase (inorganic) 1
MRPS36	0.8933	mitochondrial ribosomal protein S36
EIF2S2	0.8842	eukaryotic translation initiation factor 2 subunit beta
EIF2S1	0.8717	eukaryotic translation initiation factor 2 subunit alpha
MRPS6	0.8577	mitochondrial ribosomal protein S6
TARS	0.8574	threonyl-tRNA synthetase
MRPS10	0.8426	mitochondrial ribosomal protein S10
MRPL13	0.8036	mitochondrial ribosomal protein L13
RPS27L	0.7718	ribosomal protein S27 like
EIF3J	0.759	eukaryotic translation initiation factor 3 subunit J
EEF1E1	0.7548	eukaryotic translation elongation factor 1 epsilon 1
SSR1	0.7449	signal sequence receptor subunit 1
EIF4E	0.7173	eukaryotic translation initiation factor 4E
SRP54	0.7132	signal recognition particle 54
SRP72	0.6255	signal recognition particle 72
MRPS22	0.6075	mitochondrial ribosomal protein S22
MRPL42	0.5945	mitochondrial ribosomal protein L42
RPN1	0.55	ribophorin I
GARS	0.5323	glycyl-tRNA synthetase

In summary, our results showed the high impact of AZA in the gene expression profile of CD34+ cells of MDS/AML patients. Usually these patients show a high expression of ribosomal proteins leading to an over expression of protein synthesis. AZA will restore the levels to those seen in matched healthy population (Supplementary Figure 2). In addition, no differences in the mutational level were shown after AZA treatment.

Gene expression signatures regarding the response to 5-Azacytidine

Patients responding to AZA showed a specific GEP

To further elucidate gene signatures involved in AZA response we used the gene expression profiles from the patients before AZA treatment and we compared between blast responders and non-responders groups. We assessed a cut-off ratio higher to 3 (% blast count before / % blast count during the treatment) or a shift higher than 15%. Figure 5 shows the 413 DE genes (pval <0.01), 190 upregulated and 223 down in response patients. Immune system was highly enriched in blast responder patients (NES = 2.98, ES 0.54 and FDR <0.0001). Moreover, neutrophil degranulation was also enriched in these patients, *CXCR1*, *CR1*, *ALOX5* (Fold Change >2). These data suggest that in hematopoietic stem cell, genes related to the immune system are still active and AZA may boost its expression.

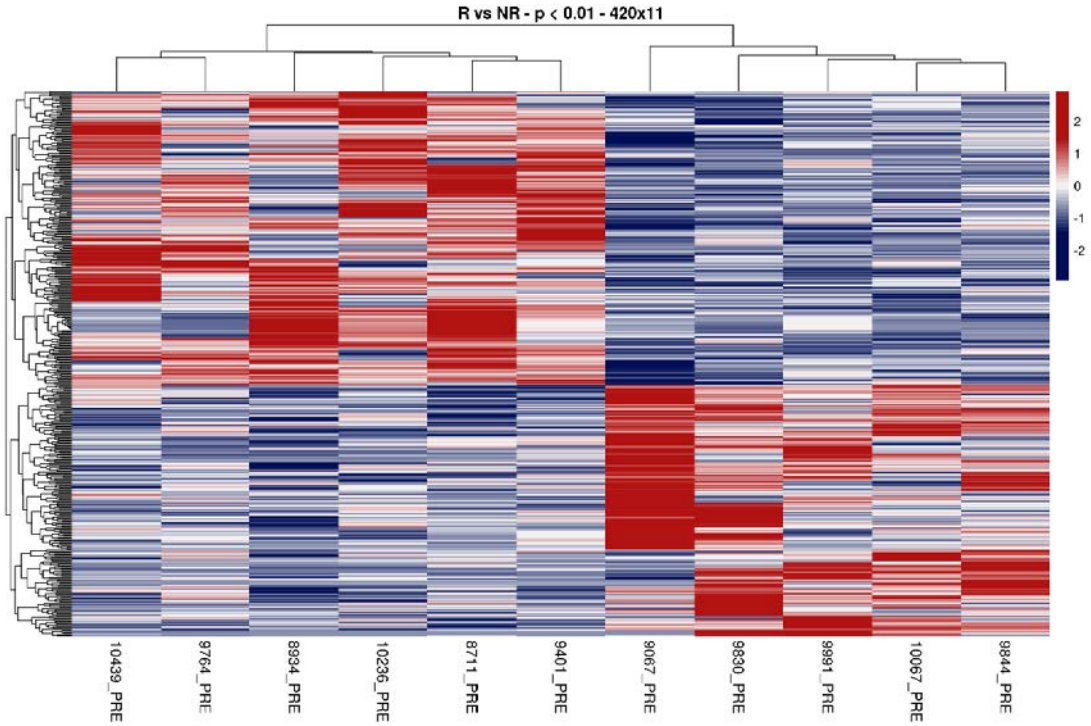

Figure 5. **Heatmap of the significant genes (pval < 0.01) of patients obtaining blast response to 5-Azacytidine vs those who did not achieving blast response (before treated samples)**. Gene expression profile clusters patients regarding its response. Red color means overexpression while blue color means underexpression of the genes.

We also analyzed the different pathways involved during the treatment. Neutrophil degranulation was upregulated in comparison to healthy control samples (ES = 0.75, NES = 3.09, FDR < 0.0001). The activation of immune response by neutrophils shows how azacytidine triggers an inflammatory response that it might be one of the reasons of the blast response. Furthermore, blast response patients were also enriched in heme metabolism (ES = 0.86, NES = 4.06 and FDR =<0.0001), protein secretion (ES = 0.90, NES = 3.03 and FDR =<0.0001) and oxidative phosphorylation (ES = 0.85, NES = 2.45 and FDR =<0.0001). In contrast, no pathways were enriched in non-response blast patients, showing the heterogeneity of the non-response patients.

Mechanisms involved in hematological and blast response to 5-Azacytidine

We evaluated the differences in GEP between patients getting a hematological response against the patients that did not. Interestingly, 426 genes were DE, 263 upregulated and 161 downregulated in response patients, pval < 0.01 (Figure 6).

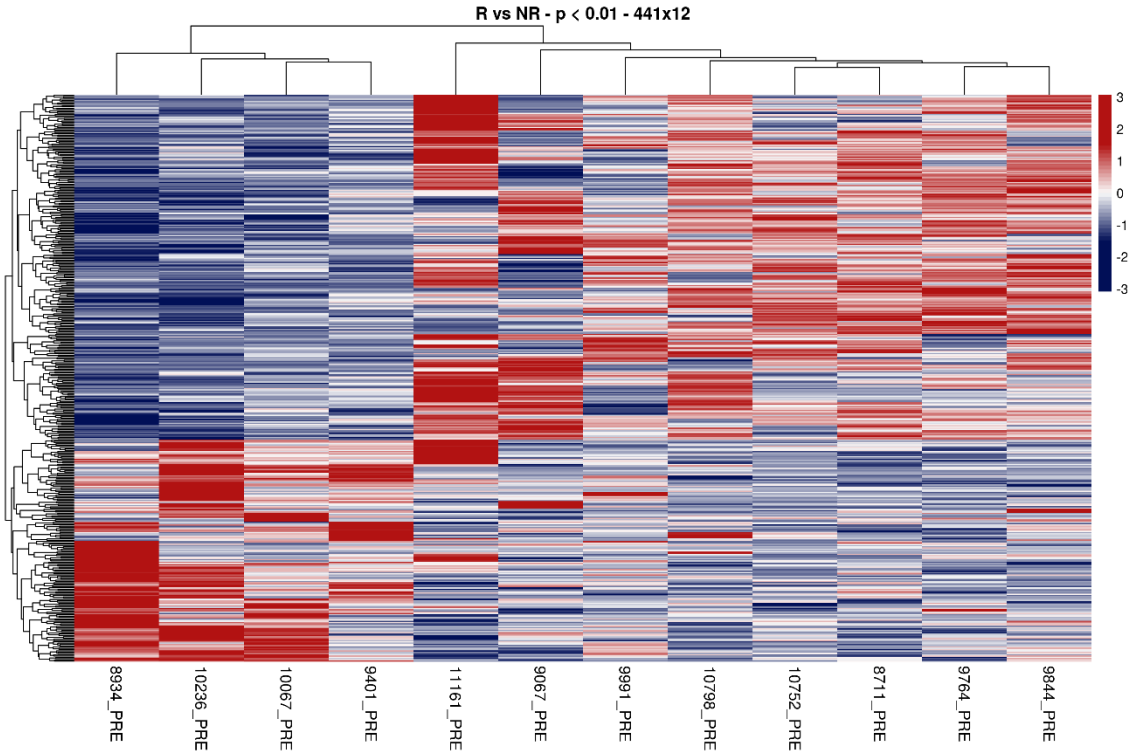

Figure 6. **Heatmap of the significant genes (pval < 0.01) from patients with hematological response *vs* non-responder patients in pretreated samples**. Gene expression profile clusters patients regarding its response. Red color means overexpression while blue color means underexpression of the genes. Gene signature of hematological responder patients showed a downregulation in transcription, specifically in RNA Polymerase II Transcription

Gene signature of hematological responder patients showed a downregulation in transcription, specifically in RNA Polymerase II Transcription (ES = -0.46, NES = -2.09, FDR = 0.028). Members of the nuclear receptor as *NR5A2* and *NR4A2*, or zinc finger protein as *ZNF14*, *ZNF3*, *ZNF484*, *ZNF92*, *ZNF664* and *ZNF169* were upregulated in non-response patients. Transcription is closely related to metabolism and so, the absent of mRNA may lead to a decreased rate of metabolism and moreover, to protection from cellular and genetic damage [32]. To further validate these results, we analyzed the genes expression in hematological responder patients, and compared to healthy controls. GSEA enrichment analysis, show the overrepresentation of oxidative phosphorylation (ES = 0.54, NES = 2.04 and FDR =0.025) and MYC targets (ES = 0.54 NES = 1.93 and FDR = 0.027). Oxidative phosphorylation is the metabolic pathway used by proliferative cells

where mitochondria produces ATP, suggesting that both pathways can be targeted by AZA [18]. Also, non-response patients were enriched in histone cluster 1, with a deregulated condensation of prophase chromosome and nucleosome assembly.

In summary, as expected blast and hematological responses were achieved by different pathways. Blast response needs the activation of immune system (neutrophil degranulation) while hematological response a narrow control of transcription. Recently Yuichi Murakami et al showed cytidine deaminase (*CDA*) as predictive gene for AZA therapeutic efficacy; Our data corroborate that this gene is upregulated in patients which respond to 5-Azacytidine [22].

To conclude, 5-Azacytidine induces changes in the mutational profile of patients with myeloid malignancies and reduces the mutation burden of *TP53* mutations. However, its action is not enough in most of the patients, and that could be the reason for the response and the relapse rate observed in the patients. The mutational status and the response to AZA are similar in BMMCS and hematopoietic stem cells. Moreover, AZA downregulated ribosomal proteins and enhanced immune cellular functions as well as upregulated genes related to all hematopoietic lineages that could be also related to the clinical benefit observed in patients treated with this drug.

Acknowledgments

This work was supported by grants from the Spanish Fondo de Investigaciones Sanitarias PI17/01741, PI18/01500, Instituto de Salud Carlos III (ISCIII), European Regional Development Fund (ERDF) “Una manera de hacer Europa”, “Consejería de Educación, Junta de Castilla y León” (SA271P18), “Proyectos de Investigación del SACYL”, Spain: GRS 1847/A/18, GRS 1653/A17, GRS 1850/A/18, from Red Temática de Investigación Cooperativa en Cáncer (RTICC) and Centro de Investigación Biomédica en Red de Cáncer (CIBERONC CB16/12/00233). JM Hernández Sánchez and AE Rodríguez Vicente are supported by a research grant by FEHH (“Fundación Española de Hematología y Hemoterapia”).

We are grateful to J. Blanco and F. Pescador for their contribution in the data collection of healthy donors. We thank I. Rodríguez, S. González, T.Prieto, M. Á. Ramos, A. Martín, A. Díaz, A.Simón, M.del Pozo, V. Gutiérrez and S.Pujante from Centro de Investigación del Cáncer, Salamanca, for their excelent technical assistance.

Authorship Contributions

JMHS designed the experiment, interpreted the results, performed bioinformatic analysis and wrote the manuscript; MDR, SC and AERV contributed to the interpretation of the results; MDC and JMHR performed patient selection and provided clinical data; JMHR, CP and AERV contributed to the interpretation of the results and wrote the manuscript. All authors revised the manuscript.

Conflict-of-interest disclosure

The authors declare no competing financial interests.

References

1. Nimer, S. D. Myelodysplastic syndromes. *Blood* **111**, 4841–4851 (2008).
2. Tefferi, A. & Vardiman, J. W. Myelodysplastic Syndromes. *N Engl J Med* **361**, 1872–1885 (2009).
3. Jabbour, E. *et al.* Acquisition of cytogenetic abnormalities in patients with IPSS defined lower-risk myelodysplastic syndrome is associated with poor prognosis and transformation to acute myelogenous leukemia. *Am. J. Hematol.* **88**, 831–837 (2013).
4. Bejar, R. *et al.* Clinical Effect of Point Mutations in Myelodysplastic Syndromes. *New England Journal of Medicine* **364**, 2496–2506 (2011).
5. Haferlach, T. *et al.* Landscape of genetic lesions in 944 patients with myelodysplastic syndromes. *Leukemia* **28**, 241–247 (2014).
6. Papaemmanuil, E. *et al.* Clinical and biological implications of driver mutations in myelodysplastic syndromes. *Blood* **122**, 3616–3627 (2013).
7. Fenaux, P. *et al.* Efficacy of azacitidine compared with that of conventional care regimens in the treatment of higher-risk myelodysplastic syndromes: a randomised, open-label, phase III study. *The Lancet Oncology* **10**, 223–232 (2009).
8. Montalban-Bravo, G. & Garcia-Manero, G. Myelodysplastic syndromes: 2018 update on diagnosis, risk-stratification and management. *Am J Hematol* **93**, 129–147 (2018).
9. Kaminskas, E. FDA Drug Approval Summary: Azacitidine (5-azacytidine, VidazaTM) for Injectable Suspension. *The Oncologist* **10**, 176–182 (2005).
10. Pierre Fenaux *et al.* Azacitidine (AZA) treatment prolongs overall survival (OS) in higher-risk MDS patients compared with conventional care regimens (CCR): Results of the AZA-001 phase III study. **110**, 817 (2007).
11. Silverman, L. R. *et al.* Randomized controlled trial of azacitidine in patients with the myelodysplastic syndrome: a study of the cancer and leukemia group B. *J. Clin. Oncol.* **20**, 2429–2440 (2002).

12. on behalf of The Spanish Group on Myelodysplastic Syndromes and PETHEMA Foundation, Spanish Society of Hematology *et al.* Effectiveness of azacitidine in unselected high-risk myelodysplastic syndromes: results from the Spanish registry. *Leukemia* **29**, 1875–1881 (2015).
13. Silverman, L. R. *et al.* Continued azacitidine therapy beyond time of first response improves quality of response in patients with higher-risk myelodysplastic syndromes: Continued Azacitidine in MDS. *Cancer* **117**, 2697–2702 (2011).
14. Xu, L. *et al.* Genomic landscape of CD34+ hematopoietic cells in myelodysplastic syndrome and gene mutation profiles as prognostic markers. *Proc. Natl. Acad. Sci. U.S.A.* **111**, 8589–8594 (2014).
15. Polgarova, K. *et al.* Somatic mutation dynamics in MDS patients treated with azacitidine indicate clonal selection in patients-responders. *Oncotarget* **8**, 111966–111978 (2017).
16. Bejar, R. *et al.* TET2 mutations predict response to hypomethylating agents in myelodysplastic syndrome patients. *Blood* **124**, 2705–2712 (2014).
17. Shastri, A., Will, B., Steidl, U. & Verma, A. Stem and progenitor cell alterations in myelodysplastic syndromes. *Blood* **129**, 1586–1594 (2017).
18. Stevens, B. M. *et al.* Characterization and targeting of malignant stem cells in patients with advanced myelodysplastic syndromes. *Nat Commun* **9**, 3694 (2018).
19. **.**Hollenbach, P. W. et al. A *Comparison of Azacitidine and Decitabine Activities in Acute Myeloid Leukemia Cell Lines*. PLoS ONE 5, e9001 (2010).
20. Öz, S. *et al.* Quantitative determination of decitabine incorporation into DNA and its effect on mutation rates in human cancer cells. *Nucleic Acids Research* **42**, e152–e152 (2014).
21. Signer, R. A. J., Magee, J. A., Salic, A. & Morrison, S. J. Haematopoietic stem cells require a highly regulated protein synthesis rate. *Nature* **509**, 49–54 (2014).

22. Murakami, Y. *et al.* The augmented expression of the cytidine deaminase gene by 5-azacytidine predicts therapeutic efficacy in myelodysplastic syndromes. *Oncotarget* **10**, 2270–2281 (2019).
23. Shvarts, A. *et al.* Isolation and identification of the human homolog of a new p53-binding protein, Mdmx. *Genomics* **43**, 34–42 (1997).
24. Gao, J. *et al.* Integrative Analysis of Complex Cancer Genomics and Clinical Profiles Using the cBioPortal. *Science Signaling* **6**, pl1–pl1 (2013).
25. Pant, V. *et al.* Tumorigenesis promotes *Mdm4-S* overexpression. *Oncotarget* **8**, (2017).
26. Collins, C. T. & Hess, J. L. Role of HOXA9 in leukemia: dysregulation, cofactors and essential targets. *Oncogene* **35**, 1090–1098 (2016).
27. Galili, N. & Raza, A. Clinical implications of gene expression profiling in myelodysplastic syndromes: recognition of ribosomal and translational gene dysregulation and development of predictive assays. *Best Pract Res Clin Haematol* **22**, 223–237 (2009).
28. Monika Belickova, M. *et al.* Up-regulation of ribosomal genes is associated with a poor response to azacitidine in myelodysplasia and related neoplasms. *International Journal of Hematology* **104**, 566–573 (2016).
29. Rinker, E. B. *et al.* Differential expression of ribosomal proteins in myelodysplastic syndromes. *J Clin Pathol* **69**, 176–180 (2016).
30. Gagnon-Kugler, T., Langlois, F., Stefanovsky, V., Lessard, F. & Moss, T. Loss of Human Ribosomal Gene CpG Methylation Enhances Cryptic RNA Polymerase II Transcription and Disrupts Ribosomal RNA Processing. *Molecular Cell* **35**, 414–425 (2009).
31. Sridhar, K., Ross, D. T., Tibshirani, R., Butte, A. J. & Greenberg, P. L. Relationship of differential gene expression profiles in CD34+ myelodysplastic syndrome marrow cells to disease subtype and progression. *Blood* **114**, 4847–4858 (2009).
32. Freter, R., Osawa, M. & Nishikawa, S.-I. Adult Stem Cells Exhibit Global Suppression of RNA Polymerase II Serine-2 Phosphorylation. *STEM CELLS* **28**, 1571–1580 (2010).

General Discussion

Precision medicine (PM) moves away from the "one size fit all" approach. The main purpose of this concept is to individually tailored health care bases on person´s genes [112]. After a decade of work and more than 3 billion (US $) the first human genome was sequenced in 2001 [13,14]. Technological advances have empowered the implementation of precision medicine, mainly due to the lower cost and time to sequence. Nowadays, today, one genome can be sequenced in 1 day for less than 1,000$ [113]. The evidences that genetics influence in drug response have rapidly increased the interest in pharmacogenomics (PKG). This relative new field use "*omic*" information to individualize therapy. Firstly, PKG was focused on single nucleotide polymorphism (SNP) to identify which could anticipate any clinical characteristic in terms of efficacy (response) and security (side adverse effects) [114]. Furthermore RNA analysis has also showed the utility as a predictive factor to identify patients that will benefit from specific therapies [102] . One of the most major proof of concept is the use of multigene mRNA-based prognosis assays in breast cancer. RNA is a dynamic and diverse biomolecule that has an essential role in biological process, physiologic or disease related. The most widely used techniques for quantify messenger RNA (mRNA) are qPCR and arrays as well as, through the knowledge acquired during the human genome sequenced, the RNAseq [115].

Pharmacogenomics studies are relevant for the detection of unexpected side effects in patients, not only adverse but also therapeutic. Thus, it could be implemented in the clinical settings for the better study of patients. Moreover, there is a need to carry out studies from bench to bedside and back again. These studies will foreground the biological pathways upset by the therapy. Besides, PM can be performed in any patient with a specific disease and therapy. Cancer precision medicine aim to personalize

treatments in cancer patients, however the implementation is associated with a number of challenges, including the tumor heterogeneity and the clinical presentations.

To overtake this issue, paired analysis, in which the patient is suited before receiving and during the therapy, can be used. This new approach will be focus in the therapy-induced changes while avoiding patients´ heterogeneity. This PhD work strongly supports the idea to combine new massive tools with the use of paired patient samples to better understand how the drugs are modifying the gene expression profiles at cellular level.

Primary immune thrombocytopenia a rare autoimmune disorder, usually treated with thrombopoietin receptor agonist as second line therapy. At present, romiplostim and eltrombopag are approved for this indication. Recently, eltrombopag has demonstrated a role in aplastic anemia however the biological mechanisms of this effect are not fully elucidated. In this PhD work, eltrombopag showed an upregulation of megakaryocytic lineage related genes, such as *PPBP*, *ITGB3*, *ITGA2B*, *F13A1, F13A1*, *MYL9* and *ITGA2B* evidencing one of the effects induced by the treatment. These results confirmed previous reports *in vitro* and *ex vivo* experiments [116]. Thus, our results confirm *in vivo* the ability of eltrombopag inducing megakaryopoiesis, hence confirming that the increment in platelet count can be the effect of an increment of megakaryocytes and not only the consequence of the decrease in destruction. Thus, these findings point that the platelet increment could be due to a crucial change in megakaryopoiesis-related genes

Moreover, the treatment induced an upregulation of several genes related with the transcription factor *RUNX1* such as *GP1BA, PF4, ITGA2B* and *MYL9*. *RUNX1* have been revealed as required for the hemostasis of hematopoietic stem cell and progenitor cells

suggesting that the hematopoiesis improvement observed in ITP and an aplastic anemia can be governed by this gene[117].

Gene expression studies also show an immunomodulatory effect induced by eltrombopag. This was the result of the regulation of TNFα and IFN-γ, standing out key hematopoietic regulators genes, as *KLF4*, *HES1* and *EGR1* which have been proposed to play an important role in aplastic anemia [118]. Moreover, *IFN-γ, IFN-α* and *IL2-STAT5*, are involved in the innate and adaptive immune response, which is altered in ITP patients and could be related to a reduction in platelet counts [119].

Evaluation of eltrombopag relapse patients show up only 21 genes differentially expressed when compared with responder patients during the treatment. Interestingly all the genes were identified as GATA-1 target genes or related directly with erythropoiesis. Among all the twenty-one genes *BCL2L1,* also known as Bcl-X, highlighted. This proapoptotic gene plays an important role in erythropoiesis. Thus, Bcl-X is upregulated in a GATA-1-dependent manner during erythroid differentiation [120]. The overexpression of Bcl-X in patients who did not response to eltrombopag, was correlated with GATA-1 expression. Thus, the regulation between *GATA-1* and *Bcl-X* is altered in non-responder patients, since an increment in the hemoglobin levels but not in platelet counts was observed.

Myelodysplastic syndromes (MDS) are a group of heterogeneous clonal hematopoietic stem cell disorders associated with a myeloid differentiation blockade leading to bone marrow (BM) accumulation of myeloid progenitor cells and peripheral blood (PB) cytopenias [121]. MDS patients can be classify according with the international prognostic scoring system. The IPSS-R classifies MDS patients based on the proportion of blasts in

the BM, cytogenetic abnormalities, and the degree of peripheral cytopenias, each considered individually (hemoglobin, platelet and neutrophil levels). Low risk MDS (very low or low), usually present anemia and red blood cell transfusions are required. However, patients that become transfusion dependence finally get iron overload [122]. Iron overload have shown a negative impact in survival of MDS patients [123], for this reason iron chelation is required. Deferasirox, is an orally chelation widely used in low low-risk MDS and also in high-risk MDS [124,125]. Gene expression profile of low risk MDS patients showed how Deferasirox upregulated more than 1,400 genes and 50 miRNAs. Treatment induced a downregulation of Nf kB pathway through the downregulation of *NFKBIA*, *RELA*, *TANK*, *CXCL* and *INFG* among others as well as in ROS (*NFE2L2/NRF2*) regulation, which was previously reported in cell lines [126]. These data provided a biological explanation for the hemoglobin improvement showed in some patients treated with this iron chelator [127] and support the utility of PKG studies in patients. Moreover, *GFI1* a critical player in hematopoiesis, which activate erythroid and megakaryocyte lineages [128], was upregulated by deferasirox suggesting the importance of its activation for the improvement in hemoglobin and platelet levels in patients treated with deferasirox [129].

MDS patients can have a higher risk score by the IPSS-R, comprising intermediate to high or very high [60]. These patients showed a shorter overall survival ranging from 0.8-3 years. The only curative therapy is the stem cell transplantation, however not all the patients are eligible because the usually are elderly. Hypomethylating agents are the first line treatment for most of the patients with intermediate-high risk MDS [56]. 5-Azacytidine and decitabine were approved after clinical trials comparing with best supportive care

therapy. However in daily clinical used these results could not be confirmed by the Spanish MDS group, suggesting the need to select patients that will benefit for the treatment [71]. To further evaluate the biological pathways deregulated by the therapy in hematopoietic stem cells, isolated bone marrow CD34+ cells were isolated from fourteen 14 patients. Of note, both DNA and RNA-seq studies were carried out in these serial samples [130].

Gene target sequencing highlight a strong correlation between CD34+ cells and mononuclear bone marrow cells. All the mutations were present in both cell types and interestingly they also displayed a similar variant allele frequency (VAF). These results suggest the needless isolation of CD34+ to track mutations in MDS since similar results can be obtained analyzing bone marrow mononuclear cells. Previous studies have shown different mutations pattern among common myeloid progenitor (CMP), granulocyte-macrophage progenitor (GMP) and megakaryocyte-erythroid progenitor (MEP) [131,132]; however, isolation of these progenitor is laborious and not feasible for clinical routine. Our study will support the use of mononuclear cells to track NDA mutations, allowing the use of this approach in the clinical setting.

Interestingly, the dynamics of mutational profile, comparing mutations before and during AZA treatment, showed a shift in some of the patients and more important in those patients harboring *TP53*, point out the effect of the therapy on *TP53* clones [133]. Moreover, three mutations in *NRAS* and *KRAS* arise during the therapy. Mutations in these genes have been correlated with high risk of progression to AML [134]. All together, these results showed that next generation sequencing is a feasible technique to track MDS/AML mutations along treatment.

We further analyzed changes in the gene expression profile (GEP) in CD34+ cells before and during AZA treatment by RNAseq. It is already known how AZA target ribosomal complex due to its interaction with RNA [135]. In our study, we compared the GEP from patients before the treatment and healthy control (aged matched), identifying the upregulation of ribosomal complex. Interestingly we further analyze the GEP during the treatment and confirmed not only the downregulation of the rRNA but also that there were not significantly differences with control samples. By contrast, translation gene set was still upregulated in the MDS patients groups. Some recent studies suggested to pharmacologically target this pathway to eradicated MDS stem cell [132]. Protein synthesis plays an important role in leukemogenesis and to maintain the self-renewal and survival in normal HSC [136]. This data will support the use of a drug that can inhibit protein translation in combination with 5-Azacytidine.

Moreover, the comparison between pre-treated samples and AZA shows an upregulation in immune system genes, involving the upregulation of neutrophil degranulation and the immunoglobulin genes. Our results suggest how AZA therapy stimulate the differentiation of hematopoietic cell lineages: T-Lymphocytes (*CD3*, *CD4*, *CD7* and *CD38*), B-Lymphocytes (*CD38* and *CD35*), neutrophils (*CD125* and *CD121*) and megakaryocytes (*CD9*, *CD14*, *CD41* and *CD61*). All these data, performed in CD34+ cells, are providing new insights in the knowledge of the mechanism of action of AZA: these drug is not just a demethylating agent. However AZA also works upregulating the immune system and the subsets of hematolpoietic cells as well as decreasing the protein synthesis.

Taking all these data together, we showed in this PhD work how pharmacogenomics can help to understand the biological pathways altered by drugs. Moreover, the implementation of wide-transcriptome analysis in clinical trials can lay the groundwork for the use of therapies in other pathologies based in patients' response. The combination of the new massive methodologies to analyze the genome with the isolation of specific subsets of hematopoietic cells to be analyze and the use of serial samples of patients is providing an in-deep knowledge of the cellular mechanisms involved by the therapies currently used in the management of patients with hematological diseases.

Concluding remarks

1. General

1.1. Gene expression profile (GEP) can be used for the better understanding of the drug mechanisms of action. GEP identify biological pathways involved in clinical outcomes. Paired studies, where the same patient is analyzing before and during the treatment, boost the identification of the biological pathways affected by the therapy.

1.2. Next Generation Sequencing (NGS) allows the efficient screening of DNA and RNA samples. This technique is feasible by its implementation in clinical routine laboratories. Integration of NGS and pharmacogenetics, in addition to the increased genetics information from daily clinical laboratories, will enhance the personalize medicine.

2. Specific

2.1. Eltrombopag increased the number of platelets while stimulates megakaryocyte proliferation and differentiation:

2.1.1. Eltrombopag upregulated *PPBP, ITGB3, TUBB1, TREML1, MYL9, ITGA2B,* and *F13A1* genes, which are involved in megakaryocyte differentiation. In addition, eltrombopag deregulated IFN-γ and *IFN-α*, involved in the innate and adaptive immune response, which is altered in ITP patients. Taking all together, eltrombopag increased platelet counts by two ways, stimulating megakaryopoiesis and regulating the immune response.

2.1.2. This drug regulated TNFα. This effect could be related to the hematopoiesis improvement observed in patients with aplastic anemia treated with eltrombopag.

2.1.3. Relapsed ITP patients to eltrombopag showed a high expression of *BCL2L1*, being this overexpression correlated with the transcription factor *GATA-1*. Both proteins are involved in erythropoiesis and might be used as biomarkers to predict the lack of response to eltrombopag.

2.2. The use of the iron chelation deferasirox in patients with MDS downregulated Nf kB pathway, nitric oxide (NO) and reactive oxygen species (ROS) as well as the hypoxia-related genes while stimulating erythropoiesis:

2.2.1. The *in vivo* downregulation of Nf kB pathway is carried out by *BCL10*, *IL1B*, *NFKBIA*, *RIPK1*, *RELA*, *BID*, *BIRC2* and *TANK*. Reduction of pro-inflammatory cytokines could be related to the decreased need of transfusions observed in these patients.

2.2.2. Transcriptional Regulator Nuclear Factor Erythroid 2 *NFE2L2/NRF2* is inhibited by deferasirox decreasing ROS. In addition, deferasirox activated Growth factor Independent 1 Transcriptional Repressor (*GFI1*), which is a master regulator of hematopoiesis, activating mega and erythropoiesis. Furthermore, *IL-1* and gamma interferon (inhibitors of erythropoiesis) were downregulated by the treatment.

Taking all together, these results provided the biological basis for some of the clinical results observed in MDS patients treated with deferasirox.

2.3. The hypomethylating agent 5-Azacytidine restored the expression of high-risk MDS in CD34+ isolated cells. Moreover, also induced a reduction in some DNA mutations in MDS patients:

2.3.1. Ribosomal complex proteins, which are overexpressed in high-risk MDS, showed a reduction during AZA treatment.

2.3.2. AZA induced the overexpression of immune system, showing an upregulation of immunoglobulin genes, IG heavy chain, kappa and lambda related genes.

2.3.3. *MDM4*, *HOXA6* and *HOXA9*, which have been proposed to have a leukemogenic effect in MDS and AML, were downregulated by the treatment.

2.3.4. AZA showed an overexpression of markers of hematopoietic cell lineages, that could be related to hematological improvement observed in the patients

2.3.5. Patients who achieved any type of response to AZA showed an involvement of immune system genes. CD34+ cells from responder patients displayed an activation of neutrophil degranulation.

2.3.6. AZA reduced the number of mutations in *TP53*, supporting the use if this drug in patients with myeloid malignancies and *TP53* mutations.

References

1. Badalian-Very, G. Personalized medicine in hematology — A landmark from bench to bed. *Computational and Structural Biotechnology Journal* **10**, 70–77 (2014).
2. Daly, A. K. Pharmacogenetics: a general review on progress to date. *British Medical Bulletin* 1–15 (2017). doi:10.1093/bmb/ldx035
3. Jameson, J. L. & Longo, D. L. Precision Medicine — Personalized, Problematic, and Promising. *N Engl J Med* **372**, 2229–2234 (2015).
4. Collins, F. S. & Varmus, H. A New Initiative on Precision Medicine. *N Engl J Med* **372**, 793–795 (2015).
5. Porche, D. J. Precision Medicine Initiative. *Am J Mens Health* **9**, 177–177 (2015).
6. Zampieri, M., Sekar, K., Zamboni, N. & Sauer, U. Frontiers of high-throughput metabolomics. *Current Opinion in Chemical Biology* **36**, 15–23 (2017).
7. Afghahi, A. & Sledge, G. W. Targeted Therapy for Cancer in the Genomic Era: *The Cancer Journal* **21**, 294–298 (2015).
8. Weinshilboum, R. M. & Wang, L. Pharmacogenomics: Precision Medicine and Drug Response. *Mayo Clinic Proceedings* **92**, 1711–1722 (2017).
9. Manolio, T. A. *et al.* Implementing genomic medicine in the clinic: the future is here. *Genet Med* **15**, 258–267 (2013).
10. Pirmohamed, M. & Hughes, D. A. Pharmacogenetic tests: the need for a level playing field. *Nat Rev Drug Discov* **12**, 3–4 (2013).
11. Rodríguez-Vicente, A. E. *et al.* Pharmacogenetics and pharmacogenomics as tools in cancer therapy. *Drug Metabolism and Personalized Therapy* **31**, (2016).
12. Wadelius, M. & Alfirevic, A. Pharmacogenomics and personalized medicine: the plunge into next-generation sequencing. *Genome Med* **3**, 78 (2011).
13. International Human Genome Sequencing Consortium. Initial sequencing and analysis of the human genome. *Nature* **409**, 860–921 (2001).

14. Venter, J. C. *et al.* The sequence of the human genome. *Science* **291**, 1304–1351 (2001).
15. Haga, S. B. & LaPointe, N. M. A. The potential impact of pharmacogenetic testing on medication adherence. *Pharmacogenomics J* **13**, 481–483 (2013).
16. Evans, W. E. & McLeod, H. L. Pharmacogenomics--drug disposition, drug targets, and side effects. *N. Engl. J. Med.* **348**, 538–549 (2003).
17. The International Warfarin Pharmacogenetics Consortium. Estimation of the Warfarin Dose with Clinical and Pharmacogenetic Data. *N Engl J Med* **360**, 753–764 (2009).
18. Mega, J. L. *et al.* Cytochrome P-450 Polymorphisms and Response to Clopidogrel. *N Engl J Med* **360**, 354–362 (2009).
19. Wang, L. & Weinshilboum, R. Thiopurine S-methyltransferase pharmacogenetics: insights, challenges and future directions. *Oncogene* **25**, 1629–1638 (2006).
20. Hulsen, T. *et al.* From Big Data to Precision Medicine. *Front. Med.* **6**, 34 (2019).
21. Abul-Husn, N. S. & Kenny, E. E. Personalized Medicine and the Power of Electronic Health Records. *Cell* **177**, 58–69 (2019).
22. Li, J., Li, X., Zhang, S. & Snyder, M. Gene-Environment Interaction in the Era of Precision Medicine. *Cell* **177**, 38–44 (2019).
23. Evans, J. P., Meslin, E. M., Marteau, T. M. & Caulfield, T. Deflating the Genomic Bubble. *Science* **331**, 861–862 (2011).
24. Deng, X. & Nakamura, Y. Cancer Precision Medicine: From Cancer Screening to Drug Selection and Personalized Immunotherapy. *Trends in Pharmacological Sciences* **38**, 15–24 (2017).
25. Hirsch, F. R. *et al.* Epidermal Growth Factor Receptor in Non–Small-Cell Lung Carcinomas: Correlation Between Gene Copy Number and Protein Expression and Impact on Prognosis. *JCO* **21**, 3798–3807 (2003).
26. O'Brien, S. G. *et al.* Imatinib compared with interferon and low-dose cytarabine for newly diagnosed chronic-phase chronic myeloid leukemia. *N. Engl. J. Med.* **348**, 994–1004 (2003).

27. Hurvitz, S. A. & Pietras, R. J. Rational management of endocrine resistance in breast cancer: A comprehensive review of estrogen receptor biology, treatment options, and future directions. *Cancer* **113**, 2385–2397 (2008).
28. Pierre Fenaux *et al.* Azacitidine (AZA) treatment prolongs overall survival (OS) in higher-risk MDS patients compared with conventional care regimens (CCR): Results of the AZA-001 phase III study. **110**, 817 (2007).
29. Silverman, L. R. *et al.* Randomized controlled trial of azacitidine in patients with the myelodysplastic syndrome: a study of the cancer and leukemia group B. *J. Clin. Oncol.* **20**, 2429–2440 (2002).
30. Cheng, G. *et al.* Eltrombopag for management of chronic immune thrombocytopenia (RAISE): a 6-month, randomised, phase 3 study. *The Lancet* **377**, 393–402 (2011).
31. Ghanima, W., Cooper, N., Rodeghiero, F., Godeau, B. & Bussel, J. B. Thrombopoietin receptor agonists: Ten Years Later. *Haematologica* haematol.2018.212845 (2019). doi:10.3324/haematol.2018.212845
32. Rodeghiero, F. *et al.* Standardization of bleeding assessment in immune thrombocytopenia: report from the International Working Group. *Blood* **121**, 2596–2606 (2013).
33. Lambert, M. P. & Gernsheimer, T. B. Clinical updates in adult immune thrombocytopenia. *Blood* **129**, 2829–2835 (2017).
34. Cuker, A., Cines, D. B. & Neunert, C. E. Controversies in the treatment of immune thrombocytopenia: *Current Opinion in Hematology* **23**, 479–485 (2016).
35. Matschke, J. *et al.* A Randomized Trial of Daily Prednisone versus Pulsed Dexamethasone in Treatment-Naïve Adult Patients with Immune Thrombocytopenia: EIS 2002 Study. *Acta Haematol* **136**, 101–107 (2016).

36. Mithoowani, S. *et al.* High-dose dexamethasone compared with prednisone for previously untreated primary immune thrombocytopenia: a systematic review and meta-analysis. *The Lancet Haematology* **3**, e489–e496 (2016).
37. Neunert, C. *et al.* The American Society of Hematology 2011 evidence-based practice guideline for immune thrombocytopenia. *Blood* **117**, 4190–4207 (2011).
38. Wang, B., Nichol, J. L. & Sullivan, J. T. Pharmacodynamics and pharmacokinetics of AMG 531, a novel thrombopoietin receptor ligand. *Clin. Pharmacol. Ther.* **76**, 628–638 (2004).
39. Erickson-Miller, C. L. *et al.* Discovery and characterization of a selective, nonpeptidyl thrombopoietin receptor agonist. *Exp. Hematol.* **33**, 85–93 (2005).
40. Toltl, L. J. & Arnold, D. M. Pathophysiology and management of chronic immune thrombocytopenia: focusing on what matters: Annotation. *British Journal of Haematology* **152**, 52–60 (2011).
41. Ogawara, H. *et al.* High Th1/Th2 ratio in patients with chronic idiopathic thrombocytopenic purpura. *Eur. J. Haematol.* **71**, 283–288 (2003).
42. Schifferli, A. & Kühne, T. Thrombopoietin receptor agonists: a new immune modulatory strategy in immune thrombocytopenia? *Seminars in Hematology* **53**, S31–S34 (2016).
43. Audia, S., Mahévas, M., Samson, M., Godeau, B. & Bonnotte, B. Pathogenesis of immune thrombocytopenia. *Autoimmunity Reviews* **16**, 620–632 (2017).
44. Gonzalez-Porras, J. R. & Bastida, J. M. Eltrombopag in immune thrombocytopenia: efficacy review and update on drug safety. *Therapeutic Advances in Drug Safety* **9**, 263–285 (2018).
45. Garnock-Jones, K. P. & Keam, S. J. Eltrombopag: *Drugs* **69**, 567–576 (2009).
46. Desmond, R., Townsley, D. M., Dunbar, C. & Young, N. S. Eltrombopag in Aplastic Anemia. *Seminars in Hematology* **52**, 31–37 (2015).
47. Tefferi, A. & Vardiman, J. W. Myelodysplastic Syndromes. *N Engl J Med* **361**, 1872–1885 (2009).

48. Arber, D. A. *et al.* The 2016 revision to the World Health Organization classification of myeloid neoplasms and acute leukemia. *Blood* **127**, 2391–2405 (2016).
49. Neukirchen, J. *et al.* Incidence and prevalence of myelodysplastic syndromes: Data from the Düsseldorf MDS-registry. *Leukemia Research* **35**, 1591–1596 (2011).
50. Rollison, D. E. *et al.* Epidemiology of myelodysplastic syndromes and chronic myeloproliferative disorders in the United States, 2001-2004, using data from the NAACCR and SEER programs. *Blood* **112**, 45–52 (2008).
51. Nisse, C. *et al.* Exposure to occupational and environmental factors in myelodysplastic syndromes. Preliminary results of a case-control study. *Leukemia* **9**, 693–699 (1995).
52. Sun, L.-M., Lin, C.-L., Lin, M.-C., Liang, J.-A. & Kao, C.-H. Radiotherapy- and Chemotherapy-Induced Myelodysplasia Syndrome: A Nationwide Population-Based Nested Case–Control Study. *Medicine* **94**, e737 (2015).
53. Malcovati, L. *et al.* Diagnosis and treatment of primary myelodysplastic syndromes in adults: recommendations from the European LeukemiaNet. *Blood* **122**, 2943–2964 (2013).
54. Adès, L., Itzykson, R. & Fenaux, P. Myelodysplastic syndromes. *The Lancet* **383**, 2239–2252 (2014).
55. Bastida, J. M. *et al.* Hidden myelodysplastic syndrome (MDS): A prospective study to confirm or exclude MDS in patients with anemia of uncertain etiology. *International Journal of Laboratory Hematology* **41**, 109–117 (2019).
56. Montalban-Bravo, G. & Garcia-Manero, G. Myelodysplastic syndromes: 2018 update on diagnosis, risk-stratification and management. *Am J Hematol* **93**, 129–147 (2018).
57. Gerstung, M. *et al.* Combining gene mutation with gene expression data improves outcome prediction in myelodysplastic syndromes. *Nat Commun* **6**, 5901 (2015).
58. Kennedy, J. A. & Ebert, B. L. Clinical Implications of Genetic Mutations in Myelodysplastic Syndrome. *JCO* **35**, 968–974 (2017).

59. Greenberg, P. *et al.* International scoring system for evaluating prognosis in myelodysplastic syndromes. *Blood* **89**, 2079–2088 (1997).
60. Greenberg, P. L. *et al.* Revised International Prognostic Scoring System for Myelodysplastic Syndromes. *Blood* **120**, 2454–2465 (2012).
61. Della Porta, M. G. *et al.* Validation of WHO classification-based Prognostic Scoring System (WPSS) for myelodysplastic syndromes and comparison with the revised International Prognostic Scoring System (IPSS-R). A study of the International Working Group for Prognosis in Myelodysplasia (IWG-PM). *Leukemia* **29**, 1502–1513 (2015).
62. Malcovati, L. *et al.* Time-dependent prognostic scoring system for predicting survival and leukemic evolution in myelodysplastic syndromes. *J. Clin. Oncol.* **25**, 3503–3510 (2007).
63. Ok, C. Y. *et al.* Application of the international prognostic scoring system-revised in therapy-related myelodysplastic syndromes and oligoblastic acute myeloid leukemia. *Leukemia* **28**, 185–189 (2014).
64. DeZern, A. E. Nine years without a new FDA-approved therapy for MDS: how can we break through the impasse? *Hematology* **2015**, 308–316 (2015).
65. Gattermann, N. *et al.* Deferasirox in iron-overloaded patients with transfusion-dependent myelodysplastic syndromes: Results from the large 1-year EPIC study. *Leukemia Research* **34**, 1143–1150 (2010).
66. Derissen, E. J. B., Beijnen, J. H. & Schellens, J. H. M. Concise Drug Review: Azacitidine and Decitabine. *The Oncologist* **18**, 619–624 (2013).
67. Esteller, M. Epigenetics in Cancer. *N Engl J Med* **358**, 1148–1159 (2008).
68. Issa, J.-P. Epigenetic Changes in the Myelodysplastic Syndrome. *Hematology/Oncology Clinics of North America* **24**, 317–330 (2010).
69. Stresemann, C. & Lyko, F. Modes of action of the DNA methyltransferase inhibitors azacytidine and decitabine. *Int. J. Cancer* **123**, 8–13 (2008).

70. Garcia-Manero, G. Myelodysplastic syndromes: 2015 Update on diagnosis, risk-stratification and management: Myelodysplastic Syndromes: 2015 Update. *Am. J. Hematol.* **90**, 831–841 (2015).
71. on behalf of The Spanish Group on Myelodysplastic Syndromes and PETHEMA Foundation, Spanish Society of Hematology *et al.* Effectiveness of azacitidine in unselected high-risk myelodysplastic syndromes: results from the Spanish registry. *Leukemia* **29**, 1875–1881 (2015).
72. Sanchez-Garcia, J. *et al.* Prospective randomized trial of 5 days azacitidine versus supportive care in patients with lower-risk myelodysplastic syndromes without 5q deletion and transfusion-dependent anemia. *Leukemia & Lymphoma* **59**, 1095–1104 (2018).
73. Steensma, D. P. Myelodysplastic syndromes current treatment algorithm 2018. *Blood Cancer Journal* **8**, 47 (2018).
74. Shenoy, N., Vallumsetla, N., Rachmilewitz, E., Verma, A. & Ginzburg, Y. Impact of iron overload and potential benefit from iron chelation in low-risk myelodysplastic syndrome. *Blood* **124**, 873–881 (2014).
75. Hellström-Lindberg, E. *et al.* Erythroid response to treatment with G-CSF plus erythropoietin for the anaemia of patients with myelodysplastic syndromes: proposal for a predictive model. *Br. J. Haematol.* **99**, 344–351 (1997).
76. Santini, V. *et al.* Can the revised IPSS predict response to erythropoietic-stimulating agents in patients with classical IPSS low or intermediate-1 MDS? *Blood* **122**, 2286–2288 (2013).
77. List, A. *et al.* Lenalidomide in the Myelodysplastic Syndrome with Chromosome 5q Deletion. *N Engl J Med* **355**, 1456–1465 (2006).
78. List, A. *et al.* Efficacy of lenalidomide in myelodysplastic syndromes. *N. Engl. J. Med.* **352**, 549–557 (2005).

79. Malcovati, L. *et al.* Prognostic factors and life expectancy in myelodysplastic syndromes classified according to WHO criteria: a basis for clinical decision making. *J. Clin. Oncol.* **23**, 7594–7603 (2005).

80. Kontoyiannis, D. P. *et al.* Increased bone marrow iron stores is an independent risk factor for invasive aspergillosis in patients with high-risk hematologic malignancies and recipients of allogeneic hematopoietic stem cell transplantation. *Cancer* **110**, 1303–1306 (2007).

81. Pullarkat, V. *et al.* Iron overload adversely affects outcome of allogeneic hematopoietic cell transplantation. *Bone Marrow Transplant.* **42**, 799–805 (2008).

82. Sánchez, M., Sabio, L., Gálvez, N., Capdevila, M. & Dominguez-Vera, J. M. Iron chemistry at the service of life. *IUBMB Life* **69**, 382–388 (2017).

83. Piga, A. *et al.* High nontransferrin bound iron levels and heart disease in thalassemia major. *Am. J. Hematol.* **84**, 29–33 (2009).

84. Brissot, P., Ropert, M., Le Lan, C. & Loréal, O. Non-transferrin bound iron: A key role in iron overload and iron toxicity. *Biochimica et Biophysica Acta (BBA) - General Subjects* **1820**, 403–410 (2012).

85. Shah, J., Kurtin, S. E., Arnold, L., Lindroos-Kolqvist, P. & Tinsley, S. Management of Transfusion-Related Iron Overload in Patients With Myelodysplastic Syndromes. *Clinical Journal of Oncology Nursing* **16**, 37–46 (2012).

86. Killick, S. B. Iron chelation therapy in low risk myelodysplastic syndrome. *Br. J. Haematol.* **177**, 375–387 (2017).

87. Lyons, R. M. *et al.* Relation between chelation and clinical outcomes in lower-risk patients with myelodysplastic syndromes: Registry analysis at 5 years. *Leuk. Res.* **56**, 88–95 (2017).

88. Santini, V. *et al.* Clinical management of myelodysplastic syndromes: update of SIE, SIES, GITMO practice guidelines. *Leukemia Research* **34**, 1576–1588 (2010).

89. Cermak, J. *et al.* A comparative study of deferasirox and deferiprone in the treatment of iron overload in patients with myelodysplastic syndromes. *Leukemia Research* **37**, 1612–1615 (2013).

90. Ghoti, H. *et al.* Increased serum hepcidin levels during treatment with deferasirox in iron-overloaded patients with myelodysplastic syndrome: Increased Serum Hepcidin Levels During Treatment. *British Journal of Haematology* **153**, 118–120 (2011).

91. Tataranni, T. *et al.* The iron chelator deferasirox affects redox signalling in haematopoietic stem/progenitor cells. *Br J Haematol* **170**, 236–246 (2015).

92. Adams, D. R. & Eng, C. M. Next-Generation Sequencing to Diagnose Suspected Genetic Disorders. *N Engl J Med* **379**, 1353–1362 (2018).

93. Bastida, J. M. *et al.* Introducing high-throughput sequencing into mainstream genetic diagnosis practice in inherited platelet disorders. *Haematologica* **103**, 148–162 (2018).

94. Cyranoski, D. China embraces precision medicine on a massive scale. *Nature* **529**, 9–10 (2016).

95. Bombard, Y., Bach, P. B. & Offit, K. Translating genomics in cancer care. *J Natl Compr Canc Netw* **11**, 1343–1353 (2013).

96. Bastida, J. M. *et al.* Two novel variants of the *ABCG5* gene cause xanthelasmas and macrothrombocytopenia: a brief review of hematologic abnormalities of sitosterolemia. *Journal of Thrombosis and Haemostasis* **15**, 1859–1866 (2017).

97. Dasi, M. A. *et al.* Uniparental disomy causes deficiencies of vitamin K-dependent proteins. *Journal of Thrombosis and Haemostasis* **14**, 2410–2418 (2016).

98. Bejar, R. *et al.* Clinical Effect of Point Mutations in Myelodysplastic Syndromes. *New England Journal of Medicine* **364**, 2496–2506 (2011).

99. Ortmann, C. A. *et al.* Effect of Mutation Order on Myeloproliferative Neoplasms. *N Engl J Med* **372**, 601–612 (2015).

100. Papaemmanuil, E. *et al.* Genomic Classification and Prognosis in Acute Myeloid Leukemia. *N Engl J Med* **374**, 2209–2221 (2016).

101. Beck, T. F., Mullikin, J. C., on behalf of the NISC Comparative Sequencing Program & Biesecker, L. G. Systematic Evaluation of Sanger Validation of Next-Generation Sequencing Variants. *Clinical Chemistry* **62**, 647–654 (2016).

102. Byron, S. A., Van Keuren-Jensen, K. R., Engelthaler, D. M., Carpten, J. D. & Craig, D. W. Translating RNA sequencing into clinical diagnostics: opportunities and challenges. *Nat Rev Genet* **17**, 257–271 (2016).

103. Heid, C. A., Stevens, J., Livak, K. J. & Williams, P. M. Real time quantitative PCR. *Genome Res.* **6**, 986–994 (1996).

104. Lockhart, D. J. *et al.* Expression monitoring by hybridization to high-density oligonucleotide arrays. *Nat. Biotechnol.* **14**, 1675–1680 (1996).

105. Mook, S., Van't Veer, L. J., Rutgers, E. J. T., Piccart-Gebhart, M. J. & Cardoso, F. Individualization of therapy using Mammaprint: from development to the MINDACT Trial. *Cancer Genomics Proteomics* **4**, 147–155 (2007).

106. Paik, S. *et al.* A Multigene Assay to Predict Recurrence of Tamoxifen-Treated, Node-Negative Breast Cancer. *N Engl J Med* **351**, 2817–2826 (2004).

107. Cooperberg, M. R. *et al.* Validation of a Cell-Cycle Progression Gene Panel to Improve Risk Stratification in a Contemporary Prostatectomy Cohort. *JCO* **31**, 1428–1434 (2013).

108. Mortazavi, A., Williams, B. A., McCue, K., Schaeffer, L. & Wold, B. Mapping and quantifying mammalian transcriptomes by RNA-Seq. *Nat Methods* **5**, 621–628 (2008).

109. Dehm, S. M., Schmidt, L. J., Heemers, H. V., Vessella, R. L. & Tindall, D. J. Splicing of a Novel Androgen Receptor Exon Generates a Constitutively Active Androgen Receptor that Mediates Prostate Cancer Therapy Resistance. *Cancer Research* **68**, 5469–5477 (2008).

110. Learn, C. A. *et al.* Resistance to tyrosine kinase inhibition by mutant epidermal growth factor receptor variant III contributes to the neoplastic phenotype of glioblastoma multiforme. *Clin. Cancer Res.* **10**, 3216–3224 (2004).

111. Postel, M., Roosen, A., Laurent-Puig, P., Taly, V. & Wang-Renault, S.-F. Droplet-based digital PCR and next generation sequencing for monitoring circulating tumor DNA: a cancer diagnostic perspective. *Expert Review of Molecular Diagnostics* **18**, 7–17 (2018).

112. Hodson, R. Precision medicine. *Nature* **537**, S49–S49 (2016).

113. Scott, A. R. Technology: Read the instructions. *Nature* **537**, S54–S56 (2016).

114. Relling, M. V. & Evans, W. E. Pharmacogenomics in the clinic. *Nature* **526**, 343–350 (2015).

115. San Segundo-Val, I. & Sanz-Lozano, C. S. Introduction to the Gene Expression Analysis. in *Molecular Genetics of Asthma* (ed. Isidoro García, M.) **1434**, 29–43 (Springer New York, 2016).

116. Raslova, H., Vainchenker, W. & Plo, I. Eltrombopag, a potent stimulator of megakaryopoiesis. *Haematologica* **101**, 1443–1445 (2016).

117. Ichikawa, M. *et al.* A role for RUNX1 in hematopoiesis and myeloid leukemia. *Int. J. Hematol.* **97**, 726–734 (2013).

118. Scheinberg, P. Activity of eltrombopag in severe aplastic anemia. *Blood Adv* **2**, 3054–3062 (2018).

119. Lazarus, A. H., Semple, J. W. & Cines, D. B. Innate and Adaptive Immunity in Immune Thrombocytopenia. *Seminars in Hematology* **50**, S68–S70 (2013).

120. Gregory, T. *et al.* GATA-1 and erythropoietin cooperate to promote erythroid cell survival by regulating bcl-xL expression. *Blood* **94**, 87–96 (1999).

121. Nimer, S. D. Myelodysplastic syndromes. *Blood* **111**, 4841–4851 (2008).

122. Ault, P. & Jones, K. Understanding Iron Overload: Screening, Monitoring, and Caring for Patients With Transfusion-Dependent Anemias. *Clinical Journal of Oncology Nursing* **13**, 511–517 (2009).

123. Malcovati, L. Impact of transfusion dependency and secondary iron overload on the survival of patients with myelodysplastic syndromes. *Leukemia Research* **31**, S2–S6 (2007).

124. Gattermann, N. Iron overload in myelodysplastic syndromes (MDS). *Int J Hematol* **107**, 55–63 (2018).

125. Musto, P. *et al.* Iron-chelating therapy with deferasirox in transfusion-dependent, higher risk myelodysplastic syndromes: a retrospective, multicentre study. *Br J Haematol* **177**, 741–750 (2017).

126. Messa, E. *et al.* Deferasirox is a powerful NF- B inhibitor in myelodysplastic cells and in leukemia cell lines acting independently from cell iron deprivation by chelation and reactive oxygen species scavenging. *Haematologica* **95**, 1308–1316 (2010).

127. Gattermann, N. *et al.* Hematologic responses to deferasirox therapy in transfusion-dependent patients with myelodysplastic syndromes. *Haematologica* **97**, 1364–1371 (2012).

128. Anguita, E., Candel, F. J., Chaparro, A. & Roldán-Etcheverry, J. J. Transcription Factor GFI1B in Health and Disease. *Front. Oncol.* **7**, (2017).

129. Nolte, F. *et al.* Results from a 1-year, open-label, single arm, multi-center trial evaluating the efficacy and safety of oral Deferasirox in patients diagnosed with low and int-1 risk myelodysplastic syndrome (MDS) and transfusion-dependent iron overload. *Ann Hematol* **92**, 191–198 (2013).

130. Jordan, C. T. The leukemic stem cell. *Best Practice & Research Clinical Haematology* **20**, 13–18 (2007).

131. Shastri, A., Will, B., Steidl, U. & Verma, A. Stem and progenitor cell alterations in myelodysplastic syndromes. *Blood* **129**, 1586–1594 (2017).

132. Stevens, B. M. *et al.* Characterization and targeting of malignant stem cells in patients with advanced myelodysplastic syndromes. *Nat Commun* **9**, 3694 (2018).

133. Polgarova, K. *et al.* Somatic mutation dynamics in MDS patients treated with azacitidine indicate clonal selection in patients-responders. *Oncotarget* **8**, 111966–111978 (2017).

134. Al-Kali, A. *et al.* Prognostic impact of *RAS* mutations in patients with myelodysplastic syndrome. *Am. J. Hematol.* **88**, 365–369 (2013).

135. Hollenbach, P. W. *et al.* A Comparison of Azacitidine and Decitabine Activities in Acute Myeloid Leukemia Cell Lines. *PLoS ONE* **5**, e9001 (2010).

136. Signer, R. A. J., Magee, J. A., Salic, A. & Morrison, S. J. Haematopoietic stem cells require a highly regulated protein synthesis rate. *Nature* **509**, 49–54 (2014).

List of Abbreviations:

5-Azacytidine AZA

AML Acute Myeloid Leukemia

ASCT allogeneic hematopoietic stem cell transplantation

BM Bone Marrow

BSC Best Supportive Care

CC: corticosteroids

CCUS: clonal cytopenia of undetermined significance

CHIP: clonal hematopoiesis of undetermined potential

CPM Cancer Precision Medicine

CR Complete Response

DAC: 5-aza-2'-deoxycytidine

DAVID: Database for Annotation, Visualization and Integrated Discovery

ddPCR: droplet digital PCR

DEG: differentially expressed genes

ES: enrichment score

ESA Erythropoiesis Stimulating Agents

FDA Food and Drug Administration

FDR: dales discovery rate

GEP Gene Expression Profile

GO: gene ontology

GP: glycoprotein

GSEA: Gene set enrichment analysis

HIC: Hepatic iron concentration

HMA Hypomethylating Agents

HSC Hematopoietic Stem Cell

HTS: high-throughput sequencing

ICT: Iron chelation therapies

ICUS: idiopathic cytopenia of undetermined significance

IgG Immunoglobulin G

Indels: small insertions and deletions

IO Iron overload

IPSS-R International Prognostic Scoring System

IQR: inter-quartile range

ITP Immune thrombocytopenia

IVIG: immunoglobulins

LDH: lactate dehydrogenase

lincRNA long intergenic non-coding RNA

lncRNA long non-coding RNA

LPI: labile plasma iron

MDS: Myelodysplastic Syndromes

MEP: megakaryocyte-erythroid progenitor

MeV4: multiexperiment viewer 4

MK Megakaryocyte

ncRNAs Non-coding RNAs

NES: normalized enrichment score

NGS Next Generation Sequencing

NO: nitric oxide

NR: No response

NT nucleotides

NTBI: non-transferrin-bound iron

OS Overall Survival

PB Peripheral blood

PBMC: Peripheral blood mononuclear cells

PKG: Pharmacogenomics

PM Personalize/precision Medicine

qRT: quantitative reverse transcriptome

R: response

RARS: refractory anemia with ring sideroblasts

RBC: red blood cells

RIN: RNA integrity number

RMA: Robust microarray analysis

RNAseq: RNA sequencing

RT: reverse transcriptome

ROS: reactive oxygen species

SAM: significance analysis of microarray

SCT: stem cell transplantation

SF: serum ferritin

SNV Single Nucleotide Variants

t-MDS therapy related MDS

TPO Thrombopoietin

TPO-R TPO receptor

TPO-RA: TPO-R agonist

WPSS: WHO classification-based prognostic scoring system

WHO World Health Organization

Supplementary Appendix

Chapter 1

Supplementary Table 1. **Differentially expressed genes in the paired analysis, of 14 immune thrombocytopeina patients, before and during eltrombopag treatment**. A total of 142 probsets were signicantly deregulated by eltrombopag, FDR < 0.1

nº	probeset ID	d.value	p.value	q.value	FC Post/Pre	Mean Diff Post-Pre	GeneName	Description
1	16967788	5,132573706	7,46E-07	0,003333333	3,023290599	278,6066273	PF4V1	platelet factor 4 variant 1
2	17123310	5,088349286	7,46E-07	0,003333333	3,749717308	112,8028842	PROS1	protein S (alpha)
3	16976821	5,029616334	7,46E-07	0,003333333	2,181168911	3355,042971	PPBP	pro-platelet basic protein (chemokine (C-X-C motif) ligand 7)
4	16991246	4,96133867	1,49E-06	0,005	3,336150238	267,3314198	NA	NA
5	17048450	4,874875484	2,24E-06	0,006	3,018121063	394,2428814	GNG11	guanine nucleotide binding protein (G protein), gamma 11
6	17019019	4,814366099	2,98E-06	0,006153846	3,262121969	1330,437836	TREML1	triggering receptor expressed on myeloid cells-like 1
7	17123308	4,723395651	3,73E-06	0,006153846	3,314219748	72,48854659	PROS1	protein S (alpha)
8	16913341	4,692470455	3,73E-06	0,006153846	3,011190673	1321,058926	MYL9	myosin, light chain 9, regulatory
9	17123306	4,605955563	5,22E-06	0,006153846	3,179984277	95,91525207	PROS1	protein S (alpha)
10	16956569	4,583705134	5,22E-06	0,006153846	3,193234852	153,374371	PROS1	protein S (alpha)
11	16761242	4,530761402	5,97E-06	0,006153846	2,918758542	179,9358569	CLEC1B	C-type lectin domain family 1, member B
12	17109832	4,510501133	5,97E-06	0,006153846	2,735168764	125,9947686	PCYT1B	phosphate cytidylyltransferase 1, choline, beta
13	17123302	4,510381658	5,97E-06	0,006153846	3,12555697	159,3430769	PROS1	protein S (alpha)
14	17006801	4,378423165	8,95E-06	0,008571429	2,236292103	155,5651219	C6orf25	chromosome 6 open reading frame 25
15	16970022	4,350641146	1,12E-05	0,009375	3,734586916	41,27418827	NA	NA
16	17121256	4,344021813	1,12E-05	0,009375	1,805324447	208,3109214	WHAMMP3	WAS protein homolog associated with actin, golgi membranes and microtubules pseudogene 3
17	16688864	4,276056161	1,49E-05	0,011764706	1,895186999	32,66949536	TTLL7	tubulin tyrosine ligase-like family member 7
18	16960114	4,220550223	1,79E-05	0,013333333	2,357063187	37,78620102	PLOD2	procollagen-lysine, 2-oxoglutarate 5-dioxygenase 2
19	16845681	4,200866777	1,94E-05	0,013684211	3,331875007	940,1086541	ITGA2B	integrin, alpha 2b (platelet glycoprotein IIb of IIb/IIIa complex, antigen CD41)
20	17123594	4,143972262	2,54E-05	0,016153846	2,52780796	27,21318984	NA	NA
21	17083900	4,042662396	3,13E-05	0,016153846	2,121583904	87,87596439	ACER2	alkaline ceramidase 2

22	17090670	4,042588756	3,13E-05	0,016153846	1,863747863	157,425827	GFI1B	growth factor independent 1B transcription repressor
23	17040851	4,027941729	3,13E-05	0,016153846	2,466850532	711,0527597	C6orf25	chromosome 6 open reading frame 25
24	17035555	4,027941729	3,13E-05	0,016153846	2,466850532	711,0527597	C6orf25	chromosome 6 open reading frame 25
25	17030760	4,027941729	3,13E-05	0,016153846	2,466850532	711,0527597	C6orf25	chromosome 6 open reading frame 25
26	17027934	4,027941729	3,13E-05	0,016153846	2,466850532	711,0527597	C6orf25	chromosome 6 open reading frame 25
27	17033465	4,002586937	3,43E-05	0,017037037	2,347931092	374,6733783	C6orf25	chromosome 6 open reading frame 25
28	16782318	3,967502908	3,95E-05	0,018	2,052346191	155,5492713	CMTM5	CKLF-like MARVEL transmembrane domain containing 5
29	16962316	3,961090379	4,03E-05	0,018	2,774083846	98,63869833	LIPH	lipase, member H
30	17122924	3,957572307	4,03E-05	0,018	1,804550184	427,2790176	TPTEP1	transmembrane phosphatase with tensin homology pseudogene 1
31	17038255	3,936700928	4,33E-05	0,018709677	2,564679062	750,3613986	C6orf25	chromosome 6 open reading frame 25
32	17005600	3,875774332	5,60E-05	0,022727273	2,380994632	177,0124306	HIST1H2BH	histone cluster 1, H2bh
33	16846864	3,866380479	5,60E-05	0,022727273	2,423418373	887,9775263	MMD	monocyte to macrophage differentiation-associated
34	16764084	3,84307173	6,57E-05	0,025882353	2,061417211	1002,111947	NA	NA
35	16908305	3,800011686	7,61E-05	0,029142857	3,074273128	895,9028363	CXCR2P1	chemokine (C-X-C motif) receptor 2 pseudogene 1
36	16857905	3,764058724	8,43E-05	0,031025641	1,867142845	676,2459517	MARCH2	membrane-associated ring finger (C3HC4) 2, E3 ubiquitin protein ligase
37	16733620	3,75642021	8,73E-05	0,031025641	2,096735592	109,1755867	JAM3	junctional adhesion molecule 3
38	16818359	3,751468919	8,80E-05	0,031025641	2,144723195	128,4298985	TGFB1I1	transforming growth factor beta 1 induced transcript 1
39	16976815	3,74330257	9,03E-05	0,031025641	1,841809055	100,0279658	PF4	platelet factor 4
40	16712576	3,705402034	9,85E-05	0,031428571	2,124542894	38,77904198	PRTFDC1	phosphoribosyl transferase domain containing 1
41	17088760	3,704972991	9,85E-05	0,031428571	2,492762176	642,7513843	PTGS1	prostaglandin-endoperoxide synthase 1 (prostaglandin G/H synthase and cyclooxygenase)
42	16853817	3,702420408	9,85E-05	0,031428571	1,95577186	42,13837455	LOC102724397	uncharacterized LOC102724397
43	16835158	3,667545743	0,000110415	0,034418605	3,029960764	1960,156517	ITGB3	integrin, beta 3 (platelet glycoprotein IIIa, antigen CD61)

44	17070695	3,654999441	0,000114145	0,034772727	1,823217274	38,40493522	LINC00534	long intergenic non-protein coding RNA 534
45	16709249	3,622867217	0,000127574	0,03787234	2,314795359	98,29383659	NA	NA
46	16990862	3,616314264	0,000130558	0,03787234	2,23974657	141,7136952	ABLIM3	actin binding LIM protein family, member 3
47	16679717	3,608293658	0,000132796	0,03787234	1,728999508	103,4111182	GCSAML	germinal center-associated, signaling and motility-like
48	17092490	3,578153868	0,000147717	0,041	1,582508404	20,49557993	NA	NA
49	16716782	3,570038306	0,000149955	0,041	2,177071684	534,792471	PDLIM1	PDZ and LIM domain 1
50	17010544	3,560921059	0,000152939	0,041	2,362689699	495,3166894	SH3BGRL2	SH3 domain binding glutamate-rich protein like 2
51	17050154	3,554324681	0,00015667	0,041176471	2,140637452	610,0945274	PRKAR2B	protein kinase, cAMP-dependent, regulatory, type II, beta
52	17001927	3,543168732	0,000161146	0,041538462	1,836943058	204,1822491	SPARC	secreted protein, acidic, cysteine-rich (osteonectin)
53	17005862	3,530025828	0,000174575	0,042413793	2,779597814	246,317534	NA	NA
54	16970404	3,521333246	0,000178305	0,042413793	1,865350643	35,71010765	FGF2	fibroblast growth factor 2 (basic)
55	17033451	3,514841449	0,000182781	0,042413793	1,896906756	146,7307247	NA	NA
56	17030746	3,514841449	0,000182781	0,042413793	1,896906756	146,7307247	NA	NA
57	17006787	3,514841449	0,000182781	0,042413793	1,896906756	146,7307247	NA	NA
58	16878947	3,512705967	0,000183527	0,042413793	2,228447085	190,7419937	LTBP1	latent transforming growth factor beta binding protein 1
59	16971712	3,502201222	0,000191734	0,042833333	2,035550021	108,8308165	GUCY1A3	guanylate cyclase 1, soluble, alpha 3
60	16714699	3,501780675	0,000191734	0,042833333	1,765350186	84,5084894	RHOBTB1	Rho-related BTB domain containing 1
61	16918939	3,492045258	0,00019994	0,043787879	2,112655343	115,5910112	NA	NA
62	16898660	3,485252723	0,000203671	0,043787879	2,497915063	543,4534868	NA	NA
63	16696217	3,470812492	0,000214115	0,043787879	3,01637992	334,912298	SELP	selectin P (granule membrane protein 140kDa, antigen CD62)
64	17004657	3,46994193	0,000214115	0,043787879	2,154234765	154,7015732	BMP6	bone morphogenetic protein 6
65	16906184	3,468758844	0,000214861	0,043787879	1,841165798	82,626897	NCKAP1	NCK-associated protein 1
66	16773453	3,466370094	0,000215607	0,043787879	1,865755523	90,60602104	WASF3	WAS protein family, member 3
67	16800229	3,446560981	0,000235751	0,046666667	1,663002678	49,13203041	MAP1A	microtubule-associated protein 1A
68	16673842	3,436909694	0,000240227	0,046666667	1,973193734	96,56068628	DNM3	dynamin 3
69	16745658	3,435915657	0,000240227	0,046666667	1,831046235	138,7656848	SIAE	sialic acid acetylesterase
70	16979339	3,428783865	0,000247687	0,047428571	2,210788147	94,41399115	PDE5A	phosphodiesterase 5A, cGMP-specific
71	16811638	3,422088375	0,00025291	0,047746479	1,302832039	66,94595165	SEMA7A	semaphorin 7A, GPI membrane anchor

								(John Milton Hagen blood group)
72	16996564	3,40646825	0,000265592	0,048767123	2,126254347	90,79067166	ELOVL7	ELOVL fatty acid elongase 7
73	16738671	3,376222557	0,000287974	0,051084337	1,371661084	19,38378579	LOC283194	uncharacterized LOC283194
74	17011949	3,373719822	0,000290212	0,051084337	1,48297046	26,93483033	FAM26E	family with sequence similarity 26, member E
75	16911804	3,355644543	0,000300657	0,051084337	1,860344335	49,76552659	SLC24A3	solute carrier family 24 (sodium/potassium/calcium exchanger), member 3
76	16780271	3,352420865	0,000301403	0,051084337	1,745013091	118,2211922	ABCC4	ATP-binding cassette, sub-family C (CFTR/MRP), member 4
77	16875549	3,347330249	0,000308117	0,051084337	2,168015278	233,92882	GP6	glycoprotein VI (platelet)
78	16843078	3,345854267	0,000308117	0,051084337	1,629423207	49,12578379	SLC6A4	solute carrier family 6 (neurotransmitter transporter), member 4
79	16813922	3,344141275	0,000311101	0,051084337	1,666366489	60,08639482	NA	NA
80	17035542	3,33769632	0,000316323	0,051084337	2,012522936	182,8755418	NA	NA
81	17027921	3,33769632	0,000316323	0,051084337	2,012522936	182,8755418	NA	NA
82	16764085	3,32627214	0,000326768	0,052142857	1,986620902	143,2751927	NA	NA
83	17071871	3,287762366	0,000367055	0,057045455	2,028800658	58,75188087	PKHD1L1	polycystic kidney and hepatic disease 1 (autosomal recessive)-like 1
84	17071208	3,284478797	0,000368547	0,057045455	2,475817009	152,2661597	LAPTM4B	lysosomal protein transmembrane 4 beta
85	17001404	3,281484102	0,000371531	0,057045455	1,522637064	23,84658922	SH3TC2	SH3 domain and tetratricopeptide repeats 2
86	16968293	3,278678481	0,000374515	0,057045455	1,793090624	93,36768693	LINC00989	long intergenic non-protein coding RNA 989
87	17002052	3,24673227	0,000417786	0,062777778	1,723477452	137,9155679	FAXDC2	fatty acid hydroxylase domain containing 2
88	16795368	3,245417535	0,000421516	0,062777778	1,853035994	88,3281633	STON2	stonin 2
89	16950877	3,230756782	0,000439421	0,064086022	1,646385421	58,18331763	TMEM40	transmembrane protein 40
90	17052244	3,229288493	0,000440913	0,064086022	1,84319656	68,80271209	CLEC2L	C-type lectin domain family 2, member L
91	16945305	3,224051818	0,000444643	0,064086022	2,08017703	95,87786963	GP9	glycoprotein IX (platelet)
92	16829967	3,210643818	0,000466279	0,066489362	1,941634907	213,1809227	GP1BA	glycoprotein Ib (platelet), alpha polypeptide
93	16746930	3,206216113	0,000472247	0,066631579	1,551816639	45,33133727	TSPAN9	tetraspanin 9
94	17106546	3,196224399	0,000490152	0,0684375	1,831966953	916,3443533	PGRMC1	progesterone receptor membrane component 1
95	16729276	3,180125872	0,00052447	0,071938776	2,490131382	92,41895491	NA	NA
96	16742381	3,171674514	0,000536407	0,072626263	1,457046885	27,1549449	NA	NA
97	17038243	3,150469429	0,000569979	0,0764	1,546021711	81,34413428	NA	NA

98	16898348	3,147976862	0,00057744	0,076633663	1,617676509	48,30170685	NA	NA
99	16958356	3,141629348	0,000589376	0,077184466	1,678763387	121,7343624	ITGB5	integrin, beta 5
100	16969729	3,138527376	0,000593107	0,077184466	1,965188056	58,00533961	EGF	epidermal growth factor
101	16810572	3,128554603	0,000622202	0,080192308	1,661659487	81,02948931	RBPMS2	RNA binding protein with multiple splicing 2
102	16797117	3,097871508	0,000697553	0,089047619	1,560928805	10,53417281	RD3L	retinal degeneration 3-like
103	16671405	3,091992355	0,000707252	0,089433962	1,896771065	98,20026113	AQP10	aquaporin 10
104	17016406	3,087792361	0,000718442	0,09	1,848653203	155,035472	HIST1H4H	histone cluster 1, H4h
105	17123476	3,079924381	0,000737839	0,09	1,721783053	34,91139035	NA	NA
106	16753406	3,079413466	0,000737839	0,09	1,688702204	15,16064335	NA	NA
107	17099463	3,078881089	0,000738585	0,09	1,855624559	115,3400212	ABO	ABO blood group (transferase A, alpha 1-3-N-acetylgalactosaminyltransferase; transferase B, alpha 1-3-galactosyltransferase)
108	16667258	3,046683652	0,000810952	0,097927928	1,492954993	35,18502572	FNBP1L	formin binding protein 1-like
109	16732891	3,042418825	0,000823635	0,098571429	2,470984907	618,5522747	NRGN	neurogranin (protein kinase C substrate, RC3)
110	17109078	3,039424768	0,000840048	0,099646018	1,510845691	33,79080142	ARHGAP6	Rho GTPase activating protein 6
111	16968878	3,027346919	0,000867651	0,102017544	1,938843448	81,36998675	MMRN1	multimerin 1
112	16877667	3,025172133	0,000878842	0,102434783	1,545103137	37,4365485	FKBP1B	FK506 binding protein 1B, 12.6 kDa
113	16745693	3,011350395	0,000916144	0,105546218	1,81897902	145,8012289	ESAM	endothelial cell adhesion molecule
114	16712587	3,009288333	0,000922113	0,105546218	1,952046598	31,89642457	ENKUR	enkurin, TRPC channel interacting protein
115	16728389	3,00330921	0,000933303	0,105546218	1,692896554	60,52246747	CTTN	cortactin
116	17109447	3,001302034	0,000937034	0,105546218	2,184939145	109,8897334	BEND2	BEN domain containing 2
117	17080666	2,991518035	0,000962399	0,106942149	1,883045705	21,71326598	NA	NA
118	17125130	2,990507922	0,000965383	0,106942149	1,297069364	14,84021136	NA	NA
119	16915395	2,981298746	0,001001194	0,11	2,428381829	1684,725421	TUBB1	tubulin, beta 1 class VI
120	17075731	2,979238678	0,001010146	0,110081301	1,921432034	166,9484881	CLU	clusterin
121	17024751	2,959107074	0,001079528	0,116693548	1,546619805	8,461550105	NA	NA
122	17051872	2,953874328	0,001095195	0,11744	1,411914371	23,59215975	CALD1	caldesmon 1
123	17044758	2,944715102	0,001131752	0,12023622	1,570651259	98,75831815	MTURN	maturin, neural progenitor differentiation regulator homolog (Xenopus)
124	16663498	2,942705242	0,001139212	0,12023622	1,676303536	86,40984002	MPL	MPL proto-oncogene, thrombopoietin receptor
125	16709128	2,931061461	0,001171292	0,12265625	1,584306739	127,1238999	DUSP5	dual specificity phosphatase 5
126	16726856	2,91517649	0,001223515	0,127131783	1,716991931	24,68748703	NA	NA
127	16889710	2,904513467	0,001266786	0,130615385	1,77385374	68,82298045	NA	NA
128	16911108	2,892130725	0,001324232	0,13530303	1,712549387	165,2147785	SMOX	spermine oxidase

129	16906615	2,890956556	0,001332438	0,13530303	2,143317238	295,9896114	SDPR	serum deprivation response
130	16795755	2,864041319	0,001444345	0,145223881	1,673752347	83,37178708	TTC7B	tetratricopeptide repeat domain 7B
131	16734877	2,86173109	0,001451805	0,145223881	1,905128051	85,96660302	HBE1	hemoglobin, epsilon 1
132	16673598	2,854585278	0,001487616	0,146714286	1,390104772	14,66248431	NA	NA
133	16830238	2,851319732	0,001504775	0,146714286	1,98699332	116,4793524	ALOX12	arachidonate 12-lipoxygenase
134	16746057	2,849017186	0,00151895	0,146714286	1,358586885	48,5675623	ARHGAP32	Rho GTPase activating protein 32
135	16677556	2,848666008	0,00151895	0,146714286	1,480370112	18,19918967	TGFB2	transforming growth factor, beta 2
136	16714405	2,846310473	0,001527902	0,146714286	2,351791648	44,50800635	NA	NA
137	16971737	2,845025665	0,001532378	0,146714286	1,978822432	123,4069659	GUCY1B3	guanylate cyclase 1, soluble, beta 3
138	17096188	2,837328693	0,001574903	0,149716312	1,409072325	101,3369484	SLC35D2	solute carrier family 35 (UDP-GlcNAc/UDP-glucose transporter), member D2
139	16655053	2,792553862	0,001821844	0,171971831	1,730972287	50,87487796	NA	NA
140	16700400	2,777720617	0,001908386	0,175479452	1,627281781	51,17248204	C1orf198	chromosome 1 open reading frame 198
141	17105712	2,777000394	0,00191137	0,175479452	1,498032358	23,31658043	NGFRAP1	nerve growth factor receptor (TNFRSF16) associated protein 1
142	16784519	2,776792793	0,00191137	0,175479452	1,757702624	22,43058863	NA	NA

Supplementary Table 2. Gene Ontology enrichment analysis of the differentially expressed genes in the paired comparison (before and during eltrombopag treatment).

GO biological process complete	fold Enrichment	P-value
platelet aggregation (GO:0070527)	21.53	6.13E-03
platelet degranulation (GO:0002576)	18.50	1.45E-10
regulation of megakaryocyte differentiation (GO:0045652)	17.87	1.66E-02
homotypic cell-cell adhesion (GO:0034109)	16.91	2.23E-02
platelet activation (GO:0030168)	14.87	1.12E-07
blood coagulation (GO:0007596)	10.89	6.21E-11
coagulation (GO:0050817)	10.81	7.02E-11
hemostasis (GO:0007599)	10.70	8.42E-11
wound healing (GO:0042060)	7.71	5.36E-10
regulation of body fluid levels (GO:0050878)	7.49	9.64E-10
response to wounding (GO:0009611)	6.74	2.32E-09
extracellular matrix organization (GO:0030198)	6.26	2.19E-03
extracellular structure organization (GO:0043062)	5.93	1.40E-03
cell adhesion (GO:0007155)	3.45	1.42E-02
biological adhesion (GO:0022610)	3.43	1.56E-02
regulation of cell differentiation (GO:0045595)	2.55	3.49E-02
regulation of biological quality (GO:0065008)	2.05	1.24E-03

Supplementary Table 3. Differentially expressed genes in the comparation of non-responder patients versus responder patients during eltrombopag treatment. A total of 21 genes (22 probset) with an FDR < 0.2

nº	probeset ID	d.value	p.value	q.value	R.fold	Genename	Description
1	16707192	4,493832699	8,95E-06	0,12	9,12527523	IFIT1B	interferon-induced protein with tetratricopeptide repeats 1B
2	16845623	4,067181368	2,83E-05	0,145	7,380052915	SLC4A1	solute carrier family 4 (anion exchanger), member 1 (Diego blood group)
3	17111520	3,935913326	3,51E-05	0,145	9,196665547	ALAS2	5'-aminolevulinate synthase 2
4	16808046	3,863115142	4,33E-05	0,145	6,215093724	EPB42	erythrocyte membrane protein band 4.2
5	16818394	3,509610133	9,55E-05	0,19	8,94428682	AHSP	alpha hemoglobin stabilizing protein
6	16693082	3,489606156	9,77E-05	0,19	5,503435376	SELENBP1	selenium binding protein 1
7	16852179	3,486248167	9,92E-05	0,19	4,233585327	SLC14A1	solute carrier family 14 (urea transporter), member 1 (Kidd blood group)
8	16734849	3,35574393	0,00013205	0,203636364	6,090591215	HBD	hemoglobin, delta
9	16855477	3,3258078	0,000146225	0,203636364	4,494483745	FECH	ferrochelatase
10	16679742	3,294431204	0,000152193	0,203636364	3,4711051	TRIM58	tripartite motif containing 58
11	17093377	3,256043817	0,000167114	0,203636364	3,821351356	DCAF12	DDB1 and CUL4 associated factor 12
12	16669278	3,160954707	0,000208147	0,221538462	3,276073471	FAM46C	family with sequence similarity 46, member C
13	16845657	3,146283597	0,000214861	0,221538462	4,448676759	SLC25A39	solute carrier family 25, member 39
14	16713614	3,07339135	0,000255148	0,244285714	2,335887806	MARCH8	membrane-associated ring finger (C3HC4) 8, E3 ubiquitin protein ligase
15	16980267	2,932428772	0,000357356	0,313125	3,76755755	GYPA	glycophorin A (MNS blood group)
16	16834764	2,919786602	0,000373769	0,313125	6,309287856	NA	NA
17	17051860	2,881610233	0,000413309	0,325882353	2,717411205	BPGM	2,3-bisphosphoglycerate mutase
18	17087329	2,739973262	0,000607281	0,452222222	4,465654921	TMOD1	tropomodulin 1
19	16793999	2,710623217	0,000655774	0,462631579	4,910219644	PLEK2	pleckstrin 2
20	16918244	2,673059045	0,000727395	0,4875	2,859060136	BCL2L1	BCL2-like 1
21	16822330	2,646337846	0,000782602	0,495	2,449887294	NPRL3	nitrogen permease regulator-like 3 (S. cerevisiae)
22	17078722	2,6320535	0,000812444	0,495	2,935699007	CA1	carbonic anhydrase I

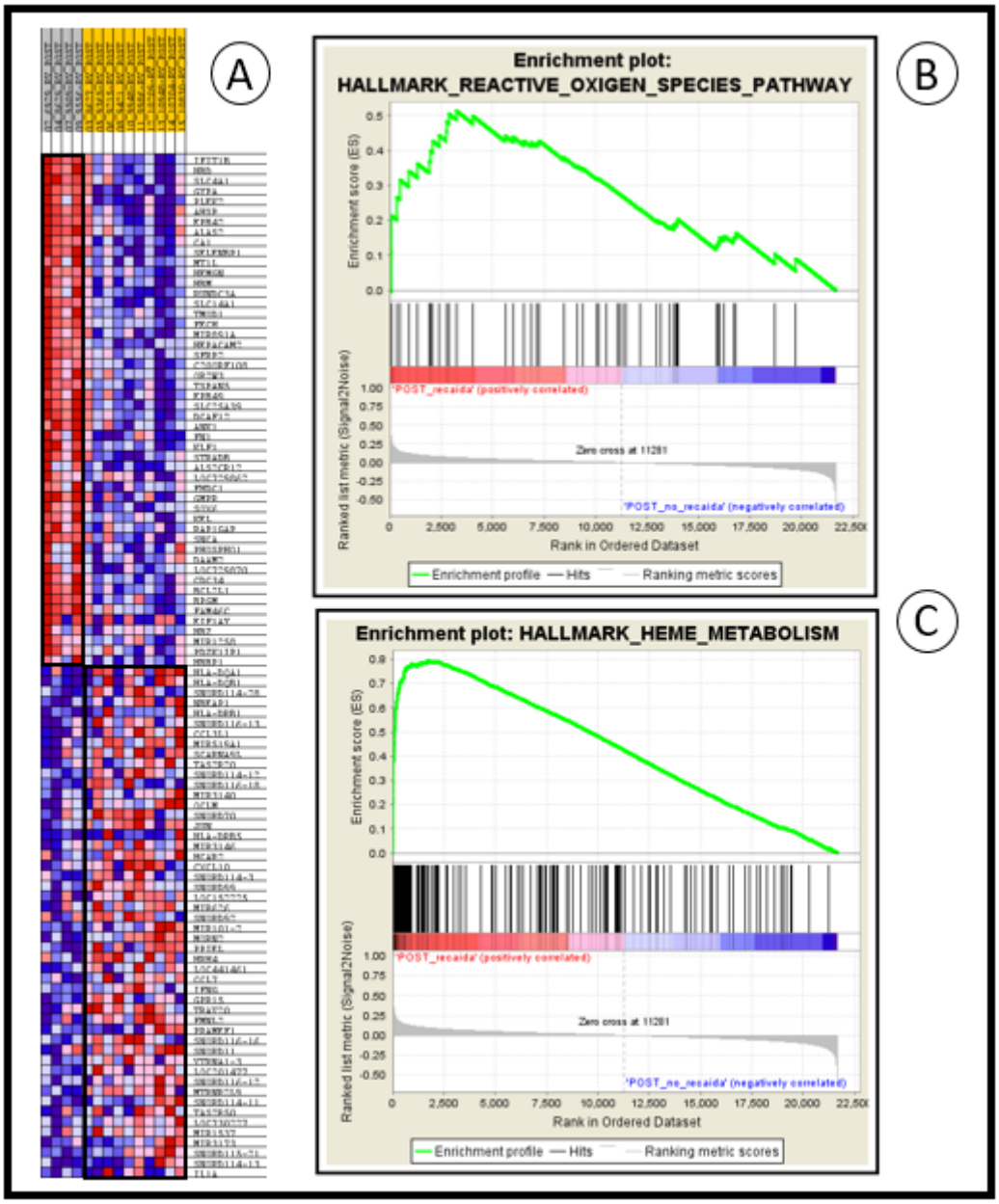

Supplementary Figure 1: GEPs of ITP patients after ETP. A. Heatmap depicts differential GEPs responders versus relapse in PBMMC. GSEA enriched hallmark: B. reactive oxygen species (ROS) C. Heme metabolism

Chapter 2

Supplementary Table 1. Primers used for droplet digital PCR

Gene	Forward	Reverse
BID	CCCTGCAGCTCAGGAACA	CAGCACCAGCATGGTCTTC
BIRC2	TGGACAAACAGCAACAAACAA	AAACCAGCACGAGCAAGACT
NFKBIA	CTACACCTTGCCTGTGAGCA	GACACGTGTGGCCATTGTAG
REL	ACAGCACAGACAACAACCGA	GGATGAGGTTTATATGGGTCATTCT
RELA	CCGCCTGTCCTTTCTCATC	AGGAAGATCTCATCCCCACC
TANK	ACAGGAACAGCTGTCACTTCAAC	TCAAGCAGAGGAACACAGCC
TRAF6	CCAAATGAAGGTTGTTTGCAC	GAATTTTTGGAAGGGACGCT

Supplementary Table 2. Genes significantly deregulated after deferasirox treatment in MDS patients.

Gene Symbol	Gene Title	Diff exp
A2ML1	alpha-2-macroglobulin like 1	0,1075945
AAED1	AhpC/TSA antioxidant enzyme domain containing 1	-0,363174
ABCA9	ATP binding cassette subfamily A member 9	0,0641326
ABCC11	ATP binding cassette subfamily C member 11	0,1433699
ABHD13	abhydrolase domain containing 13	-0,3302583
ACACA	acetyl-CoA carboxylase alpha	0,0607356
ACAT2	acetyl-CoA acetyltransferase 2	-0,4192949
ACO1	aconitase 1	0,0921777
ACOXL	acyl-CoA oxidase like	0,1015779
ACP2	acid phosphatase 2, lysosomal	0,1018519
ACSM5	acyl-CoA synthetase medium chain family member 5	0,2031634
ADAM1A	ADAM metallopeptidase domain 1A (pseudogene)	0,1626205
ADAMTS20	ADAM metallopeptidase with thrombospondin type 1 motif 20	0,0491409
ADD3-AS1	ADD3 antisense RNA 1	0,1564767
ADH4	alcohol dehydrogenase 4 (class II), pi polypeptide	0,1095826
ADH6	alcohol dehydrogenase 6 (class V)	0,0817777
ADIPOQ	adiponectin, C1Q and collagen domain containing	0,0720223
ADRB2	adrenoceptor beta 2	0,1523233
AFAP1	actin filament associated protein 1	0,072749
AFAP1L2	actin filament associated protein 1 like 2	0,1496131
AGBL1-AS1	AGBL1 antisense RNA 1	0,1911797
AGBL5	ATP/GTP binding protein like 5	0,1017884
AIMP1	aminoacyl tRNA synthetase complex interacting multifunctional protein 1	-0,4875946
AKAP2	A-kinase anchoring protein 2	0,0775938
AKIRIN1	akirin 1	-0,3633273
AKNAD1	AKNA domain containing 1	0,0842878
AKR1E2	aldo-keto reductase family 1 member E2	0,0579924
ALKBH1	alkB homolog 1, histone H2A dioxygenase	-0,1684293
ALMS1-IT1	ALMS1 intronic transcript 1	-0,130147
ALOX12P2	arachidonate 12-lipoxygenase pseudogene 2	0,1357529
ALOX15	arachidonate 15-lipoxygenase	0,1674166
ALOX15B	arachidonate 15-lipoxygenase, type B	0,1696449
ALS2	ALS2, alsin Rho guanine nucleotide exchange factor	0,090589
AMELX	amelogenin, X-linked	0,1188127
AMPD3	adenosine monophosphate deaminase 3	0,101584
ANAPC10	anaphase promoting complex subunit 10	-0,1649768
ANKRA2	ankyrin repeat family A member 2	-0,333526
ANKRD10	ankyrin repeat domain 10	-0,2591074
ANKRD16	ankyrin repeat domain 16	0,1435051
ANKRD35	ankyrin repeat domain 35	0,1681886
ANKRD37	ankyrin repeat domain 37	-0,127842
ANKRD49	ankyrin repeat domain 49	-0,4136012

ANXA2P3	annexin A2 pseudogene 3	0,1879186
AP3M2	adaptor related protein complex 3 mu 2 subunit	-0,2603859
AP3S1	adaptor related protein complex 3 sigma 1 subunit	-0,2233534
AP4B1-AS1	AP4B1 antisense RNA 1	0,130645
APCDD1L-AS1	APCDD1L antisense RNA 1 (head to head)	0,195631
APOBEC3D	apolipoprotein B mRNA editing enzyme catalytic subunit 3D	0,1802703
APOBEC3F	apolipoprotein B mRNA editing enzyme catalytic subunit 3F	0,1651787
APOL5	apolipoprotein L5	0,182378
APOL6	apolipoprotein L6	-0,427511
APTX	aprataxin	-0,1624524
AQP9	aquaporin 9	-0,7307724
ARHGAP31	Rho GTPase activating protein 31	0,1407798
ARHGAP32	Rho GTPase activating protein 32	0,1215098
ARHGEF39	Rho guanine nucleotide exchange factor 39	0,087605
ARHGEF9	Cdc42 guanine nucleotide exchange factor 9	0,088181
ARID4A	AT-rich interaction domain 4A	-0,207871
ARID4B	AT-rich interaction domain 4B	-0,3547557
ARID5A	AT-rich interaction domain 5A	-0,2674026
ARID5B	AT-rich interaction domain 5B	-0,380096
ARL5B	ADP ribosylation factor like GTPase 5B	-0,620996
ARL8B	ADP ribosylation factor like GTPase 8B	-0,3601579
ARMCX4	armadillo repeat containing, X-linked 4	0,0504189
ARNTL	aryl hydrocarbon receptor nuclear translocator like	-0,202015
ARPC5L	actin related protein 2/3 complex subunit 5 like	-0,2183876
ARRDC2	arrestin domain containing 2	-0,2196653
ASNSD1	asparagine synthetase domain containing 1	-0,4786706
ATAD1	ATPase family, AAA domain containing 1	-0,2071071
ATG12	autophagy related 12	-0,2841366
ATP10D	ATPase phospholipid transporting 10D (putative)	0,1597062
ATP13A4	ATPase 13A4	0,079586
ATP2B1	ATPase plasma membrane Ca2+ transporting 1	-0,4827634
ATP5EP2	ATP synthase, H+ transporting, mitochondrial F1 complex, epsilon subunit pseudogene 2	-0,432536
ATP5S	ATP synthase, H+ transporting, mitochondrial Fo complex subunit s (factor B)	-0,1293283
ATP6V0A2	ATPase H+ transporting V0 subunit a2	0,0667916
ATP6V0B	ATPase H+ transporting V0 subunit b	-0,463752
ATP6V1D	ATPase H+ transporting V1 subunit D	-0,2633966
ATP6V1F	ATPase H+ transporting V1 subunit F	-0,402804
ATP8B1	ATPase phospholipid transporting 8B1	0,0765319
ATRN	attractin	0,1165466
AZI2	5-azacytidine induced 2	-0,2192125
AZIN1	antizyme inhibitor 1	-0,5000545
B3GNT2	UDP-GlcNAc:betaGal beta-1,3-N-acetylglucosaminyltransferase 2	-0,2496596

B3GNT5	UDP-GlcNAc:betaGal beta-1,3-N-acetylglucosaminyltransferase 5	-0,168026
BACE1	beta-secretase 1	0,1039503
BACE1-AS	BACE1 antisense RNA	0,1641676
BAG3	BCL2 associated athanogene 3	-0,1195507
BAG4	BCL2 associated athanogene 4	-0,1543947
BANF2	barrier to autointegration factor 2	0,1560032
BARHL2	BarH like homeobox 2	0,1236021
BBS5	Bardet-Biedl syndrome 5	0,0484813
BCAS2	BCAS2, pre-mRNA processing factor	-0,728758
BCHE	butyrylcholinesterase	0,0648079
BCL10	B-cell CLL/lymphoma 10	-0,3406605
BCL2A1	BCL2 related protein A1	-0,5185847
BCL2L11	BCL2 like 11	-0,1242451
BCL7B	BCL tumor suppressor 7B	-0,1663576
BCLAF1	BCL2 associated transcription factor 1	-0,5336427
BCORP1	BCL6 corepressor pseudogene 1	0,1309498
BEND4	BEN domain containing 4	0,0838882
BEX4	brain expressed X-linked 4	-0,2823136
BEX5	brain expressed X-linked 5	-0,4769875
BHLHE40	basic helix-loop-helix family member e40	-0,3963199
BID	BH3 interacting domain death agonist	-0,3677584
BIRC2	baculoviral IAP repeat containing 2	-0,4759385
BLOC1S2	biogenesis of lysosomal organelles complex 1 subunit 2	-0,5372935
BMP8B	bone morphogenetic protein 8b	0,1465017
BMPR1A	bone morphogenetic protein receptor type 1A	0,2332658
BNIP1	BCL2 interacting protein 1	-0,2733421
BNIP3P1	BCL2 interacting protein 3 pseudogene 1	-0,2482339
BORA	bora, aurora kinase A activator	-0,1088054
BRDT	bromodomain testis associated	0,0388895
BRI3	brain protein I3	-0,3025466
BRI3BP	BRI3 binding protein	0,1323771
BRIX1	BRX1, biogenesis of ribosomes	-0,276144
BRWD1-AS1	BRWD1 antisense RNA 1	0,2056748
BTBD2	BTB domain containing 2	0,1423111
BTG3	BTG anti-proliferation factor 3	-0,4465451
BTN2A1	butyrophilin subfamily 2 member A1	-0,1023576
BZW1	basic leucine zipper and W2 domains 1	-0,5745992
C10orf105	chromosome 10 open reading frame 105	0,177787
C10orf91	chromosome 10 open reading frame 91 (putative)	0,1344313
C11orf49	chromosome 11 open reading frame 49	0,084522
C11orf58	chromosome 11 open reading frame 58	-0,291447
C14orf28	chromosome 14 open reading frame 28	-0,1614092
C15orf41	chromosome 15 open reading frame 41	0,1515003
C15orf65	chromosome 15 open reading frame 65	0,1444385
C16orf97	chromosome 16 open reading frame 97	0,2512288

C17orf67	chromosome 17 open reading frame 67	0,1004448
C18orf21	chromosome 18 open reading frame 21	-0,2586425
C1D	C1D nuclear receptor corepressor	-0,6339902
C1orf189	chromosome 1 open reading frame 189	0,1094446
C1orf195	chromosome 1 open reading frame 195	0,1562801
C1orf52	chromosome 1 open reading frame 52	-0,3847547
C20orf24	chromosome 20 open reading frame 24	-0,3575459
C2CD2	C2 calcium dependent domain containing 2	0,1546886
C2orf27A	chromosome 2 open reading frame 27A	0,1377513
C2orf69	chromosome 2 open reading frame 69	-0,2432963
C3orf38	chromosome 3 open reading frame 38	-0,4233347
C4orf46	chromosome 4 open reading frame 46	-0,1268147
C4orf51	chromosome 4 open reading frame 51	0,1235675
C5AR1	complement C5a receptor 1	-0,6957283
C5orf24	chromosome 5 open reading frame 24	-0,1190836
C6orf10	chromosome 6 open reading frame 10	0,1247464
C6orf136	chromosome 6 open reading frame 136	-0,1366875
C6orf47	chromosome 6 open reading frame 47	0,3079824
C6orf47-AS1	C6orf47 antisense RNA 1	-0,1449566
C7orf26	chromosome 7 open reading frame 26	-0,1196313
C8orf17	chromosome 8 open reading frame 17	0,251323
C9	complement C9	0,1340862
C9orf135-AS1	C9orf135 antisense RNA 1 (head to head)	-0,1340494
C9orf72	chromosome 9 open reading frame 72	-0,5296359
CABLES1	Cdk5 and Abl enzyme substrate 1	0,1078727
CABP5	calcium binding protein 5	0,2377563
CACNA1C-IT2	CACNA1C intronic transcript 2	0,1412998
CACNA1D	calcium voltage-gated channel subunit alpha1 D	0,0944103
CACNA2D1	calcium voltage-gated channel auxiliary subunit alpha2delta 1	0,0456353
CACUL1	CDK2 associated cullin domain 1	-0,2043423
CALHM1	calcium homeostasis modulator 1	-0,2095856
CAMLG	calcium modulating ligand	-0,4799805
CAPN3	calpain 3	0,0838499
CASC1	cancer susceptibility 1	0,066449
CASP2	caspase 2	0,1036086
CAST	calpastatin	-0,2074973
CCDC11	Cilia And Flagella Associated Protein 53	0,1109947
CCDC13-AS1	CCDC13 antisense RNA 1	0,2326486
CCDC158	coiled-coil domain containing 158	0,0617437
CCDC171	coiled-coil domain containing 171	0,0473917
CCDC174	coiled-coil domain containing 174	-0,1824679
CCDC22	coiled-coil domain containing 22	0,1166828
CCDC28A	coiled-coil domain containing 28A	-0,3207227
CCDC36	coiled-coil domain containing 36	0,067524
CCDC59	coiled-coil domain containing 59	-0,6815795
CCDC71L	coiled-coil domain containing 71 like	-0,269733

CCDC79	Telomere Repeat Binding Bouquet Formation Protein 1	0,0784327
CCDC84	coiled-coil domain containing 84	-0,2205884
CCDC93	coiled-coil domain containing 93	-0,2791571
CCL16	C-C motif chemokine ligand 16	0,1953883
CCL3L3	C-C motif chemokine ligand 3 like 3	-0,8482828
CCNH	cyclin H	-0,4710265
CCNJ	cyclin J	-0,087297
CCNK	cyclin K	-0,3834707
CCNYL2	cyclin Y-like 2 (pseudogene)	0,0924777
CCRL2	C-C motif chemokine receptor like 2	-0,3552041
CD101	CD101 molecule	0,1553652
CD1B	CD1b molecule	0,1021519
CD300E	CD300e molecule	-0,3100473
CD55	CD55 molecule (Cromer blood group)	-0,3864808
CD59	CD59 molecule (CD59 blood group)	-0,1677372
CD69	CD69 molecule	-0,967943
CD83	CD83 molecule	-0,6309963
CDADC1	cytidine and dCMP deaminase domain containing 1	-0,2296107
CDC37L1	cell division cycle 37 like 1	-0,1764697
CDC40	cell division cycle 40	-0,441555
CDC42BPB	CDC42 binding protein kinase beta	0,0815643
CDC42EP3	CDC42 effector protein 3	-0,5140497
CDCA4	cell division cycle associated 4	-0,1020283
CDCA7	cell division cycle associated 7	0,0816308
CDK7	cyclin dependent kinase 7	-0,376061
CEBPA	CCAAT/enhancer binding protein alpha	-0,2029061
CEBPB	CCAAT/enhancer binding protein beta	-0,2577453
CEBPD	CCAAT/enhancer binding protein delta	-0,2572385
CEBPG	CCAAT/enhancer binding protein gamma	-0,2272048
CEBPZ	CCAAT/enhancer binding protein zeta	-0,5126538
CELF2-AS2	CELF2 antisense RNA 2	0,1261224
CEND1	cell cycle exit and neuronal differentiation 1	0,152089
CENPC1	Centromere Protein C	-0,368321
CENPO	centromere protein O	0,0955127
CEP41	centrosomal protein 41	0,0639069
CEP89	centrosomal protein 89	0,08901
CES5A	carboxylesterase 5A	0,0782187
CFHR3	complement factor H related 3	0,058038
CFI	complement factor I	0,0687655
CFL2	cofilin 2	-0,2858331
CHAMP1	chromosome alignment maintaining phosphoprotein 1	-0,1322077
CHD1	chromodomain helicase DNA binding protein 1	-0,60082
CHIC2	cysteine rich hydrophobic domain 2	-0,2622226
CHKA	choline kinase alpha	-0,3733628
CHMP1B	charged multivesicular body protein 1B	-0,4242443

CHMP2B	charged multivesicular body protein 2B	-0,630846
CHORDC1	cysteine and histidine rich domain containing 1	-0,2060394
CHRND	cholinergic receptor nicotinic delta subunit	0,1660328
CHST3	carbohydrate sulfotransferase 3	0,1440296
CHSY1	chondroitin sulfate synthase 1	-0,1890254
CIB1	calcium and integrin binding 1	-0,364563
CIR1	corepressor interacting with RBPJ, 1	-0,6298003
CIRH1A	UTP4 Small Subunit Processome Component	-0,1893301
CKAP2	cytoskeleton associated protein 2	-0,1728114
CKM	creatine kinase, M-type	0,1499086
CLDND1	claudin domain containing 1	-0,2951463
CLEC5A	C-type lectin domain containing 5A	-0,1761465
CLEC7A	C-type lectin domain containing 7A	-0,4413506
CLK1	CDC like kinase 1	-0,4982133
CLK2P	CDC Like Kinase 2, Pseudogene 1	0,2317057
CLK4	CDC like kinase 4	-0,2573252
CLNK	cytokine dependent hematopoietic cell linker	0,109061
CLRN1-AS1	CLRN1 antisense RNA 1	0,0930773
CLRN3	clarin 3	0,1905902
CLSTN1	calsyntenin 1	0,1215104
CLYBL-AS1	CLYBL antisense RNA 1	0,1373034
CNOT2	CCR4-NOT transcription complex subunit 2	-0,344881
CNR1	cannabinoid receptor 1	0,0788473
CNR2	cannabinoid receptor 2	0,153215
CNTF	ciliary neurotrophic factor	-0,198538
CNTN3	contactin 3	0,0719386
COIL	coilin	-0,2117097
COL6A4P1	collagen type VI alpha 4 pseudogene 1	0,2315874
COPS2	COP9 signalosome subunit 2	-0,568008
COQ10B	coenzyme Q10B	-0,4915727
COX6A1P2	cytochrome c oxidase subunit 6A1 pseudogene 2	-0,4024726
COX6C	cytochrome c oxidase subunit 6C	-0,1641717
CPED1	cadherin like and PC-esterase domain containing 1	0,0688233
CR2	complement C3d receptor 2	0,1033514
CREBRF	CREB3 regulatory factor	-0,511832
CRK	CRK proto-oncogene, adaptor protein	-0,2646736
CRNKL1	crooked neck pre-mRNA splicing factor 1	-0,3223164
CRY1	cryptochrome circadian regulator 1	-0,5081964
CSH2	chorionic somatomammotropin hormone 2	0,236938
CSNK1A1	casein kinase 1 alpha 1	-0,29273
CSNK1D	casein kinase 1 delta	-0,338034
CSRP2BP	Lysine Acetyltransferase 14	0,0779023
CSTB	cystatin B	-0,2872858
CTDSPL2	CTD small phosphatase like 2	-0,2515282
CTSL1P8	Cathepsin L Pseudogene 8	0,1137987
CUL3	cullin 3	-0,2821875
CWC15	CWC15 spliceosome associated protein homolog	-0,511698

CX3CR1	C-X3-C motif chemokine receptor 1	0,5001405
CXCL1	C-X-C motif chemokine ligand 1	-0,3849987
CXCL16	C-X-C motif chemokine ligand 16	-0,434037
CXCL2	C-X-C motif chemokine ligand 2	-0,514133
CXorf40B	chromosome X open reading frame 40B	-0,105125
CYB561A3	cytochrome b561 family member A3	0,0829597
CYCSP52	cytochrome c, somatic pseudogene 52	-0,2072205
CYLC2	cylicin 2	0,097523
CYLD	CYLD lysine 63 deubiquitinase	-0,4109273
CYP2E1	cytochrome P450 family 2 subfamily E member 1	0,1190737
CYP2G1P	cytochrome P450 family 2 subfamily G member 1, pseudogene	0,2372658
CYP3A43	cytochrome P450 family 3 subfamily A member 43	0,0388406
CYP3A5	cytochrome P450 family 3 subfamily A member 5	0,0888397
CYP51A1	cytochrome P450 family 51 subfamily A member 1	-0,1983039
DARC	Atypical Chemokine Receptor 1	0,2676387
DBF4	DBF4 zinc finger	-0,4568637
DBIL5P	diazepam binding inhibitor-like 5, pseudogene	0,2541073
DBP	D-box binding PAR bZIP transcription factor	-0,1313367
DCAF16	DDB1 and CUL4 associated factor 16	-0,3127141
DCAKD	dephospho-CoA kinase domain containing	0,1032416
DCC	DCC netrin 1 receptor	0,1101525
DCP1A	decapping mRNA 1A	-0,3631946
DCTN4	dynactin subunit 4	-0,2408134
DCUN1D2-AS1	Defective In Cullin Neddylation 1 Domain Containing 2 Antisense	0,1635745
DDA1	DET1 and DDB1 associated 1	-0,32433
DDIT3	DNA damage inducible transcript 3	-1,0100787
DDIT4	DNA damage inducible transcript 4	-0,3600021
DDX20	DEAD-box helicase 20	-0,1541633
DDX21	DExD-box helicase 21	-0,525637
DDX39A	DExD-box helicase 39A	-0,2778926
DDX39B	DExD-box helicase 39B	-0,358609
DDX43	DEAD-box helicase 43	0,0784517
DDX47	DEAD-box helicase 47	-0,4473095
DEDD2	death effector domain containing 2	-0,2290326
DEFB114	defensin beta 114	0,1276596
DERL1	derlin 1	-0,2288916
DERL2	derlin 2	-0,398728
DGKG	diacylglycerol kinase gamma	0,1257482
DHRS4L2	dehydrogenase/reductase 4 like 2	0,0929799
DIS3	DIS3 homolog, exosome endoribonuclease and 3'-5' exoribonuclease	-0,3088564
DKFZp434L192	uncharacterized protein DKFZp434L192	0,2745295
DLX5	distal-less homeobox 5	0,1219797
DNAI2	dynein axonemal intermediate chain 2	0,1714125
DNAJB11	DnaJ heat shock protein family (Hsp40) member B11	-0,553125

DNAJB14	DnaJ heat shock protein family (Hsp40) member B14	-0,1694545
DNAJB6	DnaJ heat shock protein family (Hsp40) member B6	-0,2464473
DNAJB9	DnaJ heat shock protein family (Hsp40) member B9	-0,3005538
DNAJC11	DnaJ heat shock protein family (Hsp40) member C11	0,0969691
DNAJC3	DnaJ heat shock protein family (Hsp40) member C3	-0,3999701
DNTTIP2	deoxynucleotidyltransferase terminal interacting protein 2	-0,335541
DOCK9	dedicator of cytokinesis 9	0,1020057
DPH3	diphthamide biosynthesis 3	-0,4046257
DPM1	dolichyl-phosphate mannosyltransferase subunit 1, catalytic	-0,541493
DPPA4	developmental pluripotency associated 4	0,1066785
DRG1	developmentally regulated GTP binding protein 1	-0,2787614
DSC3	desmocollin 3	0,0718075
DUSP12	dual specificity phosphatase 12	-0,252275
DYNC2H1	dynein cytoplasmic 2 heavy chain 1	0,0373021
DYNLT3	dynein light chain Tctex-type 3	-0,4628654
E2F3	E2F transcription factor 3	-0,242815
EAF1	ELL associated factor 1	-0,3414703
ECD	ecdysoneless cell cycle regulator	-0,5031671
EDA2R	ectodysplasin A2 receptor	0,088952
EDAR	ectodysplasin A receptor	0,1498928
EDNRA	endothelin receptor type A	0,110748
EED	embryonic ectoderm development	-0,2116604
EFCAB3	EF-hand calcium binding domain 3	0,0734539
EGFEM1P	EGF like and EMI domain containing 1, pseudogene	0,0950231
EGR2	early growth response 2	0,1475288
EHMT2-AS1	EHMT2 and SLC44A4 antisense RNA 1	0,2444458
EID2	EP300 interacting inhibitor of differentiation 2	-0,0977543
EIF1B	eukaryotic translation initiation factor 1B	-0,325919
EIF2A	eukaryotic translation initiation factor 2A	-0,2743136
EIF2AK2	eukaryotic translation initiation factor 2 alpha kinase 2	-0,5077743
EIF3J	eukaryotic translation initiation factor 3 subunit J	-0,2884853
EIF4A3	eukaryotic translation initiation factor 4A3	-0,3688584
EIPR1	EARP Complex And GARP Complex Interacting Protein 1	0,1128912
ELOVL3	ELOVL fatty acid elongase 3	0,2392903
EMC7	ER membrane protein complex subunit 7	-0,4325557
EMD	emerin	-0,2475003
EML4	echinoderm microtubule associated protein like 4	-0,4131684
EMP1	epithelial membrane protein 1	-0,2006998
ENAH	ENAH, actin regulator	0,0742272
ENO4	enolase family member 4	0,1111567
ENOX1-AS1	ENOX1 antisense RNA 1	0,2112077
ENSA	endosulfine alpha	-0,1887026
ENTPD7	ectonucleoside triphosphate diphosphohydrolase 7	0,0991555

EPS8L3	EPS8 like 3	0,1863075
ERCC6	ERCC excision repair 6, chromatin remodeling factor	0,0667078
ERI2	ERI1 exoribonuclease family member 2	0,1452076
ERMP1	endoplasmic reticulum metallopeptidase 1	0,0930291
ERN1	endoplasmic reticulum to nucleus signaling 1	-0,163672
ERVK3-1	endogenous retrovirus group K3 member 1	-0,4085723
ESYT1	extended synaptotagmin 1	0,2064395
ETF1	eukaryotic translation termination factor 1	-0,588295
ETS2	ETS proto-oncogene 2, transcription factor	-0,2910966
ETV3	ETS variant 3	-0,213347
ETV5-AS1	ETV5 antisense RNA 1	0,1576367
EXOSC5	exosome component 5	0,2390947
EXOSC9	exosome component 9	-0,3447447
FAF2	Fas associated factor family member 2	-0,222896
FAM103A1	family with sequence similarity 103 member A1	-0,577174
FAM120AOS	family with sequence similarity 120A opposite strand	-0,1248133
FAM133B	family with sequence similarity 133 member B	-0,2492294
FAM13A-AS1	FAM13A antisense RNA 1	-0,1198521
FAM160B1	family with sequence similarity 160 member B1	-0,309174
FAM168B	family with sequence similarity 168 member B	-0,219472
FAM170B-AS1	FAM170B antisense RNA 1	0,2303555
FAM175B	Family With Sequence Similarity 175 Member B	-0,3242087
FAM189A1	family with sequence similarity 189 member A1	0,2872818
FAM193A	family with sequence similarity 193 member A	0,08196
FAM21D	Family With Sequence Similarity 21, Member D	-0,5796253
FAM227A	family with sequence similarity 227 member A	0,0841089
FAM49A	family with sequence similarity 49 member A	-0,389692
FAM5C	BMP/Retinoic Acid Inducible Neural Specific 3	0,1000066
FAM60A	SIN3-HDAC Complex Associated Factor	-0,3478236
FAM76B	family with sequence similarity 76 member B	-0,4306777
FAM83F	family with sequence similarity 83 member F	0,1432268
FAM8A1	family with sequence similarity 8 member A1	-0,324306
FAM98A	family with sequence similarity 98 member A	0,0563163
FASLG	Fas ligand	0,132304
FBXL12	F-box and leucine rich repeat protein 12	-0,1846547
FBXO10	F-box protein 10	-0,0852799
FBXO18	F-box protein, helicase, 18	0,1170356
FBXO28	F-box protein 28	-0,1962913
FBXO33	F-box protein 33	-0,2975566
FBXO8	F-box protein 8	-0,2220259
FBXW12	F-box and WD repeat domain containing 12	0,0751379
FCRL1	Fc receptor like 1	0,1187426
FDX1	ferredoxin 1	-0,35694
FEM1C	fem-1 homolog C	-0,2972714
FERD3L	Fer3 like bHLH transcription factor	0,278082
FEZ1	fasciculation and elongation protein zeta 1	0,0977184

FGF12-AS3	FGF12 antisense RNA 3	0,1173771
FGF13-AS1	FGF13 antisense RNA 1	0,1770084
FIBIN	fin bud initiation factor homolog (zebrafish)	0,2109258
FIGF	Vascular Endothelial Growth Factor D	0,0855233
FLJ10038	NA	-0,2982662
FLJ14082	NA	0,1623372
FLJ16779	uncharacterized LOC100192386	0,2020602
FLJ25715	NA	0,1236404
FLJ37035	uncharacterized LOC399821	0,0911708
FLJ37453	uncharacterized LOC729614	-0,3686843
FLJ41941	NA	0,1439829
FLJ43663	NA	-0,3123146
FLNB-AS1	FLNB antisense RNA 1	0,1219722
FLOT1	flotillin 1	-0,2161216
FMNL3	formin like 3	0,1233436
FMO4	flavin containing monooxygenase 4	0,0632178
FN3K	fructosamine 3 kinase	0,128427
FNIP2	folliculin interacting protein 2	-0,120202
FOSL2	FOS like 2, AP-1 transcription factor subunit	-0,3582921
FOXO1	forkhead box O1	-0,2526584
FRG1B	NA	-0,1711694
FTH1P3	ferritin heavy chain 1 pseudogene 3	-0,282131
FTH1P4	ferritin heavy chain 1 pseudogene 4	-0,273973
FUT9	fucosyltransferase 9	0,0608428
FXR1	FMR1 autosomal homolog 1	-0,2123783
G0S2	G0/G1 switch 2	-0,769169
GAB2	GRB2 associated binding protein 2	-0,3812619
GABRA2	gamma-aminobutyric acid type A receptor alpha2 subunit	0,0822451
GABRB1	gamma-aminobutyric acid type A receptor beta1 subunit	0,0970022
GADD45GIP1	GADD45G interacting protein 1	-0,48443
GAN	gigaxonin	0,128136
GANC	glucosidase alpha, neutral C	0,0913103
GAS5-AS1	GAS5 antisense RNA 1	0,1708446
GCNT1	glucosaminyl (N-acetyl) transferase 1, core 2	0,1266412
GGCX	gamma-glutamyl carboxylase	0,0488152
GGNBP2	gametogenetin binding protein 2	-0,350725
GLOD5	glyoxalase domain containing 5	0,1220002
GMDS	GDP-mannose 4,6-dehydratase	-0,108799
GMFB	glia maturation factor beta	-0,343118
GMPPA	GDP-mannose pyrophosphorylase A	0,1050363
GNA13	G protein subunit alpha 13	-0,4012315
GNA15	G protein subunit alpha 15	-0,1930155
GNB3	G protein subunit beta 3	0,1449873
GNL3	G protein nucleolar 3	-0,16398
GOLT1A	golgi transport 1A	0,133796

GPBAR1	G protein-coupled bile acid receptor 1	0,1636
GPBP1	GC-rich promoter binding protein 1	-0,4553986
GPBP1L1	GC-rich promoter binding protein 1 like 1	-0,2473664
GPCPD1	glycerophosphocholine phosphodiesterase 1	-0,4512694
GPR114	Adhesion G Protein-Coupled Receptor G5	0,1822047
GPR132	G protein-coupled receptor 132	-0,2641423
GPR148	G protein-coupled receptor 148	0,2342998
GPR158	G protein-coupled receptor 158	0,0844096
GPR183	G protein-coupled receptor 183	-0,78225
GPR20	G protein-coupled receptor 20	0,2514983
GPR56	Adhesion G Protein-Coupled Receptor G1	0,205677
GPR68	G protein-coupled receptor 68	0,1566806
GPR84	G protein-coupled receptor 84	-0,4831648
GPR98	Adhesion G Protein-Coupled Receptor V1	0,060791
GPX6	glutathione peroxidase 6	0,1317108
GRAMD2	GRAM Domain Containing 2A	0,0841976
GRIK1-AS2	GRIK1 Antisense RNA 2	-0,287742
GRIN3A	glutamate ionotropic receptor NMDA type subunit 3A	0,1276059
GRM5-AS1	GRM5 antisense RNA 1	0,1597842
GRM7-AS1	GRM7 antisense RNA 1	0,2814643
GSDMC	gasdermin C	0,12986
GSTA3	glutathione S-transferase alpha 3	0,1160732
GSTA5	glutathione S-transferase alpha 5	0,1261859
GTF2A1L	general transcription factor IIA subunit 1 like	0,0637341
GTF2B	general transcription factor IIB	-0,6260007
GTPBP4	GTP binding protein 4	-0,2753853
GUSBP11	glucuronidase, beta pseudogene 11	-0,1465469
GXYLT2	glucoside xylosyltransferase 2	0,11812
GYG2-AS1	GYG2 antisense RNA 1	-0,3277404
GZF1	GDNF inducible zinc finger protein 1	-0,318765
GZMK	granzyme K	-0,6613321
H2AFV	H2A histone family member V	-0,3857717
HACL1	2-hydroxyacyl-CoA lyase 1	-0,2417953
HARS	histidyl-tRNA synthetase	0,0864046
HAUS2	HAUS augmin like complex subunit 2	-0,5489287
HBP1	HMG-box transcription factor 1	-0,4850913
HBS1L	HBS1 like translational GTPase	-0,2598983
HCFC2	host cell factor C2	-0,1649551
HCG23	HLA complex group 23 (non-protein coding)	0,2447768
HCG24	HLA complex group 24 (non-protein coding)	0,3994102
HCP5	HLA complex P5 (non-protein coding)	-0,4174484
HDAC9	histone deacetylase 9	0,0587294
HDDC3	HD domain containing 3	0,1385924
HERPUD1	homocysteine inducible ER protein with ubiquitin like domain 1	-0,491228
HES1	hes family bHLH transcription factor 1	-0,3376028

HEXA-AS1	HEXA antisense RNA 1	0,1031334
HGSNAT	heparan-alpha-glucosaminide N-acetyltransferase	0,0900333
HHLA1	HERV-H LTR-associating 1	0,091958
HIAT1	Major Facilitator Superfamily Domain Containing 14A	-0,612375
HIF1A	hypoxia inducible factor 1 alpha subunit	-0,7389716
HIF1A-AS2	HIF1A antisense RNA 2	-0,1474743
HILPDA	hypoxia inducible lipid droplet associated	-0,1774382
HINFP	histone H4 transcription factor	0,1090622
HINT1	histidine triad nucleotide binding protein 1	-0,1506376
HIST1H2AA	histone cluster 1 H2A family member a	-0,1720832
HIVEP1	human immunodeficiency virus type I enhancer binding protein 1	-0,3470305
HLA-DMA	major histocompatibility complex, class II, DM alpha	-0,3560264
HLA-F	major histocompatibility complex, class I, F	-0,25347
HMGN1P30	high mobility group nucleosome binding domain 1 pseudogene 30	-0,1968913
HMGXB4	HMG-box containing 4	-0,1409073
HNF1A-AS1	HNF1A antisense RNA 1	0,2506087
HNRNPH2	heterogeneous nuclear ribonucleoprotein H2	-0,452934
HNRNPL	heterogeneous nuclear ribonucleoprotein L	-0,2316203
HOXB-AS2	HOXB cluster antisense RNA 2	0,2536835
HOXC9	homeobox C9	0,1114762
HRH2	histamine receptor H2	0,2678361
HRH2	histamine receptor H2	-0,442144
HS1BP3-IT1	HS1BP3 intronic transcript 1	0,2357419
HS3ST5	heparan sulfate-glucosamine 3-sulfotransferase 5	0,125685
HSBP1L1	heat shock factor binding protein 1 like 1	-0,4056883
HSD3B2	hydroxy-delta-5-steroid dehydrogenase, 3 beta- and steroid delta-isomerase 2	0,1407026
HSPA13	heat shock protein family A (Hsp70) member 13	-0,5317947
HTR2A	5-hydroxytryptamine receptor 2A	0,165176
HTR3B	5-hydroxytryptamine receptor 3B	0,1239137
HTRA1	HtrA serine peptidase 1	0,0743013
HUS1	HUS1 checkpoint clamp component	-0,200336
HYALP1	hyaluronoglucosaminidase pseudogene 1	0,1844359
ICMT	isoprenylcysteine carboxyl methyltransferase	0,0980286
ID2	inhibitor of DNA binding 2	-0,2900162
IDI1	isopentenyl-diphosphate delta isomerase 1	-0,5850692
IER3	immediate early response 3	-0,7387855
IER5L	immediate early response 5 like	-0,2226043
IFIH1	interferon induced with helicase C domain 1	-0,555409
IFNA17	interferon alpha 17	0,2444072
IFNA6	interferon alpha 6	0,0953751
IFNAR1	interferon alpha and beta receptor subunit 1	-0,4931394
IFNG	interferon gamma	-0,991313
IFNGR2	interferon gamma receptor 2	-0,4277846

IFNW1	interferon omega 1	0,0846924
IFT57	intraflagellar transport 57	-0,2667586
IGHV1-46	immunoglobulin heavy variable 1-46	0,2798327
IGHV1-58	immunoglobulin heavy variable 1-58	0,2069124
IGKV2-40	immunoglobulin kappa variable 2-40	0,1400754
IGKV4-1	immunoglobulin kappa variable 4-1	-0,2065397
IGKV6D-41	immunoglobulin kappa variable 6D-41 (non-functional)	0,2094671
IGLC7	immunoglobulin lambda constant 7	-0,4351992
IGLV3-16	immunoglobulin lambda variable 3-16	0,2414131
IKZF5	IKAROS family zinc finger 5	-0,5304054
IL17F	interleukin 17F	0,1480891
IL1B	interleukin 1 beta	-0,788842
IL1RAP	interleukin 1 receptor accessory protein	-0,1762492
IL1RAPL1	interleukin 1 receptor accessory protein like 1	0,1126196
IL20RB-AS1	IL20RB antisense RNA 1	0,1713095
IL22RA1	interleukin 22 receptor subunit alpha 1	0,2025406
IL36A	interleukin 36 alpha	0,3566182
IL8	interleukin 8	-0,718772
IL9	interleukin 9	0,1465867
IMPA1P	Inositol Monophosphatase 1 Pseudogene 1	0,1154737
ING1	inhibitor of growth family member 1	-0,1354661
ING3	inhibitor of growth family member 3	-0,4120735
INPP5K	inositol polyphosphate-5-phosphatase K	-0,2141066
INTS5	integrator complex subunit 5	-0,141417
INTS9	integrator complex subunit 9	0,052851
IQCK	IQ motif containing K	0,0718069
IRF7	interferon regulatory factor 7	-0,221036
IRS1	insulin receptor substrate 1	0,1088802
IRX6	iroquois homeobox 6	0,1360452
IST1	IST1, ESCRT-III associated factor	-0,3829303
ITGB5	integrin subunit beta 5	0,1464918
ITLN2	intelectin 2	0,1509512
IVD	isovaleryl-CoA dehydrogenase	0,0894388
IVNS1ABP	influenza virus NS1A binding protein	-0,6301893
JMJD1C-AS1	JMJD1C antisense RNA 1	0,117125
JMJD6	arginine demethylase and lysine hydroxylase	-0,3795383
JRKL	JRK like	0,1105584
JTB	jumping translocation breakpoint	-0,3579914
JUNB	JunB proto-oncogene, AP-1 transcription factor subunit	-0,5432667
KATNAL2	katanin catalytic subunit A1 like 2	0,1184942
KAZN	kazrin, periplakin interacting protein	0,1038972
KBTBD2	kelch repeat and BTB domain containing 2	-0,3253073
KCNA5	potassium voltage-gated channel subfamily A member 5	0,2336802

KCND3	potassium voltage-gated channel subfamily D member 3	0,1678259
KCNF1	potassium voltage-gated channel modifier subfamily F member 1	0,22598
KCNJ13	potassium voltage-gated channel subfamily J member 13	0,0696777
KCNJ9	potassium voltage-gated channel subfamily J member 9	0,1536423
KCNK13	potassium two pore domain channel subfamily K member 13	-0,1633957
KCNK2	potassium two pore domain channel subfamily K member 2	0,1127698
KCTD21	potassium channel tetramerization domain containing 21	0,1870505
KDM8	lysine demethylase 8	0,0804994
KHDRBS2	KH RNA binding domain containing, signal transduction associated 2	0,0888454
KIAA0125	Family With Sequence Similarity 30 Member A	0,149634
KIAA1024L	KIAA1024 like	0,2081725
KIAA1143	KIAA1143	-0,4642543
KIAA1549	KIAA1549	0,1071924
KIAA1644	Shisa Like 1	0,2040546
KIAA2022	Neurite Extension And Migration Factor	0,1255217
KIF20B	kinesin family member 20B	-0,1750753
KIF2C	kinesin family member 2C	0,1013906
KIF3C	kinesin family member 3C	0,1126855
KIF4A	kinesin family member 4A	0,0934351
KIF5C	kinesin family member 5C	0,0903272
KIN	Kin17 DNA and RNA binding protein	-0,2576127
KIR3DL3	killer cell immunoglobulin like receptor, three Ig domains and long cytoplasmic tail 3	0,2065286
KIR3DS1	killer cell immunoglobulin like receptor, three Ig domains and short cytoplasmic tail 1	0,2188025
KLHDC2	kelch domain containing 2	-0,3622179
KLHL2	kelch like family member 2	-0,2101126
KLHL24	kelch like family member 24	-0,334063
KLHL40	kelch like family member 40	0,1111057
KPNA3	karyopherin subunit alpha 3	-0,4563916
KPRP	keratinocyte proline rich protein	0,3738589
KRAS	KRAS proto-oncogene, GTPase	-0,1999497
KRR1	KRR1, small subunit processome component homolog	-0,5730572
KRT17P2	keratin 17 pseudogene 2	0,1434777
KRT20	keratin 20	0,1170951
KRT79	keratin 79	0,1660595
KRTAP19-1	keratin associated protein 19-1	0,2113199
KRTAP21-3	keratin associated protein 21-3	0,2258093

LACTB	lactamase beta	-0,5192399
LAMP3	lysosomal associated membrane protein 3	0,1410889
LAMTOR3	late endosomal/lysosomal adaptor, MAPK and MTOR activator 3	-0,681635
LAMTOR5	late endosomal/lysosomal adaptor, MAPK and MTOR activator 5	-0,4122364
LBH	limb bud and heart development	0,1257987
LCP2	lymphocyte cytosolic protein 2	-0,5459006
LCTL	lactase like	0,0474744
LEUTX	leucine twenty homeobox	0,254315
LGALS17A	galectin 14 pseudogene	0,1242704
LHFPL3-AS2	LHFPL3 antisense RNA 2	0,1082446
LIMK2	LIM domain kinase 2	-0,2884544
LIN54	lin-54 DREAM MuvB core complex component	-0,1288657
LINC00035	Williams Beuren Syndrome Chromosome Region 26	0,229373
LINC00222	long intergenic non-protein coding RNA 222	0,1849818
LINC00271	long intergenic non-protein coding RNA 271	0,0969014
LINC00272	long intergenic non-protein coding RNA 272	0,1929369
LINC00305	long intergenic non-protein coding RNA 305	0,1408672
LINC00326	long intergenic non-protein coding RNA 326	0,113925
LINC00327	long intergenic non-protein coding RNA 327	0,1476606
LINC00343	long intergenic non-protein coding RNA 343	0,1041097
LINC00365	long intergenic non-protein coding RNA 365	0,1409105
LINC00434	long intergenic non-protein coding RNA 434	0,2598805
LINC00460	long intergenic non-protein coding RNA 460	0,1502721
LINC00469	long intergenic non-protein coding RNA 469	0,1802406
LINC00478	Mir-99a-Let-7c Cluster Host Gene	0,063264
LINC00502	long intergenic non-protein coding RNA 502	0,2899549
LINC00507	long intergenic non-protein coding RNA 507	0,071273
LINC00523	long intergenic non-protein coding RNA 523	0,1460237
LINC00575	long intergenic non-protein coding RNA 575	0,2265671
LINC00649	Long Intergenic Non-Protein Coding RNA 649	0,1393414
LINC00667	long intergenic non-protein coding RNA 667	-0,2818708
LINC00681	long intergenic non-protein coding RNA 681	0,0825606
LINC00694	long intergenic non-protein coding RNA 694	0,2498712
LINC00707	long intergenic non-protein coding RNA 707	0,1332194
LINC00857	long intergenic non-protein coding RNA 857	0,14189
LINC00858	long intergenic non-protein coding RNA 858	0,1370604
LINC00864	long intergenic non-protein coding RNA 864	0,1936782
LINC00933	long intergenic non-protein coding RNA 933	0,1201332
LINC00961	Small Regulatory Polypeptide Of Amino Acid Response	0,2913807
LMTK2	lemur tyrosine kinase 2	-0,264824
LOC100129316	uncharacterized LOC100129316	0,2068705
LOC100130264	uncharacterized LOC100130264	0,12572
LOC100130880	uncharacterized LOC100130880	0,1819086
LOC100132215	uncharacterized LOC100132215	0,102837

LOC100132741	uncharacterized LOC100132741	0,1920771
LOC100271832	uncharacterized LOC100271832	0,165941
LOC100272217	uncharacterized LOC100272217	0,1570866
LOC100288637	OTU deubiquitinase 7A pseudogene	0,1548819
LOC100499194	uncharacterized LOC100499194	0,2986472
LOC100506071	uncharacterized LOC100506071	0,0989819
LOC100506274	uncharacterized LOC100506274	0,1105936
LOC100506691	uncharacterized LOC100506691	0,1732455
LOC100506804	uncharacterized LOC100506804	0,167781
LOC100507006	uncharacterized LOC100507006	-0,3289231
LOC100507250	uncharacterized LOC100507250	-0,117438
LOC100507480	uncharacterized LOC100507480	0,2262557
LOC100507562	uncharacterized LOC100507562	0,2599179
LOC100996263	uncharacterized LOC100996263	0,1637148
LOC284578	uncharacterized LOC284578	0,1895754
LOC284632	uncharacterized LOC284632	0,2001157
LOC285593	uncharacterized LOC285593	0,1288819
LOC285819	uncharacterized LOC285819	0,292491
LOC285847	uncharacterized LOC285847	0,2112223
LOC286177	uncharacterized LOC286177	0,2743578
LOC399815	chromosome 10 open reading frame 88 pseudogene	0,1339522
LOC401127	WD repeat domain 5 pseudogene	0,275989
LOC554206	leucine carboxyl methyltransferase 1 pseudogene	0,2815827
LOC645188	uncharacterized LOC645188	0,1771894
LOC645513	septin 7 pseudogene	-0,2225275
LONRF1	LON peptidase N-terminal domain and ring finger 1	-0,2389086
LRCOL1	leucine rich colipase like 1	0,1420903
LRRC1	leucine rich repeat containing 1	0,0775338
LRRC16A	Capping Protein Regulator And Myosin 1 Linker 1	0,0682676
LRRC3C	leucine rich repeat containing 3C	0,2783894
LRRC55	leucine rich repeat containing 55	0,2176336
LRRN3	leucine rich repeat neuronal 3	0,1211476
LRRTM3	leucine rich repeat transmembrane neuronal 3	0,052637
LSAMP-AS2	Long Intergenic Non-Protein Coding RNA 903	0,133174
LSM7	LSM7 homolog, U6 small nuclear RNA and mRNA degradation associated	-0,3366403
LUC7L	LUC7 like	-0,14612
LY6G6D	lymphocyte antigen 6 family member G6D	0,246377
LY86-AS1	LY86 antisense RNA 1	0,1288328
LYPD8	LY6/PLAUR domain containing 8	0,1963796
LYSMD3	LysM domain containing 3	-0,2704183
MAB21L1	mab-21 like 1	0,1252845
MAB21L3	mab-21 like 3	0,1275431
MAD2L2	mitotic arrest deficient 2 like 2	-0,1089903
MAFA	MAF bZIP transcription factor A	0,2023289
MAFB	MAF bZIP transcription factor B	-0,3388383
MAFF	MAF bZIP transcription factor F	-0,1638717

MAGEA11	MAGE family member A11	0,1759157
MAGEB17	MAGE family member B17	0,1755449
MAGEB18	MAGE family member B18	0,1050385
MAGEL2	MAGE family member L2	0,2570725
MAP1B	microtubule associated protein 1B	0,0638497
MAP1LC3B2	microtubule associated protein 1 light chain 3 beta 2	-0,3483785
MAP3K10	mitogen-activated protein kinase kinase kinase 10	0,160606
MAP3K15	mitogen-activated protein kinase kinase kinase 15	0,0918603
MAP3K19	mitogen-activated protein kinase kinase kinase 19	0,0753246
MAP6D1	MAP6 domain containing 1	0,1332331
MAPK1IP1L	mitogen-activated protein kinase 1 interacting protein 1 like	-0,37345
MAPK6	mitogen-activated protein kinase 6	-0,7801395
MARCKS	myristoylated alanine rich protein kinase C substrate	-0,5476958
MAST4	microtubule associated serine/threonine kinase family member 4	0,088934
MATR3	matrin 3	-0,1806674
MBD4	methyl-CpG binding domain 4, DNA glycosylase	-0,4515263
MBIP	MAP3K12 binding inhibitory protein 1	-0,378818
MC2R	melanocortin 2 receptor	0,1166898
MC4R	melanocortin 4 receptor	0,1294765
MCPH1	microcephalin 1	-0,0884114
MED21	mediator complex subunit 21	-0,621127
MED24	mediator complex subunit 24	0,111753
MED27	mediator complex subunit 27	-0,1906293
MED28	mediator complex subunit 28	-0,404232
MED30	mediator complex subunit 30	-0,322473
MED6	mediator complex subunit 6	-0,3538342
METTL14	methyltransferase like 14	-0,1551841
MFN1	mitofusin 1	-0,2791766
MGAT1	mannosyl (alpha-1,3-)-glycoprotein beta-1,2-N-acetylglucosaminyltransferase	-0,1256115
MIDN	midnolin	-0,3751305
MIER1	MIER1 transcriptional regulator	-0,2762341
MINA	Ribosomal Oxygenase 2	0,090833
MIOS	meiosis regulator for oocyte development	-0,2230454
MIS12	MIS12, kinetochore complex component	-0,2383005
MKL2	MKL1/myocardin like 2	0,0736502
MLN	motilin	0,2688828
MMADHC	methylmalonic aciduria and homocystinuria, cblD type	-0,3786683
MMP14	matrix metallopeptidase 14	0,16465
MMP28	matrix metallopeptidase 28	0,1417075
MMP7	matrix metallopeptidase 7	0,1555995
MNT	MAX network transcriptional repressor	-0,1820197
MOB4	MOB family member 4, phocein	-0,3660777
MORC2-AS1	MORC2 antisense RNA 1	0,1729864

MORF4L1	mortality factor 4 like 1	-0,2784554
MORF4L2	mortality factor 4 like 2	-0,379871
MORF4L2-AS1	MORF4L2 antisense RNA 1	0,1764363
MPHOSPH10	M-phase phosphoprotein 10	-0,1874842
MPP5	membrane palmitoylated protein 5	-0,1693835
MRC1	mannose receptor C-type 1	0,1021969
MRPL22	mitochondrial ribosomal protein L22	-0,2730816
MRPL47	mitochondrial ribosomal protein L47	-0,5458112
MSMB	microseminoprotein beta	0,1339441
MSMO1	methylsterol monooxygenase 1	-0,5274181
MT1E	metallothionein 1E	-0,235251
MT1F	metallothionein 1F	-0,3992157
MTHFD1	methylenetetrahydrofolate dehydrogenase, cyclohydrolase and formyltetrahydrofolate synthetase 1	0,1143658
MTHFSD	methenyltetrahydrofolate synthetase domain containing	0,1022837
MTMR6	myotubularin related protein 6	-0,377399
MTMR8	myotubularin related protein 8	0,1068087
MTOR-AS1	MTOR antisense RNA 1	0,1099555
MTPAP	mitochondrial poly(A) polymerase	-0,1318391
MUM1	melanoma associated antigen (mutated) 1	0,0718308
MUS81	MUS81 structure-specific endonuclease subunit	0,1329074
MYADML2	myeloid associated differentiation marker like 2	0,2202507
MYCBPAP	MYCBP associated protein	0,1031037
MYH8	myosin heavy chain 8	0,068799
MYNN	myoneurin	-0,3566624
MYO1C	myosin IC	0,0901005
MYO1E	myosin IE	0,0752983
MYOF	myoferlin	0,12098
MYOM1	myomesin 1	0,0960879
NAB1	NGFI-A binding protein 1	-0,0873986
NADKD1-AS1	NADK2 Antisense RNA 1	0,2730797
NAMPT	nicotinamide phosphoribosyltransferase	-0,625649
NAMPTL	Nicotinamide Phosphoribosyltransferase Pseudogene 1	-0,491431
NAP1L5	nucleosome assembly protein 1 like 5	-0,2231031
NAPG	NSF attachment protein gamma	-0,3745646
NAV2-AS5	NAV2 antisense RNA 5	0,1452876
NBEA	neurobeachin	0,054457
NBPF5P	NBPF member 5, pseudogene	0,2216356
NCAPD2	non-SMC condensin I complex subunit D2	0,2219464
NCAPD3	non-SMC condensin II complex subunit D3	0,1156686
NCAPG2	non-SMC condensin II complex subunit G2	0,0877161
NCBP2L	nuclear cap binding protein subunit 2 like	0,304358
NCK1	NCK adaptor protein 1	-0,2284107
NCR1	natural cytotoxicity triggering receptor 1	0,2338647

NDUFA1	NADH:ubiquinone oxidoreductase subunit A1	-0,399753
NDUFA6	NADH:ubiquinone oxidoreductase subunit A6	-0,4192943
NDUFAF4	NADH:ubiquinone oxidoreductase complex assembly factor 4	-0,3298886
NDUFAF5	NADH:ubiquinone oxidoreductase complex assembly factor 5	-0,2915876
NDUFB4	NADH:ubiquinone oxidoreductase subunit B4	-0,180458
NDUFS6	NADH:ubiquinone oxidoreductase subunit S6	-0,153825
NDUFV2	NADH:ubiquinone oxidoreductase core subunit V2	-0,3522662
NECAP1	NECAP endocytosis associated 1	-0,563198
NEDD4	neural precursor cell expressed, developmentally down-regulated 4, E3 ubiquitin protein ligase	0,0630997
NF2	neurofibromin 2	0,0864157
NFE2L2	nuclear factor, erythroid 2 like 2	-0,4178517
NFE2L3	nuclear factor, erythroid 2 like 3	0,1583906
NFIL3	nuclear factor, interleukin 3 regulated	-0,6278813
NFKBIA	NFKB inhibitor alpha	-0,809967
NGDN	neuroguidin	-0,4162174
NGRN	neugrin, neurite outgrowth associated	-0,3019767
NHP2L1	Small Nuclear Ribonucleoprotein 13	-0,356268
NHS-AS1	NHS antisense RNA 1	0,3244263
NHSL2	NHS like 2	0,2348997
NID1	nidogen 1	0,1335895
NINJ1	ninjurin 1	-0,4105878
NKIRAS1	NFKB inhibitor interacting Ras like 1	-0,0878772
NLGN1-AS1	NLGN1 antisense RNA 1	0,0561492
NLRP13	NLR family pyrin domain containing 13	0,1303512
NMD3	NMD3 ribosome export adaptor	-0,32576
NME5	NME/NM23 family member 5	0,0575047
NOD1	nucleotide binding oligomerization domain containing 1	0,0745358
NOL11	nucleolar protein 11	-0,42795
NOL7	nucleolar protein 7	-0,252459
NOP58	NOP58 ribonucleoprotein	-0,505034
NOVA1	NOVA alternative splicing regulator 1	0,0860515
NOVA1-AS1	NOVA1 antisense RNA 1 (head to head)	0,133903
NPY6R	neuropeptide Y receptor Y6 (pseudogene)	0,2108513
NR1D1	nuclear receptor subfamily 1 group D member 1	-0,2426777
NR1D2	nuclear receptor subfamily 1 group D member 2	-0,325795
NR1H2	nuclear receptor subfamily 1 group H member 2	-0,179841
NR3C1	nuclear receptor subfamily 3 group C member 1	-0,2266514
NR4A2	nuclear receptor subfamily 4 group A member 2	-0,6149201
NRBF2	nuclear receptor binding factor 2	-0,4635019
NRG4	neuregulin 4	0,0695963
NRP1	neuropilin 1	0,0792024
NRSN1	neurensin 1	0,1246278
NT5E	5'-nucleotidase ecto	0,04465

NUB1	negative regulator of ubiquitin like proteins 1	-0,1786774
NUP210L	nucleoporin 210 like	0,0626981
NUP54	nucleoporin 54	-0,2945401
NUP88	nucleoporin 88	-0,3115497
NXPE4	neurexophilin and PC-esterase domain family member 4	0,0831401
NXT1	nuclear transport factor 2 like export factor 1	-0,4058418
OASL	2'-5'-oligoadenylate synthetase like	-0,4266348
OCM	oncomodulin	0,1399422
ODF3B	outer dense fiber of sperm tails 3B	-0,1692515
OGFOD2	2-oxoglutarate and iron dependent oxygenase domain containing 2	0,1396766
OMP	olfactory marker protein	0,2799484
OR10A4	olfactory receptor family 10 subfamily A member 4	0,1582667
OR10J1	olfactory receptor family 10 subfamily J member 1	0,1315566
OR10J3	olfactory receptor family 10 subfamily J member 3	0,432497
OR10V2P	olfactory receptor family 10 subfamily V member 2 pseudogene	0,2318552
OR11H2	olfactory receptor family 11 subfamily H member 2	0,1782936
OR12D3	olfactory receptor family 12 subfamily D member 3	0,1781646
OR1F2P	olfactory receptor family 1 subfamily F member 2 pseudogene	0,3919816
OR2A42	olfactory receptor family 2 subfamily A member 42	0,3000839
OR2AP1	olfactory receptor family 2 subfamily AP member 1	0,1234564
OR2B2	olfactory receptor family 2 subfamily B member 2	0,1375838
OR2B3	olfactory receptor family 2 subfamily B member 3	0,1848744
OR3A1	olfactory receptor family 3 subfamily A member 1	0,3568774
OR4D11	olfactory receptor family 4 subfamily D member 11	0,2367277
OR51A4	olfactory receptor family 51 subfamily A member 4	0,2923842
OR51L1	olfactory receptor family 51 subfamily L member 1	0,2401763
OR52B6	olfactory receptor family 52 subfamily B member 6	0,4171242
OR52D1	olfactory receptor family 52 subfamily D member 1	0,2654011
OR52E8	olfactory receptor family 52 subfamily E member 8	0,2143627
OR56A5	olfactory receptor family 56 subfamily A member 5	0,2670958
OR5AP2	olfactory receptor family 5 subfamily AP member 2	0,185633
OR5AS1	olfactory receptor family 5 subfamily AS member 1	0,1737484
OR5D16	olfactory receptor family 5 subfamily D member 16	0,277415
OR5H6	olfactory receptor family 5 subfamily H member 6 (gene/pseudogene)	0,105003
OR5R1	olfactory receptor family 5 subfamily R member 1 (gene/pseudogene)	0,2977291
OR6N2	olfactory receptor family 6 subfamily N member 2	0,1195521
OR6P1	olfactory receptor family 6 subfamily P member 1	0,1754256
OR6S1	olfactory receptor family 6 subfamily S member 1	0,2896493
OR6T1	olfactory receptor family 6 subfamily T member 1	0,1076554
OR7A5	olfactory receptor family 7 subfamily A member 5	0,1834735
OSER1	oxidative stress responsive serine rich 1	-0,4601984

OSGIN2	oxidative stress induced growth inhibitor family member 2	-0,660769
OSM	oncostatin M	-0,4262143
OTC	ornithine carbamoyltransferase	0,1158574
OTOL1	otolin 1	0,2068648
OTX1	orthodenticle homeobox 1	0,1152823
OVOL2	ovo like zinc finger 2	0,0967172
P2RX4	purinergic receptor P2X 4	-0,1490697
PABPN1	poly(A) binding protein nuclear 1	-0,1721705
PAG1	phosphoprotein membrane anchor with glycosphingolipid microdomains 1	-0,2581658
PAIP1	poly(A) binding protein interacting protein 1	-0,2309695
PARM1	prostate androgen-regulated mucin-like protein 1	0,2112255
PART1	prostate androgen-regulated transcript 1 (non-protein coding)	0,1686056
PATE4	prostate and testis expressed 4	0,1832048
PCDH11X	protocadherin 11 X-linked	0,0682117
PCDH12	protocadherin 12	0,148576
PCDH8	protocadherin 8	0,1413877
PCDHB10	protocadherin beta 10	-0,1393
PCDHB11	protocadherin beta 11	0,1187238
PCDHB2	protocadherin beta 2	0,1311407
PCDHB9	protocadherin beta 9	0,1263998
PCDHGA9	protocadherin gamma subfamily A, 9	0,3305473
PCYOX1L	prenylcysteine oxidase 1 like	0,0967504
PDE12	phosphodiesterase 12	-0,1453359
PDGFD	platelet derived growth factor D	-0,108804
PDGFRB	platelet derived growth factor receptor beta	0,1303587
PDIA5	protein disulfide isomerase family A member 5	0,0603941
PDK4	pyruvate dehydrogenase kinase 4	0,2995239
PEAR1	platelet endothelial aggregation receptor 1	0,1228335
PFDN1	prefoldin subunit 1	-0,2924848
PFDN2	prefoldin subunit 2	-0,3025544
PFKFB3	6-phosphofructo-2-kinase/fructose-2,6-biphosphatase 3	-0,47728
PGLYRP4	peptidoglycan recognition protein 4	0,2101607
PGS1	phosphatidylglycerophosphate synthase 1	-0,2595598
PHF11	PHD finger protein 11	-0,2286474
PHF5A	PHD finger protein 5A	-0,3470745
PIGH	phosphatidylinositol glycan anchor biosynthesis class H	-0,188768
PIM2	Pim-2 proto-oncogene, serine/threonine kinase	-0,4304353
PIM3	Pim-3 proto-oncogene, serine/threonine kinase	-0,3983521
PIP4K2C	phosphatidylinositol-5-phosphate 4-kinase type 2 gamma	-0,11178
PIP4P1	Phosphatidylinositol-4,5-Bisphosphate 4-Phosphatase 1	-0,2013455

PIP5K1C	phosphatidylinositol-4-phosphate 5-kinase type 1 gamma	0,1499487
PKP4	plakophilin 4	0,0865217
PLAA	phospholipase A2 activating protein	-0,2681883
PLAUR	plasminogen activator, urokinase receptor	-0,6824031
PLCB1-IT1	PLCB1 intronic transcript 1	-0,1468887
PLCE1	phospholipase C epsilon 1	0,0516713
PLEK	pleckstrin	-0,6246173
PLEKHF2	pleckstrin homology and FYVE domain containing 2	-0,3168721
PLIN3	perilipin 3	-0,242454
PLS3	plastin 3	0,0427981
PMFBP1	polyamine modulated factor 1 binding protein 1	0,0976383
PNPLA8	patatin like phospholipase domain containing 8	-0,5185044
PNRC2	proline rich nuclear receptor coactivator 2	-0,4546563
POFUT1	protein O-fucosyltransferase 1	0,137696
POLA2	DNA polymerase alpha 2, accessory subunit	0,1096857
POLR1B	RNA polymerase I subunit B	0,0403952
POLR2C	RNA polymerase II subunit C	-0,1915053
POLR2J	RNA polymerase II subunit J	-0,190534
POLR2K	RNA polymerase II subunit K	-0,5259483
POLR3F	RNA polymerase III subunit F	-0,1301713
POMP	proteasome maturation protein	-0,5009744
POMT2	protein O-mannosyltransferase 2	0,0761944
POSTN	periostin	0,0428303
POU2AF1	POU class 2 associating factor 1	0,0840021
POU3F4	POU class 3 homeobox 4	0,1257455
PPCDC	phosphopantothenoylcysteine decarboxylase	-0,25328
PPIF	peptidylprolyl isomerase F	-0,6825867
PPIG	peptidylprolyl isomerase G	-0,562394
PPIL4	peptidylprolyl isomerase like 4	-0,3495751
PPM1E	protein phosphatase, Mg2+/Mn2+ dependent 1E	0,0695517
PPM1L	protein phosphatase, Mg2+/Mn2+ dependent 1L	0,1026599
PPP1R14D	protein phosphatase 1 regulatory inhibitor subunit 14D	0,1435551
PPP1R15A	protein phosphatase 1 regulatory subunit 15A	-0,6455555
PPP1R17	protein phosphatase 1 regulatory subunit 17	0,1115423
PPP1R2	protein phosphatase 1 regulatory inhibitor subunit 2	-0,4477854
PPP1R2P3	protein phosphatase 1 regulatory inhibitor subunit 2 pseudogene 3	-0,145723
PPP1R3D	protein phosphatase 1 regulatory subunit 3D	-0,1131244
PPP2CA	protein phosphatase 2 catalytic subunit alpha	-0,3715691
PPP2R2A	protein phosphatase 2 regulatory subunit Balpha	-0,2129707
PPP4R2	protein phosphatase 4 regulatory subunit 2	-0,2370715
PPP6C	protein phosphatase 6 catalytic subunit	-0,43909
PRDM11	PR/SET domain 11	0,1541745
PRDM2	PR/SET domain 2	-0,188828
PRELID1	PRELI domain containing 1	-0,3395913

PRG3	proteoglycan 3, pro eosinophil major basic protein 2	0,2065404
PRKRA	protein activator of interferon induced protein kinase EIF2AK2	-0,0966677
PRMT6	protein arginine methyltransferase 6	-0,1498355
PROX2	prospero homeobox 2	0,1119828
PRPF3	pre-mRNA processing factor 3	-0,2041969
PRPF40A	pre-mRNA processing factor 40 homolog A	-0,27246
PRR23B	proline rich 23B	0,1283459
PRR33	Proline Rich 33	-0,1919466
PSAPL1	prosaposin like 1 (gene/pseudogene)	0,2926701
PSAT1P4	phosphoserine aminotransferase 1 pseudogene 4	0,200032
PSCA	prostate stem cell antigen	0,2881887
PSD4	pleckstrin and Sec7 domain containing 4	0,1203895
PSMB4	proteasome subunit beta 4	-0,4634843
PSMB8	proteasome subunit beta 8	-0,3313461
PSMC1	proteasome 26S subunit, ATPase 1	-0,2956089
PSMC3IP	PSMC3 interacting protein	0,1163
PSMD12	proteasome 26S subunit, non-ATPase 12	-0,4393236
PSMD6	proteasome 26S subunit, non-ATPase 6	-0,343742
PSMD7	proteasome 26S subunit, non-ATPase 7	-0,4688966
PSMD9	proteasome 26S subunit, non-ATPase 9	-0,178089
PSMG2	proteasome assembly chaperone 2	-0,489052
PSPN	persephin	0,2574335
PTBP1	polypyrimidine tract binding protein 1	-0,1966486
PTCD2	pentatricopeptide repeat domain 2	0,0552405
PTCH1	patched 1	0,1136007
PTDSS2	phosphatidylserine synthase 2	0,1709536
PTP4A1	protein tyrosine phosphatase type IVA, member 1	-0,5299516
PTPMT1	protein tyrosine phosphatase, mitochondrial 1	-0,1243885
PTPN11	protein tyrosine phosphatase, non-receptor type 11	-0,1467503
PTPRE	protein tyrosine phosphatase, receptor type E	-0,4362295
PTS	6-pyruvoyltetrahydropterin synthase	-0,3278427
PTX3	pentraxin 3	-0,2187467
PWP1	PWP1 homolog, endonuclein	-0,274482
PWRN2	Prader-Willi region non-protein coding RNA 2	0,1627738
PXMP4	peroxisomal membrane protein 4	0,1421556
PYROXD1	pyridine nucleotide-disulphide oxidoreductase domain 1	-0,2243655
PZP	PZP, alpha-2-macroglobulin like	0,0932885
QKI	QKI, KH domain containing RNA binding	-0,2714744
RAB1A	RAB1A, member RAS oncogene family	-0,477146
RAB20	RAB20, member RAS oncogene family	-0,6352615
RAB21	RAB21, member RAS oncogene family	-0,583859
RAB22A	RAB22A, member RAS oncogene family	-0,2292771
RAB24	RAB24, member RAS oncogene family	-0,1960293
RAB2A	RAB2A, member RAS oncogene family	-0,2473055
RAB37	RAB37, member RAS oncogene family	0,1135559

RAB5A	RAB5A, member RAS oncogene family	-0,2882843
RABGEF1	RAB guanine nucleotide exchange factor 1	-0,4864068
RABGGTB	Rab geranylgeranyltransferase beta subunit	-0,3198627
RAD1	RAD1 checkpoint DNA exonuclease	-0,1246768
RAD52	RAD52 homolog, DNA repair protein	0,0896652
RAG2	recombination activating 2	0,1198971
RALA	RAS like proto-oncogene A	-0,1460354
RALGDS	ral guanine nucleotide dissociation stimulator	-0,181039
RAP2C	RAP2C, member of RAS oncogene family	-0,3033383
RAPGEF5	Rap guanine nucleotide exchange factor 5	0,0652154
RASA2	RAS p21 protein activator 2	-0,4261353
RASAL2	RAS protein activator like 2	0,0874584
RASGRF1	Ras protein specific guanine nucleotide releasing factor 1	0,1137958
RB1CC1	RB1 inducible coiled-coil 1	-0,4339968
RBFA	ribosome binding factor A	0,091728
RBM11	RNA binding motif protein 11	-0,2743955
RBM15	RNA binding motif protein 15	-0,2745517
RBM15B	RNA binding motif protein 15B	-0,0862116
RBM18	RNA binding motif protein 18	-0,4810636
RBM25	RNA binding motif protein 25	-0,382894
RBM34	RNA binding motif protein 34	-0,376472
RBM39	RNA binding motif protein 39	-0,4147595
RBM48	RNA binding motif protein 48	-0,3092699
RBM7	RNA binding motif protein 7	-0,2831703
RBM8A	RNA binding motif protein 8A	-0,2703793
RBPJ	recombination signal binding protein for immunoglobulin kappa J region	-0,3620429
RCN2	reticulocalbin 2	-0,2807237
RDH12	retinol dehydrogenase 12 (all-trans/9-cis/11-cis)	0,1889149
RDH14	retinol dehydrogenase 14 (all-trans/9-cis/11-cis)	-0,169206
RDH8	retinol dehydrogenase 8 (all-trans)	0,1999874
REL	REL proto-oncogene, NF-kB subunit	-0,428815
RELA	RELA proto-oncogene, NF-kB subunit	-0,304492
REN	renin	0,2040032
RGMB-AS1	RGMB antisense RNA 1	0,0943642
RGS1	regulator of G protein signaling 1	-0,6300223
RHBDL3	rhomboid like 3	0,2003825
RHOB	ras homolog family member B	-0,4981031
RHOBTB2	Rho related BTB domain containing 2	0,1222106
RHOQ	ras homolog family member Q	-0,2141444
RHOQP2	ras homolog family member Q pseudogene 2	0,180284
RINL	Ras and Rab interactor like	0,1324157
RIPK1	receptor interacting serine/threonine kinase 1	-0,1407124
RIPK2	receptor interacting serine/threonine kinase 2	-0,5198696
RIPK4	receptor interacting serine/threonine kinase 4	0,205315
RIT2	Ras like without CAAX 2	0,0976243

RLIM	ring finger protein, LIM domain interacting	-0,3585955
RMI2	RecQ mediated genome instability 2	0,1048803
RNA5-8SP4	RNA, 5.8S ribosomal pseudogene 4	-0,1238229
RNA5-8SP6	RNA, 5.8S ribosomal pseudogene 6	-0,2796087
RNA5SP133	RNA, 5S ribosomal pseudogene 133	0,3471375
RNA5SP292	RNA, 5S ribosomal pseudogene 292	0,1734867
RNASEH2A	ribonuclease H2 subunit A	0,1313362
RNASEK	ribonuclease K	-0,3645014
RNASET2	ribonuclease T2	-0,1121947
RNF103	ring finger protein 103	-0,3478312
RNF113B	ring finger protein 113B	0,1734412
RNF114	ring finger protein 114	-0,5457384
RNF126	ring finger protein 126	-0,165103
RNF138	ring finger protein 138	-0,534062
RNF139	ring finger protein 139	-0,1907859
RNF157	ring finger protein 157	0,1158602
RNF166	ring finger protein 166	-0,212828
RNF168	ring finger protein 168	-0,2703015
RNF185-AS1	RNF185 antisense RNA 1	-0,3351427
RNF19B	ring finger protein 19B	-0,520148
RNF208	ring finger protein 208	0,2212144
RNF7	ring finger protein 7	-0,260397
RNMT	RNA guanine-7 methyltransferase	-0,5599717
RNU6-63P	RNA, U6 small nuclear 63, pseudogene	0,1277505
RNU6-64P	RNA, U6 small nuclear 64, pseudogene	0,380795
RNU6-75P	RNA, U6 small nuclear 75, pseudogene	0,3292536
RNU6-82P	RNA, U6 small nuclear 82, pseudogene	-0,5397003
RNU7-13P	RNA, U7 small nuclear 13 pseudogene	-0,3734827
RNU7-23P	RNA, U7 small nuclear 23 pseudogene	-0,1905664
RNU7-30P	RNA, U7 small nuclear 30 pseudogene	-0,1141732
RNU7-41P	RNA, U7 small nuclear 41 pseudogene	-0,2177415
RNU7-54P	RNA, U7 small nuclear 54 pseudogene	0,2441505
RNU7-66P	RNA, U7 small nuclear 66 pseudogene	-0,0655899
RNU7-69P	RNA, U7 small nuclear 69 pseudogene	-0,2550532
RNU7-6P	RNA, U7 small nuclear 6 pseudogene	-0,4177063
RNY1P6	RNA, Ro-associated Y1 pseudogene 6	0,0966579
RNY4P17	RNA, Ro-associated Y4 pseudogene 17	0,2146162
RNY4P20	RNA, Ro-associated Y4 pseudogene 20	0,1818969
ROBO2	roundabout guidance receptor 2	0,0790133
ROCK1P1	Rho associated coiled-coil containing protein kinase 1 pseudogene 1	-0,2672447
RORA	RAR related orphan receptor A	-0,3160344
RPF1	ribosome production factor 1 homolog	-0,5017319
RPL22P11	ribosomal protein L22 pseudogene 11	-0,2462395
RPL23P8	ribosomal protein L23 pseudogene 8	-0,2220356
RPL34-AS1	RPL34 antisense RNA 1 (head to head)	0,1568363
RPS25	ribosomal protein S25	-0,353231

RPS27L	ribosomal protein S27 like	-0,2318868
RRAGC	Ras related GTP binding C	-0,3977044
RRNAD1	ribosomal RNA adenine dimethylase domain containing 1	0,0980149
RRP1B	ribosomal RNA processing 1B	-0,1300962
RSRC2	arginine and serine rich coiled-coil 2	-0,4989868
RTCB	RNA 2',3'-cyclic phosphate and 5'-OH ligase	-0,2297249
RTF1	RTF1 homolog, Paf1/RNA polymerase II complex component	-0,2863478
RTL1	retrotransposon Gag like 1	0,2523625
RWDD1	RWD domain containing 1	-0,3893206
RWDD4	RWD domain containing 4	-0,2727079
RXRB	retinoid X receptor beta	0,132277
SAMD13	sterile alpha motif domain containing 13	0,0593168
SAMD14	sterile alpha motif domain containing 14	0,1332206
SAMD8	sterile alpha motif domain containing 8	-0,2317035
SAMSN1	SAM domain, SH3 domain and nuclear localization signals 1	-0,7355437
SAP18	Sin3A associated protein 18	-0,176115
SAP30BP	SAP30 binding protein	-0,339764
SAR1A	secretion associated Ras related GTPase 1A	-0,410616
SASH1	SAM and SH3 domain containing 1	0,082073
SASH3	SAM and SH3 domain containing 3	-0,2641005
SAT1	spermidine/spermine N1-acetyltransferase 1	-0,5471502
SBDSP1	SBDS, ribosome maturation factor pseudogene 1	-0,4722528
SBK1	SH3 domain binding kinase 1	0,2020824
SCML1	Scm polycomb group protein like 1	-0,1362536
SDAD1P1	SDA1 domain containing 1 pseudogene 1	-0,2216496
SDHAP1	succinate dehydrogenase complex flavoprotein subunit A pseudogene 1	-0,1142304
SDR42E2	short chain dehydrogenase/reductase family 42E, member 2	0,1479595
SEC14L5	SEC14 like lipid binding 5	0,1559341
SEC24B	SEC24 homolog B, COPII coat complex component	-0,3146006
SEC62	SEC62 homolog, preprotein translocation factor	-0,5050097
SECISBP2L	SECIS binding protein 2 like	-0,3020167
SELK	Selenoprotein K	-0,5465932
SENP8	SUMO/sentrin peptidase family member, NEDD8 specific	0,2374613
SEPSECS	Sep (O-phosphoserine) tRNA:Sec (selenocysteine) tRNA synthase	-0,104806
SEPT7P2	septin 7 pseudogene 2	-0,2114521
SERPINA12	serpin family A member 12	0,1514098
SERPINA4	serpin family A member 4	0,1980882
SERTM1	serine rich and transmembrane domain containing 1	0,1395651
SETBP1	SET binding protein 1	0,2365646
SETD5-AS1	NA	-0,2388506

SF3B14	Splicing Factor 3b Subunit 6	-0,6200125
SFPQ	splicing factor proline and glutamine rich	-0,4833943
SFRP5	secreted frizzled related protein 5	0,134841
SGCB	sarcoglycan beta	-0,0722418
SGK1	serum/glucocorticoid regulated kinase 1	-0,5930367
SGTB	small glutamine rich tetratricopeptide repeat containing beta	-0,4264517
SH2B2	SH2B adaptor protein 2	-0,1704515
SHANK2	SH3 and multiple ankyrin repeat domains 2	0,1598949
SHROOM2	shroom family member 2	0,1252568
SI	sucrase-isomaltase	0,0495483
SIK1	salt inducible kinase 1	-0,2179345
SIRT4	sirtuin 4	0,1287972
SKA1	spindle and kinetochore associated complex subunit 1	0,0742966
SLA	Src like adaptor	-0,1988846
SLC11A1	solute carrier family 11 member 1	-0,1563835
SLC15A2	solute carrier family 15 member 2	0,1055613
SLC15A4	solute carrier family 15 member 4	-0,3674244
SLC15A5	solute carrier family 15 member 5	0,0965042
SLC16A9	solute carrier family 16 member 9	0,134307
SLC17A2	solute carrier family 17 member 2	0,1569445
SLC17A5	solute carrier family 17 member 5	-0,2576566
SLC25A13	solute carrier family 25 member 13	-0,07409
SLC25A19	solute carrier family 25 member 19	0,117986
SLC25A20	solute carrier family 25 member 20	0,2401413
SLC25A21-AS1	SLC25A21 antisense RNA 1	0,146362
SLC25A31	solute carrier family 25 member 31	0,107222
SLC2A3	solute carrier family 2 member 3	-0,4505863
SLC35B2	solute carrier family 35 member B2	-0,177346
SLC35D1	solute carrier family 35 member D1	0,0921855
SLC35D3	solute carrier family 35 member D3	0,2218894
SLC36A4	solute carrier family 36 member 4	-0,2879025
SLC37A2	solute carrier family 37 member 2	0,1876697
SLC3A1	solute carrier family 3 member 1	0,1122149
SLC43A3	solute carrier family 43 member 3	-0,1568215
SLC6A16	solute carrier family 6 member 16	0,1445498
SLC7A8	solute carrier family 7 member 8	0,1888034
SLC7A9	solute carrier family 7 member 9	0,1191816
SLC9A4	solute carrier family 9 member A4	0,1157487
SLC9A8	solute carrier family 9 member A8	-0,2682939
SLMO2	PRELI Domain Containing 3B	-0,3957826
SLU7	SLU7 homolog, splicing factor	-0,3177357
SMAD3	SMAD family member 3	-0,1526442
SMAD5-AS1	SMAD5 antisense RNA 1	0,1958521
SMCP	sperm mitochondria associated cysteine rich protein	0,2422336
SMEK1	Protein Phosphatase 4 Regulatory Subunit 3A	-0,2692528

SMIM19	small integral membrane protein 19	-0,3177434
SMIM21	small integral membrane protein 21	0,1518519
SMN1	survival of motor neuron 1, telomeric	-0,2759147
SMNDC1	survival motor neuron domain containing 1	-0,5423622
SNAP25-AS1	SNAP25 antisense RNA 1	0,0826593
SNAPC1	small nuclear RNA activating complex polypeptide 1	-0,4512622
SNHG9	small nucleolar RNA host gene 9	-0,431009
SNORA16B	small nucleolar RNA, H/ACA box 16B	-0,3053067
SNORA29	small nucleolar RNA, H/ACA box 29	-0,4009907
SNORA70D	small nucleolar RNA, H/ACA box 70D	-0,3214114
SNORA72	small nucleolar RNA, H/ACA box 72	-0,3451751
SNORA9	small nucleolar RNA, H/ACA box 9	-0,3450396
SNORD125	small nucleolar RNA, C/D box 125	-0,5288713
SNORD70	small nucleolar RNA, C/D box 70	-0,6703425
SNORD72	small nucleolar RNA, C/D box 72	-0,3357547
SNORD88A	small nucleolar RNA, C/D box 88A	-0,381514
SNRNP27	small nuclear ribonucleoprotein U4/U6.U5 subunit 27	-0,4255991
SNRPA1	small nuclear ribonucleoprotein polypeptide A'	-0,540038
SNRPC	small nuclear ribonucleoprotein polypeptide C	-0,2739626
SNRPD1	small nuclear ribonucleoprotein D1 polypeptide	-0,5072413
SNRPE	small nuclear ribonucleoprotein polypeptide E	-0,1870786
SNW1	SNW domain containing 1	-0,4763354
SNX16	sorting nexin 16	-0,2278199
SNX19	sorting nexin 19	0,1273386
SOCS4	suppressor of cytokine signaling 4	-0,1417096
SOSTDC1	sclerostin domain containing 1	0,1247668
SP100	SP100 nuclear antigen	-0,2506725
SP3	Sp3 transcription factor	-0,2595549
SPACA1	sperm acrosome associated 1	0,1491781
SPAG1	sperm associated antigen 1	-0,0744517
SPAG17	sperm associated antigen 17	0,0565498
SPAM1	sperm adhesion molecule 1	0,1028924
SPATA25	spermatogenesis associated 25	0,2225571
SPATS1	spermatogenesis associated serine rich 1	0,0975468
SPC25	SPC25, NDC80 kinetochore complex component	0,1107835
SPCS3	signal peptidase complex subunit 3	-0,383986
SPINK6	serine peptidase inhibitor, Kazal type 6	0,1383227
SPINK8	serine peptidase inhibitor, Kazal type 8 (putative)	0,0831616
SPPL2A	signal peptide peptidase like 2A	-0,396709
SPR	sepiapterin reductase	0,197456
SQSTM1	sequestosome 1	-0,2255035
SRA1	steroid receptor RNA activator 1	-0,2627554
SREK1IP1	SREK1 interacting protein 1	-0,2313616
SRP19	signal recognition particle 19	-0,1675176
SRPX2	sushi repeat containing protein, X-linked 2	0,1301017
SRRM1	serine and arginine repetitive matrix 1	-0,283784

SRRM2	serine/arginine repetitive matrix 2	-0,380574
SRRM5	serine/arginine repetitive matrix 5	0,4905514
SRSF4	serine and arginine rich splicing factor 4	-0,2011134
SS18L2	SS18 like 2	-0,4095763
ST6GAL1	ST6 beta-galactoside alpha-2,6-sialyltransferase 1	0,1359596
STAG3L4	stromal antigen 3-like 4 (pseudogene)	-0,2904065
STARD4	StAR related lipid transfer domain containing 4	-0,2503027
STAT1	signal transducer and activator of transcription 1	-0,5003073
STAU1	staufen double-stranded RNA binding protein 1	-0,2379241
STEAP2-AS1	STEAP2 antisense RNA 1	0,1408598
STK17B	serine/threonine kinase 17b	-0,4524889
STK4-AS1	STK4 antisense RNA 1 (head to head)	0,1225665
STRAP	serine/threonine kinase receptor associated protein	-0,6720656
STUB1	STIP1 homology and U-box containing protein 1	-0,1567678
STX12	syntaxin 12	-0,26937
STX3	syntaxin 3	-0,325131
STYK1	serine/threonine/tyrosine kinase 1	0,1355581
SUB1	SUB1 homolog, transcriptional regulator	-0,3900255
SUB1P1	SUB1 homolog, transcriptional regulator pseudogene 1	-0,3710248
SUMO1	small ubiquitin-like modifier 1	-0,3840624
SUPV3L1	Suv3 like RNA helicase	-0,2123792
SVIP	small VCP interacting protein	-0,6014393
SWSAP1	SWIM-type zinc finger 7 associated protein 1	0,1138291
SYAP1	synapse associated protein 1	-0,4684048
SYF2	SYF2 pre-mRNA splicing factor	-0,452525
SYP	synaptophysin	0,1133309
SYS1	SYS1, golgi trafficking protein	-0,1488838
SYT16	synaptotagmin 16	0,1332969
TACR2	tachykinin receptor 2	0,1722077
TAF11	TATA-box binding protein associated factor 11	-0,3848213
TAF7	TATA-box binding protein associated factor 7	-0,548896
TAF9B	TATA-box binding protein associated factor 9b	-0,2095036
TANK	TRAF family member associated NFKB activator	-0,4370277
TAS2R1	taste 2 receptor member 1	0,1484467
TAS2R10	taste 2 receptor member 10	0,16742
TAS2R50	taste 2 receptor member 50	0,2078958
TAX1BP1	Tax1 binding protein 1	-0,4943356
TBC1D15	TBC1 domain family member 15	-0,5229957
TBC1D16	TBC1 domain family member 16	0,1097932
TBC1D23	TBC1 domain family member 23	-0,289825
TBC1D7	TBC1 domain family member 7	-0,3324163
TBC1D9	TBC1 domain family member 9	0,2148333
TBK1	TANK binding kinase 1	-0,3217724
TBR1	T-box, brain 1	0,0673544
TCEA2	transcription elongation factor A2	0,098655
TCEB1	Transcription Elongation Factor B Polypeptide 1	-0,2932474

TCF19	transcription factor 19	0,13028
TCF4	transcription factor 4	0,0700664
TCFL5	transcription factor like 5	0,1010215
TCTN2	tectonic family member 2	0,0921245
TDRD7	tudor domain containing 7	-0,2141001
TDRKH	tudor and KH domain containing	0,1055548
TEX101	testis expressed 101	0,1531257
TEX15	testis expressed 15, meiosis and synapsis associated	0,0794132
TEX21P	testis expressed 21, pseudogene	0,1413337
TEX33	testis expressed 33	0,145288
TFAP2A	transcription factor AP-2 alpha	0,0875719
TGS1	trimethylguanosine synthase 1	-0,214341
THAP6	THAP domain containing 6	0,057889
THAP9-AS1	THAP9 antisense RNA 1	-0,2926566
THEMIS2	thymocyte selection associated family member 2	-0,3331993
THRSP	thyroid hormone responsive	0,2782876
THUMPD2	THUMP domain containing 2	-0,1569865
THUMPD3	THUMP domain containing 3	-0,432115
TIMD4	T-cell immunoglobulin and mucin domain containing 4	0,0762822
TIMM17A	translocase of inner mitochondrial membrane 17A	-0,378911
TK2	thymidine kinase 2, mitochondrial	0,0717457
TLE3	transducin like enhancer of split 3	-0,4298624
TLR2	toll like receptor 2	-0,6637993
TM2D3	TM2 domain containing 3	-0,282218
TMEM126A	transmembrane protein 126A	-0,560223
TMEM132B	transmembrane protein 132B	0,157582
TMEM156	transmembrane protein 156	-0,142555
TMEM167B	transmembrane protein 167B	-0,4217734
TMEM170A	transmembrane protein 170A	-0,2666934
TMEM176A	transmembrane protein 176A	0,1029258
TMEM183B	transmembrane protein 183B	-0,2460657
TMEM229B	transmembrane protein 229B	0,1669721
TMEM232	transmembrane protein 232	0,0527016
TMEM243	transmembrane protein 243	-0,2541623
TMEM254-AS1	TMEM254 antisense RNA 1	0,1280203
TMEM75	transmembrane protein 75	0,2383688
TMEM87A	transmembrane protein 87A	-0,3489861
TMEM91	transmembrane protein 91	-0,1141505
TMLHE-AS1	TMLHE antisense RNA 1	0,2019863
TMPRSS4	transmembrane protease, serine 4	0,1376023
TMUB2	transmembrane and ubiquitin like domain containing 2	-0,153433
TNFRSF13B	TNF receptor superfamily member 13B	0,1856866
TNFRSF8	TNF receptor superfamily member 8	0,1827894
TNFSF11	TNF superfamily member 11	0,0940149
TNNI3	troponin I3, cardiac type	0,12286

TNP1	transition protein 1	0,2036898
TOM1	target of myb1 membrane trafficking protein	-0,2642622
TOM1L2	target of myb1 like 2 membrane trafficking protein	0,1263543
TOMM20	translocase of outer mitochondrial membrane 20	-0,410152
TOMM5	translocase of outer mitochondrial membrane 5	-0,3340843
TP53	tumor protein p53	0,1131239
TPST2	tyrosylprotein sulfotransferase 2	-0,1149063
TRA2A	transformer 2 alpha homolog	-0,4442792
TRAF3	TNF receptor associated factor 3	-0,2154935
TRAF3IP1	TRAF3 interacting protein 1	0,0773526
TRAF6	TNF receptor associated factor 6	-0,1996092
TRAK1	trafficking kinesin protein 1	0,109988
TRAPPC12	trafficking protein particle complex 12	0,091838
TRAPPC4	trafficking protein particle complex 4	-0,25742
TRBV11-2	T cell receptor beta variable 11-2	0,2610818
TRBV6-6	T cell receptor beta variable 6-6	0,23197
TRGV4	T cell receptor gamma variable 4	0,2754741
TRIM40	tripartite motif containing 40	0,213584
TRIM41	tripartite motif containing 41	0,1085823
TRIM59	tripartite motif containing 59	-0,1333659
TRIM64	tripartite motif containing 64	0,2132302
TRIM64B	tripartite motif containing 64B	0,2155164
TRIM9	tripartite motif containing 9	0,1431789
TRIO	trio Rho guanine nucleotide exchange factor	0,06342
TROVE2	TROVE domain family member 2	-0,2453732
TRPV5	transient receptor potential cation channel subfamily V member 5	0,1777706
TSG101	tumor susceptibility 101	-0,4105943
TSGA13	testis specific 13	0,0769055
TSPAN18	tetraspanin 18	0,1405055
TSPY5P	testis specific protein, Y-linked 5, pseudogene	-0,1051105
TSPYL5	TSPY like 5	0,2182723
TSR2	TSR2, ribosome maturation factor	-0,1803233
TTI1	TELO2 interacting protein 1	0,1161289
TTLL12	tubulin tyrosine ligase like 12	0,175627
TWISTNB	TWIST neighbor	-0,716525
TXN	thioredoxin	-0,483547
TXNL4A	thioredoxin like 4A	-0,2254586
TYMP	thymidine phosphorylase	-0,164056
TYW5	tRNA-yW synthesizing protein 5	-0,2038668
UACA	uveal autoantigen with coiled-coil domains and ankyrin repeats	0,085464
UAP1	UDP-N-acetylglucosamine pyrophosphorylase 1	-0,2327347
UBE2A	ubiquitin conjugating enzyme E2 A	-0,28043
UBE2B	ubiquitin conjugating enzyme E2 B	-0,4141146
UBE2D3	ubiquitin conjugating enzyme E2 D3	-0,2578911
UBE2J1	ubiquitin conjugating enzyme E2 J1	-0,5408657

UBE2J2	ubiquitin conjugating enzyme E2 J2	-0,0764607
UBE2S	ubiquitin conjugating enzyme E2 S	-0,3071451
UBE2U	ubiquitin conjugating enzyme E2 U (putative)	0,091833
UBE3B	ubiquitin protein ligase E3B	0,1326636
UBE3D	ubiquitin protein ligase E3D	0,1035993
UBXN1	UBX domain protein 1	-0,192868
UCHL1	ubiquitin C-terminal hydrolase L1	0,0721996
UCMA	upper zone of growth plate and cartilage matrix associated	0,1145707
UGDH	UDP-glucose 6-dehydrogenase	0,0850444
UHRF1BP1L	UHRF1 binding protein 1 like	-0,4108024
UIMC1	ubiquitin interaction motif containing 1	-0,1718677
UNC119	unc-119 lipid binding chaperone	-0,1485053
UNQ6975	NA	0,1241491
UPF3AP1	UPF3A pseudogene 1	0,2930695
UPF3B	UPF3B, regulator of nonsense mediated mRNA decay	-0,1690535
UPK1A-AS1	UPK1A antisense RNA 1	0,1436222
USP16	ubiquitin specific peptidase 16	-0,538198
USP21	ubiquitin specific peptidase 21	0,0930092
USP29	ubiquitin specific peptidase 29	0,1045036
USP3	ubiquitin specific peptidase 3	-0,5093756
USP40	ubiquitin specific peptidase 40	0,0479029
USP42	ubiquitin specific peptidase 42	-0,2359291
USPL1	ubiquitin specific peptidase like 1	-0,409381
UTP15	UTP15, small subunit processome component	-0,1246132
VAV2	vav guanine nucleotide exchange factor 2	0,0843963
VEGFA	vascular endothelial growth factor A	-0,1637674
VEZF1	vascular endothelial zinc finger 1	-0,4988189
VSTM4	V-set and transmembrane domain containing 4	0,1117823
WBP11	WW domain binding protein 11	-0,3724827
WBP2NL	WBP2 N-terminal like	0,1073897
WBP4	WW domain binding protein 4	-0,2803654
WBSCR16	Williams-Beuren Syndrome Chromosomal Region 16 Protein	0,1593046
WDFY2-AS1	NA	0,1498796
WDR43	WD repeat domain 43	-0,2203253
WDR48	WD repeat domain 48	-0,3078714
WDR92	WD repeat domain 92	0,1219144
WTAP	WT1 associated protein	-0,452335
WWC3-AS1	WWC3 antisense RNA 1	0,1453163
XPC	XPC complex subunit, DNA damage recognition and repair factor	0,1230977
XYLT1	xylosyltransferase 1	0,1842608
YPEL5	yippee like 5	-0,505436
YRDC	yrdC N6-threonylcarbamoyltransferase domain containing	-0,2542019

YTHDF1	YTH N6-methyladenosine RNA binding protein 1	-0,195153
ZBTB21	zinc finger and BTB domain containing 21	-0,4440427
ZBTB43	zinc finger and BTB domain containing 43	-0,2421944
ZC3H12B	zinc finger CCCH-type containing 12B	0,0811924
ZC3H15	zinc finger CCCH-type containing 15	-0,3732725
ZC3H7A	zinc finger CCCH-type containing 7A	-0,4086183
ZCCHC10	zinc finger CCHC-type containing 10	-0,5479622
ZDHHC16	zinc finger DHHC-type containing 16	0,1288834
ZEB2-AS1	ZEB2 antisense RNA 1	-0,3005629
ZFAND2A	zinc finger AN1-type containing 2A	-0,427644
ZFP36L1	ZFP36 ring finger protein like 1	-0,5240275
ZFPM2	zinc finger protein, FOG family member 2	0,0799877
ZFX	zinc finger protein, X-linked	-0,1558225
ZFYVE16	zinc finger FYVE-type containing 16	-0,1286452
ZNF107	zinc finger protein 107	-0,1139117
ZNF169	zinc finger protein 169	-0,095917
ZNF227	zinc finger protein 227	-0,1899262
ZNF267	zinc finger protein 267	-0,6174126
ZNF280A	zinc finger protein 280A	0,1199956
ZNF292	zinc finger protein 292	-0,2752294
ZNF311	zinc finger protein 311	0,1321739
ZNF326	zinc finger protein 326	-0,2614566
ZNF337	zinc finger protein 337	0,111341
ZNF347	zinc finger protein 347	0,0714916
ZNF350	zinc finger protein 350	-0,5069773
ZNF365	zinc finger protein 365	0,0767296
ZNF397	zinc finger protein 397	0,0647709
ZNF44	zinc finger protein 44	-0,082737
ZNF470	zinc finger protein 470	0,0786399
ZNF479	zinc finger protein 479	-0,0842731
ZNF500	zinc finger protein 500	0,1139885
ZNF511	zinc finger protein 511	-0,121195
ZNF546	zinc finger protein 546	0,0799399
ZNF564	zinc finger protein 564	0,0655355
ZNF609	zinc finger protein 609	0,1643395
ZNF613	zinc finger protein 613	0,162894
ZNF644	zinc finger protein 644	-0,2090564
ZNF669	zinc finger protein 669	-0,2046728
ZNF684	zinc finger protein 684	-0,1804953
ZNF701	zinc finger protein 701	-0,1122767
ZNF706	zinc finger protein 706	-0,1321484
ZNF721	zinc finger protein 721	-0,1866219
ZNF732	zinc finger protein 732	-0,1116851
ZNF750	zinc finger protein 750	0,114587
ZNF75D	zinc finger protein 75D	0,0965267
ZNF776	zinc finger protein 776	-0,1818919
ZNF787	zinc finger protein 787	-0,1011157

ZNF792	zinc finger protein 792	0,1695748
ZNF800	zinc finger protein 800	-0,2482035
ZNF829	zinc finger protein 829	0,12409
ZNF860	zinc finger protein 860	0,0839808
ZNF865	zinc finger protein 865	-0,254967
ZNF876P	zinc finger protein 876, pseudogene	-0,1295217
ZNFX1	zinc finger NFX1-type containing 1	-0,320408
ZPBP	zona pellucida binding protein	0,0463659
ZSCAN29	zinc finger and SCAN domain containing 29	0,0743669

Diff exp: differential gene expression before and after treatment. The positive sign means overexpressed after treatment and the negative sign, underexpressed.

Supplementary Table 3. **miRNAs significantly deregulated after deferasirox treatment in MDS patients**.

miRNA	Diff exp
hsa-miR-1180	0,2818094
hsa-miR-1206	0,0844527
hsa-miR-1231	0,3409856
hsa-miR-125B2	0,1431346
hsa-miR-1266	0,2043175
hsa-miR-130B	0,0962923
hsa-miR-146B	0,2673414
hsa-miR-147B	-1,0768079
hsa-miR-1538	-0,2216387
hsa-miR-181B1	-0,2614442
hsa-miR-1827	0,1762043
hsa-miR-2110	-0,4144737
hsa-miR-216B	-0,095797
hsa-miR-22HG	-0,4664754
hsa-miR-2682	0,4834731
hsa-miR-30E	-0,1695322
hsa-miR-3121	0,0843949
hsa-miR-3126	0,2977903
hsa-miR-346	0,2620387
hsa-miR-3612	0,1934545
hsa-miR-3613	0,184538
hsa-miR-365A	0,2440205
hsa-miR-3671	-0,1951743
hsa-miR-3678	0,1189779
hsa-miR-382	0,1478329
hsa-miR-3913-1	0,1032954
hsa-miR-3936	0,3209752
hsa-miR-4253	0,2277345
hsa-miR-4280	0,1472996
hsa-miR-4290	0,2774847
hsa-miR-4305	0,250656
hsa-miR-4317	0,1089995
hsa-miR-4423	-0,129565

hsa-miR-4470	**-0,1485335**
hsa-miR-4511	**0,1857179**
hsa-miR-4668	**-0,1467339**
hsa-miR-4693	**-0,1754647**
hsa-miR-4698	**0,2388169**
hsa-miR-4712	**-0,0880747**
hsa-miR-4729	**0,2098998**
hsa-miR-4742	**-0,1588204**
hsa-miR-4755	**0,2828486**
hsa-miR-4787	**-0,180955**
hsa-miR-4790	**-0,1133828**
hsa-miR-517B	**0,1322046**
hsa-miR-518D	**-0,1746959**
hsa-miR-519E	**-0,1170266**
hsa-miR-552	**0,0848758**
hsa-miR-579	**-0,1099302**
hsa-miR-621	**0,0808752**
hsa-miR-632	**-0,4749223**
hsa-miR-636	**-0,3505116**
hsa-miR-665	**0,2216156**
hsa-miR-920	**0,2907838**

miRNA: microRNA

Diff exp: differential gene expression before and after treatment. The positive sign means overexpressed after treatment and the negative sign, underexpressed.

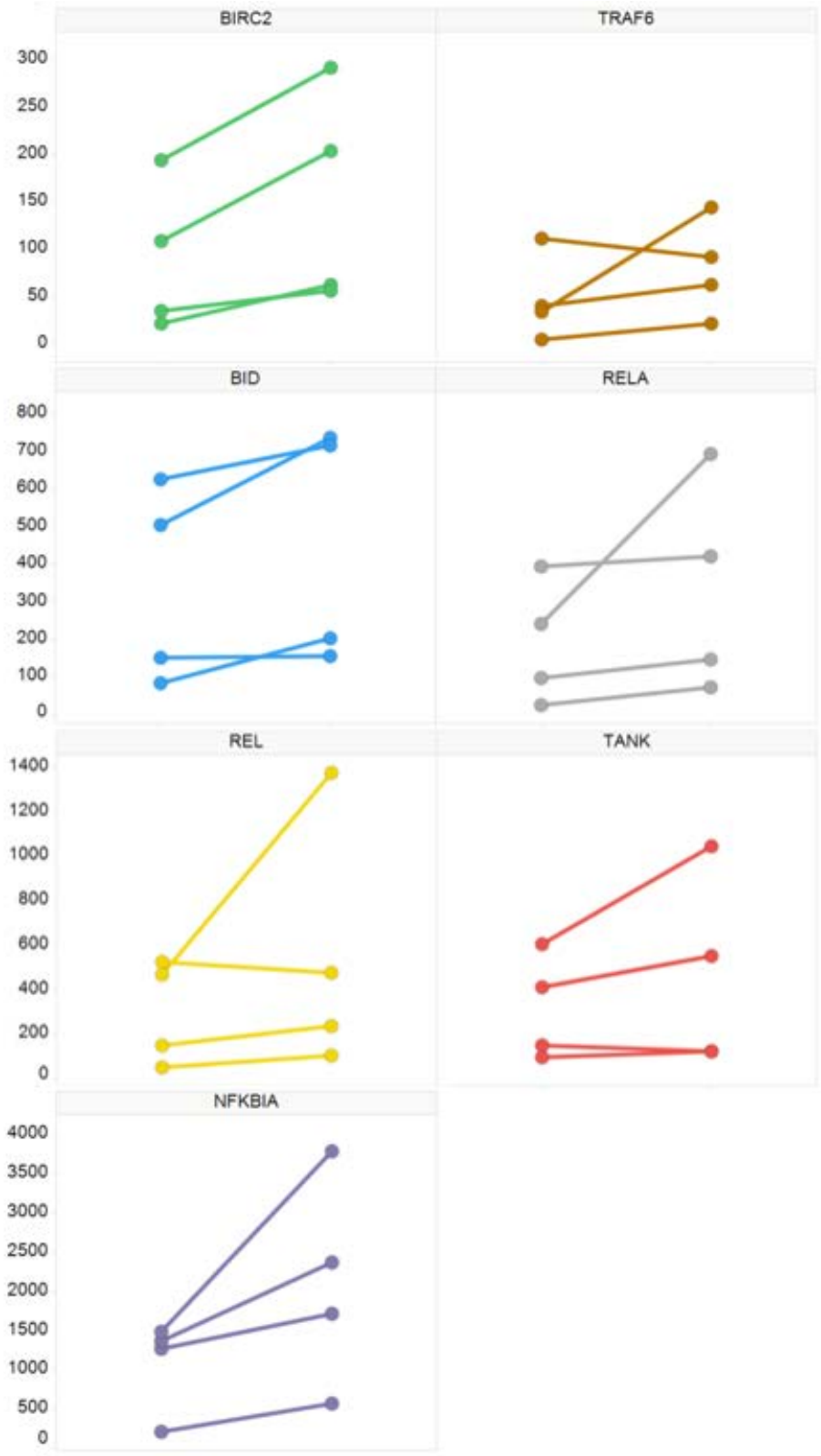

Supplementary Figure 1: Validation by ddPCR. Expression changes in *BIRC2*, *TRAF6*, *BID*, *RELA*, *REL*, *TANK* and *NFKBIA* were validate when RNA was available.

Chapter 3:

Supplementary Table 1. Clinical, biological and follow-up characteristics of the patients treated with 5-Azacytidine

SAMPLE PAIR	ID	TREATMENT	Age (years)	Sex (male/female)	MDS/AML	FAB	WHO 2016	Karyotype	IPSS-R Karyo Risk	IPSS-R Score	IPSS-R Category	WBC (10E9/L)	Hemoglobin (g/dL)	Platelet Count (X10E9/L)	Bone Marrow Blast (%)	ANC (X10E9/L)	Treatment duration between pre-Aza and during Aza (months)	Blast Resp	Blast %	Ratio	Hematological Response	Clinical Response	RESPONSE (YES/NO/STABLE) any type of response
1	8711	PRE-AZA	64	F	MDS	RAEB	MDS-EB-2	46,XX[15]	Good	5	high	2.9	9.7	112	11	1.6	--		11	1			
	9143	POST-AZA						46,XX[15]	Good			4.1	9.7	170	11	2.4	4	NR	11	1	R	Stable	YES
2	8934	PRE-AZA	73	F	AML	M0	AML-MDS	46,XX,de(5)(q31q35)[12]	NA		NA	1.2	8.6	54	70	0.1	--		70	1.3			
	9517	POST-AZA						46,XX,de(5)(q31q35)[8]/45,XX,sl,-13[3]	NA			4.3	7.7	9	56	0.1	6	R	56	0.8	NR	NO	YES
3	9067	PRE-AZA	64	M	MDS	RAEB	MDS-EB-1	46,XY[25]	Good	5	high	5.5	7.6	68	5	3.9	--		5	3.8			Progresion (22/4/14)
	9674	POST-AZA						46,XY[21]	Good			3.3	13.6	151	1	1.1	6	R	1.3	0.3	R	Progression	YES
4	9401	PRE-AZA	78	M	MDS	RAEB	MDS-EB-2	46,XY[22]	Good	4.5	Intermediate	2.1	10.6	470	15	0.6	--		15	1.2			
	10214	POST-AZA						46,XY[21]	Good			2.4	10	100	13	0.7	6	NR	13	0.9	NR	Stable	STABLE
5	9844	PRE-AZA	76	F	MDS	RAEB	MDS-EB-2	46,XX[12]	Good	5	high	3.3	8.6	35	8	1.9	--		7.6	3.8			

	10333	POST-AZA						46,XX[22]	Good			7.2	12	156	2	4.7	6	R	2	0.3	R	Complete	YES - FULL
6	9991	PRE-AZA	62	F	MDS	RAEB	MDS-EB-1	47,XX,+8[12]/46,XX[10]	Intermediate	6	high	3.7	8.6	53	8	0.6	--		7.6	9.5			
	10554	POST-AZA						46,XX[22]	Good			4.6	11	330	1	2.5	6	R	0.8	0.1	R	Complete	YES - FULL
	10236	PRE-AZA	85	F	MDS	RAEB	MDS-EB-1	46,XX[22]	Good	5.5	high	3.4	7.4	19	9	2.2	--		9	1.3			
7	10708	POST-AZA						46,XX[21]	Good			2.2	7.2	30	7	1.5	6	NR	7.2	0.8	NR	NO	STABLE
8	10067	PRE-AZA	77	F	MDS	RAEB	MDS-EB-1	47,XX,del(5)(q31q35),+8[5]/46,XX[10]	Intermediate	5	high	4.9	10.1	25	7	2.5	--		6.6	6.6			
	10370	POST-AZA						46,XX[20]	Good			2.5	8.7	187	1	1.3	4	R	1	0.2	NR	Complete	YES
	10439	PRE-AZA	67	M	AML	NA	AML-MDS	46,XY[20]	NP		NP	36.6	9	211	32	NA	--		32	1.1			
9	11047	POST-AZA						46,XY[13]	Good			12.0	10.4	214	30	NA	8	NR	30	0.9	U	Stable	STABLE
	9764	PRE-AZA	71	F	MDS	RARS	MDS-MLD	46,XX,del(5)(q31q35)[2]/47,XX,sl,+del(1)(p21p36)del(7)(21q35)[15]/47,XX,sldel(7)(q21q35)+8[2]	Very poor	4	Intermediate	2.8	10.5	220	2	1.1	--		2	2			
10	10746	POST-AZA			MDS	RARS	MDS-MLD	50,XX,-4,del(5)(q31q35),del(7)(q21q35),+8,add(11)(p13	Very poor			3	12.9	118	1	1.2	12	R	1	0.5	R	Progression	YES

								),+11,+13,+16,+22[6]/46,XX[7]															
11	10798	PRE-AZA	79	M	AML	RAEBt	AML-MDS	46,XY[18]	Good	5	high	15.7	8.3	247	25	9.1	--		25	NA			
	11066	POST-AZA						46,XY[15]	Good			NA	NA	NA	6	NA	4	NA	NA	NA	R	Stable	STABLE
12	10752	PRE-AZA	65	M	MDS	RA	MDS-MLD	47,XY,+8[15]/46,XY[6]	Intermediate	5	high	2.3	14.6	80	5	0.6	--		5	NA			
	12082	POST-AZA						ND				2.5	13.4	32	4	0.7	8	NA	NA	NA	R	Stable	STABLE
13	11161	PRE-AZA	65	M	MDS	RAEB	MDS-EB-2	46,XY[17]	Good	5	high	6.9	9.2	32	6	2.4	--		6	0.4			
	12183	POST-AZA						46,XY[18]	Good			6.8	14.9	343	15	4.9	4	NA	NA	NA	R	Complete	YES
14	9830	PRE-AZA	49	F	MDS	RAEB	MDS-EB-2	46,XX[12]	Intermediate		NA	NA	NA	NA	NA	NA	--		0,5	5			
	10195	POST-AZA						46,XX[16]	Good			NA	NA	NA	1	NA	4	R	0,1	0.2	U	Stable	STABLE

NA:Not applicable, ND: Not Done, NR: no-response, R: Reponse, U: Undefined

Control ID	ID	Age (years)	Sex
1	13409	69	Female
2	13477	74	Female
3	13670	67	Female
4	13701	77	Female
5	13718	83	Female
6	13720	74	Female

Supplementary Table 2. Myeloid-related genes included in the NGS panel

Signaling pathway	**RNA splicing**	**Transcription**
CSF3R	LUC7L2	AEBP2
EGFR	SF1	ATRX
FLT3	SF3A1	BCOR
GNAS	SF3B1	BCORL1
HRAS	SFPQ	CALR
JAK1	SRSF2	CBFb
JAK2	U2AF1	CEBPA
JAK3	USB1	CREBBP
JKAMP	ZRSR2	CTNNA1
KIT	**DNA Methylation**	CUX1
KRAS	DNMT3A	UBR5
MPL	IDH1	ETV6
MTOR	IDH2	GATA1
NF1	TET2	GATA2
NRAS	**Cohesin Complex**	IKZF1
NTRK1	CTCF	IRF1
PDGFRA	RAD21	JARID2
PDGFRB	SMC1A	MECOM
RET	SMC3	NOTCH1
TCL1B	STAG1	NPM1
SPARC	STAG2	PBRM1
PTEN	**Telomerase**	PHF19
PTPN1	TERC	PHF6
PTPN11	TERT	RPS14
PHLPP1	**Chromatine modification**	RUNX1
BCR	ASXL1	SALL4
SETBP1	EP300	SBDS
CBL	EZH2	SUZ12
UMODL1	KDM6A	TIMM50
TYK2	KMT2A	TNFAIP3
GNB1	KMT2D	TP53
BRAF	ARID2	WT1
ABL1	SETD2	EIF2AK2
NUP98	**Others**	NR2F6
ENG	GCAT	RARA
CSNK1A1	BCAS1	
BMI1	WASF3	
CDH23		
CDH3		
CDK2		
CDKN2A		
CBLB		
CBLC		
FBXW7		
TGM2		
IL3		
SH2B3		
CD177		
CDH13		
G3BP1		

Supplementary table 3. Detailed description of all mutations presented in CD34 positive cells

Sample	Gene	Chr	Start	End	Ref	Alt	FREQ	Function	Exonic consequence	AA change & Transcript
1_POST	AEBP2	chr12	19646908	19646908	C	T	17,13	exonic	stopgain	NM_001114176:c.C1162T:p.R388X
1_POST	RUNX1	chr21	36259171	36259171	C	G	52,34	exonic	nonsynonymous SNV	NM_001001890:c.G239C:p.R80P
1_POST	RET	chr10	43606670	43606670	G	C	49,11	exonic	nonsynonymous SNV	NM_020630:c.G1279C:p.V427L
1_POST	SRSF2	chr17	74732959	74732959	G	A	53,61	exonic	nonsynonymous SNV	NM_001195427:c.C284T:p.P95L
1_POST	STAG2	chrX	123220456	123220456	G	A	12,23	exonic	stopgain	NM_006603:c.G3113A:p.W1038X
1_POST	GATA2	chr3	128205729	128205729	A	-	45,04	exonic	frameshift deletion	NM_001145662:c.146delT:p.F49fs
1_PRE	AEBP2	chr12	19646908	19646908	C	T	16,08	exonic	stopgain	NM_001114176:c.C1162T:p.R388X
1_PRE	RUNX1	chr21	36259171	36259171	C	G	51,66	exonic	nonsynonymous SNV	NM_001001890:c.G239C:p.R80P
1_PRE	RET	chr10	43606670	43606670	G	C	47,87	exonic	nonsynonymous SNV	NM_020630:c.G1279C:p.V427L
1_PRE	SRSF2	chr17	74732959	74732959	G	A	56,28	exonic	nonsynonymous SNV	NM_001195427:c.C284T:p.P95L
1_PRE	STAG2	chrX	123220456	123220456	G	A	13,35	exonic	stopgain	NM_006603:c.G3113A:p.W1038X
1_PRE	GATA2	chr3	128205729	128205729	A	-	44,42	exonic	frameshift deletion	NM_001145662:c.146delT:p.F49fs
10_POST	TP53	chr17	7577124	7577124	C	T	28,74	exonic	nonsynonymous SNV	NM_001126115:c.G418A:p.V140M
10_POST	TP53	chr17	7578433	7578433	G	T	28,99	exonic	stopgain	NM_001126115:c.C101A:p.S34X
10_POST	TGM2	chr20	36769764	36769764	G	A	43,41	exonic	nonsynonymous SNV	NM_004613:c.C1019T:p.S340L
10_POST	CUX1	chr7	101870887	101870887	C	T	45,68	exonic	nonsynonymous SNV	NM_001202543:c.C3404T:p.P1135L
10_PRE	TP53	chr17	7577124	7577124	C	T	45,37	exonic	nonsynonymous SNV	NM_001126115:c.G418A:p.V140M
10_PRE	TP53	chr17	7578433	7578433	G	T	44,62	exonic	stopgain	NM_001126115:c.C101A:p.S34X
10_PRE	TGM2	chr20	36769764	36769764	G	A	47,99	exonic	nonsynonymous SNV	NM_004613:c.C1019T:p.S340L
10_PRE	CUX1	chr7	101870887	101870887	C	T	80,49	exonic	nonsynonymous SNV	NM_001202543:c.C3404T:p.P1135L
11_POST	SRSF2	chr17	74732959	74732959	G	A	35,98	exonic	nonsynonymous SNV	NM_001195427:c.C284T:p.P95L
11_POST	IDH2	chr15	90631934	90631934	C	T	11,11	exonic	nonsynonymous SNV	NM_001290114:c.G29A:p.R10Q
11_POST	SF3B1	chr2	198267359	198267359	C	G	41,27	exonic	nonsynonymous SNV	NM_012433:c.G1998C:p.K666N
11_PRE	SRSF2	chr17	74732959	74732959	G	A	53,6	exonic	nonsynonymous SNV	NM_001195427:c.C284T:p.P95L
11_PRE	IDH2	chr15	90631934	90631934	C	T	6,47	exonic	nonsynonymous SNV	NM_001290114:c.G29A:p.R10Q
11_PRE	SF3B1	chr2	198267359	198267359	C	G	46,13	exonic	nonsynonymous SNV	NM_012433:c.G1998C:p.K666N
12_POST	SRSF2	chr17	74732959	74732959	G	T	46,56	exonic	nonsynonymous SNV	NM_001195427:c.C284A:p.P95H
12_PRE	SRSF2	chr17	74732959	74732959	G	T	46,48	exonic	nonsynonymous SNV	NM_001195427:c.C284A:p.P95H
12_PRE	STAG2	chrX	123171416	123171416	C	T	16,39	exonic	stopgain	NM_006603:c.C328T:p.R110X
13_POST	DNMT3A	chr2	25457242	25457242	C	T	9,09	exonic	nonsynonymous SNV	NM_153759:c.G2078A:p.R693H
13_PRE	NPM1	chr5	170837543	170837543	-	TCTG	23,72	exonic	frameshift insertion	NM_199185:c.772_773insTCTG:p.L258fs
13_PRE	DNMT3A	chr2	25457242	25457242	C	T	43,15	exonic	nonsynonymous SNV	NM_153759:c.G2078A:p.R693H
13_PRE	PTPN11	chr12	112888195	112888195	T	C	19,5	exonic	nonsynonymous SNV	NM_002834:c.T211C:p.F71L
13_PRE	PTPN11	chr12	112926885	112926885	C	T	8,41	exonic	nonsynonymous SNV	NM_002834:c.C1505T:p.S502L
13_PRE	RPS14	chr5	149823879	149823879	C	G	18,17	exonic	nonsynonymous SNV	NM_001025070:c.G426C:p.R142S
2_POST	MTOR	chr1	11316102	11316102	T	G	39,6	exonic	nonsynonymous SNV	NM_004958:c.A652C:p.I218L
2_POST	KRAS	chr12	25398284	25398284	C	T	7,19	exonic	nonsynonymous SNV	NM_004985:c.G35A:p.G12D
2_PRE	KRAS	chr12	25398284	25398284	C	T	1,83	exonic	nonsynonymous SNV	NM_004985:c.G35A:p.G12D
2_POST	RUNX1	chr21	36252865	36252865	C	T	29,87	exonic	nonsynonymous SNV	NM_001001890:c.G416A:p.R139Q
2_POST	NRAS	chr1	115258745	115258745	C	G	15,29	exonic	nonsynonymous SNV	NM_002524:c.G37C:p.G13R
2_PRE	NRAS	chr1	115258745	115258745	C	G	1,27	exonic	nonsynonymous SNV	NM_002524:c.G37C:p.G13R
2_PRE	MTOR	chr1	11316102	11316102	T	G	42,07	exonic	nonsynonymous SNV	NM_004958:c.A652C:p.I218L
2_PRE	RUNX1	chr21	36252865	36252865	C	T	48,77	exonic	nonsynonymous SNV	NM_001001890:c.G416A:p.R139Q

4_POST	STAG2	chrX	123197770	123197770	T	C	35	exonic	nonsynonymous SNV	NM_006603:c.T1894C:p.C632R
4_POST	DNMT3A	chr2	25469071	25469071	C	A	42,74	exonic	stopgain	NM_153759:c.G820T:p.E274X
4_POST	SUZ12	chr17	30323835	30323835	G	T	18,59	exonic	nonsynonymous SNV	NM_015355:c.G1813T:p.D605Y
4_POST	BCOR	chrX	39914629	39914629	A	-	39,29	exonic	frameshift deletion	NM_001123384:c.4577delT:p.F1526fs
4_PRE	BCOR	chrX	39930400	39930400	-	C	26,47	exonic	frameshift insertion	NM_001123384:c.3009dupG:p.R1004fs
4_POST	BCOR	chrX	39930400	39930400	-	C	28,42	exonic	frameshift insertion	NM_001123384:c.3009dupG:p.R1004fs
4_POST	KIT	chr4	55603390	55603390	A	G	43,2	exonic	nonsynonymous SNV	NM_000222:c.A2746G:p.T916A
4_POST	TET2	chr4	106155858	106155861	CAGT	-	41,6	exonic	frameshift deletion	NM_001127208:c.759_762del:p.N253fs
4_POST	TET2	chr4	106196336	106196336	-	T	36,79	exonic	frameshift insertion	NM_001127208:c.4670dupT:p.V1557fs
4_POST	SF3B1	chr2	198267359	198267359	C	G	46,28	exonic	nonsynonymous SNV	NM_012433:c.G1998C:p.K666N
4_PRE	STAG2	chrX	123197770	123197770	T	C	44,44	exonic	nonsynonymous SNV	NM_006603:c.T1894C:p.C632R
4_PRE	DNMT3A	chr2	25469071	25469071	C	A	43,81	exonic	stopgain	NM_153759:c.G820T:p.E274X
4_PRE	SUZ12	chr17	30323835	30323835	G	T	19,44	exonic	nonsynonymous SNV	NM_015355:c.G1813T:p.D605Y
4_PRE	BCOR	chrX	39914629	39914629	A	-	65,22	exonic	frameshift deletion	NM_001123384:c.4577delT:p.F1526fs
4_PRE	KIT	chr4	55603390	55603390	A	G	36,03	exonic	nonsynonymous SNV	NM_000222:c.A2746G:p.T916A
4_PRE	TET2	chr4	106155858	106155861	CAGT	-	48,94	exonic	frameshift deletion	NM_001127208:c.759_762del:p.N253fs
4_PRE	TET2	chr4	106196336	106196336	-	T	37,14	exonic	frameshift insertion	NM_001127208:c.4670dupT:p.V1557fs
4_PRE	SF3B1	chr2	198267359	198267359	C	G	47,95	exonic	nonsynonymous SNV	NM_012433:c.G1998C:p.K666N
5_POST	TP53	chr17	7577114	7577114	C	T	15,88	exonic	nonsynonymous SNV	NM_001126115:c.G428A:p.C143Y
5_POST	TP53	chr17	7577114	7577114	C	T	17,65	exonic	nonsynonymous SNV	NM_001126115:c.G428A:p.C143Y
5_POST	NRAS	chr1	115258747	115258747	C	A	6,62	exonic	nonsynonymous SNV	NM_002524:c.G35T:p.G12V
5_PRE	TP53	chr17	7577114	7577114	C	T	81,25	exonic	nonsynonymous SNV	NM_001126115:c.G428A:p.C143Y
5_PRE	KRAS	chr12	25398285	25398285	C	T	6,88	exonic	nonsynonymous SNV	NM_004985:c.G34A:p.G12S
5_PRE	NRAS	chr1	115258747	115258747	C	A	28,06	exonic	nonsynonymous SNV	NM_002524:c.G35T:p.G12V
7_POST	BCOR	chrX	39913190	39913190	G	C	19,75	exonic	stopgain	NM_001123384:c.C4769G:p.S1590X
7_POST	TET2	chr4	106180857	106180857	C	A	96,59	exonic	stopgain	NM_001127208:c.C3885A:p.Y1295X
7_PRE	BCOR	chrX	39913190	39913190	G	C	22,18	exonic	stopgain	NM_001123384:c.C4769G:p.S1590X
7_PRE	TET2	chr4	106180857	106180857	C	A	89,87	exonic	stopgain	NM_001127208:c.C3885A:p.Y1295X
8_POST	ASXL1	chr20	31023472	31023472	A	G	49,75	exonic	nonsynonymous SNV	NM_015338:c.A2957G:p.N986S
8_POST	TP53	chr17	7577129	7577129	A	G	3,98	exonic	nonsynonymous SNV	NM_001126115:c.T413C:p.F138S
8_POST	DNMT3A	chr2	25457242	25457242	C	T	10,08	exonic	nonsynonymous SNV	NM_153759:c.G2078A:p.R693H
8_POST	KMT2A	chr11	118343474	118343474	T	C	43,47	exonic	nonsynonymous SNV	NM_001197104:c.T1600C:p.S534P
8_POST	STAG1	chr3	136062845	136062845	T	G	54,29	exonic	nonsynonymous SNV	NM_005862:c.A3275C:p.E1092A
8_PRE	ASXL1	chr20	31023472	31023472	A	G	46,74	exonic	nonsynonymous SNV	NM_015338:c.A2957G:p.N986S
8_PRE	TP53	chr17	7577129	7577129	A	G	87,48	exonic	nonsynonymous SNV	NM_001126115:c.T413C:p.F138S
8_PRE	DNMT3A	chr2	25457242	25457242	C	T	41,71	exonic	nonsynonymous SNV	NM_153759:c.G2078A:p.R693H
8_PRE	KMT2A	chr11	118343474	118343474	T	C	45,02	exonic	nonsynonymous SNV	NM_001197104:c.T1600C:p.S534P
8_PRE	STAG1	chr3	136062845	136062845	T	G	43,37	exonic	nonsynonymous SNV	NM_005862:c.A3275C:p.E1092A
9_POST	KRAS	chr12	25380285	25380285	G	A	7,59	exonic	nonsynonymous SNV	NM_004985:c.C173T:p.T58I

Supplementary table 4: DEG in paired analysis, treated vs pre-treated samples

gene	baseMean	log2FC	log2FCunshrunk	pvalue	padj
SEPT5	1493,6	1,07567	1,18783	0,000309	0,016306821
A2M	4603,1	1,81603	2,10375	1,81E-05	0,00254968
ABCA6	35,2	1,52936	2,08863	0,000357	0,017805818
ABCA7	602,7	0,82255	0,88154	0,000455	0,020584393
ABCA8	43,6	1,8119	3,07696	0,000489	0,021459615
ABCB10	2236	0,88437	0,94041	0,000113	0,008948831
ABI3	451,1	1,39138	1,7946	0,000293	0,015758062
ABLIM3	284,9	2,22774	3,98682	4,99E-06	0,000954564
ABTB1	1626,6	0,61571	0,64002	0,001907	0,045083656
AC011933.2	98,2	-0,57265	-0,58974	0,000985	0,030749642
AC016739.2	1292,9	-0,62522	-0,64625	0,00111	0,033173621
AC079250.1	1101,7	-0,58259	-0,59907	0,001103	0,033047483
AC079922.2	82,9	-0,8983	-0,91842	3,92E-09	3,9857E-06
AC090602.2	46,9	-0,75634	-0,79438	0,000619	0,024412448
AC104843.3	67,3	-0,69812	-0,72216	0,000109	0,008759934
ACAD9	914,8	0,69795	0,73359	0,000698	0,025792662
ACAT1	1414,9	0,55801	0,57765	0,002136	0,04783587
ACSM5	119,3	2,03622	2,92631	2,36E-05	0,00293909
ACTN1	9019,2	0,73654	0,77684	0,000963	0,030683161
ADAM28	1405	-0,7446	-0,78774	0,000683	0,025518894
ADCY3	1008,5	0,44305	0,45199	0,001916	0,045127922
ADPGK	4230,4	-0,40247	-0,40857	0,00205	0,046638014
ADPRM	868,5	-0,7323	-0,77052	0,001994	0,045988551
AFAP1L2	132,3	1,72895	2,99515	0,0001	0,008272848
AKAP1	782,7	0,7603	0,81567	0,001845	0,044162524
AKR1C1	115,1	1,56213	2,18312	0,000192	0,011695352
ALAD	1604,7	0,76009	0,80326	0,000658	0,025048504
ALG1	623,4	0,59221	0,61165	0,000807	0,02773474
ALOX15	96,2	1,92806	3,11452	0,0001	0,008272848
ALOX5	716,2	1,3507	1,6648	0,000204	0,01215525
ALOX5AP	1381,2	1,08241	1,18196	0,000797	0,02753612
ALPL	520,1	2,10338	3,12356	2,93E-06	0,000679469
ANAPC10	716,2	-0,5119	-0,52294	0,001515	0,039842806
ANK1	1361,4	1,37135	1,87991	0,001097	0,032986888
ANKH	704,8	1,13096	1,28807	0,00014	0,009821226
AOAH	1463,6	1,15292	1,40122	0,000452	0,020544705
AP000936.1	260,7	-0,60731	-0,62385	0,000311	0,016344218
AP001189.4	145,7	1,5694	2,11202	0,000975	0,030683161
AP1B1	3104,7	0,51427	0,52674	0,001241	0,034957259
APEH	3239,7	0,80619	0,87931	0,000897	0,029338273
APOE	19265	1,60946	1,73113	5,09E-05	0,005047348
APOL4	296,9	1,48924	1,95861	0,000908	0,029541708
APTR	194,6	-0,69377	-0,71706	0,000203	0,01215525
AQP10	91,2	2,19155	3,53548	3,54E-06	0,00074554
AQP3	291,8	1,34871	1,7415	0,000913	0,029624734
ARG1	311	1,93864	2,23407	9,65E-08	5,13908E-05
ARHGAP29	127,9	1,49877	1,95531	0,000348	0,017574342
ARHGEF37	47,4	1,57002	2,2206	0,000491	0,021529945
ASAP2	151,9	1,21755	1,67723	0,001962	0,045734393

ASH1L-AS1	241,2	-0,58761	-0,60679	0,001514	0,039842806
ASTN2	53,7	1,39759	2,13604	0,000768	0,027152452
ATP2A3	6419	0,55738	0,57722	0,001723	0,042409155
ATP8B1	39,3	1,4275	2,20027	0,001171	0,033830134
ATP8B4	2040,3	-0,55703	-0,56715	0,001799	0,04366828
B3GNT7	106,1	1,21947	1,58882	0,002093	0,047269398
B4GALT2	646,9	0,8991	0,95463	3,53E-05	0,003933385
BAG4	1476,5	-0,56055	-0,57055	6,43E-05	0,006087345
BANK1	630,4	0,89713	0,96972	0,000179	0,011313527
BEX1	1589,9	-1,19497	-1,23609	0,000132	0,009504105
BMP5	75,2	1,61989	3,45256	0,002151	0,048045222
BMX	65,3	1,98014	3,47002	1,16E-05	0,001847703
BPI	1860,2	2,18173	2,89191	2,6E-07	0,000111368
BRWD1	2827,4	-0,51235	-0,52554	0,001605	0,040824928
BTBD6	571,6	0,79156	0,85911	0,001792	0,043557961
BTN3A2	672,6	0,90128	0,99377	0,001097	0,032986888
BTN3A3	398,5	0,8809	0,95952	0,000833	0,028180264
C16orf87	1244	-0,67723	-0,70913	0,000785	0,027448636
C1QA	10237,7	1,48907	1,7241	0,000717	0,026062136
C1QB	10385,7	1,60106	1,85377	0,000283	0,015480219
C1QC	4509,3	1,66454	1,96678	0,000135	0,009671593
C1S	537,2	1,40691	2,09738	0,00197	0,045794379
C2	471,8	1,69387	2,18169	8,68E-05	0,007545759
C3orf14	43,7	1,63428	2,93112	0,001215	0,0345706
C5AR1	1660,1	1,62272	1,88493	3,2E-06	0,00071843
C5AR2	72,4	1,51223	2,38445	0,000793	0,027458893
C5orf30	485,8	0,65474	0,67488	0,000207	0,012228546
C6orf48	2365	-0,55624	-0,57159	0,001725	0,042409155
C7	1146,2	1,44183	2,01456	0,001266	0,035367536
CA4	60,5	1,66587	3,74602	0,001025	0,03152073
CACFD1	127	1,37508	1,77583	0,000309	0,016306821
CAD	1220,8	0,73307	0,79688	0,002236	0,04910934
CAHM	58,7	-0,7916	-0,85846	0,001879	0,044589297
CALD1	269,5	1,64964	2,71793	0,000333	0,017095338
CAMP	1103,8	3,23493	4,15739	4E-15	3,5907E-11
CCL13	38,8	1,58268	2,47392	0,000883	0,029166128
CCL2	1657,8	1,33694	1,69938	0,00192	0,045127922
CCL5	2424,5	1,46262	1,61585	0,000618	0,024412448
CCL8	372,7	1,63604	2,12848	0,000425	0,019583543
CCNI	10960,1	-0,47832	-0,48653	0,000393	0,01854025
CCR1	2126,9	1,86514	2,31748	9,91E-06	0,001624308
CD101	57,8	1,63354	3,18696	0,001275	0,035493686
CD14	2448,1	1,78945	2,20913	2,19E-06	0,000564797
CD163	4457,4	2,16639	2,62785	6,95E-07	0,000241849
CD163L1	64,2	1,64398	3,74909	0,001499	0,039592062
CD177	228,2	1,61191	2,77998	0,001537	0,039902942
CD209	112,6	2,14631	4,09757	9,76E-06	0,001614089
CD24P4	127,5	2,01448	2,39074	3,19E-07	0,000132721
CD27	89,5	1,6626	2,59647	0,000889	0,029299337
CD320	993,2	0,54346	0,55822	0,00047	0,020971493
CD38	2103,5	1,11516	1,29053	7,72E-05	0,006957981

CD3E	166,9	1,5936	2,17863	0,000404	0,018807907
CD3G	32,8	2,45457	4,10174	2,55E-06	0,000620472
CD4	3884,6	1,22837	1,48844	0,002262	0,049225707
CD5L	7092,1	1,87011	2,31739	2,01E-05	0,002746387
CD7	303,6	1,01587	1,19768	0,002253	0,049163834
CD96	881,5	1,32977	1,83593	0,000606	0,024264032
CDA	420,9	1,5872	2,14502	3,11E-05	0,003529871
CDC14B	223,7	1,54806	2,44711	0,000716	0,026062136
CDC20	1413,6	0,85947	0,94892	0,000816	0,027882864
CDC42	7165,7	-0,67945	-0,70608	0,001014	0,031243258
CDC42P6	185,9	-0,75687	-0,79129	0,000657	0,025048504
CDC73	2500,9	-0,36321	-0,36757	0,001761	0,042927857
CDS1	15,6	1,64414	3,39019	0,001364	0,037275191
CEACAM3	64,2	1,66913	2,5384	0,000293	0,015758062
CEACAM8	887,1	2,5138	3,22043	4,99E-09	4,72555E-06
CEMIP	1652,5	-1,59169	-1,92207	0,000154	0,010362318
CENPA	209,3	0,8637	0,95387	0,001871	0,044457852
CES1	534,1	1,6981	3,2761	0,000521	0,022170246
CETP	1043,7	1,51311	2,24437	0,000608	0,024264032
CFH	542,3	1,18439	1,22167	0,002242	0,049163834
CH17-172B3.1	88,2	-0,65649	-0,67345	0,000114	0,008948831
CH17-373J23.1	82,7	-1,21357	-1,61883	0,001966	0,045779005
CHI3L1	536,7	1,31919	1,41341	0,000175	0,011248588
CHI3L2	114,1	1,74246	3,26678	0,000333	0,017095338
CHIC2	1995,7	-0,45872	-0,46603	0,000791	0,027458893
CHIT1	120,6	2,1515	4,10297	7,78E-06	0,001379685
CKAP4	1097,8	1,17004	1,29071	0,000375	0,018040572
CLC	2789,4	1,62044	2,28217	0,000139	0,009805743
CLCC1	499,7	0,77656	0,83456	0,001177	0,033891722
CLDND2	54,4	-0,99747	-1,07496	3,75E-05	0,0040658
CLEC1B	121	1,37391	1,75655	0,000357	0,017805818
CLEC4E	93,2	1,97709	3,40688	1,76E-05	0,002529545
CLSTN2	60,8	2,55582	5,82623	6,08E-07	0,000216028
CNDP2	3306,8	0,67437	0,70298	0,000895	0,029338273
CNNM3	1071	0,86464	0,95663	0,001577	0,040408432
COG5	872,5	0,35856	0,36185	0,000378	0,018146527
COL14A1	163,9	1,41839	1,80854	0,000546	0,022778228
COL1A1	970,6	1,54126	1,93423	0,000527	0,022213646
COL1A2	1465,2	1,63616	2,53934	0,000901	0,029415236
COL8A2	121,1	1,2814	1,85377	0,001864	0,044428637
COLGALT1	2146,4	0,81744	0,85851	6,98E-05	0,006461805
COLQ	26,8	1,70094	2,66565	0,000148	0,010179553
COMMD2	1899,8	-0,3976	-0,40321	0,001622	0,041137785
COMTD1	198	0,93311	1,02878	0,000444	0,020216143
CPM	852	1,30768	1,5529	0,002028	0,046377656
CPNE2	1879,5	0,70917	0,74298	0,000519	0,022170246
CPNE5	313,4	1,4253	1,83196	0,001659	0,041578557
CPOX	474	0,95917	1,05906	0,000425	0,019583543
CR1	206,8	1,43507	2,10905	0,000864	0,028825162
CRISP3	631,7	2,92937	3,53824	3,08E-13	1,0494E-09
CROCC	440,7	0,67771	0,71236	0,000835	0,028180264

CRYZL1	889,9	-0,3738	-0,37705	9,06E-05	0,007727685
CTB-61M7.2	397,8	1,4405	1,8067	0,000187	0,011580401
CTC-451P13.1	502,5	-0,74264	-0,77409	0,001113	0,033215893
CTD-2031P19.4	22,3	-0,66422	-0,69435	0,001251	0,035072537
CTD-3014M21.1	517,2	-0,93601	-1,02633	0,000547	0,022778228
CTD-3035D6.1	82,5	-0,78595	-0,82728	0,000788	0,027448636
CTDSPL	829,9	1,05308	1,1937	0,000726	0,026194999
CTSE	117,5	1,98821	3,03313	8,67E-05	0,007545759
CTTN	370,4	1,38376	1,97187	0,001472	0,039019246
CXCL12	1823,4	2,05848	2,78852	7,31E-06	0,001324683
CXCR1	184,1	3,10661	4,00853	0	1,725E-12
CXCR2	176,6	2,13618	2,8574	1,35E-07	6,78521E-05
CXCR2P1	1323,1	1,87087	2,54229	5,14E-05	0,005053659
CXorf65	35,6	-1,0371	-1,13228	0,001988	0,045923407
CYBB	1249,3	1,72943	2,33062	1,46E-05	0,002204736
CYP1B1	1069,6	1,61699	1,98767	0,000117	0,008948831
CYP4F3	73,2	2,52846	4,71012	2,24E-07	0,000100494
DAAM2	65,1	2,12375	4,33406	2,54E-05	0,003092874
DAPK2	87,1	2,02452	2,72528	3,4E-07	0,0001378
DARS2	582,2	0,8713	0,9532	0,001177	0,033891722
DBN1	1706,2	0,7068	0,75151	0,001354	0,037098425
DDR2	117	1,98017	2,95964	2,88E-05	0,003397523
DEFA3	4842,7	1,92734	2,38839	1,78E-05	0,002529545
DEFA4	1392,1	1,68604	2,15758	0,000286	0,015547948
DGAT2	216,5	1,03094	1,09626	0,001834	0,044099792
DMWD	378,3	1,14483	1,48891	0,00119	0,034070534
DNAAF5	552,4	1,05923	1,19113	0,000144	0,010000798
DNAJA2	2757,5	-0,37826	-0,38349	0,001815	0,043931343
DNAJB14	1134,9	-0,43387	-0,44258	0,001684	0,041839367
DTX1	82,2	1,59773	3,31168	0,001002	0,031158032
DYSF	583,7	1,45935	1,97765	0,000721	0,026158108
EEF1A1P19	765,6	-0,52163	-0,53266	0,001387	0,037632858
EEF1A1P22	71,3	-0,70918	-0,73817	0,0004	0,018715315
EEF1A1P25	128,9	-0,65304	-0,67238	0,000417	0,019297448
EEF1A1P9	1130,9	-0,54551	-0,5586	0,001123	0,033240309
EHD3	782,4	1,26805	1,6509	0,000847	0,028461883
EIF3E	9063,6	-0,46925	-0,47656	0,000648	0,024999055
EIF3H	5284	-0,48661	-0,49225	2,11E-05	0,002801012
ELAC2	2348,1	0,55978	0,57241	0,000216	0,012585691
EMILIN1	1242,8	1,10498	1,29695	0,000966	0,030683161
ENDOG	282,8	1,00208	1,10221	0,000141	0,009821226
ENKUR	181,9	1,4747	2,05139	0,001734	0,042511923
ENTPD1	404,5	1,63823	2,00924	7,85E-06	0,001379685
ENY2	3545,3	-0,42773	-0,4344	0,002119	0,047633816
EOMES	41,8	1,73952	3,34465	0,000967	0,030683161
EPN2	59,4	1,93629	2,40884	4,02E-08	2,85548E-05
EPX	4458,8	2,18864	3,01273	3,55E-07	0,000140626
ERF	375,5	-0,75446	-0,77726	1,24E-05	0,001931114
ESM1	102,4	1,64511	4,011	0,001463	0,038904153
ETV4	28,6	1,97139	3,82842	6,92E-05	0,006439682
F5	117,1	1,84096	3,19789	0,000141	0,009821226

FABP3	271,8	1,47271	1,99796	0,001233	0,034856966
FAM178B	330,6	1,67102	2,15666	1,74E-06	0,000493955
FAM210B	1900,7	0,69837	0,73359	0,001156	0,033592113
FAM213A	948,3	0,7791	0,85439	0,00096	0,030683161
FAM214A	561,1	-0,54079	-0,55576	0,000728	0,026226882
FCAR	993,1	1,62144	2,18187	1,92E-05	0,002659997
FCGR3A	4001,7	1,74577	2,29381	4,46E-05	0,004631356
FCGR3B	388,9	2,52324	3,41357	6,51E-11	1,38591E-07
FCMR	323,5	1,09676	1,2867	0,001139	0,033475788
FCN1	6173,3	1,47013	1,95065	0,000115	0,008948831
FCRL5	248,6	1,52842	1,52326	0,002094	0,047269398
FDXR	340,4	0,89908	0,952	3,38E-05	0,00378614
FGD2	144,5	1,34762	2,02995	0,001519	0,039842806
FGFR1OP2	3765,1	-0,29759	-0,29971	0,001214	0,0345706
FGR	1427,9	1,11798	1,40572	0,001999	0,046043376
FHL3	1520,4	-0,57443	-0,58671	0,000565	0,023266695
FICD	173,7	0,94075	1,01904	0,000371	0,017961305
FKBP9	314,9	1,50585	1,67335	2,93E-06	0,000679469
FKBP9P1	17,5	1,67395	2,04444	1,69E-05	0,002477337
FMO2	227,3	1,71863	2,9496	0,000756	0,026918045
FMO3	125,8	1,81147	3,3647	0,000354	0,017805818
FN3K	104,9	1,10585	1,25085	0,000835	0,028180264
FOLR2	1998	1,62117	2,02252	0,000138	0,009793117
FOLR3	46,9	1,87563	2,7637	3,35E-05	0,003780753
FOXD2	19,1	2,06348	2,77053	2,43E-06	0,000607773
FOXRED2	1133,5	1,11698	1,22959	4,89E-05	0,004868624
FPR1	1327,9	1,59098	1,72271	1,5E-07	6,89872E-05
FPR2	460,2	1,54091	1,94839	0,000182	0,011412279
FRZB	168,6	1,66523	2,40292	0,000601	0,024264032
FUCA1	3016,2	1,35246	1,48424	0,000176	0,011248588
G3BP1	4642	0,6293	0,64962	0,000625	0,024524373
GAL3ST2	100	-1,19103	-1,36214	0,000767	0,027152452
GALC	1100,7	0,70264	0,72759	0,000109	0,008759934
GALNT10	965,7	0,69375	0,73464	0,000956	0,030683161
GAS6	941,3	1,29605	1,46085	0,000937	0,030286922
GFRA2	959,6	2,03019	2,84598	3,79E-06	0,000778945
GIMAP4	500,6	1,68212	2,3902	8,95E-05	0,007699163
GIMAP8	224,1	1,43622	2,63375	0,002024	0,046377656
GLDN	62,7	2,32092	3,84313	1,84E-06	0,000496488
GNLY	221,7	1,56158	1,8156	0,000148	0,010179553
GOLGA6L5P	28,7	-1,22953	-1,45507	0,000588	0,023930667
GPATCH2L	1267,5	-0,47775	-0,48805	0,00125	0,035072537
GPD1L	615,2	0,96233	1,02233	8,66E-05	0,007545759
GPNMB	2940,8	2,18437	3,37962	9,61E-07	0,000292547
GPR35	370,1	-1,15718	-1,22791	0,00011	0,008812703
GPX3	1655,8	1,24283	1,43057	0,001753	0,042792869
GRAP2	970,8	1,45459	2,37802	0,001837	0,044099792
GRIN3A	15,1	1,67966	2,47122	0,001409	0,037983379
GRK4	224	0,68307	0,71373	0,000607	0,024264032
GRK5	63,9	1,44263	2,67941	0,002273	0,049401759
GUCY1B3	842,7	1,2329	1,34729	8,22E-07	0,000272809

GZMA	75,7	2,14191	3,80478	1,43E-05	0,00217081
GZMM	47,6	1,72371	2,36288	9,32E-05	0,007826307
HAGH	747,7	0,81505	0,86443	0,001647	0,041459823
HBA2	9972,6	1,45719	1,52571	0,00097	0,030683161
HBM	608,1	1,92732	2,35686	2,46E-05	0,003031958
HDLBP	5352,7	0,4297	0,4381	0,00126	0,035269496
HES6	541,6	1,22248	1,33232	2,2E-05	0,00281798
HESX1	106,1	-0,83166	-0,87542	7,3E-05	0,006647871
HFE	93,5	1,94382	4,41201	0,00018	0,011313527
HIST2H2AA3	967,5	-1,0185	-1,13921	0,000578	0,023670642
HIST2H2AA4	400,2	-0,95676	-1,08305	0,001697	0,042086053
HIST2H2BC	24,5	-1,05016	-1,12314	2,93E-05	0,003398793
HIST2H2BD	26,5	-1,29137	-1,42978	4,13E-05	0,004372945
HIST2H3D	18,4	-1,0827	-1,24829	0,002291	0,049601266
HIVEP1	419,1	-0,77679	-0,79884	5,98E-06	0,001120147
HK3	891,6	2,24253	3,09427	4,6E-08	3,13431E-05
HLA-DOB	42,4	1,50398	2,47746	0,001667	0,041654539
HMBS	2020,6	0,97386	1,07881	0,000864	0,028825162
HMOX1	7542,8	1,37954	1,63638	0,001226	0,034764778
HNMT	448,2	1,47073	1,84464	0,000183	0,011412279
HOXA6	125,2	-0,87481	-0,98245	0,001646	0,041459823
HOXA9	1674,7	-0,85206	-0,917	0,000443	0,020216143
HOXA-AS3	104,5	-0,83912	-0,91477	0,001459	0,038837553
HOXB2	656,3	-0,61236	-0,62557	0,000984	0,030749642
HP	462,8	2,28642	3,17896	2,61E-07	0,000111368
HPSE	226,6	1,13537	1,2928	0,000618	0,024412448
HSBP1L1	368,8	-0,53852	-0,55215	0,001434	0,038465425
HSD17B4	1818,3	0,68578	0,71679	0,000976	0,030683161
HSD3B7	177,1	0,87633	0,98125	0,000475	0,020986899
HTRA1	136,6	1,60941	3,65897	0,00145	0,038665293
HYAL3	634,3	0,91675	1,03128	0,000308	0,016306821
ICMT	812,7	0,85484	0,90581	7,1E-05	0,006505496
IDH1	1173,5	0,86125	0,91515	0,001522	0,039842806
IGF2	94,3	1,63929	2,60566	0,001301	0,035993038
IGFBP4	2267,5	1,47026	1,83168	0,000775	0,027280131
IGHA1	179324,8	1,96957	1,96666	8,55E-07	0,000274853
IGHA2	17934,7	1,54575	1,38052	0,000455	0,020584393
IGHG1	74544,6	1,47835	1,53195	0,000214	0,012548271
IGHG2	31415,3	1,64727	1,74864	0,00012	0,008980352
IGHG3	5413,5	1,72939	2,20757	0,000119	0,008948831
IGHG4	10017,5	1,91307	1,84708	1,02E-05	0,001652841
IGHGP	6461,1	1,84938	2,08677	3,94E-06	0,00080018
IGHV1-18	423,2	2,4936	3,20963	8,25E-08	4,81509E-05
IGHV1-2	673,5	2,24336	2,80381	9,24E-07	0,00029021
IGHV1-24	293,5	1,8591	2,28587	8,89E-05	0,007690477
IGHV1-46	149,9	1,84298	2,30413	0,000177	0,011248588
IGHV2-5	370,7	1,81375	2,27766	0,000204	0,01215525
IGHV3-15	372,7	2,13184	2,64941	4,34E-07	0,000163613
IGHV3-23	1423,1	1,79521	1,90304	0,000116	0,008948831
IGHV3-30	1413,3	2,12666	2,67212	8,32E-07	0,000272809
IGHV3-33	578	2,17118	2,5719	4,48E-06	0,000877693

IGHV3-43	106,5	1,92749	3,10386	0,000231	0,013394838
IGHV3-48	150	2,13843	2,71292	6,82E-06	0,001248939
IGHV3-49	238,7	1,76172	2,02258	0,00015	0,010291112
IGHV3-7	702,4	1,65102	2,50489	0,000783	0,027448636
IGHV3-72	129,8	1,68356	2,82534	0,000608	0,024264032
IGHV3-9	842,1	1,5247	1,71328	0,002044	0,046634187
IGHV4-34	258,4	2,00572	2,5331	2,57E-05	0,003101364
IGHV4-39	420,7	2,07965	2,96971	1,77E-05	0,002529545
IGHV4-61	23,7	1,84967	2,58973	4,69E-05	0,004800805
IGHV5-51	531,8	2,63203	3,36445	1,05E-09	1,37257E-06
IGHV6-1	242,6	1,96024	3,98761	0,000192	0,011695352
IGKC	200814,9	1,78138	1,80474	2,13E-05	0,002801012
IGKV1-12	604,2	2,12572	2,57652	3,41E-06	0,000736341
IGKV1-16	359,6	2,21354	2,54384	1,09E-05	0,001754816
IGKV1-17	242,3	1,62157	2,53984	0,001241	0,034957259
IGKV1-33	454,4	1,84734	1,66771	0,0001	0,008272848
IGKV1-39	666	1,82333	1,88504	0,000153	0,010362318
IGKV1-5	2392,7	1,64424	1,61557	4,76E-05	0,004808278
IGKV1-6	286,8	2,41322	3,2718	1,03E-06	0,000307267
IGKV1-9	731	2,00259	2,40929	9,35E-06	0,001561397
IGKV1D-12	147,1	1,75248	3,51144	0,00069	0,025678355
IGKV1D-17	135,5	1,76046	2,15263	0,000733	0,026354686
IGKV1D-33	301,3	1,9028	2,17745	6,6E-05	0,006180331
IGKV1D-39	401,2	1,77518	1,94589	0,000196	0,011883454
IGKV2-30	692,7	1,73324	2,64384	0,000503	0,02187519
IGKV2D-29	191,6	2,77273	3,97117	3,19E-08	2,46727E-05
IGKV2D-30	101,2	1,89381	2,63042	0,000113	0,008948831
IGKV3-11	5332,6	1,66336	2,08816	0,000171	0,011248588
IGKV3-15	2698,4	2,45485	2,99124	8,48E-08	4,81509E-05
IGKV3-20	4260,7	1,77987	1,79095	9,23E-05	0,007787129
IGKV3D-15	473,9	2,2283	2,77552	3,33E-06	0,00073611
IGKV3D-20	417,4	1,83098	2,08464	0,000122	0,009044449
IGLC2	8006,3	2,00539	2,2541	1,81E-06	0,000496488
IGLC3	6166,1	1,55751	1,67905	0,000172	0,011248588
IGLL5	93,4	2,17683	3,12609	5,11E-06	0,000967858
IGLV1-40	1613,6	1,91653	1,73033	2,18E-05	0,00281798
IGLV1-44	619,4	1,59941	2,11207	0,000363	0,017854523
IGLV1-47	1134,2	1,95358	2,43926	1,17E-05	0,001850233
IGLV1-51	1652,5	2,03913	2,48346	9,37E-07	0,00029021
IGLV2-11	620	1,61355	2,46049	0,00104	0,031773319
IGLV2-14	1783,3	1,83221	2,44825	6,5E-05	0,006117926
IGLV2-23	1030	1,66393	3,18299	0,000789	0,027448636
IGLV2-8	428,5	2,60156	4,1428	5,29E-09	4,7442E-06
IGLV3-1	588,6	1,96938	2,67505	4,7E-05	0,004800805
IGLV3-21	2400,9	1,90267	1,92538	4,09E-05	0,004372945
IGLV3-25	686	1,97499	3,29942	0,000137	0,009791764
IGLV4-60	181,4	1,84076	2,50092	0,000488	0,021459615
IGLV4-69	495,3	2,09077	3,57072	2,99E-05	0,003446918
IGLV5-45	153,9	2,79331	4,33483	6,88E-08	4,39786E-05
IGLV6-57	1138,6	2,36878	3,2616	4,42E-07	0,000163613
IGLV7-46	119,4	1,74888	1,91525	0,000715	0,026062136

IGSF21	92,5	1,5461	3,0774	0,001662	0,041578557
IGSF6	921,9	1,62885	1,94007	2,14E-05	0,002801012
IKZF3	38,7	1,99963	3,3084	0,000127	0,009208804
IL11	522,4	-1,60959	-3,02754	0,000594	0,024105632
IL18RAP	59,7	2,01391	4,24594	5,16E-05	0,005053659
IL1R2	93,4	1,54236	2,68249	0,001307	0,036046851
IL2RB	220,6	1,77504	3,23251	0,00018	0,011313527
IL5RA	30,9	1,47751	2,44982	0,001837	0,044099792
IMPDH1	2765,1	0,64983	0,68346	0,000956	0,030683161
IPO13	605,6	0,70862	0,76112	0,001542	0,039910935
IREB2	1366,7	-0,42193	-0,42785	0,001468	0,038963114
IRF6	28,5	2,11091	3,50276	8,81E-06	0,001515911
ITGA2B	9971,6	1,28204	1,72068	0,000964	0,030683161
ITGAD	284,1	1,57407	2,53023	0,000852	0,028567862
ITGB3	853,3	1,29732	1,82324	0,002105	0,047452419
JAML	627,7	1,765	2,1763	5,77E-07	0,00020929
JSRP1	134,3	1,42679	2,07988	0,000663	0,025154114
KCNAB1	183,2	1,35559	1,68781	0,001127	0,033240309
KCNH2	1824,6	1,4178	1,92666	0,000366	0,017854523
KCNJ5	73,4	1,77663	4,02334	0,000631	0,024649838
KCNMA1	254	1,53037	1,81571	0,000757	0,026918045
KCNQ1	541,9	1,08732	1,45837	0,002314	0,049779419
KIF16B	335,6	0,81517	0,85054	3,65E-05	0,003992085
KLF1	1394,3	1,30579	1,61169	0,000705	0,025837029
KLRB1	27,7	1,34203	2,07583	0,002312	0,049779419
KLRD1	58,9	1,61491	2,403	0,001434	0,038465425
KLRG1	178,2	1,16432	1,45612	0,000698	0,025792662
KMO	76,6	1,52599	2,6694	0,001719	0,042409155
KNL1	257,6	0,82186	0,89192	0,001572	0,040408432
KRT17P1	32	-1,70142	-2,494	0,000222	0,012912146
KRT17P2	44,9	-1,41478	-1,89016	0,001926	0,045156857
KRT17P6	64,4	-2,01426	-2,50252	1,44E-07	6,89872E-05
LCN2	1369,8	2,67784	3,22528	1,15E-11	2,80928E-08
LDLRAP1	1007,6	1,11511	1,25509	0,000261	0,014693231
LEF1	290,7	1,49736	2,17289	0,000175	0,011248588
LGMN	10472,9	1,88989	2,24952	3,51E-06	0,00074554
LGMNP1	36,5	1,57863	2,09211	0,000698	0,025792662
LILRB5	1191,8	2,12766	2,78942	2,86E-06	0,000679469
LINC00989	174	1,576	2,47511	0,001248	0,035072537
LINC01011	113,9	1,50262	2,45048	0,000833	0,028180264
LINC01126	81,1	-0,99999	-1,10776	0,000356	0,017805818
LLGL2	354,2	0,54214	0,55558	0,000739	0,026484786
LMLN	79,1	1,18437	1,51467	0,001027	0,031525697
LPCAT1	1326,7	1,12817	1,2288	8,72E-06	0,001515911
LRP1	711,8	1,68645	2,1652	1,48E-05	0,002208449
LRP11	110,4	1,28784	1,51381	4,81E-05	0,00482286
LRP3	1106,6	1,18263	1,34221	7,52E-05	0,006817973
LRRC45	403,8	0,68674	0,73166	0,001579	0,040408432
LRRC75A-AS1	9227,3	-0,67272	-0,70064	0,002176	0,048352524
LRRK2	83,8	1,68099	2,98221	0,000318	0,016684351
LTBP1	1058,2	1,26203	1,60771	0,000704	0,025837029

LTF	14570,8	2,75758	3,43012	1,15E-11	2,80928E-08
LUM	702,8	1,54736	2,72932	0,001528	0,039902942
LYVE1	417,4	1,73476	2,44599	0,000138	0,009793117
MAFB	5471,2	1,29037	1,48963	0,001181	0,033900569
MAN1C1	419,5	1,42346	1,87906	0,001377	0,037551909
MARCO	330,6	1,86344	2,76043	2,93E-05	0,003398793
MARK4	204,5	-0,61252	-0,63203	0,00121	0,0345706
MBD5	388,3	-0,48769	-0,49789	0,000985	0,030749642
MBOAT2	977,1	0,97685	1,11852	0,000368	0,0178889
MBOAT7	9135,2	-0,65801	-0,69059	0,001579	0,040408432
MDM4	1158	-0,55756	-0,57895	0,00219	0,048459233
MED13	552,6	-0,58472	-0,59546	3,56E-05	0,00393879
MED30	2378,1	-0,75707	-0,78211	9,22E-05	0,007787129
MEFV	70,2	1,88751	4,10168	0,000214	0,012548271
MGAT3	49,7	1,47131	2,67561	0,001556	0,040121037
MMP25	69,7	1,72953	2,02242	3,71E-07	0,000143656
MMP8	2656,4	2,37866	2,98619	3,98E-09	3,9857E-06
MMP9	1915,8	2,38643	3,03798	1,42E-09	1,72294E-06
MOSPD3	536,5	0,6483	0,6705	0,000274	0,01509638
MPEG1	4036,2	1,60341	1,99346	4,13E-05	0,004372945
MRPL45P2	161,8	-0,85611	-0,90097	0,000153	0,010362318
MS4A2	237,9	1,21057	1,62265	0,000725	0,026194999
MYLK	956,2	1,29084	1,46504	0,000267	0,014838085
NACA	13289,3	-0,39134	-0,39691	0,00186	0,044428637
NADK	1474,3	0,53372	0,54482	0,000304	0,01624655
NBDY	1835,6	-0,42296	-0,42824	0,000339	0,017242504
NBPF1	442,4	0,95225	1,09216	0,001349	0,037011556
NBPF13P	18,9	-1,13643	-1,34994	0,001569	0,040397314
NCAPG2	1200,5	0,65035	0,68196	0,000973	0,030683161
NCF1	1020	1,83547	2,47922	2,48E-06	0,000612059
NCF1B	474,9	1,84866	2,56607	2,99E-06	0,000679469
NCF1C	585,2	1,90385	2,60254	1,77E-06	0,000495142
NCOA7	7347,3	-0,52789	-0,5385	0,001845	0,044162524
NDFIP2	162,6	1,54022	2,608	0,001148	0,033592113
NECTIN1	182,7	0,71547	0,75049	5,5E-05	0,005296947
NEXN	127,8	1,23137	1,73751	0,001532	0,039902942
NFIA	841	1,10105	1,22287	0,000154	0,010362318
NLRC4	101	1,77141	2,38567	5,22E-05	0,005060267
NOMO1	1302,6	0,52964	0,54181	8,65E-05	0,007545759
NOMO2	1061,6	0,47105	0,47768	4,43E-05	0,004631356
NPL	1017,5	1,53082	1,97845	3,94E-05	0,004250255
NPM1P26	76,8	-1,28335	-1,50158	0,000326	0,01686359
NQO1	123,5	0,81743	0,8975	0,001911	0,045102685
NUFIP2	976,1	-0,54637	-0,55885	0,000528	0,022228217
NUP54	2265,1	-0,49991	-0,51057	0,0014	0,037858746
NUPR1	104,9	1,71023	2,86092	0,000288	0,015626695
NXN	66,7	1,76094	2,30866	6,52E-06	0,001206853
OGG1	329,6	0,78971	0,8565	0,00127	0,035408195
OLFM4	715,2	2,86062	4,54111	6,93E-10	1,07417E-06
OLFML3	215,1	1,60086	2,24528	0,000427	0,019623244
OPLAH	118,4	1,32514	1,87748	0,001098	0,032986888

ORM1	72,6	2,6043	3,8674	2,38E-08	1,93022E-05
P2RY13	432,7	1,18124	1,34728	0,001892	0,044846324
P3H4	254,3	1,14631	1,42443	0,000525	0,022202356
PABPC1	26476,2	-0,5708	-0,57992	2,16E-05	0,002813606
PABPC3	277,6	-0,5777	-0,58783	4,6E-05	0,004755172
PADI4	1556,2	1,1527	1,29391	0,000373	0,01799773
PAPPA	28	1,96958	3,41659	0,000122	0,009062033
PAQR4	430,2	0,63709	0,66022	0,000783	0,027448636
PARG	187,7	0,83263	0,9006	0,000512	0,022155123
PARP3	452,4	0,5511	0,57101	0,001231	0,034845094
PC	198,4	1,51889	2,47736	0,000645	0,024999055
PCBP2	1457,7	-0,65301	-0,66487	2,98E-06	0,000679469
PCED1B	73,1	1,57278	4,11254	0,002132	0,047813391
PCGF3	776,4	-0,57364	-0,58976	0,001534	0,039902942
PCSK6	315,5	1,24919	1,39378	0,000717	0,026062136
PCYOX1	582,9	0,94811	1,02152	0,000385	0,018362297
PCYT1B	131,2	1,64872	2,99638	0,000204	0,01215525
PDCD1LG2	166,7	2,08202	3,97695	2,82E-05	0,003357317
PDIA4	5452,8	0,62822	0,64771	0,000468	0,020971493
PDSS1	244,7	0,65316	0,67275	0,000114	0,008948831
PDZD4	23	1,89826	2,89351	0,000157	0,010504147
PECR	98,3	1,24297	1,72005	0,002171	0,048308492
PF4V1	116	2,02618	2,7135	4,9E-06	0,000948496
PGLYRP1	716,5	2,81288	3,46064	8,6E-14	3,66875E-10
PHF3	1924,3	-0,29057	-0,29313	0,001988	0,045923407
PHKB	1762,4	0,61463	0,64047	0,001712	0,042342733
PHOSPHO1	93,6	1,33357	1,66259	0,000747	0,026669328
PIGQ	929,9	0,53904	0,55698	0,001438	0,038465425
PILRA	766,2	1,18353	1,44441	0,000254	0,014575525
PLA2G7	788,9	1,59553	2,22797	0,000297	0,01589482
PLBD1	1040,9	2,45479	3,18737	3,53E-10	6,01915E-07
PLCG1	230,9	0,95965	1,1251	0,002302	0,049657504
PLEKHM1P1	1333,8	-0,8968	-0,94317	5,23E-05	0,005060267
PLXNC1	1050,3	0,77526	0,8277	0,001277	0,035493686
PMAIP1	4391,3	-0,8405	-0,92358	0,000935	0,030286922
PMS2CL	493,2	-0,72494	-0,75687	0,000384	0,018362297
PNMA5	30,4	3,14613	5,20543	8,32E-10	1,18204E-06
PNRC2	6868,6	-0,48918	-0,49509	2,22E-05	0,00281798
PNRC2P1	145	-0,5285	-0,5384	0,000189	0,01162912
POLB	1016,3	-0,70099	-0,72371	0,000198	0,011993663
POLR2E	6029,1	0,29178	0,29373	0,000975	0,030683161
POLR3H	790,9	0,5294	0,54376	0,002053	0,046638014
POTEF	58,8	1,02698	1,14688	0,001169	0,033830134
PPARG	438,7	1,64635	2,69637	0,000522	0,022170246
PPIC	78,7	1,55783	2,84048	0,00173	0,042491642
PPIL4	1296,3	-0,57202	-0,58735	0,000551	0,022897587
PPM1M	552,9	0,92394	1,06738	0,00215	0,048045222
PPP2R2A	688	-0,46208	-0,47151	0,001703	0,042176519
PPP5C	1185,1	0,54509	0,56552	0,001126	0,033240309
PRDX1	4890,6	0,68814	0,70881	2,09E-05	0,002801012
PRG3	1253,9	2,44134	3,21713	1,49E-07	6,89872E-05

PRKAR1B	620,9	0,67755	0,70812	0,002155	0,048073408
PRPSAP1	1022,8	0,66031	0,69188	0,000674	0,025456895
PSMD1	3177,3	0,3353	0,33882	0,002222	0,048983952
PTBP2	941,5	-1,0915	-1,21995	0,000268	0,014838085
PTRF	2645,5	0,80353	0,84358	9,75E-05	0,008146432
PUS7	655,8	0,70785	0,74921	0,001498	0,039592062
PYGB	1718,6	0,63114	0,65402	0,000811	0,027766604
QPCT	789,7	1,10187	1,26305	0,001952	0,045623447
RAB27B	344,1	1,0058	1,20074	0,001673	0,041685458
RAB42	176,2	1,5868	2,0495	0,000117	0,008948831
RASSF4	589,8	1,33968	1,69514	0,000362	0,017854523
RBFOX3	34,4	-1,34244	-2,0224	0,002194	0,048495908
RBM18	1597,4	-0,41234	-0,41833	0,001144	0,033561638
RETN	165,3	1,38282	1,89445	0,001438	0,038465425
RGL1	872,6	1,76784	2,53173	5,84E-05	0,005593679
RICTOR	923,3	-0,69542	-0,73494	0,001625	0,041137785
RIOX2	517,6	0,80971	0,86444	0,000474	0,020986899
RMND5B	577,9	0,79636	0,83081	8,23E-05	0,007343683
RND3	369,2	1,65532	2,7096	0,000606	0,024264032
RNF113A	752,1	-0,47568	-0,48329	0,000475	0,020986899
RNF123	901,6	0,69543	0,72269	0,000188	0,01162912
RNF180	30,4	1,73883	8,22574	0,000988	0,030793267
RNF7	3160,9	-0,60993	-0,63004	0,000876	0,02905428
RNU12	204,7	-1,12915	-1,34438	0,000963	0,030683161
RNU1-60P	334,2	-1,03362	-1,21584	0,00101	0,0311938
RNU2-59P	353,3	-1,84708	-2,09276	1,16E-07	6,00441E-05
RNU2-63P	25	-1,14725	-1,38541	0,001821	0,044005374
RNU4-2	30,7	-1,47925	-1,89812	9,07E-05	0,007727685
RNU5A-1	44,2	-1,13089	-1,42535	0,002215	0,048886605
RNU5D-1	16,2	-1,3596	-1,72803	0,001365	0,037275191
RNU5E-1	16,2	-1,41894	-1,78128	0,000176	0,011248588
RNU5F-1	38,5	-1,70773	-2,09161	3,39E-06	0,000736341
RNVU1-13	32,7	-1,26803	-1,57882	0,000665	0,025179174
RNVU1-15	21,9	-1,2677	-1,69193	0,002188	0,048459233
RNVU1-18	15	-1,32489	-1,66411	0,001035	0,031707832
RNVU1-20	49,6	-1,25886	-1,561	0,000504	0,02187519
RNVU1-6	34,9	-1,1052	-1,27741	0,00101	0,0311938
ROPN1L	42,1	1,29994	1,5576	0,000261	0,014693231
RP11-1094M14.1	103,4	-0,76858	-0,81274	0,00198	0,045917405
RP11-110G21.1	97,6	-0,47942	-0,48605	8,09E-05	0,007259759
RP11-120B7.1	90,1	-0,66282	-0,68402	0,000677	0,025463158
RP11-127B20.3	82,9	-0,87518	-0,94394	0,000688	0,025666683
RP11-175B9.3	373	-0,62591	-0,64552	0,00068	0,025473252
RP11-234A1.1	2119,2	-0,72454	-0,75264	0,001117	0,033215893
RP11-307O1.1	22,3	-0,99304	-1,1118	0,001127	0,033240309
RP11-314A20.1	33,7	-0,67753	-0,70819	0,001385	0,037632858
RP11-33B1.1	407,3	-0,64496	-0,66157	0,000207	0,012228546
RP11-353H3.1	42,5	-0,70437	-0,73619	0,000648	0,024999055
RP11-366M4.1	176,4	-0,69996	-0,71816	0,000104	0,00843311
RP11-372K14.2	190	-1,05994	-1,21837	0,00167	0,041664286
RP11-37B2.1	524,2	-0,87416	-0,92085	0,000127	0,009208804

RP11-393I2.4	57,2	-1,03485	-1,12942	7,02E-05	0,006461805
RP11-396F22.1	25	-1,04539	-1,25834	0,001596	0,04065101
RP11-401L13.4	67,5	-0,56555	-0,58363	0,001102	0,033047483
RP11-423H2.3	25,2	1,32894	1,7377	0,002232	0,04910934
RP11-44F14.1	38,6	1,65128	2,57931	0,000358	0,017805818
RP11-465B22.3	385	-1,45149	-1,90526	0,000281	0,015402309
RP11-466H18.1	333,9	-0,60863	-0,63201	0,001676	0,041698585
RP11-486G15.2	67,7	-0,85457	-0,92307	0,001608	0,040846394
RP11-488L18.4	161,6	-0,74629	-0,77981	0,000125	0,009208804
RP11-543P15.1	274,3	-0,63253	-0,65635	0,001167	0,033816605
RP11-613F7.1	21,2	-0,70645	-0,74233	0,00101	0,0311938
RP11-627K11.1	250	-0,62471	-0,64745	0,00175	0,042792869
RP11-69L16.5	520,7	-0,75519	-0,79224	0,000659	0,025048504
RP11-69M1.6	413,6	-0,55033	-0,56386	0,00104	0,031773319
RP11-730G20.2	75,2	-0,53634	-0,55369	0,002184	0,048454828
RP11-761N21.2	282	-0,63762	-0,65588	0,00026	0,014693231
RP11-778D9.4	699,9	-0,67904	-0,70654	0,001386	0,037632858
RP1-182O16.1	59	-0,76143	-0,80361	0,002169	0,048308492
RP11-83J16.1	55	-0,69703	-0,724	0,000238	0,013728484
RP11-848P1.5	17	-1,19229	-1,41178	0,001306	0,036046851
RP11-864N7.2	545,1	-0,64926	-0,66872	0,000581	0,023758242
RP1-228H13.1	34,6	-0,7759	-0,80775	0,000165	0,010996615
RP3-402G11.25	43,2	-1,44842	-1,72392	0,000126	0,009208804
RP4-647J21.1	28,5	-1,38944	-1,68305	0,000184	0,011451071
RPL10	25264	-0,49919	-0,50946	0,001097	0,032986888
RPL10P16	1254,2	-0,51878	-0,53039	0,000896	0,029338273
RPL10P6	126,6	-0,58348	-0,59614	0,000118	0,008948831
RPL10P9	674,6	-0,46935	-0,47877	0,002071	0,046943647
RPL11	7413,8	-0,53357	-0,54577	0,000586	0,023883365
RPL12	9633,4	-0,63128	-0,64904	0,000345	0,017505091
RPL12P12	55,9	-0,68406	-0,71064	0,001656	0,041578557
RPL12P4	253,9	-0,63589	-0,65891	0,001063	0,032284922
RPL12P42	97	-0,57572	-0,5921	0,000908	0,029541708
RPL12P6	80,1	-0,59291	-0,61222	0,002008	0,046126134
RPL13	41444,6	-0,54152	-0,55498	0,000645	0,024999055
RPL13A	29597,9	-0,56537	-0,58026	0,001924	0,045153866
RPL13AP25	1179,6	-0,62087	-0,63862	0,000983	0,030749642
RPL13P12	3693,6	-0,57067	-0,58455	0,000401	0,018715315
RPL18A	32182,2	-0,58209	-0,59773	0,000868	0,028889508
RPL18AP3	1566,3	-0,58903	-0,60554	0,00083	0,028180264
RPL21	21848,9	-0,59613	-0,61133	0,001219	0,03462861
RPL21P11	103	-0,67457	-0,69732	0,001153	0,033592113
RPL21P28	1006,6	-0,64824	-0,66601	0,000471	0,020971493
RPL21P3	27,3	-0,7564	-0,79179	0,00046	0,020696318
RPL21P75	87,2	-0,62979	-0,65174	0,001829	0,044093373
RPL21P93	107,8	-0,64499	-0,66664	0,001659	0,041578557
RPL23A	1543,4	-0,47413	-0,48368	0,000859	0,028763109
RPL24P8	147,3	-0,62743	-0,64644	0,000837	0,028204407
RPL28	4423	-0,54594	-0,55819	0,00041	0,019018057
RPL30	1882,4	-0,64844	-0,65999	1,92E-06	0,000503918
RPL30P4	63,3	-0,69078	-0,71716	0,000392	0,01854025

RPL31	15027,6	-0,61416	-0,63334	0,001182	0,033900569
RPL34	10999,7	-0,64816	-0,66995	0,001403	0,037886076
RPL34P34	218,9	-0,688	-0,71514	0,001546	0,039910935
RPL35A	6379,2	-0,4931	-0,50387	0,001947	0,04558672
RPL37	6228,2	-0,61871	-0,63605	0,000256	0,014614517
RPL3P4	555,5	-0,54045	-0,55698	0,002026	0,046377656
RPL5P17	57	-0,7609	-0,79736	0,000515	0,022155123
RPL5P3	59,6	-0,73734	-0,77641	0,001116	0,033215893
RPL5P4	164,8	-0,65528	-0,67881	0,000821	0,027965878
RPL7	35554,2	-0,58487	-0,59984	0,000263	0,01475864
RPL7AP6	380,8	-0,5072	-0,52048	0,001869	0,044457852
RPL7P1	1096,8	-0,63384	-0,65063	0,000102	0,008304657
RPL7P19	62,7	-0,67051	-0,69692	0,000891	0,029299337
RPL7P26	149,9	-0,62935	-0,6506	0,00054	0,022630496
RPL7P47	107	-0,58976	-0,60708	0,000597	0,024166573
RPL7P6	193,1	-0,63042	-0,65431	0,000571	0,023438115
RPL7P8	71,2	-0,66256	-0,68881	0,000498	0,021700206
RPL7P9	966	-0,57961	-0,59795	0,000614	0,024398847
RPLP1	26373,1	-0,63022	-0,65019	0,000515	0,022155123
RPLP2	7024,6	-0,46402	-0,4724	0,000651	0,02503636
RPS12	8560	-0,64474	-0,66283	0,000388	0,018412173
RPS15A	2612,8	-0,57445	-0,59053	0,001595	0,04065101
RPS18	39599,9	-0,70522	-0,73267	0,001538	0,039902942
RPS18P12	136,4	-0,81298	-0,8521	0,000525	0,022202356
RPS19	33982,5	-0,71397	-0,73369	2,28E-05	0,00286252
RPS19P1	109,6	-0,65774	-0,68068	0,000386	0,018362297
RPS19P3	266,5	-0,70475	-0,72105	9,06E-06	0,001529311
RPS20	9944,3	-0,7193	-0,73665	1,71E-05	0,002491475
RPS20P10	20,9	-0,80574	-0,85481	0,00088	0,029122884
RPS20P14	217,9	-0,8457	-0,87344	1,34E-05	0,002074726
RPS24	6028,2	-0,51988	-0,53345	0,001517	0,039842806
RPS27	9267,8	-0,63182	-0,64811	0,000177	0,011248588
RPS27A	16227	-0,56355	-0,57757	0,001316	0,036220315
RPS27AP16	1198,4	-0,5598	-0,57489	0,00225	0,049163834
RPS28	2623,7	-0,51257	-0,52245	0,000652	0,025041754
RPS28P7	78,1	-0,59819	-0,60944	2,03E-05	0,002746387
RPS29	4470,1	-0,63214	-0,65201	0,001902	0,04502401
RPS3	44144,3	-0,67225	-0,69772	0,001119	0,033232138
RPS3AP26	2406,3	-0,69235	-0,71988	0,002253	0,049163834
RPS3AP49	150,1	-0,79955	-0,83755	0,00087	0,028889508
RPS4X	17408,1	-0,55249	-0,56586	0,000806	0,02773474
RPS4XP13	43,1	-0,59859	-0,62153	0,001724	0,042409155
RPS9	14251,9	-0,56644	-0,58352	0,002297	0,049657504
RUBCNL	168,3	1,21848	1,33645	0,000207	0,012228546
S100A12	1616,4	2,90883	3,59333	6E-15	3,6109E-11
S100A8	10023,3	2,14723	2,68777	2,03E-08	1,72609E-05
S100A9	14944,2	2,04645	2,55621	6,97E-08	4,39786E-05
SAC3D1	395,7	0,92518	1,07168	0,002262	0,049225707
SAMD14	93	1,37909	1,82143	0,000338	0,017242504
SAPCD2	438,7	0,9343	1,06231	0,001322	0,036324778
SCFD2	684,2	0,92279	1,03739	0,001056	0,03214157

SCIMP	315,4	1,80432	2,79213	2,81E-05	0,003357317
SCPEP1	2392,9	0,98004	1,11552	0,001637	0,041331232
SDC1	697,5	2,43037	3,3434	8,03E-08	4,81509E-05
SDC3	2212,3	1,67562	1,90057	0,000275	0,01509638
SEC14L5	50,9	1,85605	4,20543	0,000321	0,016690294
SELENBP1	450,8	1,41365	1,68372	0,000459	0,020689429
SELENOI	631,4	-0,62446	-0,64912	0,002072	0,046943647
SELP	911,7	1,48283	1,86134	0,000176	0,011248588
SERPINF1	207,9	1,27858	1,57375	0,001584	0,040477489
SFRP1	39,5	1,60074	2,19479	0,002289	0,049601266
SGPP1	733,4	1,37673	1,6281	7,53E-06	0,001351583
SH2D4A	18	1,70182	2,51205	0,000117	0,008948831
SHMT1	1403,4	1,01545	1,16439	0,001521	0,039842806
SHPK	60,2	0,94168	1,05496	0,001399	0,037858746
SIAE	424,4	0,77166	0,83972	0,001535	0,039902942
SIGLEC1	612,9	2,10857	3,17955	4,36E-06	0,000863159
SIGLEC11	131,3	2,93569	4,30487	3,53E-10	6,01915E-07
SIGLEC7	233,6	2,49013	4,04121	3,86E-08	2,85548E-05
SIGLEC9	373,8	1,53174	1,89836	0,000321	0,016690294
SIRPB1	653,3	1,53174	2,08407	0,00012	0,008980352
SIT1	33,8	1,6205	2,38327	0,001919	0,045127922
SLAMF6	68,8	1,86219	3,1986	4,77E-05	0,004808278
SLAMF8	108,4	1,60994	2,49093	0,000517	0,022170246
SLC15A3	397,7	1,61695	3,12137	0,000553	0,022922799
SLC1A3	429,1	1,41977	1,61948	0,000789	0,027448636
SLC22A17	249,9	0,75262	0,80458	0,002075	0,046965211
SLC25A36	2618,1	-0,71975	-0,75529	0,000321	0,016690294
SLC25A4	164,5	1,3355	1,58521	0,001081	0,032773713
SLC26A6	328,4	0,636	0,67092	0,00144	0,03847517
SLC27A4	245,1	1,27376	1,48776	2,25E-05	0,002842961
SLC29A1	3246,2	0,63688	0,65663	0,000365	0,017854523
SLC2A10	148,8	1,38429	1,84	0,000256	0,014611445
SLC37A2	598,2	1,45627	1,6797	0,000172	0,011248588
SLC37A4	780	0,71477	0,75211	0,000758	0,026918045
SLC39A14	800,9	0,94949	0,98874	1,2E-06	0,000352658
SLC4A4	52	1,53054	2,56161	0,000655	0,025048504
SLC7A7	514,7	1,37115	1,76766	0,000365	0,017854523
SLC9A9	477,2	1,17483	1,40373	0,001809	0,043851228
SLCO2B1	2708,9	2,11005	2,63139	3,6E-06	0,000747317
SLCO5A1	253	-1,38512	-1,79245	0,000168	0,011110101
SMG1P2	494,4	-0,8027	-0,88422	0,001989	0,045923407
SNHG15	2443	-0,85701	-0,90744	0,00029	0,015670182
SNHG5	2949,9	-0,81678	-0,85135	6,1E-05	0,00580438
SNHG8	1117,1	-0,70582	-0,73327	0,000675	0,025456895
SNORD3A	99,4	-1,43706	-1,61374	1,92E-06	0,000503918
SNORD3B-1	54,6	-0,99143	-1,06446	0,000648	0,024999055
SNORD3B-2	137,6	-1,00696	-1,12505	0,001157	0,033592113
SNX16	350,9	-0,83097	-0,85948	4,32E-05	0,004548727
SORT1	388,3	1,64711	2,91674	0,000358	0,017805818
SPIC	111,8	1,76288	3,54054	0,00053	0,022228217
SPTA1	336	1,06352	1,23836	0,000621	0,024446894

SPX	215,6	1,42557	2,23185	0,002039	0,04657833
SRGAP3	78,5	1,3084	1,5379	1,56E-05	0,002306944
ST6GAL1	1237	1,26611	1,46887	0,000101	0,008279466
STARD3NL	4013,2	-0,64267	-0,66098	0,000398	0,018673014
STEAP4	128,5	2,22425	3,19234	8,28E-07	0,000272809
SULT1C4	141,5	-0,9539	-1,04469	0,000265	0,014769064
SYNE2	221	1,46686	1,65183	0,000116	0,008948831
TADA3	1828,3	0,56213	0,58265	0,001864	0,044428637
TAF11	809,6	-0,52657	-0,53594	0,000172	0,011248588
TANGO2	775,5	0,78895	0,82932	0,001544	0,039910935
TBC1D9	206,9	1,6003	2,54748	0,000627	0,024574539
TCF15	86,7	1,09018	1,45288	0,001627	0,041137785
TCN1	532,2	2,36696	3,14751	3,82E-09	3,9857E-06
TFF3	87,6	1,7334	2,95805	0,00019	0,01162912
TGFBI	1677,4	1,86419	2,45033	3,59E-05	0,003949822
THBS2	63	1,62983	1,77146	0,001765	0,042968188
THRB	61,8	1,94515	2,65445	9E-06	0,001529311
TIMD4	2887,5	1,65468	1,94989	0,000139	0,009805743
TIMP3	2158,2	1,16731	1,45324	0,001155	0,033592113
TLN2	78,1	1,51495	1,85277	3,07E-05	0,003507895
TMEM119	180,4	2,16109	3,55763	4,28E-06	0,000858826
TMEM217	140,3	-0,87893	-1,00711	0,001979	0,045917405
TMEM26	76,7	2,11555	3,26861	1,42E-05	0,00217081
TMEM37	579,4	1,41831	1,80635	0,002132	0,047813391
TMEM38A	55,1	1,77499	2,52658	2,54E-05	0,003092874
TMEM40	214,7	1,53367	2,65205	0,001213	0,0345706
TMEM45A	91,3	1,4767	2,11366	0,00043	0,019693888
TMEM56	131,3	1,7194	2,98196	0,000237	0,013707835
TMTC1	68,9	1,51784	2,59621	0,002301	0,049657504
TNC	450,2	1,54313	1,75859	0,001413	0,038029861
TOP2A	2509,8	1,17478	1,51631	0,001138	0,033475788
TPCN1	1128,2	0,65355	0,69048	0,002005	0,046107364
TRAP1	1238,3	0,66247	0,69287	0,000702	0,025837029
TRAPPC12	892,9	0,74877	0,79326	0,000634	0,024728887
TRAPPC3L	46	2,22554	3,06922	2,02E-05	0,002746387
TRBVB	74,3	-1,51438	-2,18764	0,00095	0,030663905
TREML1	823,4	1,50463	2,13702	0,00056	0,023156895
TRIM10	88,3	1,59399	2,89307	0,002112	0,047538625
TRIM58	2341,8	0,90146	0,96085	0,000773	0,027259193
TRPM4	186,8	1,45929	1,8827	0,000396	0,018636953
TSPAN17	1250,2	0,83214	0,86848	8,31E-05	0,007378488
TTC13	341,9	0,83128	0,87069	0,000119	0,008948831
TUBA4A	2421,3	1,13981	1,23022	0,00026	0,014693231
TUBA4B	27,2	1,12578	1,24187	0,001738	0,042541709
TUBB1	4424	2,02757	2,57838	2,35E-06	0,000597562
TUBG1	1060,7	0,7544	0,7912	0,000522	0,022170246
TWISTNB	2062,9	-0,50588	-0,52016	0,002276	0,049401759
TXNDC5	296,6	0,61294	0,62943	0,0008	0,027612451
UACA	279,8	1,06359	1,13764	0,001095	0,032986888
UBE2V1	122,2	-0,84014	-0,88144	0,000308	0,016306821
UNC13D	5194,2	0,60008	0,62754	0,001825	0,044047945

UTP20	312,8	0,7416	0,7921	0,001009	0,0311938
VCAM1	9305,6	2,41302	3,18019	9,22E-08	5,06768E-05
VCAN	1567,1	1,48167	2,03202	0,000364	0,017854523
VNN1	309,4	1,36411	2,16832	0,001286	0,035688261
VNN2	482,3	1,53802	2,28751	0,000162	0,010856983
VNN3	38,1	1,78997	3,9243	0,000265	0,014769064
VPS16	788,8	0,59638	0,61617	0,000332	0,017095338
VPS26B	1973,8	0,428	0,43456	0,000614	0,024398847
VSIG2	89,2	1,4128	1,64649	0,000811	0,027766604
VSIG4	2209,2	1,79533	2,12836	2,89E-05	0,003397523
WASHC1	112,8	-0,59333	-0,61514	0,002248	0,049163834
WDR33	2373,2	-0,37031	-0,37402	0,00074	0,026484786
WDR34	1540,4	0,7477	0,79585	0,000699	0,025792662
WDR77	671	0,62436	0,65219	0,001958	0,045712897
WLS	87,3	2,19953	3,5193	1,48E-06	0,000426395
XPO5	798,7	0,93408	1,05037	0,000963	0,030683161
YAF2	440,3	-0,66078	-0,67538	1,87E-05	0,002606661
YTHDF3-AS1	67,6	-0,71907	-0,74864	0,000338	0,017242504
YWHAG	427,6	-0,44892	-0,4578	0,001297	0,035935199
ZCRB1	1630,3	-0,35668	-0,35994	0,000368	0,0178889
ZMYM5	1380,6	-0,71201	-0,73758	0,000126	0,009208804
ZMYND11	1196,9	0,58155	0,60043	0,000496	0,021685871
ZNF131	2318,8	-0,47201	-0,48173	0,001152	0,033592113
ZNF195	1171,6	-0,5145	-0,52473	0,000561	0,023167988
ZNF292	2135,3	-0,66961	-0,69926	0,00047	0,020971493
ZNF326	1576,3	-0,57941	-0,5964	0,001042	0,031773319
ZNF669	486,5	-0,56762	-0,58867	0,00205	0,046638014
ZNF684	201	-0,65373	-0,67546	0,000679	0,025473252
ZNF791	966,7	-0,43888	-0,44857	0,002236	0,04910934

Supplementary table 5. Deregulated genes in pretreated samples from MDS/AML patients vs healthy control samples comparation.

gene	baseMean	log2FC	log2FCunshrunk	pvalue	padj
CD19	812,647254	-3,726638394	-4,472151083	7,74E-06	0,000993351
CD44	29658,99343	1,100740364	3,069770521	0,002142233	0,039048507
CD79A	3940,035254	-3,688670707	-4,904751069	9,35E-07	0,000220647
CD79B	5761,280874	-2,854327208	-4,571571518	4,84E-06	0,000730557
CDC25B	847,0188648	-1,599185039	-2,983019585	0,002854197	0,046542464
E2F2	2398,587894	-2,913223502	-4,873496833	1,10E-06	0,000246378
ESPL1	605,346242	-1,7794973	-3,635970703	0,000276936	0,010930798
GAB1	877,2768817	-1,551358469	-3,030310473	0,002443025	0,042326054
LEF1	1908,727291	-3,766183843	-3,275376085	0,001055214	0,024829223
PPP2R2C	48,3349828	-9,432422993	-8,843487615	9,28E-19	9,52E-15
TLE1	2877,793958	-3,31229033	-4,485480808	7,27E-06	0,000961264
TOP2B	15113,66721	-1,330662192	-3,280547601	0,001036058	0,02454952
07-mar	10470,72294	0,770693926	3,04655502	0,002314801	0,041194093
01-sep	1183,76395	-1,555391875	-2,989202983	0,002797062	0,045951527
09-sep	12152,34752	-1,261179784	-3,055335496	0,002248089	0,040451147
01-dic	2,147482365	-5,151023801	-3,051413899	0,002277664	0,040863887
AAGAB	2939,213029	0,640145549	3,729046573	0,000192206	0,008831428
ABCA12	9,127309227	-2,577472289	-2,952871679	0,003148328	0,048805426
ABCA7	1448,968782	-1,400874113	-3,612620959	0,000303118	0,011506884
ABCC8	6,780121988	-4,407693016	-4,316514691	1,59E-05	0,0016213
ABCD4	2604,228085	-0,841262466	-3,200117201	0,001373717	0,029492768
ABHD12B	450,1961279	2,886926323	3,198828279	0,001379873	0,029563101
ABHD17C	6680,070408	2,636495764	3,417277143	0,000632509	0,018064045
ABI3BP	125,2689967	-3,397576439	-3,846564492	0,000119786	0,00642422
ABLIM1	3793,017995	-1,27735022	-2,962269577	0,003053803	0,048133648
ABRAXAS1	437,9473811	0,886958543	3,343634588	0,000826886	0,021300931
ABRAXAS2	1725,979059	0,936015062	3,07254497	0,002122419	0,038860958
ABT1	5393,080462	0,883952342	3,036527725	0,002393201	0,04186334
ABTB1	4464,807509	-1,664408076	-4,260687027	2,04E-05	0,001948563
AC000089.1	219,264451	1,024628556	3,218879587	0,001286925	0,028413608
AC002101.1	4,227329761	-6,127070379	-4,792616352	1,65E-06	0,000349529
AC002350.1	91,47802418	1,269987209	3,064238288	0,00218225	0,039593837
AC003070.1	21,25701571	-2,562456026	-3,680190148	0,00023306	0,009856073
AC004024.1	2,186784002	-2,890199725	-3,073408057	0,002116289	0,038800482
AC004453.1	1166,252475	1,252994602	3,058056907	0,002227773	0,040226649
AC004585.1	5,906313253	-6,605617288	-3,422929381	0,000619502	0,017817457
AC004890.1	87,28403603	1,09985082	3,060331586	0,002210921	0,040016234
AC005000.1	151,1534333	0,592064603	3,115448439	0,001836655	0,035309496
AC005104.2	2,397969633	-4,101709155	-3,217426322	0,001293462	0,028413608
AC005162.3	2,599848605	-4,974162129	-3,416243304	0,000634915	0,018078505
AC005332.3	65,04370735	-5,242956416	-3,721860991	0,00019776	0,008904736
AC005332.6	34,78778319	-2,084107918	-3,314393464	0,000918422	0,022741615
AC005342.2	8,364322024	3,63665463	3,54972779	0,00038563	0,01326523
AC005736.1	2,778838695	-3,640468757	-3,037138176	0,002388359	0,04186334
AC005865.2	3,56584167	-4,711523599	-3,668824807	0,000243668	0,010136501
AC005912.1	588,1549667	1,01087294	2,964419921	0,003032542	0,048133648

AC005921.3	127,6928577	-1,907195944	-4,318780146	1,57E-05	0,0016213
AC006122.1	59,34089637	1,087236562	3,036643515	0,002392282	0,04186334
AC006511.3	943,7664212	1,061150628	3,136287275	0,001711015	0,03370251
AC007014.2	68,23291447	-1,755253487	-3,464752732	0,000530719	0,016081941
AC007038.1	26,73306772	-1,989084054	-2,973627251	0,002943023	0,047387263
AC007161.1	17,58834928	1,476336335	4,587668144	4,48E-06	0,00069903
AC007163.1	7,023048691	-3,799216643	-4,853618032	1,21E-06	0,000268509
AC007182.2	124,9491407	1,128027564	3,961917378	7,44E-05	0,004661959
AC007278.1	4,465197921	-5,299898697	-3,907535141	9,32E-05	0,005488827
AC007278.2	2,210981029	-3,920022166	-2,99771005	0,002720163	0,045341456
AC007342.5	3,486947184	-5,172668297	-3,846160203	0,000119983	0,00642422
AC007387.1	34,73344939	1,206303257	3,145296492	0,001659186	0,032934465
AC007683.1	143,773201	0,855062018	3,207666744	0,001338165	0,029012728
AC007688.1	511,3528676	1,674928208	3,879778989	0,000104551	0,005961617
AC007998.3	18,47448546	-3,607621775	-4,138698403	3,49E-05	0,002844798
AC008060.1	5,736224094	-6,56410818	-4,366031078	1,27E-05	0,001426853
AC008074.3	121,2469764	1,28910668	3,543746799	0,000394484	0,013390271
AC008083.2	2,275071233	-4,281097026	-3,046886479	0,00231225	0,041189154
AC008429.2	116,5196837	1,390013341	4,011165291	6,04E-05	0,00403502
AC008696.2	50,8238196	-4,735770285	-3,449039161	0,000562585	0,016622176
AC008802.1	233,9049443	1,726938465	3,527824617	0,00041899	0,013975552
AC008957.3	1,944016955	-5,006871422	-3,042301781	0,002347764	0,04146908
AC009053.1	372,5448047	-0,978708613	-3,322894156	0,000890887	0,022307666
AC009245.1	413,9582698	0,900402045	3,525310322	0,000422987	0,014032866
AC009413.1	34,43899649	1,575988405	3,56836086	0,000359222	0,012624833
AC009533.1	613,6355157	-1,696764717	-4,274641668	1,91E-05	0,001883072
AC009533.2	1,530882589	-4,174861104	-3,358593625	0,000783402	0,020672644
AC010343.1	281,4825677	1,17727526	3,722248541	0,000197457	0,008904736
AC010468.1	935,7064553	1,769523357	3,606269448	0,000310631	0,011705488
AC010889.1	7,154409812	6,257579004	3,230309848	0,001236561	0,027768061
AC011495.1	481,9172787	1,083486281	3,079396979	0,002074201	0,038330387
AC011773.1	71,77123931	-2,33579582	-4,023376864	5,74E-05	0,003873328
AC011933.1	206,7889711	1,438044228	4,66971676	3,02E-06	0,000523606
AC011979.1	120,6367117	1,277454773	3,10677788	0,001891385	0,035928976
AC012370.2	1,804763693	-4,636697763	-3,71567626	0,000202661	0,009003351
AC012409.5	3,065021059	-4,484032437	-3,317232927	0,000909138	0,022649273
AC012651.1	11,84630281	-3,847865139	-3,810259212	0,000138821	0,007123145
AC012676.5	60,90158668	-2,174024304	-3,005352447	0,002652733	0,044677069
AC015660.5	13,81627589	-4,977905607	-3,85982552	0,000113468	0,006257814
AC015849.6	134,5598927	1,667049932	3,612699216	0,000303026	0,011506884
AC015911.1	241,5502467	1,417024404	3,100338082	0,001932999	0,036465215
AC015914.1	2,320348965	-5,018196792	-4,074098518	4,62E-05	0,003405469
AC016168.1	38,63995379	-7,930272614	-5,698073092	1,21E-08	7,31E-06
AC016168.2	43,85726552	-5,626154353	-4,674693759	2,94E-06	0,000523606
AC016168.3	17,92127072	-3,83645549	-3,108431887	0,00188083	0,035832371
AC016700.2	637,6797697	1,689101591	3,71588075	0,000202497	0,009003351
AC018475.1	304,7210591	1,187393219	3,280677815	0,00103558	0,02454952
AC018868.1	117,0523829	1,336529353	4,671513197	2,99E-06	0,000523606
AC019084.1	1,784972485	-4,337718501	-3,578892591	0,000345053	0,012380302
AC020634.1	4,121990626	-4,592853583	-3,125719913	0,001773704	0,034495909
AC020898.1	1448,575691	1,775005275	3,540722147	0,000399034	0,013500051

AC021087.4	29,06869109	-7,038122028	-5,032553454	4,84E-07	0,00013771
AC021188.1	207,934092	-1,462514085	-2,942836526	0,003252201	0,049937912
AC022034.3	24,56800518	2,063179511	4,539446286	5,64E-06	0,000797969
AC022210.1	530,6223077	1,098240949	3,578625662	0,000345406	0,012380302
AC022905.1	1,760041098	-4,595768859	-3,593215087	0,000326623	0,01201402
AC022968.1	347,1922969	0,972916805	2,968920419	0,00298848	0,047845204
AC023232.1	55,72018905	0,906639897	4,055420908	5,00E-05	0,0035344
AC023389.1	22,92045153	-2,217340177	-4,092430499	4,27E-05	0,003229043
AC024075.2	65,53182761	-1,431477241	-3,006347981	0,002644062	0,044604243
AC024560.1	9,94003671	-6,930531668	-3,94597909	7,95E-05	0,004854728
AC024560.2	36,76084126	-3,191798074	-4,320912228	1,55E-05	0,0016213
AC024940.3	546,8036505	1,264253647	3,284108517	0,001023055	0,024377273
AC025048.1	6,400495554	6,090371997	3,403866725	0,000664392	0,018474259
AC025280.2	4,024981448	-5,158219758	-3,132207004	0,001734975	0,03404377
AC025437.2	5,833394425	-6,589272787	-3,477455574	0,000506197	0,015571261
AC025437.4	16,16061122	-7,63444465	-5,382931991	7,33E-08	3,42E-05
AC025470.2	4,061991018	-6,067106836	-4,249704966	2,14E-05	0,002027209
AC026362.2	46,38715516	-3,014876189	-3,073514702	0,002115533	0,038800482
AC026403.1	1096,855702	0,965703073	3,671897007	0,000240757	0,010070893
AC044787.1	128,5355615	0,958197958	2,987358085	0,002813999	0,046180485
AC066616.2	2,347163968	-5,271394959	-3,020145976	0,002526529	0,043354483
AC068134.3	3,728252558	-3,194763257	-3,533175331	0,0004106	0,013781003
AC068580.3	43,88857609	-3,375866074	-3,909412008	9,25E-05	0,005467266
AC068896.1	40,66800555	-4,61807942	-3,208061619	0,001336329	0,02899334
AC068993.1	37,85252683	1,843051998	5,674310985	1,39E-08	8,24E-06
AC069304.2	1,92454062	-4,990919041	-3,001239565	0,002688829	0,045087685
AC073861.1	4853,816426	1,631429199	3,553043897	0,000380801	0,013175464
AC074212.1	5,001941813	-3,25488153	-3,070581831	0,002136421	0,039011865
AC078883.4	10,74457208	4,548294585	3,079421506	0,00207403	0,038330387
AC079250.1	2535,253132	1,131403151	3,290789842	0,000999065	0,023991099
AC079331.2	6,383761087	-5,129243047	-2,962810285	0,003048444	0,048133648
AC079922.1	186,391276	1,806383208	4,944738006	7,62E-07	0,000189306
AC079944.1	9,920040097	2,242612004	2,963180838	0,003044776	0,048133648
AC080128.1	1,791022692	-4,385100485	-3,568774851	0,000358654	0,012624833
AC083873.1	100,9740224	0,616242705	3,620474249	0,000294064	0,011337574
AC084033.3	2459,670236	1,786787164	3,652120433	0,000260084	0,010475737
AC087343.1	266,1683679	1,354740838	3,666690055	0,00024571	0,010158533
AC087481.1	42,7572546	1,901169082	4,497559133	6,87E-06	0,00091268
AC087741.1	15,8360168	-3,660434731	-3,146401504	0,001652929	0,032869772
AC087749.2	49,24983206	-1,995804112	-3,328701194	0,00087252	0,022005642
AC087752.3	71,09654426	-2,192941072	-3,643874923	0,000268564	0,01069635
AC090013.1	78,57918714	1,196952744	3,215896068	0,001300379	0,028413608
AC090403.1	2,403722916	-5,302841251	-4,656441998	3,22E-06	0,000544221
AC090498.1	159,5292814	1,327265833	3,716145799	0,000202285	0,009003351
AC090602.1	97,05808714	1,320360383	3,302330032	0,000958852	0,023354565
AC090844.1	12,01249477	2,002390542	2,968105644	0,002996413	0,047922377
AC091393.1	4,670369307	-4,283159287	-3,138411295	0,001698663	0,033502082
AC092106.1	30,59684509	0,836867578	3,372488591	0,000744922	0,019977269
AC092140.1	3,960476929	-3,149607072	-3,118328311	0,001818801	0,035084849
AC092155.2	213,268914	1,570890454	3,940975713	8,12E-05	0,004942054
AC092368.3	62,5673229	-1,974525509	-4,201949562	2,65E-05	0,002334763

AC092431.2	55,33455411	1,322521402	3,568622269	0,000358863	0,012624833
AC092597.1	695,6870629	1,171715724	3,315870229	0,000913582	0,02268263
AC092746.1	8,413347483	-5,232559421	-3,348696574	0,000811927	0,021023368
AC092798.1	34,95816761	-2,514646383	-3,083876892	0,002043221	0,037962977
AC092865.1	65,54096148	1,203714618	3,525543769	0,000422614	0,014032866
AC093155.1	10,31936223	1,739882161	3,14389578	0,001667148	0,033049895
AC093157.2	20,93301004	1,639658305	3,394319841	0,000687993	0,018898261
AC093668.2	4,209845056	-2,585499471	-3,57235541	0,000353785	0,01251951
AC096541.1	2,924411853	-5,594606181	-3,095810744	0,001962756	0,036845955
AC096582.3	3,298467831	-5,763635825	-3,494355334	0,000475208	0,014974648
AC096921.1	2,988136203	-4,923932474	-3,046764885	0,002313186	0,041189154
AC097381.1	3,428504578	-5,358098266	-3,544568198	0,000393257	0,013363351
AC097523.1	169,753686	1,269520657	3,599374287	0,000318984	0,011837812
AC097638.1	95,43293514	1,189535091	3,603404268	0,000314076	0,011748623
AC097713.2	13,61137756	2,121744413	4,096541076	4,19E-05	0,00320122
AC099340.1	77,22843596	1,21195914	3,070140089	0,002139584	0,039031587
AC099791.2	15,04014765	-2,246633001	-3,161434965	0,001569939	0,031735852
AC102953.2	5,000485692	-3,333041517	-3,183505775	0,001455032	0,030329095
AC104297.1	25,71233506	1,202714261	3,17171688	0,001515407	0,031061801
AC104563.1	1110,967719	0,937239728	3,146805609	0,001650647	0,032869772
AC104619.3	330,5691943	1,087527983	3,073396873	0,002116368	0,038800482
AC104843.1	147,407328	1,294619803	4,295392526	1,74E-05	0,001747111
AC105219.1	3,636168885	-4,956942318	-5,077864952	3,82E-07	0,0001165
AC105250.1	494,2901314	1,470161853	3,687751381	0,000226245	0,009634012
AC105285.1	268,7199426	-2,083185239	-4,363342928	1,28E-05	0,001428806
AC106782.5	11,29670348	-1,962612804	-4,070278356	4,70E-05	0,003437056
AC106872.2	423,1393383	1,262994159	3,192718262	0,001409404	0,02986326
AC106872.7	56,01503535	1,382178323	3,12051421	0,001805356	0,034927814
AC107032.1	295,9227902	1,317724373	3,60745126	0,00030922	0,011666598
AC107075.1	133,182112	1,326121143	3,827445228	0,00012948	0,006745019
AC107464.1	1,682223203	-4,269972979	-3,723103696	0,000196789	0,008904736
AC107954.1	104,1129776	1,518194796	2,948679978	0,003191343	0,049199731
AC107956.1	72,06646464	1,175540728	3,709986911	0,00020727	0,009093353
AC108134.1	5,246355504	-6,435199488	-3,327613713	0,000875932	0,022050146
AC108941.2	5,807759447	4,961009067	3,620320325	0,000294239	0,011337574
AC110994.2	321,8619734	0,886972125	3,043685008	0,002336997	0,041397655
AC112198.2	5,289120407	-5,777851863	-2,959830533	0,003078083	0,048329591
AC112206.2	4,818028843	-6,310761304	-3,045754897	0,00232097	0,041256171
AC112255.1	5,711756238	-6,559605254	-3,527052205	0,000420214	0,014001218
AC112482.1	4,126473985	-5,201717218	-4,058807438	4,93E-05	0,003507014
AC112722.1	1,779855589	-4,627032226	-3,715267788	0,000202989	0,009004914
AC114728.1	209,2472729	1,091550181	2,959642956	0,003079958	0,048329591
AC114730.1	34,21873977	2,291531116	3,023083636	0,002502131	0,043054293
AC114752.2	20,25787832	-5,699122287	-4,549183172	5,39E-06	0,000774776
AC116096.1	2,835323351	-5,544877856	-3,365024109	0,00076537	0,020383596
AC116533.1	747,8165531	1,088929474	3,510074504	0,000447981	0,014457019
AC118549.1	2728,276333	0,701337217	3,263543048	0,001100285	0,025488686
AC119396.1	395,5320988	-1,722349605	-3,047742741	0,002305672	0,041189154
AC119674.1	3,776651167	-3,449411247	-3,186921606	0,001437957	0,030156945
AC120042.3	2,768423899	-5,515067538	-3,666574289	0,000245822	0,010158533
AC124248.1	177,2408278	1,346010761	3,375354491	0,000737207	0,019909106

AC124856.1	4,347413399	-3,407229836	-3,558450013	0,00037305	0,013021636
AC126696.3	3,989263595	3,948587434	3,110583149	0,001867183	0,035682786
AC126755.1	615,7843605	-1,357919096	-3,314838163	0,000916962	0,022732677
AC130324.1	11,0493129	-2,667360489	-3,403421979	0,000665474	0,018474259
AC131097.3	66,88794562	4,674271615	3,403563742	0,000665129	0,018474259
AC131097.4	929,8768127	4,331589347	4,391515079	1,13E-05	0,001312687
AC131235.1	1348,021775	1,250378126	3,298143797	0,000973263	0,023612168
AC132008.2	597,560993	-0,736268978	-3,354372755	0,000795451	0,020806762
AC133134.1	199,4783592	1,587065533	4,075993285	4,58E-05	0,003399058
AC133435.1	253,060859	1,062256136	3,76799079	0,000164567	0,00800251
AC134043.2	54,00651824	-3,706585168	-3,014657959	0,002572692	0,043881147
AC135068.6	41,77315761	1,499540167	4,264471638	2,00E-05	0,001936052
AC135983.1	12,67997373	1,444263774	2,97106248	0,002967714	0,047636606
AC136424.2	7,998736545	-7,044712547	-3,826529786	0,000129962	0,006758705
AC136428.4	4,422676952	-4,00831535	-3,224538756	0,001261758	0,028088023
AC136475.10	14,23086722	-3,080638391	-4,048551384	5,15E-05	0,003614185
AC137932.2	95,58850433	-3,939028916	-3,725074342	0,000195258	0,008879465
AC138305.3	16,45047499	1,393643385	3,026484648	0,002474154	0,042697183
AC138649.2	26,88282789	-4,54974812	-3,604937618	0,000312228	0,011708357
AC138866.1	98,19865094	-1,01107766	-3,214213394	0,001308024	0,028560385
AC138932.1	623,4008781	-1,61920757	-4,044934622	5,23E-05	0,003620947
AC138951.1	71,84875605	-2,91208624	-4,600693289	4,21E-06	0,000670954
AC138969.2	188,2479698	-1,401601088	-3,187390338	0,001435629	0,030156945
AC139099.3	7,079003617	4,822559803	3,855355453	0,000115562	0,006319351
AC139495.3	91,18529808	-2,071888507	-3,045243721	0,002324918	0,041293621
AC139713.2	98,36648638	-2,66550913	-3,726450449	0,000194195	0,008845802
AC141557.2	11,50776979	-4,057025267	-3,937970163	8,22E-05	0,00498617
AC141930.1	13,56909507	-5,716632751	-3,128216424	0,001758706	0,034273506
AC144530.1	184,0614775	1,093497823	3,218208227	0,001289941	0,028413608
AC145285.1	24,57571463	1,448091882	2,955967624	0,003116898	0,048538159
AC147651.1	94,1534768	-4,002648624	-3,310818835	0,000930234	0,022911294
AC148476.1	31,25521713	5,193460007	4,299068518	1,72E-05	0,001729732
AC226118.1	3,056470166	-5,658296432	-3,231514105	0,001231362	0,027757645
AC233702.1	4,367086241	2,477061821	3,419849182	0,000626559	0,017960764
AC234778.1	15,93308162	1,353195757	3,228988293	0,00124229	0,027852705
AC234782.3	4,379596133	-4,796067839	-4,759147736	1,94E-06	0,000396382
AC234782.4	1,762243487	-4,365676724	-3,218136639	0,001290263	0,028413608
AC240504.1	3,141713876	4,009834899	3,655684871	0,000256496	0,010390462
AC241584.1	112,342279	1,379876988	3,42309556	0,000619123	0,017817457
AC244669.2	9,203133381	3,382235614	2,966836204	0,003008812	0,04800371
AC245060.2	160,0962595	-2,31674385	-3,870784006	0,000108486	0,006117134
AC245060.6	68,99778836	-3,705506357	-4,060608928	4,89E-05	0,00349621
AC245128.3	675,3680973	-3,139900188	-3,730624661	0,000191006	0,008803128
AC246787.1	542,8104442	1,264343262	3,96793326	7,25E-05	0,004564448
ACACB	425,2432166	-2,051160655	-3,174835079	0,001499217	0,030853201
ACCSL	6,53718371	-5,905958636	-3,066368351	0,002166762	0,03936122
ACP5	882,0654378	-2,039813358	-3,082257227	0,002054372	0,038101181
ACTG1P22	5,349939553	-6,248298337	-4,581760877	4,61E-06	0,000713325
ADAM19	189,902253	-3,057877654	-3,454158496	0,000552013	0,016435996
ADAM29	3,103667003	-5,674693411	-3,638974652	0,000273726	0,010870835
ADAMTS2	251,6899434	-4,13174993	-4,047497467	5,18E-05	0,003620947

ADAMTS8	4,858168308	-6,320902021	-4,887408485	1,02E-06	0,000234744
ADAMTS9	48,60369729	-3,259375984	-2,943033405	0,003250133	0,049931067
ADAP2	378,5381386	-2,764170225	-2,984282259	0,002842444	0,046436606
ADCY3	2123,480388	-0,750244332	-3,672233987	0,000240439	0,010070893
ADM	2306,830519	-2,112564664	-3,349815994	0,000808653	0,021007294
ADPGK	9271,832682	0,609329396	2,966850572	0,003008671	0,04800371
ADTRP	35,00358106	-5,029595565	-3,133988875	0,001724474	0,033919645
AF279873.1	96,01151046	1,446581295	4,371832379	1,23E-05	0,001396121
AFTPH	3333,249635	1,129210249	5,120462329	3,05E-07	9,98E-05
AGFG2	410,0771784	-1,791867905	-4,068408748	4,73E-05	0,003437056
AGMO	8,099479388	-3,761367695	-3,322551839	0,000891981	0,022308219
AGXT	12,89797531	6,133061432	3,100387922	0,001932673	0,036465215
AHDC1	590,4311844	-1,629685844	-3,796900146	0,000146517	0,007381834
AHSA2P	1913,162514	-1,49747162	-3,117268313	0,001825354	0,035189205
AIRE	274,1552148	-5,47125584	-3,370119264	0,000751357	0,020086369
AK1	110,6015601	-1,96115388	-3,477562638	0,000505995	0,015571261
AKR1C2	118,0915853	-2,887333535	-3,739704118	0,000184237	0,008568133
AL008707.1	3,592341619	-5,440581159	-2,955062753	0,003126055	0,048582455
AL020997.1	2,831524089	-3,267990948	-3,719991218	0,00019923	0,008941232
AL021408.2	7,496113596	-5,140876589	-3,785395004	0,000153465	0,007591029
AL022324.2	154,8586492	-1,57440495	-3,024364265	0,002491562	0,04297352
AL023802.1	7,813674873	-5,284606859	-4,007161434	6,15E-05	0,004095128
AL024507.2	67,58821068	-1,593820134	-2,963882108	0,003037846	0,048133648
AL031428.1	27,69646583	-1,972724896	-3,314243994	0,000918913	0,022741615
AL031666.2	6,161836273	-3,404746736	-3,204559552	0,001352693	0,029242937
AL031727.1	185,546768	1,754844055	3,210203703	0,001326409	0,028818748
AL031985.2	70,84005942	1,318432614	3,401723958	0,000669622	0,018539266
AL033519.2	349,5662655	1,148221829	2,958455411	0,00309185	0,04836992
AL034376.1	11,55719999	-7,576109732	-4,062591378	4,85E-05	0,003482802
AL035398.1	25,2510233	1,202909636	3,351273975	0,000804407	0,020934295
AL035448.1	53,12533646	-2,367796065	-3,303391167	0,00095523	0,023321712
AL035696.3	22,80824933	-5,043567485	-4,399589234	1,08E-05	0,001269595
AL049873.1	786,2906553	1,373864412	3,633133341	0,00028	0,010995366
AL078644.1	1,535725991	-4,663565241	-3,751154639	0,000176022	0,008331944
AL109766.1	170,9438785	0,813131109	4,174730041	2,98E-05	0,002558491
AL109840.2	17,94162698	1,496316279	3,122767493	0,001791592	0,034734099
AL117190.1	29,40111709	6,541708867	3,516456485	0,000437348	0,014308867
AL118508.1	121,7953977	4,590379728	3,758191744	0,000171146	0,008245795
AL121769.1	46,57754318	0,967763682	3,471226554	0,000518087	0,01577679
AL121787.1	13,70428487	-4,491528406	-3,975693459	7,02E-05	0,004473005
AL121950.1	4,856918258	-6,322601221	-3,029273537	0,002451426	0,042431274
AL122020.1	182,8408	1,709032241	3,59396283	0,000325686	0,012008269
AL133260.1	300,7514119	1,328271651	2,966073687	0,003016282	0,048041088
AL133284.1	2,095008827	-4,618979657	-3,158580678	0,001585394	0,03200625
AL133346.1	16,92178066	-4,485943743	-3,353477418	0,000798029	0,020821124
AL135818.2	2,158970971	-5,152263852	-2,978180311	0,002899653	0,046960353
AL136084.2	1,979422277	-3,98497555	-3,2060684	0,00134562	0,029124518
AL136088.1	18,10404705	-4,638382465	-3,25346453	0,00114007	0,02609615
AL136126.1	44,41395624	0,977725698	3,230537657	0,001235576	0,027766195
AL136320.1	54,06230398	-1,921805225	-3,827536039	0,000129432	0,006745019
AL136380.1	187,2917884	0,921839855	3,379015164	0,00072746	0,019697722

AL136968.2	139,5929882	1,619758108	3,772244594	0,000161786	0,007918746
AL136988.2	2,936522301	-4,500291766	-3,314803734	0,000917075	0,022732677
AL137792.1	16,96141134	1,493649332	3,272016392	0,001067834	0,025038386
AL139039.2	130,1289353	1,394099605	3,645011086	0,00026738	0,010692391
AL139095.2	1240,606327	1,305154326	3,37003014	0,0007516	0,020086369
AL139100.1	231,9528596	1,20665766	2,949311011	0,003184833	0,049123974
AL139349.1	2,766654201	-3,192168632	-3,003902635	0,002665406	0,044792499
AL139423.1	13,97284625	3,575177628	3,490902058	0,000481393	0,015113208
AL158823.1	111,8293957	1,235127991	3,090209417	0,002000154	0,037343084
AL161781.2	1,881217034	-4,957891335	-4,181392581	2,90E-05	0,00249159
AL161787.1	172,7583083	1,40388565	3,038178796	0,002380127	0,041800894
AL161909.1	2146,529414	1,483391408	3,408099851	0,00065417	0,018392618
AL161912.2	7,931141577	-7,032737519	-3,847422682	0,000119367	0,006423385
AL161912.3	2,219323501	-5,195204292	-3,197015646	0,001388574	0,029625798
AL162578.1	47,59604219	-1,610009734	-3,548375011	0,000387616	0,01328901
AL162632.1	1,576686208	-3,930239603	-2,947674875	0,003201736	0,049310579
AL353801.3	10,76599595	-1,343349734	-3,108955976	0,001877497	0,03579102
AL354702.1	809,0227259	1,207460361	3,228814559	0,001243045	0,027852705
AL354868.1	147,2869371	1,35911896	3,569675565	0,000357424	0,012619267
AL354893.1	2,111468479	-5,126106894	-3,121407148	0,00179989	0,034851077
AL355032.1	253,2609298	1,226602305	2,980995278	0,002873132	0,046720729
AL355073.1	9,093942772	-3,767179586	-2,961898458	0,003057486	0,048148758
AL355312.3	10,96602999	-2,303782056	-4,086146341	4,39E-05	0,003309581
AL355472.2	115,5101381	0,918011357	3,5153029	0,000439253	0,014323697
AL355480.2	8,96678252	-2,379208887	-2,996537164	0,00273065	0,045442436
AL355802.1	554,9198452	0,952793584	3,03945948	0,002370031	0,041718776
AL356056.3	42,73543249	1,794018455	3,625591334	0,000288301	0,011235344
AL356512.1	104,7500894	-1,266786009	-3,066435567	0,002166275	0,03936122
AL356535.1	47,07493453	1,348291819	3,449555751	0,00056151	0,016622176
AL357060.1	516,1146974	-1,926885376	-4,261847674	2,03E-05	0,001948563
AL359399.1	4,632424259	-3,907035818	-2,9814452	0,002868914	0,046720729
AL359475.1	3,822912003	-5,977638254	-3,784759616	0,000153857	0,007591029
AL365356.1	6,90360466	-2,192440338	-3,074163508	0,002110937	0,038800482
AL365440.1	25,37435365	1,047637401	4,120553632	3,78E-05	0,002988836
AL390719.1	877,6746579	3,598811993	3,575880571	0,000349051	0,012426922
AL391335.1	5,682926838	-2,093624813	-2,980877801	0,002874235	0,046720729
AL391839.2	93,89789792	-1,300448798	-3,098712389	0,001943636	0,036621005
AL451048.1	5,626496276	-5,665200651	-3,662945979	0,000249331	0,010288876
AL512306.3	22,32500167	-7,092453964	-7,085634512	1,38E-12	3,28E-09
AL512378.1	3,941485602	-4,604431757	-3,059879687	0,002214259	0,040053113
AL512631.1	9,610363954	-3,982641002	-3,349141623	0,000810623	0,021007294
AL512631.2	62,93823868	-1,685135578	-3,043247082	0,002340401	0,041410299
AL513190.1	23,07390853	-5,05360966	-3,013355816	0,002583758	0,04397106
AL513493.1	56,37022829	-5,161296438	-3,056285555	0,002240977	0,040393083
AL583805.1	104,722701	1,193734985	3,25210186	0,00114555	0,026202107
AL590135.1	34,78433687	2,06948748	4,613809019	3,95E-06	0,000640622
AL590226.1	325,0429856	1,449595097	3,478506546	0,000504216	0,015554411
AL590867.2	3253,665501	1,447780571	3,04685658	0,00231248	0,041189154
AL590999.1	3,712305008	-5,933871824	-4,352693522	1,34E-05	0,001462649
AL591368.1	1,66467244	-4,515042171	-3,691292741	0,000223117	0,009541117
AL592114.1	326,1897073	1,152023486	2,96932454	0,002984552	0,04781658

AL592295.1	92,11023809	1,068870716	3,080777341	0,00206461	0,038267996
AL596275.1	108,9266455	1,028077837	3,50611561	0,000454698	0,01458206
AL662907.2	41,26170299	-2,646227947	-3,076695749	0,002093088	0,038633038
AL663070.1	184,5138577	1,082283981	3,465427214	0,00052939	0,016057462
AL669831.1	138,5182665	-0,945123002	-3,417488024	0,000632019	0,018064045
AL714022.1	22,66152998	1,953859587	2,950288998	0,003174768	0,049067062
AL731567.1	6,028495622	-6,632313049	-5,716767694	1,09E-08	6,69E-06
AL732372.2	33,1858933	-1,533792017	-3,546360372	0,000390592	0,013316883
ALAS1	3893,888182	1,198132989	4,184782483	2,85E-05	0,002475442
ALG13	3115,028433	1,39180142	3,180266178	0,001471398	0,030525566
ALG2	3755,179205	1,294945277	5,127120981	2,94E-07	9,74E-05
ALOX12	388,5498516	-1,721183313	-3,355589666	0,00079196	0,02076837
ALOX15B	134,8181784	-2,768916001	-3,118421244	0,001818227	0,035084849
ALPL	764,7726346	-3,345691045	-3,358520465	0,000783609	0,020672644
AMN	573,3070746	1,259390294	3,427557734	0,000609037	0,017705775
AMY1A	2,149425444	-5,142568905	-3,580091203	0,000343474	0,012369479
ANAPC10	1515,699081	1,468071246	3,916284427	8,99E-05	0,0053653
ANAPC2	430,9279767	-1,234528117	-4,52140939	6,14E-06	0,000855722
ANKRD18B	105,2454537	4,621227132	4,1441739	3,41E-05	0,00282248
ANKS1B	6,828265049	-4,001910041	-2,999906728	0,002700623	0,045198264
ANOS2P	15,29350682	21,63615749	6,641595487	3,10E-11	4,55E-08
ANTXR2	4813,484272	1,080728844	3,395376175	0,000685344	0,018855831
ANXA7	14044,9558	0,765315945	3,383079562	0,000716779	0,01947702
AOX2P	322,5467366	-4,491030279	-3,750676851	0,000176358	0,008331944
AP000553.6	2,136056214	-3,738716929	-3,785155341	0,000153613	0,007591029
AP000769.1	87,87219243	1,412403592	3,173385491	0,001506723	0,030966281
AP000936.3	589,7748151	1,034275929	3,227790061	0,001247505	0,027932316
AP001086.1	23,75688678	1,430041987	3,229202285	0,001241361	0,027852705
AP001189.1	358,7053445	-6,136879282	-6,267287695	3,67E-10	4,19E-07
AP001189.3	23,91346971	-5,185495688	-3,476738882	0,000507552	0,015579261
AP001324.1	1214,184599	1,279774669	3,406272678	0,000658564	0,018435458
AP001453.4	18,16734907	-3,886971739	-3,950377691	7,80E-05	0,004814122
AP001476.1	5,485756125	-6,055044055	-3,991846999	6,56E-05	0,004258262
AP001528.3	2,926272764	-5,593097731	-3,390978594	0,000696435	0,01904188
AP002004.1	35,87004424	-2,625491911	-3,173901626	0,001504047	0,030931918
AP002495.1	17,6245779	-2,08882096	-4,561216012	5,09E-06	0,000749173
AP002982.1	43,89524232	1,019679906	3,088275382	0,002013218	0,037541459
AP002986.1	7,589079007	-2,274587325	-3,156427633	0,001597145	0,032138109
AP003469.3	3,360409334	-5,080615377	-3,755769024	0,00017281	0,008287075
AP003555.3	2,722712593	-5,490750602	-3,447315075	0,000566188	0,016680599
AP005131.1	16,83503302	-4,429461774	-3,34343213	0,000827489	0,021300931
AP005403.1	23,48629291	1,582577954	3,236302754	0,001210889	0,027391355
AP1B1	7982,025821	-1,37217902	-4,203020221	2,63E-05	0,002334763
APOB	11,65294464	-7,163213458	-5,351810094	8,71E-08	3,78E-05
APPL1	5254,087193	0,661289046	3,037939835	0,002382015	0,041810204
APPL2	1512,631683	-0,947621525	-3,856980293	0,000114796	0,006300033
AQP10	103,0514185	-3,96419614	-3,75054307	0,000176452	0,008331944
AQP5	45,03362269	-7,32099641	-4,730946279	2,23E-06	0,000434263
AQP6	9,286927432	-6,837911316	-5,375277883	7,65E-08	3,51E-05
ARCN1	8009,984723	0,636009804	3,115302244	0,001837565	0,035309496
ARF4	10938,24945	0,780122983	3,660561662	0,000251663	0,0102919

ARFGAP3	3838,755768	0,742742751	3,303064452	0,000956344	0,023330399
ARG1	457,1403718	-2,467047703	-3,200601146	0,001371412	0,029463831
ARHGAP27	5035,666493	-1,536994509	-3,336195594	0,000849334	0,021702542
ARHGAP29	99,99633899	-2,7094386	-3,841638162	0,000122216	0,006521077
ARHGAP33	503,3352181	-1,761657862	-3,868495147	0,000109509	0,006129922
ARHGAP39	10,25136992	-6,111161825	-6,03383974	1,60E-09	1,45E-06
ARHGAP45	19586,92263	-1,034481749	-3,359242199	0,000781565	0,020654123
ARHGEF18	133,2749884	-1,217344957	-2,96865475	0,002991065	0,047861696
ARHGEF25	2,83535173	-3,751469652	-3,594872095	0,000324551	0,011980757
ARL14EP	2318,024085	0,806652801	2,999102929	0,002707758	0,045232637
ARL5A	1740,470125	0,677741511	3,670606249	0,000241976	0,010108156
ARL5B	3162,306453	1,354543223	2,999266313	0,002706306	0,045232637
ARL5C	25,53222003	-3,131417817	-4,137261555	3,51E-05	0,002855112
ARL8B	6950,962876	1,223547015	5,058880848	4,22E-07	0,000123654
ARMC3	11,17031246	-7,524551417	-5,253446908	1,49E-07	5,67E-05
ARMCX5	1104,615856	0,956989929	2,954526553	0,003131492	0,048642404
ARPP21	911,6715475	-6,110110997	-3,923453137	8,73E-05	0,005238516
ARPP21-AS1	11,07418701	-7,514438036	-4,080711297	4,49E-05	0,003346919
ARRDC5	54,63004799	-1,732827688	-3,328404441	0,00087345	0,022005642
ARX	4,152550043	-6,097459537	-3,947695223	7,89E-05	0,004839273
ASCC1	1520,27395	0,772041147	3,005672026	0,002649947	0,044654573
ATAD1	3558,81563	1,019338364	3,185171499	0,001446682	0,03023694
ATF1	1313,292609	1,208447523	3,298769646	0,000971096	0,023587686
ATF2	3893,320089	0,842159837	3,615121772	0,000300206	0,011452859
ATF6	5114,379412	0,915457768	3,546757257	0,000390004	0,013311581
ATG2A	1443,407444	-2,417732631	-4,415695611	1,01E-05	0,001196838
ATG4A	765,1083472	0,810336675	2,995290504	0,002741836	0,045494834
ATM	880,0050951	-1,499340706	-3,662624838	0,000249644	0,010288876
ATP1A3	27,28673616	-2,230624436	-3,891776343	9,95E-05	0,00574804
ATP2A3	15844,02436	-1,207542622	-4,332870425	1,47E-05	0,001562469
ATP2C2	78,28564023	-5,555722168	-3,746924812	0,000179016	0,008427151
ATP5F1AP2	6,998917776	1,379569962	3,002336998	0,002679154	0,044974437
ATP5F1B	69351,51605	0,439558068	3,290334972	0,001000682	0,023991099
ATP5PBP1	16,83894536	-2,472618037	-3,512133951	0,000444524	0,01441651
ATP6AP2	17490,85843	0,916922719	3,035203691	0,002403733	0,041973039
ATP6V0E2	1569,472556	-1,506219243	-3,407500059	0,000655609	0,01840523
ATP6V1A	5993,841526	0,911953513	3,655915391	0,000256266	0,010390462
ATP6V1H	3988,751851	0,890667178	3,315968057	0,000913263	0,02268263
ATP8B5P	98,36608989	1,5606329	3,273279871	0,001063072	0,024964748
AVPR2	8,36223295	-4,29741487	-5,316345467	1,06E-07	4,29E-05
AXL	669,0034722	-2,701487077	-3,237450388	0,001206029	0,027321573
AZIN1	13718,64544	1,197816021	4,073878591	4,62E-05	0,003405469
B4GALNT3	7,598687955	-5,631743176	-5,09167294	3,55E-07	0,000112648
BACH2	1069,164147	-3,430089941	-4,211833236	2,53E-05	0,002286973
BAG4	3258,457385	1,059311514	3,714637613	0,000203495	0,009014394
BAG6	2076,89851	-0,905243536	-5,343069754	9,14E-08	3,80E-05
BAHCC1	1894,521835	-1,630485767	-3,154126651	0,001609792	0,03234778
BASP1-AS1	4,19303112	-4,638975057	-3,457031733	0,000546161	0,016309063
BCAP29	2893,010522	0,774290328	3,047530616	0,0023073	0,041189154
BCAR1	207,1222017	-2,565283831	-3,480782918	0,000499951	0,015453792
BCL9L	153,4356372	-2,564783554	-3,869965729	0,000108851	0,006125514

BCR	16590,67138	-1,168802685	-3,272661812	0,001065399	0,025000327
BEND2	76,28741343	-6,114592893	-4,043688241	5,26E-05	0,003632098
BFAR	1937,645753	0,86731254	3,58031723	0,000343177	0,012369479
BICD2	5158,043021	-0,744520972	-2,97244893	0,002954344	0,047496279
BLOC1S6	5488,326628	0,86198266	4,306294428	1,66E-05	0,001686803
BMI1	4400,295596	1,326210973	3,167421074	0,001537975	0,031321017
BMP5	68,17234174	-4,58635369	-3,293008455	0,000991215	0,023878352
BRINP3	2,268379991	-4,740042267	-3,074737807	0,002106877	0,038771319
BTBD10	1146,201299	0,960522479	3,723569589	0,000196426	0,008904736
BTBD10P1	6,687979951	1,845581964	3,080508539	0,002066474	0,038279509
BTBD6	1403,665353	-1,519022948	-3,198962499	0,001379231	0,029563101
BTBD6P1	21,06740453	-3,354879529	-4,354546986	1,33E-05	0,001460276
BTF3	28976,68758	0,865612189	3,161830193	0,00156781	0,031713636
BTF3P10	42,51188977	1,016817201	3,284202939	0,001022713	0,024377273
BTF3P8	19,24985074	1,701862653	4,092667469	4,26E-05	0,003229043
BX255925.3	577,0866069	-1,275231378	-4,406852826	1,05E-05	0,001237182
BZW1P1	70,94821277	1,178436236	3,239829742	0,001196011	0,027134553
C11orf58	11967,51278	0,653757835	4,551331212	5,33E-06	0,000771825
C14orf180	4,059482042	-6,06664637	-3,130126316	0,001747312	0,034176925
C15orf54	19,46427162	-8,327083685	-5,919683479	3,23E-09	2,55E-06
C15orf59	10,67025772	-4,775945348	-3,162515466	0,001564124	0,031659891
C16orf87	2801,268022	0,954677836	3,345858707	0,000820282	0,021168497
C1GALT1	1973,483724	0,679568344	2,987084196	0,002816521	0,046197254
C1orf87	1,902962836	-4,974100835	-3,045808329	0,002320557	0,041256171
C21orf58	753,5714806	-1,906925929	-3,888963437	0,000100673	0,005793324
C3orf52	114,7161566	-2,485661055	-3,116820009	0,001828131	0,035220704
C4BPB	2,345488457	-5,278017942	-3,508104676	0,000451311	0,01450368
C5orf56	581,3907209	-1,433229446	-3,291345091	0,000997095	0,023982475
C6	2,223946175	-5,193360965	-3,045135	0,002325759	0,041293621
C7orf26	2615,372866	-0,587514558	-2,999716981	0,002702306	0,045198264
C7orf43	371,0292218	-1,108835977	-3,552984331	0,000380887	0,013175464
C9	1,787794279	-4,403745482	-3,458488969	0,000543215	0,016252619
C9orf131	35,7262657	-2,601935436	-3,10367494	0,001911332	0,036145073
CA12	7,331092127	-6,916688887	-5,83799656	5,28E-09	3,85E-06
CA4	228,2565306	-4,131413036	-3,585462918	0,000336481	0,012215472
CA5BP1	516,9638012	0,611607029	3,215963222	0,001300075	0,028413608
CABIN1	1327,758305	-0,527177204	-3,145436535	0,001658392	0,032934465
CABP5	73,42481469	-4,230508051	-3,112605387	0,001854438	0,03552743
CACNB1	364,0706852	-1,064675977	-3,197832984	0,001384644	0,029615377
CADM2	10,86118017	-4,993894413	-6,876999659	6,11E-12	1,05E-08
CALCR	4,269346071	-4,722185715	-3,973867976	7,07E-05	0,004498131
CALM3	9097,045325	-0,842153439	-3,011944461	0,002595801	0,044104261
CAMP	2199,5933	-4,736810905	-4,935413004	8,00E-07	0,000195427
CAMTA1	3179,492793	0,926590607	3,321105399	0,000896617	0,022369642
CAPN3	23,00735381	-2,812970424	-3,153887819	0,00161111	0,03234778
CAPZA2	23817,99718	1,326576597	3,04382438	0,002335915	0,041397655
CARD11	817,1818962	-1,346408463	-2,955741636	0,003119183	0,048549178
CARD8-AS1	898,2122619	1,882648298	3,302615698	0,000957876	0,023349261
CARMN	5,782887127	-6,137087387	-5,045529181	4,52E-07	0,000131358
CASR	5,387409438	-6,033889682	-5,407826196	6,38E-08	3,12E-05
CBX3	10666,68482	0,716246083	3,972443573	7,11E-05	0,004512988

CBX3P9	191,7036987	0,959346992	5,247561949	1,54E-07	5,72E-05
CBX5	4362,530172	-1,044074153	-3,147242402	0,001648183	0,032861064
CBX7	271,1291211	-2,192156828	-3,397265967	0,000680628	0,018793263
CC2D1A	2003,665144	-0,908244495	-3,837518644	0,000124284	0,006597113
CCBE1	13,59513403	-3,763562861	-3,492349303	0,000478792	0,015056751
CCDC126	871,0446182	1,256690601	3,958066238	7,56E-05	0,004709357
CCDC78	29,82965151	-2,411958266	-3,003518395	0,002668774	0,044824632
CCDC9B	283,6720219	-1,847247384	-3,408965264	0,000652098	0,018367919
CCL2	771,9882709	-2,134770966	-3,09558954	0,001964221	0,03685098
CCL5	1640,268297	-3,083357541	-3,602954645	0,00031462	0,011748623
CCNB1IP1	1978,654308	1,139918422	3,410351628	0,000648792	0,018308296
CCND3	16552,12583	-0,805988415	-3,394271843	0,000688114	0,018898261
CCNG1	10024,24772	0,989156875	3,166380346	0,001543488	0,031407386
CCNJ	1058,748526	1,366606098	4,606116194	4,10E-06	0,000661291
CCNJP1	2,400645643	4,63847702	3,55269361	0,000381308	0,013175464
CCNJP2	7,154925514	-3,912840029	-3,316958336	0,000910032	0,022649273
CCR1	773,9894416	-2,83720051	-3,520228618	0,000431175	0,014182248
CCSER1	397,3990921	1,020117426	3,020001731	0,002527732	0,043354483
CD177	785,1476064	-4,173491657	-3,10284705	0,001916687	0,036224084
CD24	1462,976997	-3,600668839	-4,562555867	5,05E-06	0,000747986
CD244	3018,592419	1,371964371	3,137502059	0,001703941	0,033584651
CD24P4	10,81890929	-3,138306343	-3,149465421	0,001635695	0,032700085
CD27	69,41468405	-3,037372161	-3,09430524	0,001972744	0,036920895
CD4	3944,536998	-2,200825106	-4,084146396	4,42E-05	0,003321927
CDC123	6661,772134	0,807728198	3,016330679	0,002558541	0,043688182
CDC26	629,7492194	0,633923123	3,043700487	0,002336877	0,041397655
CDC42BPG	144,2783906	-2,723789994	-3,585168329	0,000336861	0,012215472
CDC73	5258,819553	0,958738747	3,88140214	0,000103856	0,005943147
CDH4	897,5716597	2,368292888	3,00451412	0,002660054	0,044751413
CDH5	527,3188103	-2,344417807	-3,030868002	0,002438518	0,042271769
CDH7	57,53392773	-4,048738697	-3,309506146	0,000934607	0,022972774
CDH9	36,66806262	-2,567382205	-3,017034074	0,002552611	0,043649966
CDK13	5566,700487	-0,79153361	-3,038823015	0,002375043	0,041771212
CDK5R1	159,3886209	-2,991981984	-2,992234991	0,00276943	0,045658012
CDK5RAP3	388,0594674	-1,918039764	-3,500335427	0,000464673	0,014733151
CDKL1	63,18033942	-1,67874521	-3,226872399	0,001251513	0,027981349
CDRT4	1,621456327	-4,007681236	-3,993248703	6,52E-05	0,004251094
CEACAM3	157,8569201	-2,998910451	-2,957603631	0,003100405	0,04836992
CEACAM8	1032,546935	-3,351996555	-3,99684035	6,42E-05	0,004213917
CEACAMP3	11,0769352	-3,892658966	-3,411633442	0,000645749	0,018272449
CEP170P1	125,2626672	0,769583481	3,307893504	0,000940005	0,02302303
CFAP47	6,158741375	-5,236059862	-3,321623836	0,000894953	0,022364371
CFAP58	17,83812095	-4,287988363	-3,768929331	0,000163949	0,007999219
CFHR3	6,914686928	-2,629436287	-3,0177274	0,002546779	0,043608276
CGNL1	5,580570157	-4,046189895	-3,158200888	0,001587461	0,032010743
CH25H	66,50341963	-4,597334229	-2,977832341	0,002902947	0,04698898
CHI3L1	1096,923829	-2,734637373	-3,743074621	0,000181782	0,008491388
CHIT1	323,7067585	-4,242897276	-3,178559826	0,001480087	0,030590392
CHL1	166,8580749	-4,218292257	-3,455307743	0,000549665	0,016381934
CHMP2B	6608,140771	1,388274964	3,547012193	0,000389627	0,013311581
CHMP4BP1	67,55188961	-1,559198133	-3,00813367	0,002628575	0,044450154

CISH	2756,327482	2,116231881	3,460338298	0,000539497	0,016204389
CIT	550,2775662	-1,899617514	-2,955153029	0,00312514	0,048582455
CLCN3P1	4,39478677	-2,473306102	-3,424396379	0,000616167	0,017795428
CLEC16A	1787,141841	-0,994001971	-3,743150833	0,000181727	0,008491388
CLEC20A	43,9817846	-4,008936428	-3,403088525	0,000666287	0,018480157
CLEC2B	9565,566953	1,942098653	3,266714162	0,001088035	0,025319219
CLEC2D	580,6327196	-1,28069118	-3,258246466	0,00112103	0,025833196
CLEC4GP1	5,355472444	-5,57391276	-4,124511775	3,72E-05	0,002963225
CLIC1	47698,71639	0,925309185	3,139639013	0,001691561	0,033404811
CLIC1P1	241,9374499	1,067718666	3,184515086	0,001449968	0,030285041
CLSTN1	4774,44534	-0,734883204	-2,951504331	0,003162301	0,048948097
CLTCL1	174,0057608	-2,541422841	-4,688696216	2,75E-06	0,000509163
CMTM2	308,2331931	-2,144975538	-3,054342688	0,002255543	0,040561562
CNBP	49767,22388	0,755752879	3,192254856	0,001411667	0,029890644
CNIH1	4804,269734	1,053965967	3,416015406	0,000635447	0,018078505
CNIH4	1992,694692	1,085305383	3,165854757	0,00154628	0,031407427
CNOT3	2074,913163	-0,707998867	-3,738307784	0,000185263	0,0085899
CNTN5	1,845919247	-4,416700706	-3,05945587	0,002217395	0,040086274
COG8	162,6627479	-1,151973984	-3,948719144	7,86E-05	0,0048305
COL19A1	16,24956645	-6,305900119	-4,574184385	4,78E-06	0,000728644
COL4A1	172,2278623	-2,745645937	-3,032747812	0,00242338	0,042175585
COL4A2	405,2184093	-2,669470593	-3,326925845	0,000878097	0,022086588
COL4A5	556,3254452	4,478927386	3,829959457	0,000128164	0,006710538
COLCA1	8,66727112	-7,160276027	-4,658193712	3,19E-06	0,000542593
COLQ	90,70654962	-3,272787031	-3,338505966	0,000842302	0,021591972
COMMD2	4089,052943	0,90373445	4,037852643	5,39E-05	0,00369874
COMMD6	4154,377941	1,159995974	3,121879897	0,001797002	0,034817061
COPS2	6143,43249	1,21041703	3,47713664	0,000506799	0,015571692
COPS3	10951,89031	0,905936466	2,99514017	0,002743187	0,045494834
COPS4	4971,297192	0,956866895	3,50899697	0,0004498	0,014493852
CORO6	213,8248981	-2,322884984	-4,066755847	4,77E-05	0,003450674
COX6B2	67,28948292	5,676677734	4,568873551	4,90E-06	0,000736414
COX7A2L	8153,028546	1,150922981	3,182516073	0,001460014	0,030412351
CPA6	31,75926484	4,270650135	3,998140904	6,38E-05	0,00419979
CPLX1	26,9413729	-3,813049106	-4,156145245	3,24E-05	0,002707768
CPNE5	266,1276755	-2,927289648	-3,307302818	0,00094199	0,023053297
CPT1B	14,88028006	-1,890131324	-3,053110835	0,002264823	0,04068092
CRABP1	25,62824955	-2,605698967	-3,40222275	0,000668401	0,018522117
CRACR2A	832,589546	-1,072246432	-3,405050831	0,000661517	0,018458156
CRAT	2057,245779	-0,844129559	-3,424796148	0,000615261	0,01778595
CREB3L1	126,2601983	-2,642330976	-3,187335183	0,001435903	0,030156945
CREBBP	4022,798187	-1,165071417	-3,256384744	0,001128407	0,025944941
CRH	35,99913867	-5,300437951	-3,867519685	0,000109948	0,006135155
CRIPT	1217,036837	1,247151567	3,575675584	0,000349325	0,012426922
CRISP3	1071,073151	-4,220923475	-4,980274284	6,35E-07	0,000165736
CRISPLD2	493,9846148	-2,754993972	-3,515055165	0,000439663	0,014323697
CRMP1	543,281852	-5,200855494	-4,685339353	2,79E-06	0,000509163
CROCC	1295,192596	-1,769531258	-4,878346163	1,07E-06	0,000242174
CROCCP3	151,2101508	-1,301297709	-3,53170766	0,000412886	0,01383189
CRYBG1	1344,295674	-1,973915136	-3,571195407	0,000355356	0,012560659
CSF2	8,488671092	6,501209743	3,24563403	0,001171894	0,026713262

CSGALNACT1	1402,427387	-2,232228031	-3,349234514	0,000810352	0,021007294
CSPG5	4,777919244	-3,96480222	-2,995048849	0,002744009	0,045494834
CTSH	1074,714203	-1,75942899	-3,404894415	0,000661896	0,018458156
CTSS	11543,26793	-1,473977458	-3,185210834	0,001446486	0,03023694
CUL9	1209,241382	-1,171992448	-4,245910252	2,18E-05	0,002049715
CWC22	2015,664177	0,836335475	3,221185461	0,001276615	0,02825435
CXCL12	2566,09672	-3,504060505	-3,475544259	0,000509818	0,01563323
CXCL9	23,08507319	-4,537085244	-3,750155918	0,000176725	0,00833204
CXCR1	423,8111839	-3,779345201	-3,245551016	0,001172236	0,026713262
CXCR2	557,02626	-4,332960633	-4,505459748	6,62E-06	0,0008943
CYB561D1	523,7126693	-1,422478803	-3,361709885	0,000774615	0,020561987
CYCS	9370,549205	1,061095218	3,937205194	8,24E-05	0,00498617
CYCSP27	37,18211404	1,284289072	3,133733623	0,001725975	0,033919645
CYCSP45	25,49484021	1,597028861	3,95188261	7,75E-05	0,004802224
CYCSP55	34,54457322	0,998009846	3,09661478	0,001957441	0,036782544
CYFIP2	13745,44971	-1,268799424	-3,508733233	0,000450246	0,014493852
CYGB	1252,585482	-3,551172051	-4,119033321	3,80E-05	0,002995749
CYP4F3	200,821477	-4,609913679	-3,587308876	0,000334108	0,012158626
CYP4Z1	2,669698694	-4,960040092	-3,18098116	0,001467772	0,030470862
DAPK2	216,4547554	-3,15003088	-3,675335987	0,000237537	0,009990491
DBH	14,91700035	-6,094006893	-5,53128859	3,18E-08	1,69E-05
DCTN6	1770,179225	1,571264169	3,879295046	0,00010476	0,005961617
DCUN1D1	3298,081607	0,863816771	3,323285455	0,000889638	0,022307666
DCUN1D3	537,9547839	1,965261003	4,292628776	1,77E-05	0,001759244
DDR1	348,2710545	-3,174247598	-3,427183302	0,000609877	0,017713482
DDX12P	709,8264674	-1,676861273	-4,379906252	1,19E-05	0,001360821
DDX18	3844,572675	0,748426791	4,363392813	1,28E-05	0,001428806
DDX3Y	3265,874546	9,287609822	8,014697565	1,10E-15	6,80E-12
DDX51	2727,868792	-0,973399025	-3,038564765	0,00237708	0,041771212
DEFA1	1598,01841	-4,242172799	-4,244165109	2,19E-05	0,002053173
DEFA1B	1598,301342	-4,242459715	-4,244441789	2,19E-05	0,002053173
DEFA3	4443,976633	-4,336932894	-4,478338329	7,52E-06	0,000972873
DEFA4	1598,888785	-3,048500299	-3,264381178	0,001097035	0,025467396
DENND4B	3725,761101	-0,786503967	-3,521065954	0,000429816	0,014152659
DERL1	6366,697107	0,729722244	3,197902615	0,00138431	0,029615377
DEXI	155,1891417	-1,311421997	-3,632188522	0,000281028	0,011016693
DGKZ	7301,159702	-0,824104384	-3,626402514	0,000287397	0,011222961
DHX32	2021,440472	0,804710732	2,992403194	0,002767904	0,045658012
DHX37	1101,71776	-1,098222684	-3,216334824	0,001298393	0,028413608
DIS3	3603,86618	0,786531391	3,115156286	0,001838475	0,035309496
DLD	10699,42174	1,041685494	3,428620679	0,000606657	0,017653253
DLEU7	16,02948792	-3,327130057	-3,329687972	0,000869434	0,021994454
DLX5	5,256766976	-5,533587729	-3,750688878	0,000176349	0,008331944
DNAI1	5,356818592	-3,947256837	-2,975964332	0,002920688	0,047114019
DNAJA1	13118,30431	0,666299677	3,957832151	7,56E-05	0,004709357
DNAJB2	202,6904472	-1,246559532	-3,258673123	0,001119346	0,025813702
DNAJB4	1213,154344	1,602007355	4,185363082	2,85E-05	0,002475442
DNAJC1	4817,044619	1,301199883	3,502205579	0,000461423	0,014690634
DNAJC24	420,5410041	0,721390676	3,500624165	0,00046417	0,014733151
DNAJC9-AS1	1,673749771	-3,751876732	-3,757044781	0,000171932	0,008262665
DNER	4,173078951	-5,190010133	-2,963518179	0,003041441	0,048133648

DNHD1	430,1181661	-1,468249899	-3,631976271	0,000281259	0,011016693
DNM2	17983,91645	-0,605973197	-3,171049613	0,001518892	0,03109184
DNTTIP1	4089,178513	0,829839387	3,608346421	0,000308155	0,011654992
DOK7	1,494835335	-4,364180267	-3,001766371	0,002684181	0,045034266
DPYSL4	34,29093373	-5,395701257	-4,132842514	3,58E-05	0,002883291
DSC1	4,862209326	-5,43321857	-4,069146878	4,72E-05	0,003437056
DSCAM	6,250288561	-5,346498028	-3,705596933	0,000210893	0,009157654
DSTN	7401,405024	1,162945862	3,405524618	0,000660371	0,018449029
DTWD1	1397,672136	0,781261399	3,104338343	0,001907051	0,036093584
DTX1	543,2912466	-4,410026319	-3,33119057	0,000864754	0,021935081
DUSP10	6503,983905	1,003936475	3,459917811	0,00054034	0,016213895
DUSP13	40,65931643	-5,721452961	-2,995277804	0,00274195	0,045494834
DUSP14	2079,861542	1,585491745	4,228410602	2,35E-05	0,002166513
DUX4L26	6,577268145	-4,336357545	-4,25831272	2,06E-05	0,001963273
DYNC1I2	1896,133834	0,932029868	3,589890462	0,000330817	0,012131457
DYNC1I2P1	49,26460208	0,823714232	2,99475586	0,002746646	0,045503886
DYNLT3P2	3,240830343	-2,155897018	-3,014664617	0,002572636	0,043881147
DYRK2	2944,112561	-1,064633746	-2,95750659	0,003101381	0,04836992
E2F1	4101,434674	-1,492065374	-3,194320914	0,001401602	0,029759397
EBF1	3221,330346	-4,898336696	-4,415787207	1,01E-05	0,001196838
EBF3	61,77843948	-3,533497482	-3,233233427	0,001223975	0,02764675
ECD	5112,895057	0,931253877	3,4215789	0,000622587	0,017863535
ECE1	2568,486749	-1,699836845	-3,013274406	0,002584451	0,04397106
EDEM1	4110,917192	-1,110235678	-3,16827378	0,00153347	0,031303211
EEF1A1P10	175,9734898	1,06007836	3,116602496	0,001829481	0,035224655
EEF1A1P11	2999,676543	1,128704175	3,363315687	0,000770122	0,020474749
EEF1A1P12	993,8643402	1,200148383	3,499805293	0,000465598	0,014747293
EEF1A1P13	5597,367768	1,063324078	3,222668954	0,001270022	0,028231177
EEF1A1P14	25,84834461	1,369377311	2,972013149	0,00295854	0,047514124
EEF1A1P19	1685,601461	1,17752019	3,44523273	0,000570568	0,01677753
EEF1A1P22	171,336447	1,198152328	3,645351515	0,000267027	0,010692391
EEF1A1P25	303,2379781	1,287772661	3,574415245	0,000351011	0,012449989
EEF1A1P29	71,316066	1,331645152	3,489255986	0,000484367	0,015154684
EEF1A1P3	96,71257535	-1,906463341	-3,261177885	0,001109504	0,025644372
EEF1A1P38	59,5014621	1,221537967	3,370480942	0,000750371	0,020086369
EEF1A1P4	908,2459293	1,184102235	3,440995139	0,000579579	0,016976442
EEF1A1P6	5541,457791	1,006772832	3,006617466	0,00264172	0,044589158
EEF1A1P7	239,1363618	1,069245157	3,073565598	0,002115172	0,038800482
EEF1A1P8	110,7534078	1,125726922	3,170660753	0,001520927	0,031112801
EEF1A1P9	2446,651314	1,129670559	3,406221467	0,000658687	0,018435458
EEF1AKMT2	615,6823028	0,772653312	4,449054655	8,62E-06	0,001083816
EEF1B2	23586,62958	1,132842496	3,18754185	0,001434877	0,030156945
EEF1B2P1	160,0387874	1,222269108	3,158157736	0,001587696	0,032010743
EEF1B2P2	102,3928112	1,422093001	3,726657728	0,000194036	0,008845802
EEF1B2P3	1521,763596	1,203556007	3,31592297	0,00091341	0,02268263
EEF1B2P6	274,1426494	1,285090068	3,544814265	0,00039289	0,013363351
EEF1GP5	228,3630917	1,054157188	3,993601947	6,51E-05	0,004251094
EFNA1	1547,745547	1,78500339	3,116098884	0,001832608	0,035262816
EFNA5	5,349972553	-4,439958844	-3,656925125	0,000255259	0,010390462
EGFR	23,29763882	-4,561052512	-3,710006467	0,000207254	0,009093353
EHD4	1561,299915	-1,857661828	-3,613906048	0,000301618	0,011478276

EID1	11540,26004	0,406432165	3,221114849	0,00127693	0,02825435
EIF1AX	6323,408774	0,930422551	3,225722416	0,001256552	0,028012639
EIF1AXP1	193,1265791	0,891864191	2,960701083	0,003069397	0,048262267
EIF1AY	852,0008524	13,15042138	7,931598522	2,16E-15	1,11E-11
EIF2S2	3201,688723	0,927981313	4,361790437	1,29E-05	0,001429174
EIF3E	19301,50172	1,23869102	4,045747887	5,22E-05	0,003620947
EIF3EP1	110,3523323	0,941510443	3,40105033	0,000671275	0,018568314
EIF3H	11692,21776	0,885651971	3,650864094	0,00026136	0,010490842
EIF3J	2215,960666	0,677924816	4,150511286	3,32E-05	0,002767771
EIF3J-DT	698,653914	0,63265778	3,082682919	0,002051436	0,038069658
EIF3LP1	32,26577867	1,227021089	3,133653537	0,001726446	0,033919645
EIF3LP3	82,58615153	0,835476712	3,226431267	0,001253443	0,02800418
EIF4A1P2	310,0480625	0,983929141	3,349584307	0,000809329	0,021007294
EIF4A1P4	148,0573609	0,869996867	3,450597088	0,000559348	0,016590217
EIF4A1P9	1,676126926	4,163487616	3,705791648	0,000210731	0,009157654
EIF4EP5	41,68914822	1,26389114	3,511937358	0,000444853	0,01441651
ELN	2465,560718	3,110164597	4,138988157	3,49E-05	0,002844798
ELOC	4812,711783	1,063393581	3,281223549	0,001033578	0,02454952
ELOCP28	10,57324671	-2,082949675	-3,104278493	0,001907437	0,036093584
EMC2	789,6537631	1,075832956	3,218393392	0,001289109	0,028413608
EME2	406,1048587	-1,451853277	-4,90386546	9,40E-07	0,000220647
EML3	1923,739903	-1,039459648	-2,982512553	0,002858929	0,046594947
EML6	47,37027057	-2,667393843	-3,031951574	0,002429782	0,042189719
EMX2	2,178238597	-4,448474539	-2,986472085	0,002822166	0,046245757
ENKUR	128,2985652	-5,285310253	-5,166706984	2,38E-07	8,24E-05
ENTPD4	1781,22678	-1,831834116	-5,086521349	3,65E-07	0,000113722
ENY2	7550,287785	1,104358511	4,100255919	4,13E-05	0,003176399
EP400	709,2149791	-0,801037211	-3,352500729	0,00080085	0,020859373
EPB41L4B	23,14150702	-6,751437073	-5,361097326	8,27E-08	3,69E-05
EPHA5	1,681301195	-4,274440919	-2,996699585	0,002729195	0,045442436
EPHX1	626,9553147	-1,979987537	-3,670252316	0,000242311	0,010108447
ERI1	2788,194812	1,573172374	4,0752045	4,60E-05	0,003402402
ERLEC1	3662,756565	0,856594459	3,595256365	0,000324072	0,011977447
ERP27	206,9560239	-1,913332937	-4,477494247	7,55E-06	0,000972873
ERP44	9967,323758	0,840957335	3,477411763	0,00050628	0,015571261
ETFRF1	1987,604807	1,319798214	4,058174905	4,95E-05	0,003508421
EWSAT1	2,060600975	-5,0912698	-3,055539692	0,002246559	0,040447252
EYA4	5,365890703	-6,469130653	-4,481215546	7,42E-06	0,000972333
F11R	3867,311389	1,770169849	3,688972399	0,000225162	0,009601179
FAM102A	1785,791069	-1,75906267	-3,153768696	0,001611768	0,03234778
FAM122A	1644,097463	0,95672197	3,832792198	0,000126697	0,006647358
FAM149A	16,7652432	-4,759018927	-4,144650926	3,40E-05	0,00282248
FAM157B	9,97446608	-3,724380257	-4,05936481	4,92E-05	0,003506752
FAM163B	2,428391919	-5,325234339	-3,168249013	0,001533601	0,031303211
FAM193B	3320,206286	-1,376343698	-3,221849325	0,001273661	0,02825435
FAM204A	4204,067817	0,681437928	3,243204695	0,001181933	0,026874564
FAM20A	286,1416539	-2,98889929	-3,824171622	0,000131212	0,006800739
FAM53B	2434,418041	-2,048139161	-3,798178618	0,000145763	0,007368824
FAM57B	17,40458715	-2,844226382	-3,644190638	0,000268235	0,01069635
FAM83A	334,7770898	4,451956222	3,832705235	0,000126742	0,006647358
FAM9B	1,920391397	-4,984379753	-3,146248999	0,001653791	0,032869772

FAUP1	137,043248	0,905412398	2,965180058	0,003025058	0,048130473
FAXDC2	713,8886716	-1,836479117	-3,267314433	0,00108573	0,025284701
FBXO17	8,811076188	-3,651920309	-3,397332517	0,000680462	0,018793263
FBXO28	1978,473613	0,855669622	4,11404879	3,89E-05	0,003037905
FBXO30	1077,956695	1,694710311	4,532716737	5,82E-06	0,000818595
FBXO34	5280,35215	1,022644837	3,254373919	0,001136426	0,026090339
FBXO42	3269,324577	0,753088733	3,168026735	0,001534774	0,031303211
FBXO8	878,042992	1,245828577	3,18826347	0,001431301	0,030145439
FCAR	1612,576738	-3,116202584	-3,641806979	0,000270731	0,010768729
FCER1G	3516,559363	-2,36973534	-3,54867037	0,000387181	0,013288986
FCHSD1	1005,697502	-0,976275679	-3,152552288	0,001618498	0,032461699
FCMR	1114,252761	-2,655519657	-4,051210324	5,10E-05	0,003581511
FCRL1	161,0946398	-5,522281123	-3,179847681	0,001473525	0,030549097
FCRL3	27,09728679	-6,8064661	-5,182490299	2,19E-07	7,84E-05
FDFT1	11523,66464	0,954526189	3,167373449	0,001538226	0,031321017
FDX1	4690,140431	0,922359485	2,988720645	0,002801481	0,045999578
FFAR4	7,436711889	-4,758965321	-3,426203403	0,000612082	0,017744033
FGFR1OP2	7621,783332	1,161918654	4,946501415	7,56E-07	0,000189125
FHIT	1676,176752	-1,204604452	-3,164859376	0,001551579	0,03146803
FHL3	3269,252365	1,602279497	4,034025791	5,48E-05	0,003751177
FHOD3	2,310440774	-3,731316113	-3,807648211	0,000140295	0,007174837
FLJ45513	3,369654538	-4,110967723	-3,295309955	0,000983132	0,02373216
FLYWCH1	3096,70285	-0,586567594	-3,024190218	0,002492996	0,042974177
FMO2	311,790145	-4,217641965	-3,467740726	0,000524853	0,015935564
FNDC1	6,298104463	-4,705013131	-5,062580609	4,14E-07	0,000122443
FO393411.1	294,2491061	1,229932849	4,238773979	2,25E-05	0,002093125
FO538757.2	33,614716	-2,283894075	-3,067494005	0,002158618	0,039300632
FOPNL	5080,836326	0,97347966	3,46378663	0,000532629	0,016108097
FOXA1	62,66967767	6,169480436	3,767642394	0,000164797	0,00800251
FOXF2	7,249699768	-6,903672861	-3,691274387	0,000223133	0,009541117
FOXP2	7,301830328	-4,277765939	-3,517864101	0,000435035	0,014263499
FPR1	3576,271921	-2,784028904	-3,201297188	0,001368103	0,02943306
FRMD5	172,9958927	-2,171934458	-3,07598066	0,002098115	0,038702608
FSTL4	15,54243318	-4,065513305	-3,294761006	0,000985054	0,023748522
FZD10-DT	2,408146551	-5,316113735	-4,228155309	2,36E-05	0,002166513
G3BP2	14851,17584	1,093660321	4,157060697	3,22E-05	0,002704293
G6PD	696,1876829	-1,423475394	-4,157128972	3,22E-05	0,002704293
GABPB1-IT1	3809,970684	-0,998012659	-3,415799329	0,000635951	0,018078505
GABRG3	3,285679103	-5,756121284	-5,505964341	3,67E-08	1,92E-05
GADL1	3,696315334	-4,537238381	-3,257584886	0,001123646	0,025874124
GAL3ST2	217,5050689	3,845155496	3,703095772	0,000212984	0,009196566
GALNT17	13,49335473	-7,37592445	-4,937835377	7,90E-07	0,00019456
GALNT3	1333,081369	1,779707938	3,217108504	0,001294896	0,028413608
GAPDHP47	1,797603168	-3,136801913	-2,946696198	0,003211886	0,049442166
GAPDHP68	5,838299995	-3,435698934	-3,336675104	0,00084787	0,021698565
GAPDHP70	43,28003801	0,931138809	3,971611453	7,14E-05	0,004512988
GAS1	86,71308366	-2,97071308	-3,181844055	0,001463406	0,030441809
GAS5	10990,2267	1,827226851	3,265859834	0,001091323	0,025374692
GAS7	1427,330123	-1,636005665	-2,964138777	0,003035314	0,048133648
GBP2	3627,48705	1,429651552	3,037152291	0,002388248	0,04186334
GCN1	3690,933016	-1,037015924	-3,78708435	0,000152425	0,007581131

GCSAM	127,5465233	-2,466479173	-2,995034033	0,002744142	0,045494834
GDE1	6056,983002	0,766482855	2,94487972	0,003230802	0,049683672
GDI2	15422,0519	0,660218369	3,104913874	0,001903344	0,03606047
GHITM	21849,15853	0,644325299	3,321142694	0,000896497	0,022369642
GHRHR	6,848450684	-6,821011823	-4,478050782	7,53E-06	0,000972873
GIPR	15,4981279	-4,235853437	-3,329708164	0,000869371	0,021994454
GLA	4154,758018	1,061603558	3,552076321	0,000382204	0,013188579
GLDN	56,15476967	-4,231900484	-3,657247403	0,000254938	0,010390462
GLP2R	2,299346388	-5,242479669	-3,107424287	0,001887253	0,035888119
GLRA3	1,716431581	-4,813555049	-3,326070484	0,000880797	0,022136394
GLRX3	3791,764006	0,589710138	3,163843422	0,001557005	0,03155729
GLYATL1P2	8,418766118	-6,018370863	-4,065297808	4,80E-05	0,003450674
GLYCTK	365,1731726	-1,026485522	-2,97729298	0,00290806	0,047046996
GLYR1	3787,462906	-0,71529281	-3,123128615	0,001789395	0,034728339
GNAI3	12681,05073	0,724678617	3,482902593	0,000496009	0,015378271
GNAO1	15,64980688	-3,979902119	-3,132671362	0,001732233	0,034011639
GNAZ	181,4011129	-2,921810534	-3,692744295	0,000221847	0,00952581
GNG7	2542,840017	-1,745607875	-3,833541034	0,000126312	0,006647358
GNL2	6138,36261	0,568236456	3,704367678	0,000211919	0,009176288
GNPDA2	1574,430398	1,473391297	3,937492427	8,23E-05	0,00498617
GOLGA7	7362,758646	0,71139959	3,510116214	0,000447911	0,014457019
GOLPH3	16848,18954	0,982914204	3,898540882	9,68E-05	0,005632104
GOLT1B	3674,425566	1,113830606	3,029220788	0,002451854	0,042431274
GPATCH11	1990,419307	1,59352087	4,097188646	4,18E-05	0,00320122
GPATCH2	408,96238	0,873233338	3,311748638	0,000927148	0,02285357
GPBP1L1	9718,175275	0,616391706	2,950894883	0,003168547	0,048995513
GPC2	215,7375237	-2,358573694	-3,61836474	0,00029647	0,011352529
GPR176	790,7920243	-5,113227969	-4,353866777	1,34E-05	0,001460276
GPR88	99,50964109	-3,709291909	-3,185492752	0,001445077	0,03023694
GRB14	31,46103403	-4,932050291	-4,354848856	1,33E-05	0,001460276
GRB7	10,7221575	-6,380499422	-5,129170772	2,91E-07	9,74E-05
GRIA2	3,474345498	-5,368428914	-4,428878772	9,47E-06	0,001161366
GRIN2B	5,349746947	-4,589552849	-3,241171137	0,001190397	0,027037553
GSKIP	2141,078045	1,207544851	3,766909777	0,000165281	0,008013381
GTF2F2	1358,513757	0,811316587	3,656236457	0,000255945	0,010390462
GTF2IP6	2,32585469	-5,265935382	-3,185679748	0,001444144	0,03023694
GUCY1A2	4,119368864	-5,643998725	-3,977209961	6,97E-05	0,004463065
GUCY2C	7,156241888	-6,881215386	-5,835936996	5,35E-09	3,85E-06
HAMP	171,9721905	2,84146863	3,031794768	0,002431044	0,042189719
HAS1	3591,972045	4,056436779	3,177247581	0,001486801	0,03067971
HAT1	6615,21894	0,907840215	4,980186135	6,35E-07	0,000165736
HBG1	71,83965808	4,383507948	4,061057842	4,89E-05	0,00349621
HBG2	9,21490665	5,196681151	3,109544377	0,001873761	0,03574194
HCCS	1766,417293	1,036327404	3,848110261	0,000119032	0,006417956
HCFC1	3858,428729	-1,211742682	-4,29488376	1,75E-05	0,001747111
HDAC7	3892,560138	-1,087815025	-3,202449289	0,001362643	0,029377932
HELLPAR	84,26385056	-2,984145353	-5,810674559	6,22E-09	4,35E-06
HERC2P10	118,5663618	2,201009265	3,854330445	0,000116047	0,006334631
HESX1	241,82371	1,135728781	3,241060943	0,001190857	0,027037553
HGFAC	7,549670678	-6,959906837	-6,166375961	6,99E-10	6,72E-07
HHAT	522,6184632	-1,071133705	-3,127993291	0,001760042	0,034273506

HHIP	409,8566536	-4,758727191	-3,940756155	8,12E-05	0,004942054
HIP1R	1763,912451	-1,883132055	-3,800984959	0,000144122	0,007321923
HIRA	395,6321799	-1,059537429	-3,471354691	0,00051784	0,01577679
HIST1H2AI	214,0979174	2,062720733	3,191990038	0,001412962	0,0298975
HIST1H2BI	21,30973611	1,784469635	2,991155983	0,002779235	0,045736841
HIST1H2BL	25,8004654	1,951780602	3,226960577	0,001251127	0,027981349
HIST1H4I	841,3973284	1,380586744	2,991911685	0,002772365	0,045667623
HLA-W	5,291433471	-1,987156743	-3,655161657	0,00025702	0,010397995
HLF	576,2367899	-2,361408959	-3,12038924	0,001806122	0,034927814
HMGB3P12	6,015674037	-6,632969676	-3,518773575	0,000433547	0,014245035
HMGCR	2574,024265	1,268555414	3,674603657	0,000238219	0,01000552
HMHB1	27,24276582	-4,495832987	-4,600723854	4,21E-06	0,000670954
HNRNPA1P26	23,23493934	0,924227893	3,600628659	0,000317449	0,011817767
HNRNPA1P4	442,6852763	0,7321299	3,726405171	0,00019423	0,008845802
HNRNPA1P53	13,94284789	1,219212535	3,167923636	0,001535318	0,031303211
HNRNPA1P8	99,68950362	0,732006031	3,124703275	0,001779845	0,03459349
HNRNPC	56703,80048	0,654338985	3,615828563	0,000299388	0,011438542
HNRNPCL1	53,75047858	0,848558259	3,178638514	0,001479685	0,030590392
HNRNPCL2	15,21490721	1,226703319	3,176148278	0,001492446	0,030734414
HNRNPCP2	1562,877468	0,702965574	3,56922056	0,000358045	0,012624833
HOOK2	345,9153161	-1,106398949	-3,178589849	0,001479933	0,030590392
HOXA10	1821,316825	0,960187185	3,786607034	0,000152718	0,00758345
HOXA7	311,2654401	1,243620151	3,194688034	0,001399821	0,029742083
HOXA9	3320,880744	1,718166968	4,902544613	9,46E-07	0,000220647
HOXC4	3,256873833	-5,743770975	-3,426320712	0,000611818	0,017744033
HOXD-AS2	1,532583037	-4,658181032	-3,290013973	0,001001824	0,023991099
HP	682,6936186	-2,988122041	-3,325305192	0,000883218	0,022179145
HPS4	5810,741609	-1,58054837	-5,367719157	7,97E-08	3,61E-05
HRH3	3,831380868	-5,984586621	-3,555754864	0,000376895	0,013111275
HRK	55,84432878	-4,830760581	-3,244352419	0,00117718	0,026791417
HS3ST3A1	15,26699475	-3,871720924	-4,51862054	6,22E-06	0,000859328
HS3ST3B1	475,8534283	-1,886122745	-3,206888628	0,001341789	0,029070843
HS6ST3	1,650415126	-4,75799498	-3,424925434	0,000614968	0,01778595
HSD17B11	7243,12268	1,279463225	3,977894455	6,95E-05	0,004463065
HSP90AA1	29326,7876	0,632227776	3,441756146	0,000577951	0,016962228
HSP90AA2P	620,8006515	0,746884709	4,271337139	1,94E-05	0,001899678
HSP90AA6P	16,24842599	1,164623092	3,231450988	0,001231634	0,027757645
HSP90AB1	61913,49789	0,621761428	3,080131684	0,002069091	0,038281912
HSP90AB2P	95,06244108	0,86267593	3,502966383	0,000460108	0,014679099
HSP90AB3P	630,0372931	0,820442546	3,704436196	0,000211861	0,009176288
HSPA13	4995,99541	1,350706856	5,349074183	8,84E-08	3,78E-05
HSPA14	2379,239284	0,83909439	2,98398755	0,002845183	0,046436606
HSPA8P14	2,574970613	-4,641169129	-3,197341247	0,001387007	0,029615377
HTRA1	78,15998525	-3,181372403	-3,280161658	0,001037476	0,024550946
HTRA3	3187,20304	2,161907711	3,709895132	0,000207345	0,009093353
IER3IP1	2387,525553	0,925969747	4,780267192	1,75E-06	0,000361721
IFI30	217,99754	-2,686340754	-3,066327275	0,00216706	0,03936122
IFT57	4528,351647	0,889187626	4,318734209	1,57E-05	0,0016213
IGF2	12,84647051	-4,614773192	-3,73888305	0,00018484	0,008583197
IGF2R	1504,650606	-1,95341894	-3,111412573	0,001861946	0,035626931
IGHA1	41953,86176	-2,751644565	-4,11325029	3,90E-05	0,003040719

IGHA2	6490,324737	-2,306433461	-2,993637796	0,00275673	0,04560529
IGHD2-2	19,26587005	-6,986281356	-5,267045825	1,39E-07	5,34E-05
IGHD2-8	6,57909606	-5,224101197	-3,901795526	9,55E-05	0,00559776
IGHD3-22	8,231688012	-4,233581004	-4,839506648	1,30E-06	0,000284205
IGHD4-23	5,580353275	-4,542671797	-3,898910926	9,66E-05	0,005632104
IGHD6-25	36,90529215	-2,901351291	-3,644099177	0,00026833	0,01069635
IGHG2	25088,82498	-2,89489756	-3,395521719	0,000684979	0,018855831
IGHJ3P	143,5627329	-2,366471859	-3,268751351	0,001080232	0,025216006
IGHJ5	94,77430052	-2,34642868	-3,481702677	0,000498237	0,015419425
IGHJ6	70,29153873	-2,616639425	-3,391630717	0,00069478	0,019013507
IGHV1-17	2,254105051	-5,219681731	-3,166123063	0,001544854	0,031407427
IGHV1-18	142,8029753	-4,070982644	-4,438532636	9,06E-06	0,001128951
IGHV1-2	105,5116719	-3,394811994	-3,990194358	6,60E-05	0,004279015
IGHV1-24	99,48316583	-3,604505636	-5,03114568	4,88E-07	0,00013771
IGHV1-46	171,275554	-3,967283851	-3,783436594	0,000154678	0,007619302
IGHV1-69	68,02856393	-5,368352379	-6,48100452	9,11E-11	1,22E-07
IGHV1-69-2	38,02097142	-4,963494033	-3,656522436	0,00025566	0,010390462
IGHV2-5	205,069946	-4,123300833	-3,85314658	0,00011661	0,006343286
IGHV2-70	51,608149	-4,369990645	-4,780560369	1,75E-06	0,000361721
IGHV3-20	63,16876649	-3,746998135	-3,329131053	0,000871174	0,022005642
IGHV3-21	199,9431574	-3,531316379	-3,512941035	0,000443176	0,01440766
IGHV3-22	3,009794616	-3,994215376	-3,508562809	0,000450535	0,014493852
IGHV3-23	616,6875936	-3,552823164	-4,423036336	9,73E-06	0,001170885
IGHV3-30	561,0649012	-3,035923825	-3,914910791	9,04E-05	0,0053855
IGHV3-33	350,5671459	-3,042809344	-4,096150083	4,20E-05	0,00320122
IGHV3-48	277,364004	-3,827944257	-4,117930175	3,82E-05	0,003000996
IGHV3-64	16,14349534	-5,237119917	-3,449865997	0,000560865	0,016619198
IGHV3-69-1	19,99152915	-2,822118101	-3,232917567	0,001225329	0,027657044
IGHV3-72	115,0712401	-3,268453068	-3,087407168	0,002019108	0,037628502
IGHV3-74	548,3007344	-3,118339105	-3,171425896	0,001516926	0,031072249
IGHV4-34	93,00273353	-3,784586496	-4,419210693	9,91E-06	0,001186702
IGHV4-39	181,9187324	-3,180938452	-3,925831855	8,64E-05	0,005197141
IGHV4-61	50,46924186	-2,6125567	-3,750841058	0,000176242	0,008331944
IGHV5-51	240,3352886	-4,202263228	-4,381597258	1,18E-05	0,001358461
IGHV5-78	155,0476234	-4,863331084	-3,331814507	0,000862817	0,021917129
IGHV6-1	108,3742174	-4,665184917	-4,405535872	1,06E-05	0,001239972
IGKV1-13	18,06317553	-2,859725367	-3,13198422	0,001736292	0,034047913
IGKV1-16	180,7224744	-4,133332257	-5,071285311	3,95E-07	0,000118108
IGKV1-33	237,0973204	-3,260634145	-3,751004758	0,000176127	0,008331944
IGKV1-8	124,5660231	-4,694730778	-4,621855736	3,80E-06	0,000626149
IGKV1-9	371,2160215	-3,120137105	-3,623164445	0,000291021	0,011305393
IGKV1D-16	50,75365169	-4,38564247	-4,842190509	1,28E-06	0,000282395
IGKV1D-33	73,5543783	-3,362761777	-3,754084942	0,000173976	0,008317073
IGKV2-26	26,34696949	-4,920509344	-4,724001665	2,31E-06	0,000444966
IGKV2-28	688,6898303	-3,323748477	-3,553421521	0,000380255	0,013175464
IGKV2-30	480,981527	-3,642144593	-4,520462351	6,17E-06	0,000855722
IGKV2D-28	301,662006	-3,166465738	-3,487861003	0,000486901	0,015188954
IGKV2D-29	94,06588689	-4,5593736	-3,624626004	0,00028938	0,011263134
IGKV3-15	916,6468021	-3,596401237	-4,513903363	6,36E-06	0,000870865
IGKV3-20	2323,172045	-3,021215029	-4,068702192	4,73E-05	0,003437056
IGKV3D-11	82,99942254	-2,929054975	-4,132230318	3,59E-05	0,002883291

IGKV3D-15	61,38721039	-3,315666567	-3,721761266	0,000197838	0,008904736
IGLC2	10553,36961	-2,75863789	-3,295254892	0,000983324	0,02373216
IGLC5	19,12811202	-2,544411038	-3,267557796	0,001084797	0,025284701
IGLV10-54	140,22029	-8,826099042	-5,631275524	1,79E-08	1,02E-05
IGLV1-41	37,27923648	-3,278153758	-2,956246199	0,003114084	0,04851888
IGLV1-51	1177,818922	-3,090995095	-3,014454297	0,00257442	0,043886305
IGLV2-14	854,0338703	-3,014100161	-3,405644358	0,000660081	0,018449029
IGLV2-8	752,3440007	-4,101582424	-3,502269042	0,000461314	0,014690634
IGLV3-19	306,5628799	-3,70007371	-3,482974613	0,000495875	0,015378271
IGLV3-21	935,9344624	-3,782427401	-4,410838047	1,03E-05	0,001219299
IGLV4-60	94,55761348	-5,993793735	-4,63928712	3,50E-06	0,000578685
IGLV6-57	349,7243297	-3,653937739	-3,14657283	0,001651961	0,032869772
IGLV7-43	69,6043714	-3,860976453	-3,785812939	0,000153207	0,007591029
IGLV7-46	58,69660016	-3,978886242	-3,85682635	0,000114869	0,006300033
IKZF3	66,58815806	-5,070149579	-3,718171573	0,00020067	0,008966656
IL11	1368,980869	5,913533246	4,190539635	2,78E-05	0,00244096
IL13	21,90331372	-5,6292088	-4,084821099	4,41E-05	0,003320388
IL18BP	380,8107999	-2,001636438	-3,423408479	0,000618411	0,017817457
IL1RL1	418,9616214	2,837634751	3,009138849	0,002619894	0,044391118
IMPA1	2529,045113	1,667268991	5,19043116	2,10E-07	7,60E-05
IMPAD1	4588,853738	0,95802895	3,04808273	0,002303065	0,041189154
IMPG2	3,506416364	-5,395104952	-6,237751518	4,44E-10	4,88E-07
INHBA	1188,743294	4,396292215	5,161605389	2,45E-07	8,28E-05
INO80	1753,156319	-1,168415627	-3,523752595	0,000425481	0,014060381
INO80E	341,5527532	-1,094848423	-3,791921308	0,000149486	0,007483308
INPPL1	2895,587461	-1,021312302	-3,530410406	0,000414916	0,013884787
INTS1	5870,144741	-1,070842165	-3,191391864	0,001415891	0,02991835
IPO9-AS1	12,14120208	-1,685383103	-3,347782369	0,00081461	0,021070615
IPPKP1	8,897562455	5,597789824	3,361427402	0,000775407	0,020561987
IRF4	639,3691739	-4,223079205	-3,450873585	0,000558775	0,016589212
IRS2	5213,191638	-1,915913405	-3,926657869	8,61E-05	0,005189469
IRX2	6,789085378	-6,369815553	-4,208998151	2,57E-05	0,002307214
ITM2A	17200,18852	1,677740063	3,557706395	0,000374107	0,013043756
IZUMO4	20,82601571	-3,265684669	-4,716723915	2,40E-06	0,000455481
JADE2	1618,889294	-1,24633792	-3,080236571	0,002068362	0,038281912
JAGN1	2055,006767	1,055153187	3,341895491	0,000832084	0,021401307
JAM2	152,0130197	-2,137586185	-2,94939948	0,003183921	0,049123974
JCHAIN	3058,222002	-1,991781919	-3,165611953	0,001547571	0,031407427
JMJD7-PLA2G4B	82,58688036	-2,569372287	-3,010185116	0,002610885	0,044311643
KANK2	2126,211418	-1,849677152	-4,540669257	5,61E-06	0,000797969
KBTBD8	520,0793978	2,00281659	3,143509081	0,001669352	0,033057678
KCNA3	982,8651892	-1,889974437	-2,99271839	0,002765048	0,045658012
KCNE4	24,70593815	-6,090234993	-5,336892933	9,46E-08	3,88E-05
KCNT2	4,378746105	-5,735796004	-5,086003012	3,66E-07	0,000113722
KCNU1	3,256583953	-5,743710302	-4,213602029	2,51E-05	0,002282506
KCNV1	3,101128274	-5,672948257	-3,198828169	0,001379874	0,029563101
KCTD12	247,5648967	-2,404967241	-3,084049891	0,002042033	0,037962977
KCTD17	679,76942	-1,231780618	-3,852698027	0,000116823	0,006343286
KDM5C	5615,373289	-0,828254979	-3,047223467	0,002309659	0,041189154
KDM5D	639,971901	12,73760014	7,798867888	6,25E-15	2,61E-11

KIAA0319	5,227710325	-6,428403788	-4,921462205	8,59E-07	0,000208236
KIAA1586	1806,159896	1,52278616	3,416342219	0,000634684	0,018078505
KIF12	3,757003655	-5,9545152	-3,902281981	9,53E-05	0,00559776
KIF21B	554,3292705	-1,398137209	-3,409712102	0,000650315	0,018334473
KIF26A	68,29547398	-3,291869893	-3,576588563	0,000348107	0,012426922
KIF5A	9,459655586	-4,52833422	-3,679323708	0,000233853	0,009869347
KIF5C	15,4346795	-4,04013192	-3,472039564	0,00051652	0,0157759
KIR2DP1	6,538304114	-6,537308572	-4,249071027	2,15E-05	0,002027209
KLF4	1072,298072	-2,254472548	-3,039857259	0,002366903	0,041687553
KLHL14	10,73631461	-7,041152632	-7,031141492	2,05E-12	4,20E-09
KLHL4	7,539960478	-4,789242985	-3,690649162	0,000223682	0,009551335
KLKB1	3,582184093	-5,887580469	-3,946448863	7,93E-05	0,004854728
KNL1	650,984504	-1,605893593	-3,694997947	0,000219889	0,009454901
KPNA2	11670,60796	0,718106512	2,980379083	0,002878919	0,046767574
KRAS	3822,133028	1,51005481	3,455897221	0,000548464	0,01636199
KRT17P6	163,1116971	3,574986277	4,363513731	1,28E-05	0,001428806
KRT18	4331,372163	2,449518656	3,70580143	0,000210723	0,009157654
KRT18P11	18,48199629	2,445906735	3,197501608	0,001386236	0,029615377
KRT18P17	23,44861595	2,869056349	3,884307405	0,000102622	0,005884218
KRT8	1321,432995	2,672421153	4,045776266	5,22E-05	0,003620947
KRT80	27,0763979	4,453801949	2,964837984	0,003028424	0,048133648
KRT8P3	31,81437364	2,154961574	3,801210001	0,000143991	0,007321923
KRT8P32	2,490872918	4,731731728	3,147365196	0,001647491	0,032861064
KRTAP5-9	4,130451326	-4,840031	-3,063583912	0,002187029	0,03965374
KRTCAP3	81,86827017	-1,853870166	-3,20256627	0,00136209	0,029377932
L1TD1	1,605866193	-4,214741462	-3,359961498	0,000779533	0,02063585
L3HYPDH	494,6843394	-1,480291105	-4,872066622	1,10E-06	0,000246378
LAMP2	19407,68903	0,789234028	3,796564368	0,000146715	0,007381834
LAPTM4A	33181,39344	1,082096813	3,408442638	0,000653348	0,018386317
LARGE2	230,4946325	-4,658224233	-3,699266859	0,000216223	0,009323337
LCN10	44,31218038	-5,479922708	-5,303592295	1,14E-07	4,54E-05
LCN2	3127,564225	-4,757554872	-5,804393621	6,46E-09	4,42E-06
LCN6	98,84128943	-3,52511274	-3,691713274	0,000222748	0,009541117
LDB2	76,31536926	-2,841015689	-3,416402562	0,000634544	0,018078505
LDHAP7	126,012891	1,18888951	3,203431131	0,001358005	0,029319008
LDLRAD4	2192,384793	-2,137486707	-4,093828973	4,24E-05	0,003225469
LEF1-AS1	114,0221658	-3,934373416	-3,30942684	0,000934872	0,022972774
LEPROT	9639,722204	1,11847089	3,178310128	0,001481362	0,030590392
LETM2	457,0868604	1,471287921	3,618790865	0,000295983	0,011351098
LGALS3	2192,835593	-3,061537703	-4,201585462	2,65E-05	0,002334763
LGI1	2,272745981	-5,224188004	-3,072070379	0,002125796	0,038863943
LGR6	138,3236089	-3,045254113	-3,10158041	0,001924906	0,036357102
LHPP	1147,887788	-1,412310377	-3,890945146	9,99E-05	0,005756968
LHX1	3,272656704	-5,300260001	-3,575202077	0,000349957	0,012426922
LILRB1	924,0852657	-2,428193275	-3,106722978	0,001891736	0,035928976
LILRB2	2314,493021	-2,660889137	-3,599622019	0,00031868	0,011837812
LILRB5	1423,99999	-3,292240225	-2,972674223	0,002952176	0,047486231
LIMD1	1626,967244	-1,515371636	-3,87712108	0,0001057	0,00600402
LIN7C	4356,241883	1,079067753	4,026174561	5,67E-05	0,003835966
LINC00114	84,25117044	-4,43680968	-3,279848249	0,001038629	0,024555417
LINC00278	28,48196874	22,50030358	8,177433429	2,90E-16	2,23E-12

LINC00426	734,3704162	-2,877378791	-3,957563835	7,57E-05	0,004709357
LINC00494	8,040964517	-7,052335215	-5,163621049	2,42E-07	8,28E-05
LINC00544	53,16645797	-8,324194578	-7,357968261	1,87E-13	6,39E-10
LINC00574	2,387662092	-4,825401511	-3,415354423	0,000636991	0,018084804
LINC00598	11,66062088	-4,364431614	-4,183407532	2,87E-05	0,002482991
LINC00639	5,158903458	-5,953116841	-7,181504438	6,89E-13	1,77E-09
LINC00642	12,01526358	-7,632789294	-6,172966062	6,70E-10	6,66E-07
LINC00689	1,738061841	-4,839216815	-3,267404131	0,001085386	0,025284701
LINC00944	4,080439827	-4,377731374	-3,712978867	0,000204834	0,009047668
LINC00951	7,473722702	-6,94814146	-5,496308328	3,88E-08	1,96E-05
LINC00957	23,92954136	-1,989003398	-3,756897932	0,000172033	0,008262665
LINC00989	168,6145147	-4,214000515	-3,410870956	0,000647557	0,018290227
LINC01001	32,78971177	-2,196636526	-4,271264959	1,94E-05	0,001899678
LINC01091	72,1740327	3,057791714	3,208934406	0,001332279	0,028925859
LINC01114	29,81992343	5,228387204	3,916480174	8,99E-05	0,0053653
LINC01151	2,581154768	-4,926726206	-4,120178142	3,79E-05	0,002988836
LINC01226	131,0116915	-3,957113427	-2,994644996	0,002747644	0,045503886
LINC01375	36,55213469	-7,441940462	-5,574984484	2,48E-08	1,36E-05
LINC01447	4,716307809	-6,283115119	-3,999217498	6,36E-05	0,004190429
LINC01471	2,381643036	-5,294347346	-3,096502315	0,001958183	0,036782544
LINC01630	3,356039598	-5,786836474	-3,176395428	0,001491175	0,030734414
LINC01697	2,185118259	-5,164588603	-4,442872644	8,88E-06	0,001110906
LINC01750	9,241620953	-6,824216809	-4,903764462	9,40E-07	0,000220647
LINC01781	5,863962729	-4,813756551	-4,987815715	6,11E-07	0,000162072
LINC01792	21,48529641	-2,818449322	-3,07007685	0,002140037	0,039031587
LINC01874	16,53727846	7,463469942	3,605623382	0,000311404	0,011705995
LINC01973	25,92645398	-6,342770958	-3,839918175	0,000123075	0,006544249
LINC02001	1077,327185	1,0159021	3,064212441	0,002182439	0,039593837
LINC02005	1,814946554	-4,895394589	-3,987882344	6,67E-05	0,004302803
LINC02043	1,72675214	-3,283262194	-2,984455461	0,002840836	0,046436606
LINC02150	2,384454597	-4,567812833	-3,562319897	0,000367592	0,012854056
LINC02202	66,61330373	-4,674369829	-3,010939583	0,002604407	0,044226072
LINC02227	59,19495806	-4,831317269	-3,1234821	0,001787247	0,034715448
LINC02240	1,927634659	-4,517495629	-4,011752966	6,03E-05	0,004033736
LINC02355	2,399993597	-4,802772188	-3,332961545	0,000859268	0,021863049
LINC02418	2,04912311	-5,074920708	-2,985403618	0,002832044	0,046353072
LINC02471	3,900976336	-6,006180955	-3,622002028	0,000292332	0,011335038
LIX1L-AS1	11,27482045	-2,009810237	-3,356010749	0,000790755	0,02076837
LMF1	1101,509522	-1,306556126	-3,668506602	0,000243971	0,010136501
LMF2	3978,732124	-0,827418783	-4,799958697	1,59E-06	0,000341668
LPIN3	8,155532417	-4,821040761	-4,996833756	5,83E-07	0,00015739
LRIG1	1459,706738	-2,967330692	-4,378064869	1,20E-05	0,00136532
LRP10	5439,453734	-1,394068643	-3,171776244	0,001515097	0,031061801
LRP12	1662,985755	2,000068792	3,761840126	0,000168668	0,008151927
LRRC25	2234,497125	-2,418732707	-3,371817639	0,000746739	0,020008569
LRRC37A3	208,9627122	-1,35993313	-3,296403153	0,000979314	0,023721583
LRRC38	16,37337248	-5,977807615	-3,623005114	0,0002912	0,011305393
LRRC75A-AS1	18322,92681	2,047799019	4,371588511	1,23E-05	0,001396121
LSM1	1129,943203	1,125058776	3,516173312	0,000437815	0,014308931
LSM3P3	16,24187577	1,333402936	3,377219778	0,000732225	0,019791938
LTBP2	269,5847673	-3,054502571	-3,708437891	0,000208542	0,009119853

LTF	23966,24512	-3,982268797	-4,73088989	2,24E-06	0,000434263
LUZP1	3763,777204	1,190118568	3,603709924	0,000313707	0,011748623
LY6K	65,15908118	3,270740167	3,353675863	0,000797457	0,020821124
LY96	286,3426477	-2,538574611	-3,850348103	0,00011795	0,006381948
LYPLA1	12623,54879	1,072523629	3,954163543	7,68E-05	0,004767197
LYPLA1P3	197,1424007	0,999988148	3,782913333	0,000155003	0,007623146
LYRM2	2376,049808	0,869653888	3,599246421	0,000319141	0,011837812
LYSMD3	2465,154262	1,369226766	4,515092142	6,33E-06	0,00086986
MAMDC2	756,0609817	2,858444095	4,135897108	3,54E-05	0,002864573
MAP3K10	109,7712435	-2,08736654	-4,283356101	1,84E-05	0,001822424
MAP3K6	560,4599091	-1,860451249	-2,969264139	0,002985139	0,04781658
MAP3K7CL	1507,169014	-4,135758663	-5,224551138	1,75E-07	6,40E-05
MAPK3	793,4941442	-0,994554437	-4,666074002	3,07E-06	0,000525445
MARCO	253,5948817	-3,543804314	-3,951449882	7,77E-05	0,004802224
MARK1	17,57394953	-4,176536228	-2,984424608	0,002841122	0,046436606
MAST2	1209,466635	-0,92396867	-3,798879892	0,000145352	0,007360093
MBIP	3105,150605	1,260791522	3,057868097	0,002229177	0,040228408
MCM3AP	1877,214385	-1,018678265	-3,275249328	0,001055688	0,024829223
MCOLN3	8,481447322	-4,486260436	-3,197317075	0,001387124	0,029615377
MED14	1446,921383	-0,905805212	-3,295174834	0,000983605	0,02373216
MED21	2909,798561	1,072171693	3,283902675	0,001023803	0,024377273
MED8	2012,708956	1,020490313	3,284278711	0,001022438	0,024377273
MEGF9	1549,76689	-0,921324894	-4,264217052	2,01E-05	0,001936052
MEOX1	9,046682696	-7,221552911	-5,023569871	5,07E-07	0,000141955
MET	108,3208137	-4,73716877	-3,796522685	0,00014674	0,007381834
METAP2	3600,408673	0,73553108	3,580057563	0,000343519	0,012369479
METTL21EP	6,218026416	-5,277472673	-3,035935945	0,002397903	0,041921772
METTL3	1720,683904	-0,990748489	-3,143450212	0,001669688	0,033057678
MFAP5	6,301376251	-4,906867685	-3,618719517	0,000296064	0,011351098
MFGE8	1145,990984	-1,1702782	-3,085881851	0,002029494	0,037799181
MGAT5	484,5635447	-1,102851662	-2,970182482	0,002976229	0,047748391
MIA2	2616,031283	0,600450136	3,071106797	0,002132669	0,038966449
MIB2	3303,404449	-0,649721122	-4,053149394	5,05E-05	0,00356007
MINK1	1671,953827	-1,493862553	-3,55434275	0,000378925	0,013167003
MIR1244-2	538,2806961	0,725460039	3,51799585	0,000434819	0,014263499
MIR3128	5,624363969	-2,311615869	-3,278021751	0,001045373	0,024662001
MIR3939	5,48929044	-1,951783797	-3,281407363	0,001032904	0,02454952
MIR3945HG	184,2212206	2,599773647	2,992478352	0,002767223	0,045658012
MIR4432HG	62,90984732	-4,171383939	-3,579425839	0,00034435	0,012380302
MIR4747	3,339332242	-5,786641535	-3,396244834	0,000683172	0,018829743
MIR4748	3,641052123	-2,982615108	-3,833478532	0,000126344	0,006647358
MIR5195	124,9841726	-4,590182839	-3,35459058	0,000794825	0,020806762
MIR6722	12,9187717	-7,737236675	-6,298099666	3,01E-10	3,57E-07
MIR6750	3,301435565	-3,91541554	-3,66096238	0,00025127	0,0102919
MKI67	3346,533595	-1,765996401	-3,541708943	0,000397544	0,013464448
MKNK2	7144,061463	-1,188692387	-3,033368137	0,002418404	0,042112781
MLH3	761,3637811	-1,481182957	-3,019114371	0,002535148	0,04343328
MLLT1	477,4773484	-0,752538111	-3,268727411	0,001080323	0,025216006
MLXIP	16658,57664	-2,275640039	-6,197893126	5,72E-10	5,87E-07
MMADHC	8179,552181	0,869063358	3,863673504	0,000111694	0,006217215
MMGT1	1435,475065	0,581884579	3,032375986	0,002426368	0,042189719

MMP25	398,8224306	-4,602241297	-6,306590882	2,85E-10	3,51E-07
MMP8	3347,686731	-2,750995036	-2,979109307	0,002890876	0,046845463
MMP9	9521,507481	-4,867210116	-5,075257376	3,87E-07	0,000116801
MORC3	3546,765683	0,773689593	2,996944186	0,002727006	0,045430923
MORF4	338,8811077	0,899439919	3,022780755	0,002504636	0,043054293
MORF4L1P3	98,66034276	1,192360126	3,72225561	0,000197451	0,008904736
MORF4L2	12159,05139	1,073968054	4,327124539	1,51E-05	0,00159279
MPEG1	2197,407405	-2,622099887	-3,282767777	0,001027933	0,024456704
MPPED2	398,2542359	-2,711506349	-3,899635432	9,63E-05	0,005627983
MRFAP1	8030,247348	0,660371214	3,503975943	0,000458367	0,014653933
MROH1	2312,388291	-0,674504163	-3,196173176	0,001392635	0,029671317
MROH2B	2,788710638	-4,838458208	-2,96620107	0,003015033	0,048041088
MRPL13	3995,480916	1,248235541	3,091381373	0,001992276	0,037218563
MRPL15	3241,91937	1,203510451	2,992709162	0,002765131	0,045658012
MRPL47	3735,51353	0,784052001	3,107648112	0,001885825	0,035883117
MRPL50	1687,316188	1,235858425	2,975730632	0,002922915	0,047114019
MRPL57P3	4,007336369	-3,549507909	-3,163088991	0,001561046	0,031618372
MRPS10	3337,764638	0,828033218	3,847046169	0,00011955	0,006423385
MRPS36	1086,111882	1,020610934	4,379593176	1,19E-05	0,001360821
MS4A1	175,7516945	-4,408349501	-3,654631504	0,000257552	0,010405829
MSANTD4	658,700251	1,543265414	3,31217366	0,000925741	0,022845804
MSMO1	2436,620588	1,863824534	3,213012738	0,001313505	0,028659722
MSTO2P	409,8944191	-1,115011009	-3,202219055	0,001363733	0,029380849
MT1X	211,5740463	-1,812659831	-3,276426655	0,001051296	0,024763775
MTA1	1673,034987	-0,947320443	-3,151728989	0,001623068	0,032511
MTHFD2	2607,887575	1,377694452	3,392873114	0,000691637	0,018944322
MTHFD2P1	3,603781672	-5,894936302	-4,730413067	2,24E-06	0,000434263
MTHFR	761,3957444	-1,023329232	-2,963339439	0,003043208	0,048133648
MTMR2	2959,126483	0,84244225	3,280394961	0,001036619	0,02454952
MTMR4	2157,666267	-0,800523604	-2,95401689	0,003136668	0,04869824
MTOR	1386,905412	-0,89769751	-3,149216804	0,001637087	0,032706681
MUC3A	2,313391401	-4,262192224	-2,984088435	0,002844246	0,046436606
MXD3	1411,192586	-1,350008869	-3,253886715	0,001138377	0,02609615
MYBPC1	3,311393083	-3,614862407	-2,958721257	0,003089184	0,04836992
MYBPC2	9,323661857	-3,69389999	-2,99587388	0,002736596	0,045492213
MYD88	7095,914276	-0,980352816	-3,254155791	0,001137299	0,026090925
MYH11	188,587105	-1,426012495	-2,95778498	0,003098582	0,04836992
MYH14	8,639648674	-6,275819883	-6,005711411	1,90E-09	1,68E-06
MYH2	4,309785991	-6,150417551	-3,578609144	0,000345428	0,012380302
MYH9	39170,81196	-1,105185682	-3,721838016	0,000197778	0,008904736
MYL9	484,1422836	-2,699406151	-4,302936421	1,69E-05	0,001706949
MYLK	2808,806547	-3,63062205	-5,742453857	9,33E-09	5,99E-06
MYLK-AS2	1,965656284	-4,534101293	-3,816456644	0,000135382	0,006981576
MYLPF	69,34815595	0,929643575	3,0077841	0,0026316	0,044467111
MYNN	1595,785653	0,848502346	3,276824922	0,001049814	0,024747808
MYO15B	2646,2521	-1,353825709	-2,991122705	0,002779538	0,045736841
MYO18A	5205,262123	-1,537271958	-3,374842863	0,000738578	0,019911223
MYO18B	56,95672199	-6,910425022	-4,794062682	1,63E-06	0,000349426
MYO19	1049,884736	-0,794784328	-3,084819935	0,002036754	0,037911458
MYO6	78,00840453	-2,848204412	-3,347294711	0,000816044	0,021076802
NAA15	3885,950951	0,882168529	3,094586274	0,001970876	0,03690837

NAA50	11377,57983	0,734553116	2,963658983	0,00304005	0,048133648
NACA	29174,98943	0,729416109	3,517317614	0,000435932	0,014277695
NACAP1	76,42924521	0,844087715	3,181494872	0,001465171	0,030456541
NANS	3558,496611	0,782352946	2,96306505	0,003045922	0,048133648
NAPG	2307,267037	0,830818324	3,072448007	0,002123108	0,038860958
NBDY	4028,51549	0,743712286	3,047113951	0,002310501	0,041189154
NBN	4769,280005	0,633805443	3,210714229	0,001324055	0,028787918
NBPF11	656,4229687	-0,91508268	-3,384116999	0,000714076	0,019455087
NCK1	2895,727406	1,135847447	3,22232072	0,001271567	0,028245121
NCOA7	14980,25069	2,314609576	4,285362792	1,82E-05	0,001811877
NDOR1	887,7323279	-1,110261201	-3,524124875	0,000424884	0,014060381
NDUFS4	2412,375804	0,956666631	3,356640811	0,000788955	0,020742586
NDUFV2P1	376,961178	0,898594306	3,003907165	0,002665366	0,044792499
NECAB2	21,66149809	-4,889654159	-3,350722215	0,000806011	0,020958331
NECAB3	257,2819711	-0,981226401	-3,114502691	0,001842553	0,035365756
NEIL1	1816,931596	-4,479399567	-6,619853585	3,60E-11	5,03E-08
NETO2	754,212433	2,389248665	3,195500066	0,001395888	0,029684845
NEU4	7954,843179	3,43535645	3,458503671	0,000543185	0,016252619
NFATC2IP	2789,213683	-0,71827963	-3,089517958	0,002004816	0,037407434
NFE2L2	7275,325751	0,984148165	3,667189268	0,000245231	0,010158533
NFU1	2494,064014	0,885741495	2,973474973	0,002944484	0,047387263
NGB	5,16297283	-6,41309676	-3,373416473	0,000742416	0,019944809
NGFR	232,2064452	-2,994090518	-2,959739971	0,003078988	0,048329591
NID2	284,445222	-1,84949466	-3,471536596	0,000517489	0,01577679
NIFK	2344,175928	1,037553447	3,966068679	7,31E-05	0,004590896
NLRC5	3905,847706	-1,517409393	-4,34963909	1,36E-05	0,001462777
NLRP1	4229,713724	-1,659056437	-3,711849161	0,000205751	0,009075134
NLRP14	2,200016715	-3,388503176	-2,985548731	0,0028307	0,046353072
NLRP6	192,9942008	-3,084856021	-3,073909277	0,002112737	0,038800482
NLRP7	5,20815284	-5,038480175	-4,553880242	5,27E-06	0,00076844
NMD3	6833,212454	0,958657417	3,901398717	9,56E-05	0,00559776
NMUR2	2,347225586	-5,271277885	-3,028318021	0,002459191	0,042510458
NOL12	266,1574563	-1,17866525	-4,000736026	6,31E-05	0,004180793
NPAS3	6,455070337	-4,055237757	-4,456006138	8,35E-06	0,001057505
NPIPA7	3,742503799	-2,136536361	-3,557069904	0,000375014	0,013060597
NPIPB13	46,42275357	-1,263884266	-2,951885872	0,003158396	0,048936865
NPIPB3	261,5067346	-1,399432909	-3,340257688	0,000837007	0,021474109
NPIPB5	578,5167307	-1,393630303	-3,149814902	0,001633739	0,032682218
NPY	723,0157409	-6,218684774	-4,431072781	9,38E-06	0,001154703
NPY1R	5,352577554	-6,025920757	-4,13332605	3,58E-05	0,002883291
NRBF2P3	58,17420631	0,986134376	2,975974068	0,002920596	0,047114019
NRG4	276,892087	2,646662162	4,038078207	5,39E-05	0,00369874
NRGN	3160,227243	-3,268055778	-5,175095466	2,28E-07	8,05E-05
NRIP2	158,4094057	-1,514619341	-4,349766952	1,36E-05	0,001462777
NRXN3	83,27351896	-4,414291398	-3,216772158	0,001296415	0,028413608
NSUN5P1	751,9161445	-1,450677761	-3,374021316	0,000740786	0,019944809
NSUN5P2	47,08642604	-1,710079291	-3,591540338	0,000328729	0,012077074
NTNG1	8,953431168	-5,496711276	-4,317426964	1,58E-05	0,0016213
NUMA1	5454,585896	-0,856809644	-3,022791129	0,00250455	0,043054293
OBSCN	515,8385317	-1,114331569	-3,290555817	0,000999897	0,023991099
OCIAD1	5910,65586	0,695048122	3,59661387	0,000322386	0,011929463

OCM	2,816503558	-3,152205214	-3,211250664	0,001321586	0,02877034
OFCC1	3,016030663	-5,164802663	-3,372816625	0,000744035	0,019970882
OGDH	2200,771357	-0,819418749	-3,01915799	0,002534783	0,04343328
OLA1	6632,746556	0,812505297	3,105684604	0,001898391	0,036001659
OLAH	10,42871116	-4,281822851	-3,526000762	0,000421886	0,014026562
OLFM4	369,1281248	-3,063579811	-3,487838297	0,000486942	0,015188954
OLFM5P	2,39395655	-4,107507133	-2,966786866	0,003009295	0,04800371
OMD	15,24706126	-4,35263235	-4,211832321	2,53E-05	0,002286973
OR1A1	2,493956585	-5,35768372	-3,008748256	0,002623264	0,044423775
OR2D3	2,185128008	-5,16688833	-2,992992713	0,002762563	0,045658012
OR51F5P	2,244182503	-5,206020478	-3,157323595	0,001592245	0,032067592
OR6K3	2,239840329	-5,201059513	-4,018643479	5,85E-05	0,003943307
OR8K2P	2,726402516	-5,026097522	-3,31275688	0,000923812	0,022826175
OR9G1	4,26613651	-4,752755373	-3,461894904	0,000536387	0,016135687
ORC4	3462,208728	0,857872532	3,039975378	0,002365975	0,041687553
ORC5	936,2541644	0,930145394	3,188286236	0,001431188	0,030145439
ORM1	222,2707975	-4,416095723	-3,911532614	9,17E-05	0,005429895
OSBPL11	806,8327156	-0,999569722	-3,289928276	0,001002129	0,023991099
OSBPL9	6814,812399	0,866663485	4,031345631	5,55E-05	0,00377743
OSGIN2	4655,741343	1,307616317	3,566001612	0,000362469	0,012709952
OTUD6B-AS1	1852,294652	1,052463152	4,055376837	5,01E-05	0,0035344
OTX1	5,776779525	-6,14245324	-4,166553511	3,09E-05	0,002635055
P2RY14	319,024588	-2,811380591	-3,583964675	0,000338418	0,012246885
P4HA2	280,5495183	-1,920332146	-3,15220113	0,001620446	0,032479606
PA2G4P6	60,55401733	-1,163475078	-3,620440577	0,000294102	0,011337574
PABPC3	606,1945194	1,027352556	3,503413261	0,000459336	0,014669693
PACS1	6796,973031	-0,849336926	-3,369568901	0,000752859	0,020102567
PALM2	3,761925492	-5,512499814	-3,204381091	0,001353532	0,029242937
PAN2	1703,145399	-1,225701189	-3,769554187	0,000163539	0,007991885
PAPPA	36,5661572	-4,223626699	-3,034489831	0,002409429	0,04202781
PAQR4	1044,064571	-1,541627024	-4,330247863	1,49E-05	0,001575761
PARL	553,6524571	0,653998445	4,66895787	3,03E-06	0,000523606
PARP11	744,9662213	0,63325373	3,155276649	0,00160346	0,032244101
PART1	8,630330183	-6,728998675	-4,992231111	5,97E-07	0,000159787
PASK	915,6184529	-1,172196921	-3,032038268	0,002429084	0,042189719
PAX5	521,6515146	-6,347610146	-3,894973558	9,82E-05	0,005704857
PCA3	5,13536206	-4,272650249	-3,462325471	0,000535529	0,016135687
PCDH11X	4,30574878	-5,22726584	-3,719052862	0,000199971	0,008961446
PCDH15	4,527173106	-5,317570905	-4,201266436	2,65E-05	0,002334763
PCDH19	5,015259914	-5,463839647	-3,70351162	0,000212635	0,009194392
PCDH9	1092,222144	-2,3286581	-3,17828737	0,001481478	0,030590392
PCED1B-AS1	339,2063598	-2,997602532	-3,589690011	0,000331071	0,012131457
PCF11	1853,154244	-0,619384062	-2,959808266	0,003078306	0,048329591
PCNP	18126,88056	1,014756941	3,253558992	0,001139691	0,02609615
PCNT	2408,059205	-0,822211929	-3,165697172	0,001547118	0,031407427
PCSK9	9,674329488	-7,318487579	-3,743422207	0,000181531	0,008491388
PDE5A	226,2165187	-1,399950518	-3,226148513	0,001254682	0,028011534
PDZD4	52,98550739	-4,068862209	-3,113282427	0,001850189	0,035468095
PDZK1IP1	320,9718055	-3,286873174	-4,433965325	9,25E-06	0,001143886
PDZRN4	38,45687786	-4,084714529	-3,033473725	0,002417558	0,042112781
PEAK3	171,2938939	-2,149612202	-3,195443224	0,001396162	0,029684845

PELI3	323,0192254	-1,182790628	-2,943322973	0,003247095	0,049909288
PEX13	1540,774791	0,936437913	3,040435547	0,002362362	0,041655243
PEX2	3768,087017	1,392374882	3,789308305	0,000151067	0,007537942
PF4V1	347,908116	-5,506938885	-5,544399052	2,95E-08	1,59E-05
PFAS	3879,904321	-1,10555955	-3,271625346	0,001069312	0,025053958
PFDN2	2588,216082	0,886778511	4,587044007	4,50E-06	0,00069903
PFKFB2	586,3864449	-3,051328065	-5,970378302	2,37E-09	1,97E-06
PGLYRP1	1673,197712	-3,989284158	-4,170885339	3,03E-05	0,002594818
PIEZO1	6266,50941	-0,874024832	-3,385056958	0,000711635	0,019409975
PIGA	2501,526953	1,539903774	3,468399622	0,000523568	0,015912231
PIGQ	2055,230479	-0,883959048	-2,989646537	0,002793004	0,045909358
PIK3CB	2700,617213	1,103091027	3,544744079	0,000392994	0,013363351
PIK3CD	8676,075266	-1,574634519	-5,283993278	1,26E-07	4,93E-05
PIK3CD-AS1	409,0885414	-2,720795703	-4,162758448	3,14E-05	0,002659404
PILRA	1316,331338	-2,780075001	-3,84870221	0,000118745	0,006413702
PKD1P5	393,7119186	-1,576483136	-4,203771171	2,63E-05	0,002334763
PKD1P6	1072,009047	-1,396030085	-3,33242764	0,000860919	0,021886952
PKHD1	8,836420472	-5,490822153	-4,752175928	2,01E-06	0,000402308
PLBD1	2989,34283	-3,633942673	-3,605757617	0,000311244	0,011705995
PLBD1-AS1	1,786510299	-4,874414841	-3,297186163	0,000976587	0,023674172
PLCB3	439,093503	-1,211511201	-4,716952902	2,39E-06	0,000455481
PLCG1	782,9180767	-2,325247844	-3,626203544	0,000287619	0,011222961
PLIN4	89,82820344	-2,844744985	-3,047741937	0,002305678	0,041189154
PLVAP	825,2373136	-2,513738267	-3,564994332	0,000363864	0,012744349
PLXDC1	62,4462175	-4,066480274	-3,633589366	0,000279506	0,010989959
PLXNA1	518,266766	-2,376517043	-3,729106598	0,00019216	0,008831428
PLXNA3	292,2806688	-1,165010324	-2,945378382	0,003225599	0,049628448
PLXNC1	2421,894141	-1,368889538	-4,266246746	1,99E-05	0,001936052
PMP2	5,771774738	-6,137459797	-4,509730808	6,49E-06	0,00088424
PNO1	2413,460987	0,806713897	2,961580771	0,003060642	0,048173817
PNPLA6	1313,838425	-1,497663916	-4,080762552	4,49E-05	0,003346919
PNPLA7	1330,677551	-2,638531796	-4,790755332	1,66E-06	0,00035037
PNRC2	14972,11521	0,953723244	4,066373314	4,78E-05	0,003450674
PNRC2P1	310,0135107	1,145006894	4,893229378	9,92E-07	0,000229617
POC1B	1908,248223	0,533598373	3,250784689	0,00115087	0,026304253
POF1B	3,155693884	-4,78997848	-3,548668916	0,000387184	0,013288986
POLE	2594,976357	-1,308031569	-3,008496954	0,002625434	0,04443609
POLG	3990,560756	-0,676307523	-3,344064127	0,000825607	0,021288063
POLR1D	4869,005852	0,682933276	3,183816233	0,001453473	0,030329095
POLR2J2	228,5459602	-1,178055424	-3,306491371	0,000944723	0,023101807
POLR2K	3295,851334	0,898475293	3,259852743	0,001114701	0,025725855
POU2AF1	1048,862679	-4,57984408	-3,620990675	0,000293477	0,011337574
POU4F1	33,32151105	-4,785767895	-3,861909339	0,000112504	0,006240848
POU6F2	8,46913236	-6,463292734	-3,602783159	0,000314828	0,011748623
PPA1	7864,484817	1,195780419	4,046316169	5,20E-05	0,003620947
PPARG	244,3950643	-3,094027392	-3,440756864	0,00058009	0,016976442
PPBP	8140,818411	-2,393056117	-2,966069891	0,003016319	0,048041088
PPHLN1	6677,161391	0,914893695	3,336162402	0,000849435	0,021702542
PPIL4	2873,890936	1,015538781	3,205953209	0,001346159	0,029124518
PPP1R12C	1075,533422	-1,283116984	-3,81361053	0,000136951	0,007046752
PPP1R32	152,6089391	-1,407121232	-3,360816804	0,000777124	0,02058976

PPP1R37	288,2656372	-1,125240134	-3,695097881	0,000219802	0,009454901
PPP1R3F	447,1942244	-1,253231258	-3,760441408	0,000169614	0,008184796
PPP2R3C	2226,887036	0,776306252	3,047990109	0,002303775	0,041189154
PRAMENP	3,12524099	-5,68738717	-3,474858085	0,000511124	0,015657676
PRCD	166,0063676	-2,975753275	-3,836363309	0,00012487	0,006605433
PRELID3A	35,11295515	-1,249333703	-3,016346103	0,002558411	0,043688182
PREX1	8043,069505	-1,26745276	-3,383257883	0,000716313	0,01947702
PRG3	916,6339779	-3,91475239	-4,712599352	2,45E-06	0,000459133
PRKD1	27,99126856	-4,215013739	-3,551841926	0,000382545	0,013188579
PRKG2	603,2845131	-2,663670247	-3,238783809	0,001200405	0,027214195
PRKX	3388,014105	-1,047923234	-3,440966107	0,000579641	0,016976442
PRKY	412,9112022	4,739187521	4,506484537	6,59E-06	0,000893915
PRPF4	3475,930228	0,921977006	3,483226344	0,000495409	0,015378271
PRR13P2	49,32456974	-1,897967674	-3,328846479	0,000872065	0,022005642
PRRC2A	1636,520113	-1,086855992	-4,316962457	1,58E-05	0,0016213
PRRC2B	4157,724462	-1,038743775	-3,803093021	0,000142901	0,007295991
PRSS33	17,89845056	-7,784494623	-4,4974406	6,88E-06	0,00091268
PSAP	105188,5211	-1,812473805	-4,351861121	1,35E-05	0,001462649
PSMB1	15196,53377	0,695259538	3,381038921	0,000722123	0,019570427
PSMB2	9215,544748	0,589780192	3,182239814	0,001461408	0,030420794
PSMC1P3	39,47985097	0,899952313	2,953012212	0,003146895	0,048805426
PSMC1P9	60,42500464	0,756773064	3,490260153	0,000482551	0,015113208
PSMD12	7429,772796	1,06743152	3,12300171	0,001790167	0,034728339
PSMD14	4710,567494	0,553002783	2,962625111	0,003050278	0,048133648
PTCRA	281,4358295	-4,096369246	-4,140015986	3,47E-05	0,002844798
PTDSS1	13020,89668	0,906942077	3,547590968	0,000388771	0,013311581
PTGES3	20818,61645	0,689849876	4,281937511	1,85E-05	0,001828205
PTGES3P1	290,3119269	0,857865513	4,687501705	2,77E-06	0,000509163
PTGES3P3	44,97086495	1,21673381	4,001586429	6,29E-05	0,004174771
PTH2R	439,6666573	3,011778577	3,532970111	0,000410919	0,013781003
PTMAP4	69,41306096	0,98702057	4,314759915	1,60E-05	0,00162882
PTP4A1	25539,05897	1,142113826	3,2119338	0,001318448	0,028726854
PTP4A2P2	39,66132464	-2,582085539	-3,754386927	0,000173766	0,008317073
PTPN2	4089,073985	0,774940319	2,975750547	0,002922725	0,047114019
PTPN3	1,29868806	-4,425328385	-3,169535192	0,00152683	0,031212819
PTPN5	7,08971946	-6,870268828	-3,578083613	0,000346123	0,012390791
PTPRG-AS1	6,678375376	-5,661464871	-6,203466438	5,52E-10	5,86E-07
PUS10	569,94742	1,009494915	3,432162257	0,000598789	0,017457313
PYURF	7806,103156	0,670129296	4,599851596	4,23E-06	0,000670954
RAB43	102,3582057	-1,629964412	-3,128022709	0,001759866	0,034273506
RAB4A	3376,948257	0,666404267	4,122494481	3,75E-05	0,002981578
RAB6C	86,65082836	0,71742829	3,004907748	0,002656614	0,044717976
RAB8B	6399,252593	1,746594516	3,436708022	0,00058883	0,017206631
RAD51-AS1	417,565753	-1,461859214	-3,373636099	0,000741824	0,019944809
RAG1	1201,435209	-4,92977642	-3,234623412	0,001218033	0,027532726
RALA	5190,158266	1,514317026	4,695131846	2,66E-06	0,000497135
RALBP1	3687,990871	0,578151132	3,043335912	0,00233971	0,041410299
RALGPS1	143,2966879	-2,076494619	-4,752963623	2,00E-06	0,000402308
RANBP3	670,9526297	-0,773372133	-3,713181436	0,00020467	0,009047668
RAPH1	159,8441793	-3,034745841	-3,61113827	0,000304856	0,011544408
RASGRP2	12021,19353	-1,1317366	-3,522361961	0,00042772	0,014113834

RBM14-RBM4	30,19848834	-1,660878684	-3,473701825	0,000513331	0,015709668
RBM7	3497,768441	0,978622344	3,340310297	0,000836848	0,021474109
RBMS3-AS2	1,963953784	-4,78196714	-3,260649889	0,001111572	0,025672893
RBMXP2	188,4513209	0,640173806	2,965486291	0,003022048	0,048107444
RCHY1	2602,52125	0,962182924	3,41806982	0,000630669	0,018044995
RCSD1	10939,69098	-1,484497516	-4,260868061	2,04E-05	0,001948563
REM2	53,43072399	-2,601647262	-3,036634095	0,002392357	0,04186334
RERG	2,532347454	-5,386846103	-3,217657062	0,001292422	0,028413608
RETN	449,314015	-3,220963431	-3,140249743	0,001688039	0,03335664
RF00003	26,54643606	2,405310634	3,236685616	0,001209266	0,027374749
RF00012	38,69393254	1,723424457	3,279256066	0,001040811	0,024573208
RF00017	1,025264892	-4,0775595	-2,956567683	0,003110839	0,048492868
RF00019	25,5453791	-3,514311884	-5,093410389	3,52E-07	0,000112648
RF00086	23,20271668	2,037448209	2,957511609	0,003101331	0,04836992
RFX1	159,1022688	-1,050549025	-3,742785888	0,000181991	0,008491388
RGP1	655,6501894	-0,941029368	-3,265666719	0,001092067	0,025374692
RGPD2	55,39355091	-1,808755183	-2,963888328	0,003037785	0,048133648
RGS11	8,427993491	-5,240705923	-3,098226504	0,001946826	0,036658669
RGS6	123,5917469	-2,670109917	-3,061185228	0,002204627	0,039925788
RHEBP1	30,00781589	1,561874635	3,633910094	0,000279158	0,010989959
RIC3	67,64050165	-2,740840503	-3,000547015	0,002694951	0,045165743
RIMS3	607,0193083	-4,306387124	-4,665940762	3,07E-06	0,000525445
RIPK2	8736,253489	1,18240662	3,3230624	0,00089035	0,022307666
RLIMP1	47,81995439	-3,987742326	-5,445637436	5,16E-08	2,56E-05
RN7SL610P	2,810503673	-3,024563436	-3,099615038	0,001937723	0,036531955
RNF133	2,836357072	-5,549684871	-3,03863194	0,00237655	0,041771212
RNF2	2691,326201	1,162975124	4,20852048	2,57E-05	0,002307214
RNF219	685,9976849	1,599096648	3,109767589	0,001872346	0,035737085
RNF219-AS1	2,196066025	-5,177517811	-2,963894984	0,003037719	0,048133648
RNF43	187,0429863	-1,986412282	-3,682272272	0,000231164	0,009802832
RNU1-85P	9,867632057	5,738769183	4,757112864	1,96E-06	0,000397763
RNU2-63P	84,20143153	2,38491079	3,913731411	9,09E-05	0,005401438
RNU4-78P	1,974184723	-3,357788495	-3,009218206	0,002619209	0,044391118
RNU6-1294P	1,465725846	-3,57520782	-3,521562772	0,000429011	0,014141289
RNU7-113P	1,261160169	-3,82425584	-3,461815777	0,000536544	0,016135687
RNVU1-3	10,33967242	3,282075821	3,058449723	0,002224854	0,040197525
RNVU1-6	71,44053605	2,289627386	3,853026767	0,000116667	0,006343286
RP2	4033,505486	0,896665029	3,013197672	0,002585105	0,04397106
RPF2	2302,672073	1,156093478	4,539067782	5,65E-06	0,000797969
RPF2P1	17,82389601	2,181769192	4,238480273	2,25E-05	0,002093125
RPL10AP2	169,5089764	1,231861205	3,111073205	0,001864087	0,035645747
RPL11	16605,0507	0,94565551	3,495723222	0,000472779	0,014913362
RPL12	21712,46488	1,203611896	3,540061738	0,000400033	0,013519022
RPL12P12	111,7847356	1,813511069	4,559238757	5,13E-06	0,00075266
RPL12P13	14,78992337	1,691447355	4,141399281	3,45E-05	0,00284157
RPL12P14	75,5429545	1,227231712	3,225830394	0,001256078	0,028012639
RPL12P35	10,99857444	1,847826637	3,048414635	0,002300523	0,041189154
RPL12P42	210,9148206	1,305683872	3,867401663	0,000110001	0,006135155
RPL12P6	179,0174231	1,321686766	3,501407079	0,000462808	0,014719504
RPL13	93440,94334	0,872102427	3,07326784	0,002117284	0,038800482
RPL13P12	8016,405702	1,076556108	3,582669137	0,000340101	0,012289551

RPL14P3	56,69292954	1,239978592	3,244297837	0,001177406	0,026791417
RPL15P18	666,9119833	1,240478697	3,791478828	0,000149753	0,007484485
RPL15P2	1104,602378	1,252272657	3,505377951	0,00045596	0,014592126
RPL15P20	49,43447939	1,286113033	3,533491398	0,000410109	0,013781003
RPL17P36	302,4073179	1,200776774	3,499149771	0,000466744	0,014768405
RPL18AP16	9,300497904	1,679076526	3,894049124	9,86E-05	0,005709822
RPL19	38335,79174	0,832625992	3,06705727	0,002161774	0,039334839
RPL19P16	106,3092349	1,214103273	4,002967085	6,26E-05	0,004159437
RPL19P21	25,26389594	1,252871906	3,221066393	0,001277146	0,02825435
RPL21	50700,30859	1,177121777	3,141361967	0,001681641	0,033251553
RPL21P11	234,9169215	1,26468798	3,212541896	0,00131566	0,02868641
RPL21P120	403,7989975	1,389430122	3,651671683	0,000260539	0,010475737
RPL21P23	1,311816584	-4,432715057	-3,423898161	0,000617297	0,017811376
RPL21P28	2230,769562	1,332259947	3,575289786	0,00034984	0,012426922
RPL21P3	63,47580623	1,412754261	3,352514844	0,000800809	0,020859373
RPL21P39	161,5753453	1,436171283	3,742725378	0,000182035	0,008491388
RPL21P93	249,9941894	1,34307841	3,483642148	0,00049464	0,015378271
RPL22	6596,118311	0,952130914	5,345814243	9,00E-08	3,80E-05
RPL22P1	114,4906704	0,643261427	2,980951502	0,002873543	0,046720729
RPL22P16	22,41671194	1,501719171	3,585205123	0,000336813	0,012215472
RPL22P2	56,74206523	1,011312283	3,488415185	0,000485893	0,015186991
RPL23	14336,54169	0,912308396	3,193605086	0,001405082	0,029812719
RPL23A	2754,138701	0,848487998	4,463169101	8,08E-06	0,001027373
RPL23AP2	51,18451535	1,200075808	4,22882516	2,35E-05	0,002166513
RPL23AP3	113,4880103	1,254931134	4,970275006	6,69E-07	0,00017153
RPL23AP42	162,9954695	0,920891817	3,178916897	0,001478265	0,030590392
RPL23AP43	55,14263102	1,24548412	3,740173062	0,000183894	0,008565102
RPL23AP65	451,7577906	0,969624882	3,813336102	0,000137103	0,007046752
RPL24	13417,97992	1,065663077	3,028866378	0,002454732	0,042457215
RPL24P4	470,6525894	1,153813769	3,219129987	0,001285802	0,028413608
RPL24P8	332,7584035	1,242309235	3,481648233	0,000498338	0,015419425
RPL27A	40250,03152	1,367390715	2,97365011	0,002942804	0,047387263
RPL3	155609,3189	0,882981424	2,980129247	0,002881268	0,046767574
RPL30	3495,557049	0,918174136	3,58942787	0,000331405	0,012131457
RPL30P4	135,8543661	1,160586287	3,661865418	0,000250385	0,0102919
RPL31	33610,64434	1,328819228	3,527998287	0,000418715	0,013975552
RPL31P2	25,46930856	1,555694631	3,291850827	0,000995304	0,023958109
RPL31P49	25,32102932	1,422383451	3,483827055	0,000494299	0,015378271
RPL31P63	163,1702555	1,400706042	3,46271524	0,000534754	0,016135687
RPL32	32316,66319	1,197317485	2,948125665	0,003197071	0,049263372
RPL34	25127,75893	1,414744671	3,358200762	0,000784516	0,020678851
RPL34P18	1349,764339	1,494132958	3,485259627	0,00049166	0,015320575
RPL34P27	25,2219318	1,966674878	3,708978596	0,000208097	0,009113347
RPL34P33	178,7094417	1,471032634	3,432715656	0,000597568	0,017438236
RPL34P34	495,5566633	1,458938654	3,357112244	0,000787611	0,020742586
RPL35A	14162,26305	0,957308379	3,15725884	0,001592599	0,032067592
RPL35P5	382,8193935	1,187972665	3,462422275	0,000535337	0,016135687
RPL36AP21	110,7410302	0,832115158	3,216158992	0,001299188	0,028413608
RPL37	14013,31673	1,038827514	3,73544951	0,00018738	0,008661972
RPL37A	10163,3555	0,873288128	3,075108971	0,002104257	0,038771319
RPL37P2	206,2408877	1,344589154	4,388084266	1,14E-05	0,001328528

RPL37P6	106,2680204	0,970216694	3,033713047	0,002415641	0,042112306
RPL38	5244,354367	0,978943544	3,644970335	0,000267423	0,010692391
RPL39	10600,26715	1,479273177	3,334311091	0,00085511	0,021811317
RPL39P3	325,9576012	1,451882107	3,105578692	0,001899071	0,036001659
RPL39P38	97,80954077	1,381274477	3,147953407	0,001644179	0,032827068
RPL3P2	1503,46915	1,071737838	3,607789676	0,000308817	0,011665692
RPL3P7	264,5975411	1,053887773	3,220989329	0,001277489	0,02825435
RPL4	42704,60535	0,704186451	3,407166148	0,000656412	0,01840523
RPL4P3	53,68587232	0,978450018	3,176281476	0,001491761	0,030734414
RPL4P4	1408,021007	0,822990393	4,039600938	5,35E-05	0,003687706
RPL4P5	326,6792363	0,975138667	4,112176517	3,92E-05	0,003040724
RPL5	55688,88821	1,243901242	3,436596275	0,000589073	0,017206631
RPL5P1	918,8864196	1,353289433	3,587399352	0,000333993	0,012158626
RPL5P12	66,8457341	1,273942426	3,261637791	0,001107706	0,025628564
RPL5P17	95,96009952	1,448689911	3,634933022	0,000278053	0,010960837
RPL5P18	36,4080433	1,463178075	3,16015982	0,001576826	0,031854165
RPL5P23	329,1401192	1,154300007	3,012178293	0,002593802	0,044094635
RPL5P29	68,29225889	1,148338752	3,128309757	0,001758148	0,034273506
RPL5P3	131,6736252	1,364313826	3,828635188	0,000128856	0,006735288
RPL5P34	768,2334498	1,385313567	3,81923607	0,000133866	0,006914967
RPL5P4	312,0307655	1,381857429	3,999175543	6,36E-05	0,004190429
RPL5P5	46,61617157	1,635501336	3,419233521	0,000627978	0,017984708
RPL5P9	71,41103565	1,627336363	4,341148708	1,42E-05	0,001515188
RPL6	15034,95368	0,664536857	3,084040311	0,002042099	0,037962977
RPL6P27	709,4953917	0,665649052	3,036913833	0,002390138	0,04186334
RPL7	76601,85534	1,306426829	4,422951966	9,74E-06	0,001170885
RPL7AP30	231,9821504	1,015417425	3,353980689	0,000796579	0,020818578
RPL7AP50	145,2439366	1,223364963	4,228033239	2,36E-05	0,002166513
RPL7AP6	827,8941938	0,919094162	3,393050401	0,000691189	0,018944322
RPL7P1	2297,503383	1,326323485	4,427258822	9,54E-06	0,001161366
RPL7P10	27,60959597	1,45166557	3,666860277	0,000245547	0,010158533
RPL7P15	78,24412388	1,655129452	4,614712569	3,94E-06	0,000640622
RPL7P16	109,0925566	1,090209497	3,03109297	0,002436702	0,042264083
RPL7P19	133,224038	1,631112627	4,591403587	4,40E-06	0,000695115
RPL7P23	1141,961346	1,444439317	4,745745536	2,08E-06	0,000412625
RPL7P26	301,7671232	1,395068891	4,588600626	4,46E-06	0,00069903
RPL7P32	252,1495327	1,522504468	5,292487628	1,21E-07	4,76E-05
RPL7P36	7,310886295	2,834388181	4,065672528	4,79E-05	0,003450674
RPL7P46	17,89218014	-1,643492159	-3,082771629	0,002050825	0,038069658
RPL7P47	203,7138922	1,48255431	4,780758212	1,75E-06	0,000361721
RPL7P50	23,3294081	1,157715358	3,356834275	0,000788404	0,020742586
RPL7P59	42,78587723	1,580740094	3,977668955	6,96E-05	0,004463065
RPL7P6	382,9863367	1,570179527	5,72282738	1,05E-08	6,58E-06
RPL7P8	128,1014371	1,484829395	4,883395239	1,04E-06	0,0002378
RPL7P9	1977,13389	1,243981328	4,138888584	3,49E-05	0,002844798
RPL9	34164,56881	1,455896412	3,309124278	0,000935883	0,022976894
RPL9P18	248,4441373	1,57062907	3,774997757	0,000160009	0,007844268
RPL9P21	80,79304785	2,015403829	4,675227759	2,94E-06	0,000523606
RPL9P28	111,3310724	1,986184087	4,334079813	1,46E-05	0,001559282
RPL9P3	310,8041855	1,673855569	4,045212831	5,23E-05	0,003620947
RPL9P32	301,8134891	1,682854895	4,149104248	3,34E-05	0,00277731

RPL9P7	309,3357402	1,554430981	3,187205203	0,001436548	0,030156945
RPLP0	83123,0495	0,889552204	3,403789296	0,00066458	0,018474259
RPLP0P6	3622,776993	0,871225796	3,144402249	0,001664265	0,033013999
RPLP1	59871,73008	1,034530798	3,587312157	0,000334104	0,012158626
RPP14	298,1352328	1,056746832	3,981473329	6,85E-05	0,004411262
RPS12	19498,05054	1,229271957	3,396679373	0,000682088	0,018816716
RPS13	20039,38229	1,006011825	3,048578153	0,002299271	0,041189154
RPS13P2	647,0976555	1,028297314	3,109929139	0,001871322	0,035737085
RPS15AP11	72,04818098	1,362647683	3,301996215	0,000959994	0,023363893
RPS18	91676,51454	1,652096328	3,529501896	0,000416343	0,01391742
RPS18P12	310,5099998	1,899052099	4,161317048	3,16E-05	0,002668916
RPS18P9	236,1594567	1,272718219	3,09524351	0,001966514	0,036871534
RPS19	77890,94217	1,127269565	3,638712752	0,000274004	0,010870835
RPS19P1	180,5409885	1,177324608	3,430878229	0,000601631	0,017523559
RPS19P3	611,7065763	1,149546163	3,707145192	0,000209609	0,009153511
RPS2	143517,7162	0,864669987	3,393972955	0,000688865	0,018902037
RPS20	22472,55232	1,434584569	4,099407411	4,14E-05	0,003180115
RPS20P14	495,311839	1,574357571	4,318215555	1,57E-05	0,0016213
RPS20P15	9,87572518	-4,713948508	-3,37736776	0,000731831	0,019791938
RPS21	8455,021477	1,433500052	2,949615579	0,003181695	0,049123974
RPS23P8	1523,5705	0,923542767	3,022126451	0,002510057	0,043099339
RPS24	13068,06167	1,197739976	4,500181002	6,79E-06	0,000908827
RPS24P8	527,117002	1,268082285	4,673276771	2,96E-06	0,000523606
RPS27A	36444,74299	1,18596893	3,50042199	0,000464522	0,014733151
RPS27AP1	75,6696783	1,551869352	4,351191609	1,35E-05	0,001462649
RPS27AP11	50,29998447	1,512153132	3,765070283	0,000166502	0,008059913
RPS27AP16	2709,103758	1,247742095	3,541881419	0,000397284	0,013464448
RPS29	10219,2679	1,485537302	3,458765065	0,000542658	0,016252619
RPS2P4	66,77039445	1,02015589	3,308284183	0,000938695	0,023009239
RPS2P55	1042,092606	1,001040991	3,44309163	0,000575104	0,01689479
RPS2P7	781,1428085	1,130178963	4,081237195	4,48E-05	0,003346919
RPS3	104286,2028	1,145443855	2,979929099	0,002883151	0,046767574
RPS3A	39336,46002	1,676168095	3,411587053	0,000645859	0,018272449
RPS3AP25	747,221737	1,828856119	3,668597533	0,000243885	0,010136501
RPS3AP26	5770,79855	1,702224016	3,492413245	0,000478677	0,015056751
RPS3AP29	163,3054807	1,91437181	3,875939935	0,000106214	0,006022112
RPS3AP35	33,68670421	1,664038549	2,997762221	0,002719698	0,045341456
RPS3AP47	1640,289449	1,851589312	3,728686799	0,00019248	0,008831428
RPS3AP49	353,8258386	1,795628342	3,626510578	0,000287277	0,011222961
RPS3AP5	1845,318249	1,782533966	3,638284692	0,00027446	0,010874901
RPS3AP6	2817,79235	1,502089376	3,023100547	0,002501991	0,043054293
RPS3P6	124,6557748	1,205161245	3,112170295	0,001857173	0,035557709
RPS4XP13	66,85345695	1,249961374	3,295523941	0,000982383	0,02373216
RPS4XP16	131,5017896	1,350605904	4,166114384	3,10E-05	0,002635055
RPS4XP3	151,7291048	1,104429406	3,016932458	0,002553467	0,043649966
RPS4XP6	161,4772144	1,160773927	2,979092193	0,002891038	0,046845463
RPS4Y1	2930,26769	14,93252019	8,955993688	3,37E-19	5,18E-15
RPS5	31113,08267	1,251650646	2,957664062	0,003099797	0,04836992
RPS6	123080,4808	1,360903314	3,135607869	0,001714983	0,033759077
RPS6P12	3,703844219	-5,488866523	-3,131036813	0,001741903	0,034117697
RPS7P14	50,49055264	1,540566719	3,056116929	0,002242238	0,040393083

RPS8	24007,73303	1,074063668	3,407194691	0,000656343	0,01840523
RPS8P10	41,77315761	1,499540167	4,264471638	2,00E-05	0,001936052
RPSAP8	88,77678136	1,131033133	3,094827676	0,001969273	0,036900791
RPSAP9	206,0947023	1,352342785	4,550971763	5,34E-06	0,000771825
RRN3	4382,662688	1,061363402	3,34075544	0,000835508	0,021471435
RSL1D1	15525,60178	0,98018724	4,52483695	6,04E-06	0,000845832
RSL24D1	20736,64436	1,497699939	3,359289988	0,00078143	0,020654123
RSL24D1P1	47,62299935	1,769480182	3,744851001	0,000180501	0,008484092
RSL24D1P11	29,38729215	2,011361424	3,975879993	7,01E-05	0,004473005
RSL24D1P2	11,94180807	2,046288742	3,130910854	0,001742651	0,034117697
RTEL1-TNFRSF6B	100,8809062	-2,079656487	-5,017318633	5,24E-07	0,00014533
RTRAF	8076,048813	0,712891911	3,42253464	0,000620402	0,017817457
RUBCNL	574,2663243	-3,188991184	-3,869114371	0,000109231	0,006125514
RUNX2	2866,511594	0,863937075	2,976320978	0,002917294	0,047114019
RWDD4	1851,775723	0,691260582	3,284477546	0,001021716	0,024377273
RWDD4P1	21,55125663	1,067008937	3,151049235	0,001626851	0,032565573
RWDD4P2	221,4610566	0,842955072	3,971950964	7,13E-05	0,004512988
S100A12	4285,213509	-4,159826314	-4,298545564	1,72E-05	0,001729732
S100A8	22261,79917	-3,243580355	-3,514053553	0,000441324	0,014362618
S100A9	44674,47568	-3,421540902	-3,588818692	0,00033218	0,012131457
S100Z	613,3893448	1,597109178	3,196790125	0,00138966	0,029628436
SAGE4P	3,557334136	-4,698156931	-3,383257096	0,000716315	0,01947702
SAMD1	1964,413201	-1,415552563	-3,404642442	0,000662507	0,018458475
SAMMSON	7,852310431	-3,617369668	-3,597873485	0,00032083	0,011886138
SAP18	15397,53683	0,823803454	2,997970643	0,002717839	0,045341456
SARM1	334,413427	-1,04230149	-3,129241137	0,001752584	0,034236554
SBF1	4723,6711	-1,370571793	-4,384004367	1,17E-05	0,00134858
SCGB1C1	6,935511029	-6,411048579	-2,96241836	0,003052327	0,048133648
SCHIP1	309,74183	-1,254837337	-2,967892726	0,00299849	0,047930685
SCIMP	178,666465	-2,892714346	-3,328426004	0,000873382	0,022005642
SCML1	108,9418784	-1,785816989	-2,98387854	0,002846197	0,046436606
SCN4A	26,1038504	-5,255255759	-3,968250074	7,24E-05	0,004564448
SCN5A	13,72931729	-3,61547078	-3,300489349	0,000965164	0,023471167
SCOC	3783,051213	1,278880419	3,863276309	0,000111876	0,006217215
SCRIB	1348,387255	-1,327969886	-3,47953054	0,000502293	0,01551063
SCTR	2,253129417	-4,972198043	-4,165130662	3,11E-05	0,002639152
SDCBP2-AS1	205,9522783	-1,160656529	-3,304749059	0,000950615	0,023227441
SDHAP1	1172,730667	-0,907839384	-3,732218235	0,000189801	0,008760722
SDHD	5607,580577	0,734688466	3,415201976	0,000637347	0,018084804
SEMA3E	5,431489051	-6,050165244	-5,399478872	6,68E-08	3,20E-05
SEMA6A	234,1873187	-2,181789901	-4,077111459	4,56E-05	0,003390931
SEMA6C	393,9592324	-1,818852766	-4,646552877	3,38E-06	0,000564753
SEPHS2	6036,986285	0,773475452	4,539825979	5,63E-06	0,000797969
SERINC1	14834,38802	0,98476727	3,041815112	0,002351563	0,041512366
SERPINA1	6049,655328	-3,25905992	-3,2639931	0,001098538	0,025467396
SERTAD4	15,38394048	-7,137031849	-6,650979715	2,91E-11	4,48E-08
SETD3	4281,352805	0,747595343	3,097542386	0,001951325	0,036698497
SF3B6	7438,938927	0,906584567	3,992173171	6,55E-05	0,004258262
SFR1	995,6343908	0,755670295	3,373816337	0,000741338	0,019944809
SFRP1	36,5844869	-4,119155271	-3,076972961	0,002091143	0,038620282

SGK3	2932,678704	0,90506295	3,44776449	0,000565247	0,016680599
SGSM2	2543,754086	-1,292465663	-5,247927096	1,54E-07	5,72E-05
SH2B1	531,5447836	-0,895890444	-4,45520846	8,38E-06	0,001057505
SH3BGRL	22398,22185	0,668811828	2,942646307	0,0032542	0,049943693
SH3TC1	9626,647378	-1,737958151	-3,334065117	0,000855866	0,021812543
SHISA2	104,3557038	-3,613356166	-3,861232509	0,000112816	0,006246908
SIAH2	11906,88989	-1,256776725	-3,107837098	0,001884619	0,035882357
SIAH2-AS1	30,10825314	-2,347682093	-3,490362712	0,000482365	0,015113208
SIGLEC7	244,5895449	-4,795218392	-4,671274626	2,99E-06	0,000523606
SIM1	3,451833212	-5,830640984	-2,953373253	0,003143217	0,048775307
SINHCAF	9612,202057	1,298665596	3,840995418	0,000122536	0,006526865
SINHCAFP1	24,48772806	1,546308133	3,91261574	9,13E-05	0,005416006
SINHCAFP2	85,55430416	1,225716463	2,949634123	0,003181504	0,049123974
SLC10A7	820,3150741	0,825124522	3,129529293	0,001750866	0,034224709
SLC12A3	5,334951476	-6,461373824	-3,826020415	0,000130231	0,006761277
SLC12A9	999,0780508	-1,227016982	-3,550666546	0,000384257	0,013232794
SLC15A3	462,8866955	-4,559481586	-4,565035447	4,99E-06	0,00074277
SLC17A8	12,85762664	-5,01424074	-3,11353081	0,001848632	0,035460334
SLC19A3	4,014671337	-6,051512669	-3,044435583	0,002331173	0,041365901
SLC1A3	455,5098096	-2,305296353	-3,056308126	0,002240808	0,040393083
SLC1A6	196,5580037	-5,039951945	-3,856539152	0,000115004	0,006300033
SLC23A1	141,9357964	-2,135533735	-3,261565647	0,001107988	0,025628564
SLC23A2	1640,613762	-0,743626743	-3,190235785	0,001421568	0,030017697
SLC25A25-AS1	212,563249	-1,124393723	-3,767761447	0,000164718	0,00800251
SLC25A32	2911,14356	0,810600621	3,097579995	0,001951077	0,036698497
SLC26A1	123,4212949	-1,673703707	-3,994633761	6,48E-05	0,004244305
SLC26A10	3,304807859	-4,85102631	-3,049692363	0,002290759	0,041074893
SLC28A3	8,3043198	-4,122647699	-3,256502055	0,001127941	0,025944941
SLC2A4RG	1098,143356	-0,996053113	-3,792437204	0,000149176	0,007479936
SLC35D1	1997,213801	-1,519929032	-3,185407438	0,001445503	0,03023694
SLC35F6	587,1713768	-1,094633299	-3,217175745	0,001294593	0,028413608
SLC38A11	2,897463989	-3,882432969	-3,800270884	0,000144538	0,007330958
SLC39A8	12414,39544	1,101740535	3,188216351	0,001431534	0,030145439
SLC44A2	8296,618703	-1,526388487	-3,660500397	0,000251723	0,0102919
SLC4A10	3,010908352	-5,630021989	-3,361558379	0,00077504	0,020561987
SLC50A1	3558,206734	0,735335091	3,027472416	0,002466082	0,042581757
SLC5A9	1,985705986	-4,545918201	-2,958173402	0,00309468	0,04836992
SLC6A19	20,92086235	-8,432041508	-5,774455878	7,72E-09	5,06E-06
SLC7A3	75,07322138	-4,284984081	-2,951027701	0,003167185	0,048995513
SLC7A6	501,6991854	-1,047516428	-3,035247866	0,002403381	0,041973039
SLC8A1-AS1	107,1121289	-3,157166388	-3,57653388	0,00034818	0,012426922
SLITRK6	44,15549633	7,91675601	4,572543966	4,82E-06	0,000730557
SMARCA4	12975,19256	-0,948016447	-3,717102322	0,000201521	0,008991626
SMARCC2	7292,617854	-0,892087571	-3,683181425	0,000230341	0,009781395
SMG1P7	55,77888454	-2,019742102	-3,286665972	0,00101381	0,024251882
SMIM12	3450,624666	0,96807701	3,223334935	0,001267073	0,028185966
SMIM25	423,224789	-4,000110873	-4,215701013	2,49E-05	0,002268068
SNAPC1	601,649438	1,664035583	5,397348891	6,76E-08	3,20E-05
SNAPC4	696,7523932	-0,840068922	-3,19161378	0,001414804	0,029915909
SNCAIP	13,63921708	-4,613141001	-4,142126202	3,44E-05	0,00284017
SNHG16	2234,817724	0,993642945	3,618735635	0,000296046	0,011351098

SNHG5	6733,861857	1,343670119	3,171719241	0,001515394	0,031061801
SNHG6	2249,206089	1,214545678	3,68166999	0,000231711	0,009812508
SNHG8	2528,764627	1,306482072	3,425141264	0,00061448	0,01778595
SNRNP200	12498,75825	-0,931896328	-3,217259262	0,001294216	0,028413608
SNX25	274,2623701	-3,439402662	-4,128777239	3,65E-05	0,002916349
SNX29	932,2498517	-1,249622985	-3,575370168	0,000349733	0,012426922
SOCS2	6740,392801	-2,160882221	-3,893849573	9,87E-05	0,005709822
SOCS2-AS1	800,6020048	-2,330894851	-3,658030112	0,000254161	0,010377799
SP7	7,08881542	-4,333279712	-3,859491495	0,000113623	0,006257814
SPANXB1	5,712678307	-5,455238812	-3,463965946	0,000532274	0,016108097
SPART	7415,582781	1,003749495	3,490407397	0,000482285	0,015113208
SPATA21	36,96825129	-2,372613724	-3,538184412	0,000402889	0,013600582
SPC24	468,4757085	-1,451127647	-2,957580983	0,003100633	0,04836992
SPDYE2	138,5439459	-1,688094391	-3,988169918	6,66E-05	0,004302803
SPG7	3913,046247	-0,827359129	-3,270620221	0,001073119	0,025124046
SPPL2B	4664,69329	-1,394041866	-4,997591256	5,81E-07	0,00015739
SPRYD7	518,6929995	0,866758997	4,220514933	2,44E-05	0,002226758
SPSB1	1607,031585	2,600796449	3,36879715	0,00075497	0,020141466
SPTBN1	10084,60815	-1,435341707	-3,312067794	0,000926091	0,022845804
SPTBN5	10,64207319	-4,355422317	-3,171767916	0,00151514	0,031061801
SPTSSA	2570,847754	0,833809067	3,18359225	0,001454598	0,030329095
SRGAP2	931,8840985	-1,38254149	-3,651569094	0,000260643	0,010475737
SRP14P2	158,6143967	0,635427594	2,958702688	0,00308937	0,04836992
SRP72	13854,36422	0,793062318	4,767843295	1,86E-06	0,000382187
SRRM4	2,894707203	-4,894435139	-4,685781329	2,79E-06	0,000509163
SSPO	63,97430092	-3,544819635	-5,878292955	4,15E-09	3,19E-06
SSR1	14307,14968	0,624720715	3,092571627	0,001984303	0,037092549
ST13	14753,88271	0,66610996	4,730220486	2,24E-06	0,000434263
ST13P15	78,12945727	0,648567229	3,510746538	0,00044685	0,014455929
ST13P18	97,64953561	0,779858748	3,446642184	0,0005676	0,016706209
ST13P3	58,55784694	0,722030851	3,66169353	0,000250553	0,0102919
ST13P5	115,7218816	0,672159849	3,807965643	0,000140115	0,007174837
ST13P6	92,20629718	0,552436253	3,422588079	0,00062028	0,017817457
ST3GAL5	385,056125	-1,691932587	-3,017187806	0,002551317	0,043649966
ST8SIA3	3,597291421	-4,940067166	-3,620721814	0,000293782	0,011337574
STARD3	3769,50115	-0,683845234	-4,072970752	4,64E-05	0,003410616
STARD3NL	9170,693324	1,075781676	3,822031433	0,000132357	0,00684852
STARD9	463,9879189	-2,154251229	-5,077619998	3,82E-07	0,0001165
STEAP1	2,375965872	-5,295750043	-4,915786789	8,84E-07	0,000212687
STK3	1456,360397	0,880035007	3,127723549	0,001761658	0,034283289
STK38	1878,571725	-0,838727006	-3,119438226	0,001811963	0,034996794
STK38L	2776,303107	1,172317705	3,333319654	0,000858163	0,021852986
STPG3	3,388308515	-4,446612064	-4,437305595	9,11E-06	0,001130825
STPG3-AS1	2,904015361	-4,290432238	-3,217080671	0,001295022	0,028413608
STXBP3	4388,962609	0,849579722	4,013415622	5,98E-05	0,004022906
SUB1P3	188,1739565	1,270769347	3,230645568	0,00123511	0,027766195
SUGP2	4126,810565	-0,858786123	-3,225434189	0,001257818	0,02802057
SUMO1	14038,27441	0,905235809	3,023659638	0,002497372	0,043025518
SUMO1P1	3,467776987	-4,921327092	-3,26417735	0,001097824	0,025467396
SUMO2	8429,595099	0,56924263	3,793181329	0,000148729	0,007469713
SUMO2P3	120,7432087	0,592362165	2,962914486	0,003047412	0,048133648

SURF4	25237,48435	0,755574096	3,042474316	0,002346418	0,04146908
SYNDIG1	51,25573504	-6,549648715	-3,842778507	0,000121649	0,00650211
SYNE1	1525,266699	-1,441774854	-3,750753	0,000176304	0,008331944
SYNE2	971,5446737	-3,949956856	-5,623929301	1,87E-08	1,04E-05
SYNE3	1546,812174	-1,832177022	-2,957737866	0,003099055	0,04836992
SYNPO2	48,23607829	-2,780311456	-3,411386356	0,000646334	0,018272449
SYT6	2,955879327	-5,14664437	-3,526442577	0,000421182	0,014018319
SYT7	8,631741833	-6,722266706	-4,818904437	1,44E-06	0,000312962
SYVN1	1850,623494	-1,584278439	-4,108373412	3,98E-05	0,003074499
TACR2	14,83977849	2,446564308	2,996358358	0,002732251	0,045444529
TAF1B	772,2876464	0,959080366	3,270029691	0,001075362	0,025157423
TAF1C	2468,130095	-0,9670136	-2,95150477	0,003162297	0,048948097
TAF1D	2650,83583	0,902879693	3,72757738	0,000193329	0,008845802
TAPT1-AS1	272,9665969	-1,568694504	-4,012652427	6,00E-05	0,004027147
TARS	8633,059505	0,977409228	3,661298613	0,00025094	0,0102919
TATDN1	1164,979267	0,837694263	3,052564081	0,002268953	0,040731341
TBC1D10C	7396,851594	-1,313907192	-3,706732858	0,00020995	0,009155434
TBC1D30	61,31954674	-2,42823433	-3,273554473	0,001062039	0,024959542
TBCD	3717,330231	-1,076613023	-3,726683699	0,000194016	0,008845802
TBX18	2,039033865	-4,580089807	-3,005675368	0,002649917	0,044654573
TCEA1	12503,16792	0,912954204	3,614589564	0,000300824	0,011462206
TCEAL4	1990,855152	0,4942134	2,955462395	0,003122008	0,048568593
TCEAL8	3482,87896	1,003039093	3,317113809	0,000909526	0,022649273
TCF3	14199,9308	-1,91773119	-4,714509018	2,42E-06	0,000457639
TCF7L1	77,15713448	-2,519643271	-4,427946137	9,51E-06	0,001161366
TCL6	228,7894707	-5,101946727	-3,686146977	0,000227675	0,009681529
TCOF1	4462,012336	-1,165084177	-3,721155496	0,000198313	0,008913096
TDG	2338,345805	1,223922559	4,355521068	1,33E-05	0,001460276
TDGP1	26,0187487	1,255391267	3,141523568	0,001680713	0,033251553
TEAD1	13,26057371	-4,473621667	-4,069725829	4,71E-05	0,003437056
TECPR1	849,3248814	-0,913921197	-3,948607189	7,86E-05	0,0048305
TENM2	10,485327	-6,088406745	-4,205209612	2,61E-05	0,002327678
TERF1	2175,289908	0,591202203	2,96223222	0,003054173	0,048133648
TERF1P4	44,73920439	0,858763577	3,068860911	0,002148766	0,039144415
TEX15	4,367397782	-6,168579681	-5,796548137	6,77E-09	4,53E-06
TEX30	3220,011934	1,887118194	4,112084317	3,92E-05	0,003040724
TFAP2A-AS1	5,50394559	-5,130966802	-4,42370615	9,70E-06	0,001170885
TFEC	1486,347429	1,080880273	2,957641093	0,003100028	0,04836992
TFG	7818,319901	0,936034876	3,375112026	0,000737856	0,019909192
TFPI	10414,77808	1,719091852	3,20110339	0,001369024	0,02943306
TGDS	934,0875288	1,631653371	3,5888998	0,000332076	0,012131457
TGS1	1665,036714	0,892043101	4,207545178	2,58E-05	0,002310455
TH2LCRR	4,854781823	-4,703515206	-2,979924672	0,002883193	0,046767574
THAP1	1262,06725	0,769042763	3,188800985	0,001428642	0,030145439
THAP12	4614,220013	0,666151497	3,515416179	0,000439065	0,014323697
THAP12P3	41,98474275	1,272617985	3,053850039	0,00225925	0,040604509
THAP12P7	119,8898723	0,952872422	4,976767895	6,47E-07	0,000167271
THAP9-AS1	2349,224144	0,849636261	3,255243247	0,001132953	0,026030014
THRB	150,463391	-3,640474867	-4,954082686	7,27E-07	0,00018339
TIAM2	83,9948253	-2,286888821	-3,447529373	0,000565739	0,016680599
TIMM17A	4456,907602	0,826674129	3,181312757	0,001466093	0,030456541

TIMM23	6727,527015	0,895786496	3,246781437	0,00116718	0,026657245
TIMM9	1423,216151	0,944913737	3,074922675	0,002105571	0,038771319
TINAGL1	512,4971111	-1,674880289	-2,961381408	0,003062624	0,048180383
TLE1P1	34,94994694	-3,019120398	-2,964309704	0,003033628	0,048133648
TLN2	141,5131008	-2,087360042	-3,031902117	0,00243018	0,042189719
TMCC1	475,4786652	-1,099089853	-2,999840642	0,002701209	0,045198264
TMED10	15515,58506	0,568018268	4,026822032	5,65E-05	0,003833849
TMED2	31246,16949	0,643072058	3,384997331	0,000711789	0,019409975
TMED7	3278,312719	1,046290564	3,022401211	0,002507779	0,043084263
TMEM108-AS1	2,698399442	-5,472136998	-3,231252285	0,001232491	0,027757645
TMEM110-MUSTN1	13,34148689	-3,327267371	-3,920918615	8,82E-05	0,005283627
TMEM123	33349,38178	0,669236052	3,309397823	0,000934969	0,022972774
TMEM126A	1548,560579	0,940063901	3,092568328	0,001984325	0,037092549
TMEM131L	3013,85662	-1,722155178	-3,506842864	0,000453457	0,01455743
TMEM132B	9,008685605	-6,784036424	-4,960531882	7,03E-07	0,000178871
TMEM151B	7,512258888	-6,511437847	-6,395999631	1,60E-10	2,05E-07
TMEM167B	5986,173829	0,986954901	3,637523811	0,000275272	0,010893048
TMEM170A	2361,835	0,907465354	3,672714775	0,000239987	0,010066061
TMEM243	1924,144715	-1,631900228	-3,38155395	0,000720771	0,019550987
TMEM38B	3284,020876	1,014920752	3,86948364	0,000109066	0,006125514
TMEM45B	22,00296544	-3,385707554	-3,284142101	0,001022933	0,024377273
TMEM59	24066,80512	0,820836859	3,457461194	0,000545291	0,0162989
TMEM68	1601,992703	1,462863751	3,718354364	0,000200525	0,008966656
TMEM70	3206,652509	1,171663049	3,290639014	0,000999601	0,023991099
TMSB4Y	120,6989154	10,3310493	5,972655847	2,33E-09	1,97E-06
TMTC1	88,70389309	-4,499605694	-5,097754063	3,44E-07	0,000111386
TMX2	4759,159652	0,597042257	3,524801618	0,0004238	0,014044706
TNC	596,0232093	-4,063721159	-4,322179591	1,54E-05	0,0016213
TNFRSF13C	151,9377388	-3,218425943	-4,117453952	3,83E-05	0,003000996
TNFSF9	384,3104751	1,710576338	2,976020488	0,002920154	0,047114019
TNK2	1201,879382	-1,462637731	-4,576096358	4,74E-06	0,000725612
TOMM20	12098,56304	0,8039625	3,497856674	0,000469013	0,014813126
TOMM20P4	122,0424789	0,900302292	3,385816199	0,000709669	0,019386494
TOX2	80,27694017	-3,020662988	-3,295431765	0,000982706	0,02373216
TOX3	1,999076343	-5,047075127	-3,007292798	0,002635857	0,044514615
TPMT	2547,581426	1,2643496	5,63052952	1,80E-08	1,02E-05
TPMTP1	15,76406534	1,726691153	3,364036896	0,000768113	0,020438969
TPO	62,44464414	-4,384289269	-3,329902975	0,000868763	0,021994454
TPT1P6	63,91706239	1,367475007	2,999665297	0,002702764	0,045198264
TRAPPC2B	575,2043916	1,575946245	4,501910525	6,73E-06	0,000905398
TRAPPC3L	17,2761893	-4,911621611	-3,074754048	0,002106762	0,038771319
TRARG1	5,583431326	-6,526941003	-3,216526223	0,001297527	0,028413608
TRBV10-3	5,937562174	-6,612630051	-3,147082577	0,001649084	0,032861064
TRBV27	279,6115411	3,276570646	3,472399927	0,000515827	0,015770382
TRBV5-6	11,03850576	-4,513137797	-3,335075625	0,000852762	0,021769474
TRDN	9,629984728	-3,9761728	-3,583883796	0,000338523	0,012246885
TREML1	865,7049046	-2,792825049	-2,998506331	0,002713065	0,045296713
TRGC1	1707,764969	2,51642229	3,676833871	0,000236147	0,009945621
TRGC2	891,5143214	2,7964943	3,778910843	0,000157516	0,007734353

TRGJP2	76,43283156	3,141398138	3,851924522	0,000117193	0,006352157
TRHDE	9,735525663	-6,237980676	-7,788541997	6,78E-15	2,61E-11
TRIM40	6,967903229	-6,845193062	-3,63699466	0,000275838	0,01090143
TRIM48	2,555203833	-5,390753656	-3,601902633	0,000315897	0,011774227
TRIM73	59,1261274	-1,876894299	-7,013128163	2,33E-12	4,48E-09
TRIM74	69,5093965	-1,50278618	-4,670477896	3,00E-06	0,000523606
TRPM3	5,514912893	-4,493493343	-3,567988728	0,000359732	0,012628356
TSC22D1	63960,49128	2,112914729	3,534319112	0,000408827	0,013755805
TSC22D4	3565,257965	-0,987917304	-3,201761913	0,001365898	0,029406933
TSIX	9,504031988	-4,633035022	-3,470018466	0,000520423	0,015832263
TSLP	66,4558924	3,857821223	3,874322432	0,000106922	0,006040001
TSPAN14	8718,602146	-1,802235304	-3,505621843	0,000455542	0,014592126
TSPOAP1-AS1	512,2859543	-1,166541915	-2,976936423	0,002911444	0,047077006
TTC16	9,89165375	-6,468815182	-3,523651851	0,000425643	0,014060381
TTC21B-AS1	13,36463729	-3,044397865	-3,736553268	0,00018656	0,008637024
TTTY14	71,6143521	9,57776832	5,357954185	8,42E-08	3,70E-05
TTTY15	564,814292	11,59539374	6,934293165	4,08E-12	7,39E-09
TUBA4A	5351,031343	-2,499393339	-5,834928366	5,38E-09	3,85E-06
TUBA4B	56,67453286	-2,517502209	-5,936818179	2,91E-09	2,35E-06
TUBB1	3105,326963	-4,675011851	-5,49697318	3,86E-08	1,96E-05
TVP23B	1960,540588	1,234737383	4,579778645	4,65E-06	0,000716519
TWISTNB	4391,868717	1,206445401	4,680362141	2,86E-06	0,000518614
TXLNGY	678,435138	12,82181245	7,341646855	2,11E-13	6,50E-10
TXNDC12	7918,140252	0,731879075	3,788091258	0,000151809	0,007562697
TXNDC9	1979,44904	1,076479446	3,308622634	0,000937561	0,022999757
TXNL1	7424,892758	0,989077305	3,245572381	0,001172148	0,026713262
TXNRD1	8842,947826	0,774808708	4,652678008	3,28E-06	0,000551225
TYK2	6534,993852	-1,10997067	-4,470834436	7,79E-06	0,00099534
UBB	13261,65945	0,726321418	2,98643777	0,002822483	0,046245757
UBBP4	886,6368117	0,767604103	3,221620849	0,001274677	0,02825435
UBE2D3P2	54,17550377	1,06502486	3,313743037	0,000920561	0,022764097
UBE2W	1877,411872	1,512685046	5,173223342	2,30E-07	8,05E-05
UBXN2A	3114,88461	0,909581847	3,195649472	0,001395165	0,029684845
UBXN7-AS1	114,7616992	-2,209490519	-4,319944862	1,56E-05	0,0016213
UFM1	9489,001419	0,851063744	3,879461806	0,000104688	0,005961617
ULK4P2	126,5388113	1,11997101	3,014006363	0,002578224	0,04392683
UNC5D	4,436961394	-5,29541018	-3,908320265	9,29E-05	0,005481505
UNKL	871,7406866	-1,138596744	-3,027964494	0,00246207	0,042536337
UQCRB	3531,942764	0,857241709	3,547206954	0,000389339	0,013311581
UQCRC2	11497,06265	0,582579865	3,130822425	0,001743175	0,034117697
USP9Y	116,3324117	24,45831843	9,254259051	2,16E-20	6,64E-16
UTP11	2970,864594	1,053567572	3,32278547	0,000891234	0,022307666
UTP23	1646,502065	1,321743802	4,361707485	1,29E-05	0,001429174
UTRN	4516,307746	-1,15883451	-3,211092777	0,001322312	0,02877034
UTY	799,8006163	9,908952682	7,045326097	1,85E-12	4,07E-09
VAMP7	6176,782493	1,010723295	4,483416687	7,35E-06	0,000966466
VASN	838,0666134	-3,405454506	-4,641905221	3,45E-06	0,000574487
VAT1L	42,46041762	-9,453155294	-7,24341002	4,38E-13	1,22E-09
VBP1	5197,889619	0,839164321	3,27967689	0,00103926	0,024555417
VDAC2	10991,11466	0,730320285	3,860705884	0,00011306	0,006249149
VMA21	6318,027754	0,654653289	3,192982836	0,001408113	0,02985646

VPREB1	2943,621299	-4,14372009	-4,253962539	2,10E-05	0,001995648
VPREB3	1184,347565	-4,526158234	-3,884276547	0,000102635	0,005884218
VPS26A	8349,024872	1,035629977	5,035822135	4,76E-07	0,000136902
VPS26B	5057,177105	-1,271931586	-4,478053179	7,53E-06	0,000972873
VPS37A	2789,371097	1,129021039	4,22325218	2,41E-05	0,002206421
VPS39	4413,816631	-0,656401245	-3,35581881	0,000791304	0,02076837
VSIG10	677,4125111	-1,490942527	-3,802529934	0,000143226	0,007300492
VSIG2	79,72059759	-2,700030955	-3,572558093	0,000353511	0,01251951
VSIG4	2628,007675	-3,00936052	-2,972084988	0,002957848	0,047514124
WAPL	6406,183552	0,612341997	2,99213932	0,002770298	0,045658012
WDFY1	3927,084101	0,601536573	2,9938697	0,002754636	0,045595143
WDFY4	2217,740631	-1,164135548	-3,615766974	0,00029946	0,011438542
WDR11-AS1	59,95373079	-3,201158969	-4,131995756	3,60E-05	0,002883291
WDR33	5173,457354	0,720115594	3,298656379	0,000971488	0,023587686
WDR44	984,4641849	1,041026643	4,617762035	3,88E-06	0,000635229
WDR62	1207,807475	-1,605980502	-4,182814182	2,88E-05	0,002482991
WDR63	2,740020273	-5,496095623	-3,497795893	0,00046912	0,014813126
WDR90	1569,350139	-1,35129795	-3,4533723	0,000553624	0,016468051
WDTC1	866,4478479	-0,982154369	-3,833986406	0,000126083	0,006647358
WFS1	1022,092467	-3,326530939	-3,381944969	0,000719746	0,019540395
WNT2B	15,76557978	-2,819481954	-3,619160911	0,00029556	0,011351098
WT1	367,2888237	2,191550275	3,355196999	0,000793085	0,020780173
WT1-AS	58,98976241	4,867478242	4,188709366	2,81E-05	0,002453736
WTIP	15,72134343	-3,45278177	-3,652767016	0,00025943	0,010467967
XPO6	3898,319634	-0,919505993	-3,605144064	0,00031198	0,011708357
YAE1D1	371,8230872	1,522035908	2,980964168	0,002873424	0,046720729
YIPF6	1504,110925	0,83371026	4,566788998	4,95E-06	0,000740161
YLPM1	3500,30368	-0,744831929	-3,035054094	0,002404925	0,041973039
YME1L1	12910,38475	0,65929769	3,139211483	0,001694031	0,033432144
YPEL3	4810,841285	-1,185835169	-3,534361147	0,000408762	0,013755805
YTHDF3	8433,753049	0,996969513	3,331127702	0,000864949	0,021935081
YWHAEP5	51,43288766	1,193281695	3,711139239	0,000206329	0,009087607
Z74021.1	281,663078	1,039091375	3,452968894	0,000554453	0,016476778
Z82206.1	27,22799627	-3,41791316	-3,562149118	0,000367831	0,012854056
Z95114.3	11,25944985	-3,451681762	-3,367251147	0,000759215	0,020237191
Z97353.1	675,0982036	1,160934157	3,230841378	0,001234264	0,027766195
ZAP70	1361,672725	-3,502605453	-3,510652527	0,000447008	0,014455929
ZBTB12	2,548672491	-2,649922233	-3,061412328	0,002202955	0,039918996
ZBTB18	411,6528297	-1,330043274	-3,010000669	0,002612471	0,044314132
ZBTB40	661,5773496	-1,366051808	-3,337374056	0,00084574	0,021662072
ZBTB8A	292,9670032	2,127097006	3,961390894	7,45E-05	0,004662756
ZCCHC14	244,4458814	-1,216630059	-3,008066861	0,002629153	0,044450154
ZCCHC17	1017,097658	1,08289751	2,969604528	0,002981833	0,047813389
ZCRB1	3517,982163	0,735143723	3,449178131	0,000562296	0,016622176
ZDHHC4	2642,410391	0,762083056	4,032330448	5,52E-05	0,003769971
ZDHHC8	1318,246424	-1,019810205	-2,962152626	0,003054963	0,048133648
ZFAND1	3642,277666	1,233276898	3,874680687	0,000106765	0,006040001
ZFAND6	7474,364652	1,266633711	3,186975265	0,001437691	0,030156945
ZFAS1	1802,719121	1,508782682	2,990206983	0,002787885	0,045849682
ZFY	653,6900613	7,693119366	6,053976073	1,41E-09	1,32E-06
ZMAT4	2,225492587	-4,724760051	-3,128916055	0,001754524	0,034252719

ZMIZ2	1893,265235	-0,953911278	-3,593327232	0,000326482	0,01201402
ZMYM6	903,0265145	1,123967966	4,111025093	3,94E-05	0,003047034
ZMYND15	165,1331008	-4,806145871	-3,461744837	0,000536686	0,016135687
ZNF165	457,9104745	1,523816629	3,072137401	0,002125319	0,038863943
ZNF184	1579,531106	0,997073083	3,120050045	0,001808203	0,034946109
ZNF195	2592,567687	1,017520167	3,280635942	0,001035733	0,02454952
ZNF222	418,2547234	1,917471049	3,679147273	0,000234015	0,009869347
ZNF24	5139,285808	0,970874097	4,120155819	3,79E-05	0,002988836
ZNF267	3318,238327	1,531895374	3,75138607	0,00017586	0,008331944
ZNF35	558,721986	1,104467204	3,93406041	8,35E-05	0,005041992
ZNF419	555,8588442	1,323807716	4,996937556	5,82E-07	0,00015739
ZNF44	1421,074899	1,28063519	4,02793789	5,63E-05	0,003824126
ZNF440	906,6779372	1,330902865	3,512175074	0,000444455	0,01441651
ZNF571	425,1243238	1,39383149	3,612281886	0,000303514	0,011507755
ZNF597	386,8524053	1,633298851	3,553960917	0,000379476	0,013171269
ZNF614	1363,734406	1,280177464	3,535944966	0,000406319	0,013701373
ZNF615	841,4911236	1,234775109	3,836674375	0,000124712	0,006605433
ZNF627	1509,450968	1,19193414	3,042847132	0,002343513	0,041441557
ZNF649	836,0261211	1,299749912	2,966796284	0,003009203	0,04800371
ZNF723	13,66707556	21,06653253	6,712060919	1,92E-11	3,11E-08
ZNF764	709,9797194	0,84966783	3,105752465	0,001897955	0,036001659
ZNF823	349,5515067	1,54825659	3,040481347	0,002362003	0,041655243
ZNF839P1	14,82896977	7,305508634	3,347608708	0,00081512	0,021070615
ZNF93	1518,184427	1,549216225	3,268787396	0,001080094	0,025216006
ZNF99	3,005603855	-2,417203303	-3,41456853	0,000638831	0,018110218
ZSWIM8	1759,976096	-1,392597377	-4,185369601	2,85E-05	0,002475442

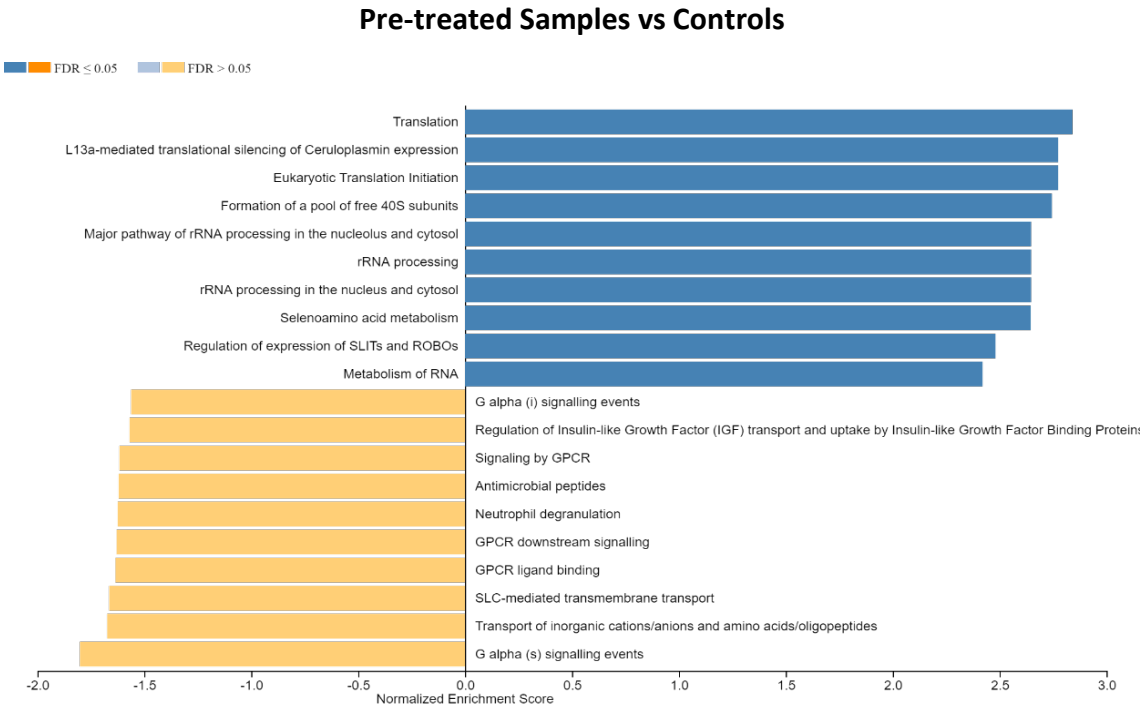

Supplementary figure 1. Reactome enrichment analysis showed an enriched pathaways from the comparation between myeloid malignancies and healthy control samples. MDS patients showed a high enrichment in translation and ribosomal complex.

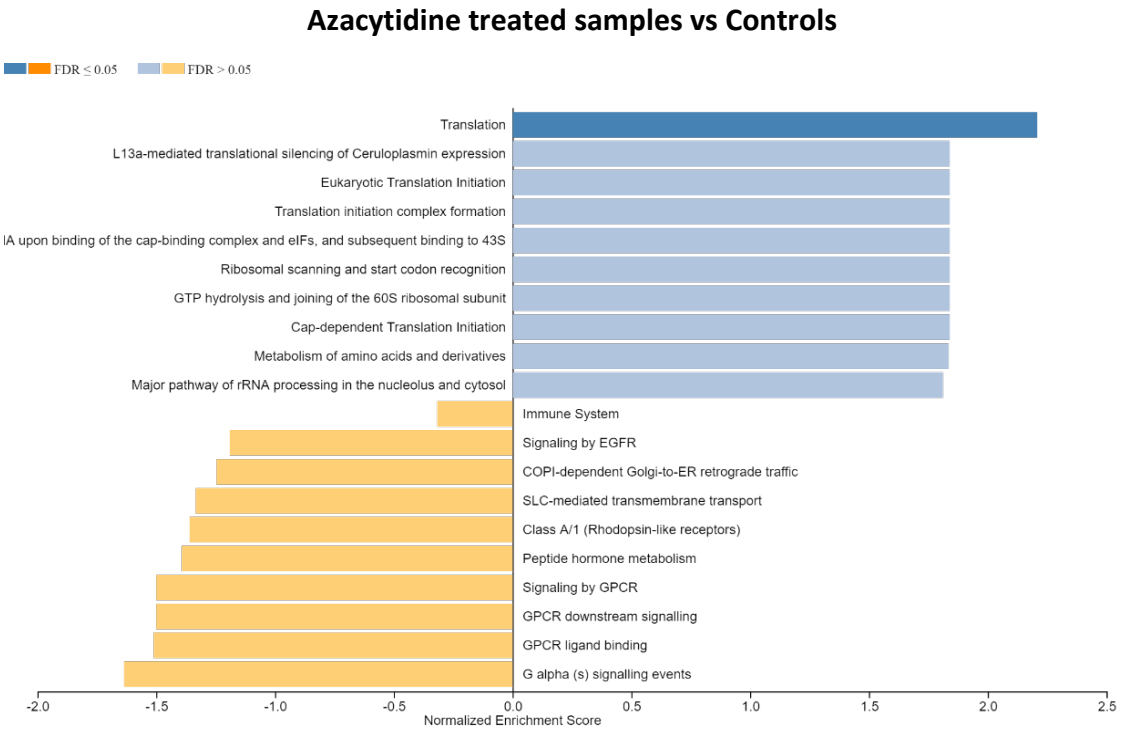

Supplementary figure 2. Reactome enrichment analysis showed an enriched pathaways from the comparation between AZA treated patients and healthy control samples. Only translation is enriched during the treatment when compared with control, suggesting the normalization of abnormal regulated pathways in MDS patients.

Departamento de **MEDICINA, HEMATOLOGÍA**

CENTRO DE INVESTIGACIÓN DEL CÁNCER-IBMCC (USAL-CSIC)

Tesis doctoral

Estudio de las modificaciones en la expresión génica inducidas por el tratamiento en enfermos con hemopatías

Con la aprobación de la Universidad de Salamanca, Departamento de Medicina, esta tesis será defendida el 2 de Septiembre de 2019

Directores:

Prof. Dr. Jesús María Hernández Rivas

Dra. M del Rocío Benito Sánchez

Dra. Ana E. Rodríguez Vicente

Jesús María Hernández Sánchez, Salamanca, 2019

BENITO SANCHEZ MARIA DEL ROCIO - 07875452E

Firmado digitalmente por BENITO SANCHEZ MARIA DEL ROCIO - 07875452E
Nombre de reconocimiento (DN): c=ES, serialNumber=IDCES-07875452E, givenName=MARIA DEL ROCIO, sn=BENITO SANCHEZ, cn=BENITO SANCHEZ MARIA DEL ROCIO - 07875452E
Fecha: 2019.07.09 12:56:08 +02'00'

RODRIGUEZ VICENTE ANA EUGENIA - 70982673G

Firmado digitalmente por RODRIGUEZ VICENTE ANA EUGENIA - 70982673G
Nombre de reconocimiento (DN): c=ES, serialNumber=IDCES-70982673G, givenName=ANA EUGENIA, sn=RODRIGUEZ VICENTE, cn=RODRIGUEZ VICENTE ANA EUGENIA - 70982673G
Fecha: 2019.07.09 11:43:40 +01'00'

HERNANDEZ RIVAS JESUS MARIA - 06541691P

Firmado digitalmente por HERNANDEZ RIVAS JESUS MARIA - 06541691P
Nombre de reconocimiento (DN): c=ES, serialNumber=IDCES-06541691P, givenName=JESUS MARIA, sn=HERNANDEZ RIVAS, cn=HERNANDEZ RIVAS JESUS MARIA - 06541691P
Fecha: 2019.07.09 12:56:50 +02'00'

Tabla de Contenidos

Los números de las paginas se refieren a la versión en inglés de la tesis doctoral

Introducción

La medicina de precisión o medicina personaliza ha sufrido una gran revolución en los últimos años. La medicina de precisión se caracteriza por el uso de los tratamientos en pacientes que muestran determinados marcadores, evitando así el uso del mismo tratamiento para todos los pacientes con una determinada enfermedad [14]. De este modo, es necesario evaluar las características genéticas, fenotípicas, biomarcadores y aspectos psicosociales, para adecuar las terapias a los pacientes [15]. Su rápida expansión en los últimos años se ha basado principalmente en el mejor conocimiento de la salud y de las enfermedades. La mejora en las técnicas de análisis genético, en el análisis de datos y en la inteligencia artificial está permitiendo su desarrollo progresivo en la práctica clínica [16].

La medicina de precisión aspira a la reclasificación de las enfermedades heterogéneas mediante el cribado genómico, el análisis mutacional y el descubrimiento de nuevas terapias dirigidas [15]. De esta manera, las nuevas terapias estarán dirigidas a los pacientes que presenten los biomarcadores para los que se ha demostrado la eficacia del tratamiento [17]. Por este motivo, la medicina de precisión usa herramientas como la farmacogenómica para su implementación. La farmacogenómica estudia las bases genéticas de los individuos para optimizar la selección del tratamiento [18]. De este modo, busca minimizar los efectos adversos y al mismo tiempo maximizar la eficacia [19]. Su uso ha permitido la detección de marcadores moleculares utilizados en la clínica como el aumento de sensibilidad a warfarina producida por polimorfismos en los genes *CYP2C9* o *VKORC1* [20], la resistencia a clopidrogrel ocasionado por variaciones en el gen *CYP2C19* [21], o los efectos adversos del tratamiento con 6-Mercaptopurina debido a variaciones en el gen *TPMT* [22].

Introducción

El aumento en la información genética debido a su uso en la práctica clínica está contribuyendo a su incorporación en los registros médicos [23]. Esta nueva información molecular ha llamado la atención de las plataformas de Big Data, cuyo objetivo es la incorporación de decenas de miles de pacientes con información clínica y molecular, para poder detectar de manera eficiente y precisa nuevos biomarcadores [24]. Sin embargo, la farmacogenética aún no ha alcanzado todo su potencial y su uso es limitado en la clínica . No obstante, las nuevas terapias dirigidas, y el uso de las técnicas de secuenciación masiva, están permitiendo su uso en cada vez mas ensayos clínicos.

En los últimos años, el termino medicina de precisión en cáncer (MPC), ha emergido en los pacientes con cáncer. La MPC incorpora tanto el cribado, como la monitorización para detectar recaídas o progresiones, además de aspirar a mejorar la selección de las terapias [25]. Alguno de los ejemplos más destacados son el uso de los inhibidores de la tirosina-quinasa en la leucemia mieloide crónica, consiguiendo una supervivencia global del 85% [26]. El cáncer de mama fue el primer tumor sólido que se benefició del uso del perfil de expresión génico y mutacional para predecir la respuesta de las pacientes.

La trombocitopenia inmune (PTI) es una enfermedad autoinmune que se caracteriza por una disminución en el número de plaquetas [43] ocasionada por una respuesta anormal de los linfocitos T. Las plaquetas son destruidas por los linfocitos y los megacariocitos no pueden recuperar el número normal de plaquetas. Sus manifestaciónes más características es la diátesis hemorrágica en forma de petequias y púrpuras [44]. La primera línea de tratamiento de esta enfermedad son los corticoides, principalmente prednisona [45], aunque en ocasiones también se usa la dexametasona [46]. Sin embargo, no todos los pacientes responden al tratamiento y por este motivo la esplenectomía es

la segunda opción terapéutica en estos pacientes. El reciente descubrimiento de los agonistas del receptor de la trombopoyetina (TPO-R), ha desplazado a la esplenectomía como fármaco de segunda línea. Actualmente, hay dos fármacos aprobados, romiplostim y eltrombopag [47,48]. Este último, es un agente mimético de la trombopoyetina que se une al dominio transmembrana del TPO-R, de este modo no compite con TPO [49]. La interacción activa la ruta de señalización de *JAK2*, que directamente fosforila STAT, estimulando la megacariopoyesis [50]

Los síndromes mielodisplásicos (SMD) son un grupo heterogéneo de neoplasias hematológicas que se surgen en la célula madre hematopoyética con un aumento del riesgo de progresion a LAM [10]. Los SMD se caracterizan por una hematopoyesis clonal e ineficiente, lo que ocasiona un fallo de la medula ósea y distintos grados citopenias en sangre periférica [12]. Los SMD presentan un curso clínico muy heterogéneo. Se observan en torno a los 70 años [27]. En el año 2016, la Organización Mundial de la Salud (OMS) actualizó la clasificación de las neoplasias mieloides. Actualmente los SMD se clasifican en: SMD con displasia unilínea, SMD con displasia multilínea, SMD con sideroblastos en anillo, SMD con del(5q) como alteración única., SMD con exceso de blastos y por último SMD inclasificables [28].

Dado que los SMD son enfermedades muy heterogéneas, es preciso disponer de buenos sistemas de estratificación pronóstica. El IPSS-R (*Revised International Prognostic Scoring System*), permite determinar el riesgo pronóstico de los SMD. Este sistema de clasificación divide a los pacientes en riesgo: muy bajo, bajo, intermedio, alto o muy alto [29].

Por desgracia, no existen aun terapias dirigidas aprobadas para los pacientes con SMD. Actualmente el único tratamiento curativo en lo SMD es el trasplante alogénico; sin embargo, solo puede ser usado en pacientes jóvenes. La FDA ha aprobado varios tratamientos como la lenalidomida en el síndrome 5q-, y la 5-Azacitidina (AZA) y la decitabina en los pacientes de riesgo intermedio y alto [12]. Sin embargo, desde hace más de doce años no se ha aprobado ningún nuevo tratamiento específico de los SMD (https://www.centerwatch.com/drug-information/fda-approved-drugs/therapeutic-area/6/hematology).

Cuando el trasplante no es posible, el tratamiento con agentes hipometilantes suele ser la elección. Tanto AZA como decitabina modifican el curso clínico de la enfermedad. Ambos tratamientos son estructuralmente similares además de análogos nucleósidos [30]. Una de las principales diferencias es la unión de AZA predominantemente al RNA (ratio ARN:ADN, 65:35), mientras que decitabina se une casi de forma exclusiva al ADN [31].

El principal mecanismo de acción de los agentes hipometilantes es restaurando la hipermetilación de las islas CpG [32]. Sin embargo, las funciones celulares alteradas por este tratamiento aún no están definidas. El gen *DNMT1* pertenece a la familia de la DNA metiltransferasa y está encargado del mantenimiento de la metilación. En un primer momento estos tratamientos se usaron a altas dosis por su efecto quimioterápico, sin embargo, a bajas dosis actúan mediante la inactivación de *DNMT1*, restaurando así la metilación [33].

La decitabina fue aprobada en Estados Unidos después de 2 ensayos clínicos aleatorizados (D-0007 y EORTC-06011) comparándola con el mejor tratamiento de

soporte, mostrando una tasa de respuesta completa del 9% y una tasa de respuesta global del 17% [34].

Por su parte AZA fue aprobado en Europa, en pacientes con SMD de alto riesgo. Los dos estudios, CALGB 9221 y AZA-001, fueron aleatorizados y multicéntricos. Los pacientes incluidos en el estudio CALGB 9221 presentaron una mediana de edad de 68 años y se obtuvo un 60% de repuestas, frente al 5% en la rama con tratamiento de soporte. Además, AZA mostró un mayor tiempo hasta progresion de LAM, 21 meses *vs* 12 meses [35]. En el segundo estudio AZA-001, se incluyeron pacientes con una mediana de edad similar a CALGB 9221, y mostró como el tratamiento mejoraba la mediana de supervivencia alargando también el tiempo de progresión a LAM. Además, AZA-001 demostró una reducción de transfusiones de glóbulos rojos, así como un menor número de infecciones [36].

Sin embargo, los resultados de estos estudios no han podido ser confirmados entre otros por el grupo cooperativo español de SMD, donde analizaron la eficacia de AZA en la práctica clínica sin encontrar una mejoría en la supervivencia [13]. Por este motivo, es necesario ahondar en el mecanismo de acción del fármaco, para así, poder seleccionar a los pacientes que van a poder beneficiarse del tratamiento.

Los pacientes con SMD de riesgo muy bajo o bajo, suelen ser pacientes asintomáticos o con leves citopenias al momento del diagnóstico. De este modo los pacientes son tratados con terapias de soporte puesto que ningún fármaco ha mostrado mejoría de la clonalidad , a excepción de los pacientes que presentan como alteración única del(5q) [37]. Los pacientes con SMD de bajo riesgo se asocian con una supervivencia larga además de transfusiones de glóbulos rojos. De este modo, los pacientes que presentan anemia

y requieren transfusiones [38], terminan por tener una sobrecarga férrica, que reduce su supervivencia [39]. Por este motivo, el tratamiento con quelantes del hierro es de elección en estos pacientes. Actualmente, 3 quelantes están disponibles, deferasirox, deferoxamina y deferiprona. Deferasirox es un fármaco de administración oral (deferoxamina se administra de forma intravenosa), facilitando así la adherencia de los pacientes. Además, deferasirox presenta menos efectos adversos que deferiprona (agranulocitosis) [40]. Deferasirox está aprobado para su uso en pacientes con SMD que presenten sobrecarga férrica [41]. Este fármaco no solo regula la homeostasis del hierro, sino que también ha demostrado su influencia en la renovación y la diferenciación de las células madre hematopoyéticas; sin embargo, se desconoce el mecanismo biológico que ocasiona la mejora hematopoyética [42].

Secuenciación de nueva generación (NGS)

Hasta hace poco, la secuenciación por el método Sanger, era la herramienta usada para el diagnóstico molecular. Esta metodología es laboriosa y con un límite de detección entre el 15-20%. Recientemente, el auge de la secuenciación de nueva generación, que permite el estudio simultáneo de todo el genoma/exoma, ha revolucionado el diagnóstico molecular [51]. Se están llevando a cabo grandes proyectos internacionales con el objetivo de su desarrollo en la clínica y así mejorar la medicina de presión [16,52].

El análisis del trascriptoma, también ha sufrido un gran avance debido a la incorporación de la secuenciación del ARN [53]. Los análisis de expresión han evolucionado de la qRT-PCR [54] a los microarrays de expresión [55] y finalmente al RNAseq. Esta nueva metodología permite cuantificar, al igual que los microarrays, la expresión tanto de los genes codificantes como de los microRNAs. Tiene una serie de ventajas sobre los microarrays,

como es la detección de transcritos de fusión, de las regiones no codificantes y de nuevas isoformas. Además, permite tienen un rango dinámico mayor, lo que facilita la detección de transcritos poco expresados, la detección de modificaciones en el *splicing* y de cambios puntuales en el ARN [56].

Resumen

Capítulo 1: Análisis del transcriptoma de pacientes con trombocitopenia inmune tratados con eltrombopag.

En los últimos años, el uso de los agonistas del receptor de la trombopoyetina, eltrombopag y romiplostim, ha mejorado el manejo de los pacientes con trombocitopenia inmune [1]. Además, eltrombopag es usado en los pacientes con anemia aplásica y síndromes mielodisplásicos [2,3]. Sin embargo, el mecanismo de acción y las rutas de señalización afectadas por este fármaco aún no se conocen de manera precisa y existe controversia al respecto [4]. Con el fin de entender mejor el mecanismo de acción de eltrombopag, se analizó en perfil de expresión génico en enfermos con trombocitopenia inmune, antes y durante el tratamiento. Para ello, se seleccionaron 14 pacientes y se analizó su transcriptoma mediante la metodología de microarrays. La mediana de edad fue de 78 años (rango, 35-87 años); la mediana de plaquetas en el momento basal $14x10^9$/L (rango, 2-68 $x10^9$/L). Diez pacientes respondieron a la terapia, 2 recayeron después de una respuesta inicial y 2 fueron refractarios al tratamiento. Eltrombopag indujo cambios en la hematopoyesis, principalmente diferenciación megacariocítica, así como activación y degranulación de las plaquetas. Además, después del tratamiento se observó una sobreexpresión de los genes *PPBP*, *ITGB3*, *ITGA2B*, *F13A1, F13A1*, *MYL9* y *ITGA2B*. Además, se observó una sobreexpresión de varios genes regulados por *RUNX1*, un factor de transcripción clave en la hematopoyesis, entre los que se encontraban *GP1BA, PF4, ITGA2B, MYL9, HIST1H4H* y *HIST1H2BH*. Además, los pacientes no respondedores, presentaban una sobreexpresión de *BCL-X*, y de genes implicados en la eritropoyesis como *SLC4A1* y *SLC25A39*. De esta manera, los estudios

del efecto de eltrombopag *in vivo*, demuestran una sobreexpresión de los genes implicados en la megacariopoyesis, adhesión plaquetaria, degranulación y agregación. Por último, los pacientes no respondedores presentaban un importante enriquecimiento del metabolismo del grupo hemo.

Capítulo 2: El estudio del transcriptoma completo permite la identificación de genes desregulados durante el tratamiento con deferasirox en pacientes con SMD de bajo riesgo.

El quelante del hierro deferasirox es ampliamente usado en los pacientes con sobrecarga férrica [5,6]. Los pacientes con SMD de bajo riesgo y dependencia transfusional son tratados con este quelante para evitar la sobrecarga férrica [7]. Además, en estos pacientes se ha observado un incremento tanto de glóbulos rojos como de plaquetas como consecuencia del tratamiento con deferasirox [8]. Sin embargo, los mecanismos responsables de estos hallazgos clínicos no se conocen con detalle. Por este motivo se estudiaron quince pacientes con SMD de bajo riesgo fueron analizados antes y durante el tratamiento con deferasirox. El análisis se llevó a cabo mediante microarrays, que permiten la detección tanto del transcriptoma completo como de los microRNAs. El tratamiento durante 14 semanas con este quelante produjo cambios en el perfil de expresión de 1.457 genes y en 54 microRNAs. Estos cambios se relacionaron con una infraexpresión de la ruta Nf kB y del interferón gamma. Estos resultados sugieren que ambas rutas pueden ser las responsables de la mejoría a nivel de serie roja observada en estos pacientes. Además, la inhibición del gen NFE2L2/ NRF2, puede desempeñar un papel clave en la reducción de las especies reactivas de oxígeno. Finalmente, el miR-125b, se encontraba sobreexpresado durante el tratamiento con deferasirox. Este microRNA está involucrado en procesos de inflamación y podría tener que ver con la estimulación de la hematopoyesis observada en los pacientes. En resumen, nuestro estudio muestra, *in vivo*, las modificaciones producidas por deferasirox en los pacientes

con SMD de bajo riesgo, y su implicación en las rutas biológicas, que pueden tener que ver con la mejoría clínica observada en algunos enfermos tratados con este fármaco.

Capítulo 3: Análisis secuencial del perfil mutacional y de expresión revela el acusado cambio producido en la población CD34+ de enfermos con SMD tratados con 5-Azacitidina

Los síndromes mielodisplásicos (SMD) son un grupo heterogéneo de enfermedades hematológicas que surgen en la célula madre hematopoyética [9]. Se caracteriza por presentar un bloqueo en la diferenciación mieloide dando lugar a una acumulación de células inmaduras tanto en la medula ósea como en sangre periférica, además de presentar citopenias [10]. Estas citopenias, pueden afectar a distintos linajes hematopoyéticos; eritrocitos, plaquetas, granulocitos y/o monocitos. Por otra parte, el 30% de los SMD progresan finalmente a leucemia aguda mieloblástica (LAM) [11]. Las terapias con agentes demetilantes, 5-azacitidina y decitabina, se usan en los pacientes que no son candidatos a trasplante. Estos tratamientos están indicados en los pacientes con SMD de riesgo intermedio y alto, así como en la leucemia mielomonocítica crónica, y en la LAM rasgos mielodisplásicos [12].

Existe controversia sobre el uso del AZA, puesto que los resultados obtenidos en los ensayos clínicos no han podido ser validados por otros grupos y su uso en la clínica solo consigue una tasa de respuesta de 30-40% [13]. Por este motivo, es necesario comprender qué pacientes se pueden beneficiar del tratamiento, y cuáles son las rutas biológicas implicadas en las respuestas. El desarrollo de las técnicas de secuenciación de nueva generación permite el análisis tanto de variantes a nivel de ADN, con una alta sensibilidad, como la cuantificación de los transcritos expresados. Este estudio se centró en el análisis de las células madre hematopoyéticas CD34+, con el objetivo de comparar el perfil mutacional antes y durante el tratamiento. Del mismo modo, secuenciamos el

transcriptoma completo. El análisis mutacional no reveló la presencia de diferencias entre las células CD34+ y las células mononucleadas de la medula ósea, mostrando una alta correlación en la frecuencia alélica observada en ambas poblaciones. El análisis de las células CD34+ antes y durante el tratamiento puso de manifiesto la reducción en la carga alélica en 3 pacientes, todos ellos con mutaciones en TP53. Además, 2 mutaciones, en *NRAS* y *KRAS,* aparecieron durante el tratamiento, ambas han sido relacionadas previamente con un aumento en el riesgo de transformación a LAM.

El perfil de expresión génico mostró una infraexpresión del complejo ribosomal, que a su vez estaba sobreexpresado en la comparación con controles sanos. Además, AZA indujo la infraexpresión en la traducción y en el metabolismo del ARN (FDR <0.0001, NES = 5.3 and ES = 0.67). Por otra parte, el tratamiento indujo la activación del sistema inmune, tanto el relacionado con la respuesta innata como con la adaptativa. Además, los genes *HOXA6* y *HOXA9*, relacionados con la leucemogénesis también se infraexpresaron por el tratamiento. Estos resultados ponen de manifiesto la afectación de nuevas rutas biológicas por el tratamiento con AZA, además de la disminución en los clones con mutación en *TP53*.

Resumen

Conclusiones

Conclusiones

1. General

    1.1. El perfil de expresión génico puede ser usado para mejorar el conocimiento de los mecanismos de acción de los medicamentos. El perfil de expresión es una técnica efectiva para la identificación de las rutas biológicas implicadas en la respuesta clínica. Los estudios pareados, donde el mismo paciente es analizado antes y durante el tratamiento, permiten definir mejor las rutas biológicas alteradas por el tratamiento.

    1.2. La secuenciación de nueva generación permite la identificación eficiente de muestras de ADN y de ARN. Esta técnica ha reducido el su coste y mejorado su desarrollo en la rutina clínica de los laboratorios. La integración de la secuenciación masiva y de la farmacogenómica, junto con el aumento de la información genética, contribuirá al mejor desarrollo de la medicina personalizada.

2. Especificos

    2.1. Eltrombopag aumenta el número de plaquetas estimulando la proliferación y la diferenciación megacariocítica.

        2.1.1. Eltrombopag sobreexpresa los genes *PPBP, ITGB3, TUBB1, TREML1, MYL9, ITGA2B* y *F13A1*, que están implicados en la diferenciación megacariocítica. Además, aumenta los niveles de IFN-γ y *IFN-α*, implicados en la respuesta innata y adaptativa, que está alterada en los enfermos con PTI. Por consiguiente, eltrombopag aumenta el número de plaquetas mediante dos mecanismos, estimulando la megacariopoyesis y regulando la respuesta inmune.

2.1.2. Eltrombopag sobreexpresa el TNFα y el interferón gamma. Este efecto puede estar relacionado con la mejora de la hematopoyesis observada en los pacientes con anemia aplásica tratos con este fármaco.

2.1.3. Los pacientes que recaen tras el tratamiento con eltrombopag presentan una sobreexpresión de *BCL2L1*, que se correlaciona con el aumento GATA-1. Ambas proteínas están involucradas en la eritropoyesis y pueden ser usadas para predecir la ausencia de respuesta al tratamiento.

2.2. Los pacientes con SMD de bajo riesgo tratados con deferasirox tienen una infraexpresión de la ruta de Nf kB, del óxido nítrico y de las especies reactivas de oxígeno, así como de los genes relacionados con la hipoxia durante la estimulación eritroide.

2.2.1. La infraexpresión *in vivo* de la ruta de Nf kB está mediada por *BCL10*, *IL1B*, *NFKBIA*, *RIPK1*, *RELA*, *BID*, *BIRC2* y *TANK*. La reducción de citoquinas proinflamatorias puede estar relacionada con la disminución de transfusiones observadas en estos pacientes.

2.2.2. Deferasirox inhibe *NFE2L2/NRF2*, disminuyendo las especies reactivas de oxígeno. Además, deferasirox activa *GFI1*, un regulador de la hematopoyesis, activando la megacarioppoyesis y la eritropoyesis.

Por todo ello, estos resultados proporcionan las bases biológicas de algunas de las características clínicas observadas en los pacientes con SMD de bajo riesgo tratados con deferasirox.

2.3. El agente hipometilante 5-Azacitidina restaura la expresión inmune en las células CD34+ en los pacientes con SMD de alto riesgo. Además, también induce la reducción de mutaciones en el ADN en estos pacientes:

2.3.1. El complejo ribosomal, que está sobreexpresado en los enfermos con SMD de alto riesgo, muestra una reducción durante el tratamiento con 5-Azacitidina.

2.3.2. AZA induce la sobreexpresión del sistema inmune, mediante el aumento en la expresión de los genes de las inmunoglobulinas, tanto de la cadena pesada como las cadenas ligeras kappa y lambda.

2.3.3. Los genes *MDM4*, *HOXA6* y *HOXA9*, que se han relacionado con un efecto leucemogénico en los SMD y en las AML, se infraexpresaron durante el tratamiento con AZA.

2.3.4. 5-Azacitidina produce una sobreexpresión de los marcadores de diferenciación en varias estirpes hematológicas, que pueden estar relacionado con la mejora hematológica observada en estos pacientes.

2.3.5. Los pacientes que alcanzan algún tipo de respuesta tenían una mayor presencia de los genes relacionados con sistema inmune. Además, las células CD34+ de estos pacientes mostraron una activación de la degranulación neutrofílica.

2.3.6. AZA reduce el número de mutaciones en *TP53*, por lo que este fármaco está indicado en el tratamiento de los enfermos que tengan mutaciones en este gen.

Referencias

1. Ghanima, W., Cooper, N., Rodeghiero, F., Godeau, B. & Bussel, J. B. Thrombopoietin receptor agonists: Ten Years Later. *Haematologica* haematol.2018.212845 (2019). doi:10.3324/haematol.2018.212845
2. Gill, H., Leung, G. M. K., Lopes, D. & Kwong, Y.-L. The thrombopoietin mimetics eltrombopag and romiplostim in the treatment of refractory aplastic anaemia. *British Journal of Haematology* **176**, 991–994 (2017).
3. Platzbecker, U. *et al.* Safety and tolerability of eltrombopag versus placebo for treatment of thrombocytopenia in patients with advanced myelodysplastic syndromes or acute myeloid leukaemia: a multicentre, randomised, placebo-controlled, double-blind, phase 1/2 trial. *The Lancet Haematology* **2**, e417–e426 (2015).
4. Gonzalez-Porras, J. R. & Bastida, J. M. Eltrombopag in immune thrombocytopenia: efficacy review and update on drug safety. *Therapeutic Advances in Drug Safety* **9**, 263–285 (2018).
5. Gattermann, N. Iron overload in myelodysplastic syndromes (MDS). *Int J Hematol* **107**, 55–63 (2018).
6. Musto, P. *et al.* Iron-chelating therapy with deferasirox in transfusion-dependent, higher risk myelodysplastic syndromes: a retrospective, multicentre study. *Br J Haematol* **177**, 741–750 (2017).
7. Olivieri, N. F., Sabouhanian, A. & Gallie, B. L. Single-center retrospective study of the effectiveness and toxicity of the oral iron chelating drugs deferiprone and deferasirox. *PLoS ONE* **14**, e0211942 (2019).

8. Gattermann, N. *et al.* Hematologic responses to deferasirox therapy in transfusion-dependent patients with myelodysplastic syndromes. *Haematologica* **97**, 1364–1371 (2012).
9. Nimer, S. D. Myelodysplastic syndromes. *Blood* **111**, 4841–4851 (2008).
10. Tefferi, A. & Vardiman, J. W. Myelodysplastic Syndromes. *N Engl J Med* **361**, 1872–1885 (2009).
11. Jabbour, E. *et al.* Acquisition of cytogenetic abnormalities in patients with IPSS defined lower-risk myelodysplastic syndrome is associated with poor prognosis and transformation to acute myelogenous leukemia. *Am. J. Hematol.* **88**, 831–837 (2013).
12. Montalban-Bravo, G. & Garcia-Manero, G. Myelodysplastic syndromes: 2018 update on diagnosis, risk-stratification and management. *Am J Hematol* **93**, 129–147 (2018).
13. on behalf of The Spanish Group on Myelodysplastic Syndromes and PETHEMA Foundation, Spanish Society of Hematology *et al.* Effectiveness of azacitidine in unselected high-risk myelodysplastic syndromes: results from the Spanish registry. *Leukemia* **29**, 1875–1881 (2015).
14. Badalian-Very, G. Personalized medicine in hematology — A landmark from bench to bed. *Computational and Structural Biotechnology Journal* **10**, 70–77 (2014).
15. Jameson, J. L. & Longo, D. L. Precision Medicine — Personalized, Problematic, and Promising. *N Engl J Med* **372**, 2229–2234 (2015).
16. Collins, F. S. & Varmus, H. A New Initiative on Precision Medicine. *N Engl J Med* **372**, 793–795 (2015).

17. Zampieri, M., Sekar, K., Zamboni, N. & Sauer, U. Frontiers of high-throughput metabolomics. *Current Opinion in Chemical Biology* **36**, 15–23 (2017).
18. Weinshilboum, R. M. & Wang, L. Pharmacogenomics: Precision Medicine and Drug Response. *Mayo Clinic Proceedings* **92**, 1711–1722 (2017).
19. Manolio, T. A. *et al.* Implementing genomic medicine in the clinic: the future is here. *Genet Med* **15**, 258–267 (2013).
20. The International Warfarin Pharmacogenetics Consortium. Estimation of the Warfarin Dose with Clinical and Pharmacogenetic Data. *N Engl J Med* **360**, 753–764 (2009).
21. Mega, J. L. *et al.* Cytochrome P-450 Polymorphisms and Response to Clopidogrel. *N Engl J Med* **360**, 354–362 (2009).
22. Wang, L. & Weinshilboum, R. Thiopurine S-methyltransferase pharmacogenetics: insights, challenges and future directions. *Oncogene* **25**, 1629–1638 (2006).
23. Abul-Husn, N. S. & Kenny, E. E. Personalized Medicine and the Power of Electronic Health Records. *Cell* **177**, 58–69 (2019).
24. Hulsen, T. *et al.* From Big Data to Precision Medicine. *Front. Med.* **6**, 34 (2019).
25. Deng, X. & Nakamura, Y. Cancer Precision Medicine: From Cancer Screening to Drug Selection and Personalized Immunotherapy. *Trends in Pharmacological Sciences* **38**, 15–24 (2017).
26. O'Brien, S. G. *et al.* Imatinib compared with interferon and low-dose cytarabine for newly diagnosed chronic-phase chronic myeloid leukemia. *N. Engl. J. Med.* **348**, 994–1004 (2003).

27. Rollison, D. E. *et al.* Epidemiology of myelodysplastic syndromes and chronic myeloproliferative disorders in the United States, 2001-2004, using data from the NAACCR and SEER programs. *Blood* **112**, 45–52 (2008).
28. Arber, D. A. *et al.* The 2016 revision to the World Health Organization classification of myeloid neoplasms and acute leukemia. *Blood* **127**, 2391–2405 (2016).
29. Greenberg, P. L. *et al.* Revised International Prognostic Scoring System for Myelodysplastic Syndromes. *Blood* **120**, 2454–2465 (2012).
30. Derissen, E. J. B., Beijnen, J. H. & Schellens, J. H. M. Concise Drug Review: Azacitidine and Decitabine. *The Oncologist* **18**, 619–624 (2013).
31. Hollenbach, P. W. *et al.* A Comparison of Azacitidine and Decitabine Activities in Acute Myeloid Leukemia Cell Lines. *PLoS ONE* **5**, e9001 (2010).
32. Issa, J.-P. Epigenetic Changes in the Myelodysplastic Syndrome. *Hematology/Oncology Clinics of North America* **24**, 317–330 (2010).
33. Stresemann, C. & Lyko, F. Modes of action of the DNA methyltransferase inhibitors azacytidine and decitabine. *Int. J. Cancer* **123**, 8–13 (2008).
34. Hussain I. Saba, Michael Lübbert & P.W. Wijermans. Response rates of phase 2 and phase 3 trials of decitabine in patients with myelodysplastic syndromes (MDS). *Blood* **106**, (2005).
35. Silverman, L. R. *et al.* Randomized controlled trial of azacitidine in patients with the myelodysplastic syndrome: a study of the cancer and leukemia group B. *J. Clin. Oncol.* **20**, 2429–2440 (2002).
36. Pierre Fenaux *et al.* Azacitidine (AZA) treatment prolongs overall survival (OS) in higher-risk MDS patients compared with conventional care regimens (CCR): Results of the AZA-001 phase III study. **110**, 817 (2007).

37. Steensma, D. P. Myelodysplastic syndromes current treatment algorithm 2018. *Blood Cancer Journal* **8**, 47 (2018).

38. Shenoy, N., Vallumsetla, N., Rachmilewitz, E., Verma, A. & Ginzburg, Y. Impact of iron overload and potential benefit from iron chelation in low-risk myelodysplastic syndrome. *Blood* **124**, 873–881 (2014).

39. Malcovati, L. *et al.* Prognostic factors and life expectancy in myelodysplastic syndromes classified according to WHO criteria: a basis for clinical decision making. *J. Clin. Oncol.* **23**, 7594–7603 (2005).

40. Killick, S. B. Iron chelation therapy in low risk myelodysplastic syndrome. *Br. J. Haematol.* **177**, 375–387 (2017).

41. Cermak, J. *et al.* A comparative study of deferasirox and deferiprone in the treatment of iron overload in patients with myelodysplastic syndromes. *Leukemia Research* **37**, 1612–1615 (2013).

42. Tataranni, T. *et al.* The iron chelator deferasirox affects redox signalling in haematopoietic stem/progenitor cells. *Br J Haematol* **170**, 236–246 (2015).

43. Rodeghiero, F. *et al.* Standardization of bleeding assessment in immune thrombocytopenia: report from the International Working Group. *Blood* **121**, 2596–2606 (2013).

44. Lambert, M. P. & Gernsheimer, T. B. Clinical updates in adult immune thrombocytopenia. *Blood* **129**, 2829–2835 (2017).

45. Cuker, A., Cines, D. B. & Neunert, C. E. Controversies in the treatment of immune thrombocytopenia: *Current Opinion in Hematology* **23**, 479–485 (2016).

46. Matschke, J. *et al.* A Randomized Trial of Daily Prednisone versus Pulsed Dexamethasone in Treatment-Naïve Adult Patients with Immune Thrombocytopenia: EIS 2002 Study. *Acta Haematol* **136**, 101–107 (2016).
47. Erickson-Miller, C. L. *et al.* Discovery and characterization of a selective, nonpeptidyl thrombopoietin receptor agonist. *Exp. Hematol.* **33**, 85–93 (2005).
48. Wang, B., Nichol, J. L. & Sullivan, J. T. Pharmacodynamics and pharmacokinetics of AMG 531, a novel thrombopoietin receptor ligand. *Clin. Pharmacol. Ther.* **76**, 628–638 (2004).
49. Garnock-Jones, K. P. & Keam, S. J. Eltrombopag: *Drugs* **69**, 567–576 (2009).
50. Desmond, R. *et al.* Eltrombopag restores trilineage hematopoiesis in refractory severe aplastic anemia that can be sustained on discontinuation of drug. *Blood* **123**, 1818–1825 (2014).
51. Adams, D. R. & Eng, C. M. Next-Generation Sequencing to Diagnose Suspected Genetic Disorders. *N Engl J Med* **379**, 1353–1362 (2018).
52. Cyranoski, D. China embraces precision medicine on a massive scale. *Nature* **529**, 9–10 (2016).
53. Byron, S. A., Van Keuren-Jensen, K. R., Engelthaler, D. M., Carpten, J. D. & Craig, D. W. Translating RNA sequencing into clinical diagnostics: opportunities and challenges. *Nat Rev Genet* **17**, 257–271 (2016).
54. Heid, C. A., Stevens, J., Livak, K. J. & Williams, P. M. Real time quantitative PCR. *Genome Res.* **6**, 986–994 (1996).
55. Lockhart, D. J. *et al.* Expression monitoring by hybridization to high-density oligonucleotide arrays. *Nat. Biotechnol.* **14**, 1675–1680 (1996).

56. Mortazavi, A., Williams, B. A., McCue, K., Schaeffer, L. & Wold, B. Mapping and quantifying mammalian transcriptomes by RNA-Seq. *Nat Methods* **5**, 621–628 (2008).